

Elucidation of the molecular and
biochemical mechanisms associated
with colour intensity and colour
retention in fresh and dry chilli peppers
(*Capsicum annuum*).

Harriet Martha Berry

This thesis was submitted for the degree of Doctor of Philosophy
at Royal Holloway University of London, September 2015

Declaration of Authorship

I, Harriet Berry, hereby declare that the work presented in this thesis is original work of the author unless otherwise stated. Original material used in the creation of this thesis has not been previously submitted either in part or whole for a degree of any description from any institution.

Signed: _____

Date: 1st September 2015

Abstract

The vibrant red colour of chilli powder determines the quality and price of the material and is therefore of highest commercial importance to the plant breeder, seed companies, and retailer. Intense red colour is the desired quality at the point of harvest and throughout storage. Therefore varieties with low colour intensity and retention are less profitable in comparison to high colour intensity and retention.

In the present study colour intensity was characterised among accessions within a colour diversity panel. This was carried out by analysing the pigment profiles of 12 chilli pepper lines throughout ripening to provide an insight into carotenoid biosynthesis and accumulation occurring within these lines. These data resulted in the discovery that carotenoid quantity and composition is directly related to the colour intensity phenotype. Identification of components responsible for the colour intensity phenotypes was attained when selected lines were analysed at a gene, transcript, and metabolite level. This revealed the role of phytoene synthase-1 and 1-deoxy-D-xylulose 5-phosphate gene products in the accumulation of carotenoids and regulatory mechanisms associated with this process. Additionally, the subchromoplast location of the carotenoids within the plastids was analysed using a subplastid fractionation techniques. This emphasised differences in sequestration mechanisms which contributed to the colour intensity phenotype. The *PSY2* gene was also sequenced and characterised on a gene expression level in chilli pepper.

Colour retention was investigated to identify mechanisms responsible for colour loss during storage. A protocol to speed up and monitor colour loss was implemented using an image analysis technique allowing identification of high and low colour retention lines. Volatile analysis revealed possible lipid peroxidation processes occurring in the high and low retention lines and analysis of superoxide dismutase activity highlighted ROS signalling pathways potentially acting in the plastid in low retention lines.

Acknowledgements

The last 4 years have been an exciting and challenging adventure which has not only allowed me to achieve my doctorate but has also resulted in me traveling the world and growing as a person. I would like to thank the people who have impacted those 4 years.

Thank you to my mum and her never ending faith and support in my endeavours, so lucky to have such a fantastic driving force behind me. Thank you to Nial for always supporting me and encouraging me to be the person I am today, could not have had a better person to share this journey with, we did it together and I could not have done it without you. And to all of my friends and family who have pretended to know what a carotenoid was!

I would like thank the wonderful people in my lab who have provided me with much fun, laughter and happiness throughout my PhD. To have such a social and enjoyable workplace kept me going through the stressful days and lifted me up on the good days. I would like to make a special mention of Dr Marilise Noguiera and Dr Margit Drapal who have been with me from start to finish and provided me with excellent example of proficient scientists, always inspiring me and providing me with great friendship. As well as team pepper which will hopefully continue to grow.

I would like to give special thanks to my supervisor Professor Paul Fraser, not only has your expert knowledge and guidance provided me with a broad skill set, but your positivity, enthusiasm and encouragement have changed me as a person making me more confident in myself and my abilities and for that I am extremely grateful. I hope we will continue to work together in the future.

I would like to acknowledge Syngenta for the opportunity for my project to take place, the provision of material, and the financial support.

'I believe the most important single thing, beyond discipline and creativity, is daring to dare'
– Maya Angelou.

Harriet

Table of Contents

Abstract.....	3
Acknowledgements.....	4
Table of Contents.....	5
Table of figures	9
Table of tables.....	12
List of abbreviations.....	13
Chapter 1. Introduction	16
1.1. Capsicum annum.....	17
1.1.1. Genus	17
1.1.2. Origins	17
1.1.3. Pungency.....	21
1.1.4. Pepper and tomato	23
1.2. Colour.....	23
1.3. Carotenoids.....	24
1.3.1. Structure and function.....	25
1.3.2. Health and nutrition.....	32
1.3.3. Biosynthesis	35
1.3.4. Genetics	46
1.3.5. Regulation of carotenoid biosynthesis	50
1.3.6. Carotenoid storage and deposition	60
1.4. Lipids	67
1.4.1. Lipid composition.....	68
1.4.2. Lipid peroxidation	70
1.4.3. Volatile compounds	71
1.5. Plant breeding: Strategies of genetic intervention for improved traits	74
1.5.1. Conventional breeding.....	74
1.5.2. Doubled haploids (DH) populations.....	74
1.5.3. Mutagenesis and TILLING	75
1.5.4. Marker assisted selection (MAS)	75
1.5.5. Genetic engineering.....	76
1.5.6. Recent advances in breeding strategies: CRISPR CAS.....	78
1.6. Aims and objectives of this study	80
Chapter 2. Materials and Methods.....	81

2.1. Plant material.....	82
2.2. Harvesting/ sampling	82
2.2.1. Fruit material	82
2.2.2. Leaf material	82
2.2.3. Storage	82
2.3. Extraction of carotenoids.....	83
2.4. Separation of carotenoids.....	83
2.5. Identificiation and quantification of carotenoids	84
2.6. Identification of carotenoids and their esters	84
2.7. Metabolite profiling	85
2.7.1. Statistical analysis and data visualisation	86
2.8. Extraction and analysis of nucleic acids	86
2.8.1. Optimised DNA extraction	86
2.8.2. Optimised RNA extraction	87
2.9. Sequencing of isoprenoid biosynthesis genes	88
2.9.1. Primer design	88
2.9.2. Nucleic acid analysis.....	89
2.9.3. Cloning of PCR amplicons.....	90
2.10. Transcription factor analysis	91
2.11. Gene expression analysis	91
2.12. Subchromoplast fractionation	93
2.13. Image analysis	94
2.13.1. Camera settings	95
2.13.2. Camera calibration.....	95
2.13.3. Whole fruit and powder imaging	96
2.13.4. Analysis	97
2.14. Colour loss during storage	97
2.14.1. Optimisation of colour loss	97
2.14.2. Long storage.....	98
2.15. Volatile analysis.....	99
2.16. Superoxide dismutase (SOD) assay.....	99
Chapter 3. Characterisation of colour intensity throughout ripening in red chilli pepper lines	101
3.1. Introduction	102
3.2. Results.....	102
3.2.1. Characterisation of colour intensity phenotypes found in the chilli pepper discovery panel	102

3.2.2. Identification and quantification of free and esterified carotenoids present in red chilli pepper fruit.....	105
3.2.3. Characterisation of carotenoid biosynthesis throughout ripening.....	115
3.2.4. Sequencing of <i>PSY1</i> , <i>PSY2</i> and <i>DXS</i> in selected lines	130
3.3. Discussion.....	152
3.3.1. Characterisation of carotenoids and carotenoid esters in chilli pepper.....	152
3.3.2. Sequencing of <i>PSY1</i> , <i>PSY2</i> and <i>DXS</i>	159
3.4. Conclusion.....	168
Chapter 4. Regulation and sequestration of carotenoids in red chilli pepper.....	170
4.1. Introduction	171
4.2. Results.....	171
4.2.1. Expression of carotenoid related genes in in ripe fruit.....	171
4.2.2. Expression of carotenoid related genes in ripe fruit	174
4.2.3. Expression of carotenoid related genes throughout ripening.....	177
4.2.4. Metabolite analysis on lines differing in ripening rates.....	185
4.2.5. Subcellular fractionation.....	196
4.3. Discussion.....	209
4.3.1. Expression of carotenoid related genes in red chilli pepper	209
4.3.2. Metabolic profiling.....	216
4.3.3. Subchromoplast fractionation	218
4.4. Conclusion.....	225
Chapter 5. Colour retention in red chilli pepper.....	227
5.1. Introduction	228
5.2. Results.....	228
5.2.1. Colour loss over time under different conditions.....	228
5.2.2. Comparison of colour measurement methods.....	238
5.2.3. Volatile analysis in fresh and dried chilli pepper fruit	242
5.2.4. Analysis of superoxide dismutase (SOD) activity in fresh and dry pepper	260
5.3. Discussion.....	263
5.3.1. Colour loss in chilli powder over time.....	263
5.3.2. Comparison of colour measurement methods.....	270
5.3.3. Volatile analysis in fresh and dry chilli pepper fruit.....	272
5.3.4. Analysis of superoxide dismutase (SOD) activity in fresh and dry pepper	277
5.4. Conclusions	278
5.4.1. Colour change in chilli powder.....	278
5.4.2. Characterisation of colour retention phenotype.....	279

5.4.3. Volatile analysis.....	280
Chapter 6. General discussion	283
6.1. Summary and general discussion.....	284
6.1.1. Aims and objectives	284
6.1.2. Summary and general conclusions	285
6.1.3. Colour intensity.....	285
6.1.4. Colour retention.....	292
6.2. Relevance to current literature and applications	293
6.2.1. Colour intensity.....	293
6.2.2. Colour retention.....	296
6.3. Future prospects and directions	297
6.3.1. Genetic engineering.....	297
6.3.2. Regulatory mechanisms.....	297
6.3.3. Lipidomics	299
6.3.4. Antioxidants and degradation.....	300
Appendices.....	302
References	312

Table of figures

Figure 1.1. A phylogenetic tree of Solanaceae.....	18
Figure 1.2. Origin of the chilli pepper.....	19
Figure 1.3. Examples of pungent and non-pungent pepper.....	20
Figure 1.4. Proposed capsaicinoid biosynthesis pathway.....	22
Figure 1.5. Carotenoids in nature.....	24
Figure 1.6. Mechanism of the xanthophyll cycle in plants.....	26
Figure 1.7. Photochemical quenching of triplet chlorophyll and singlet oxygen by carotenoids.....	27
Figure 1.8. Carotenoid reactions with radicals.....	28
Figure 1.9. Interaction between carotenoids and other antioxidants.....	29
Figure 1.10. Examples of carotenoids with different end group structures.....	31
Figure 1.11. Oxidative stress, antioxidants, and chronic diseases (adapted from Rao and Rao, 2007).....	33
Figure 1.12. Roles of carotenoids in the prevention of chronic diseases. Abbreviations: AMD, age-related macular degeneration; CVD, cardiovascular disease (Adapted from Rao and Rao, 2007).....	35
Figure 1.13. Isoprenoid biosynthesis in plants.....	37
Figure 1.14. The MEP pathway.....	38
Figure 1.15. The carotenoid biosynthesis pathway in pepper.....	41
Figure 1.16. Comparison of natural colour mutants in tomato and pepper.....	48
Figure 1.17. Different mechanisms associated with the regulation of biochemical pathways.....	51
Figure 1.18. A model for carotenoid metabolic feedback in plants.....	56
Figure 1.19. The transition from chloroplast to chromoplast.....	61
Figure 1.20. Longitudinal sections of globular plastoglobuli transforming into fibrillar plastoglobuli found in <i>Capsicum annuum</i> (Simpson and Lee, 1976).....	63
Figure 1.21. Metabolic processes present in plastoglobuli (PGs).....	65
Figure 1.22. Plant cuticle structure (adapted from Yeats and Rose, 2013).....	69
Figure 1.23. Lipid peroxidation reactions.....	71
Figure 1.24. Carotenoid derived volatiles and their potential precursors (Lewinsohn et al., 2005).....	72
Figure 1.25. Summary of the cellular processes which can result in the production of volatiles in plants.....	73
Figure 1.26. Functioning of the type II CRISPR-Cas systems in bacteria.....	79
Figure 2.1. Image analysis system.....	94
Figure 2.2. Image calibration.....	96
Figure 2.3. Examples of images containing (a) whole chilli peppers and (b) chilli powder.....	97
Figure 3.1. Typical HPLC-PDA profile of carotenoids and their esters in a red ripe chilli pepper.....	107
Figure 3.2. Example of capsanthin and capsanthin esters identified on the LCMS.....	111
Figure 3.3. Summary of coloured carotenoid content in ripe fruit.....	113
Figure 3.4. The percentage of capsanthin and corresponding esters of the total carotenoid content.....	115
Figure 3.5. Ratio of chlorophyll a to b.....	122

Figure 3.6. The determination of capsanthin and its corresponding esters during ripening, showing the transition between synthesis and accumulation.	125
Figure 3.7. PCA of carotenoid pigments throughout ripening in selected lines.	128
Figure 3.8. Ratio of red to yellow carotenoids.	130
Figure 3.9. Comparison of amino acid sequence of PSY1 between different higher plants.	132
Figure 3.10. Predicted protein structure of the PSY1 protein in chilli pepper.	133
Figure 3.11. Putative regulatory elements present in the PSY1 promoter.	135
Figure 3.12. Comparison of the predicted structure of the PSY2 protein.	139
Figure 3.13. Comparison of amino acids in PSY1 and PSY2 between different higher plants.	141
Figure 3.14 Putative regulatory elements present in the PSY2 promoter.	143
Figure 3.15. Comparison of the predicted structure of the DXS protein.	147
Figure 3.16. Comparison of the DXS amino acid sequences in different higher plants.	148
Figure 3.17. Putative regulatory elements present in the DXS promoter.	149
Figure 3.18. Overview of the synthesis and accumulation of carotenoids, chlorophylls, and tocopherols throughout ripening.	156
Figure 3.19. Diagram of proposed DXS promoter regulation.	167
Figure 4.1. Average expression stability of reference targets.	172
Figure 4.2. Comparison of plastome to genome ratio between selected lines.	173
Figure 4.3. Characterisation of phytoene synthase-1 (PSY1) and 1-deoxy-D-xylulose 5-phosphate synthase (DXS) expression in ripe fruit.	175
Figure 4.4. Characterisation of the capsanthin capsorubin synthase (CCS) and the β -carotene hydroxylase-2 (CHY2) gene expression in ripe fruit.	176
Figure 4.5. PSY1 expression throughout ripening in high and low intensity lines.	178
Figure 4.6. DXS expression throughout ripening in high and low intensity lines.	180
Figure 4.7. CCS expression throughout ripening in high and low intensity lines.	181
Figure 4.8. Contribution of PSY2 to the accumulation of carotenoids present in ripe fruit in a high and low intensity line.	183
Figure 4.9. Ripening specific acyltransferase (rsAct) expression throughout ripening in high and low intensity lines.	184
Figure 4.10. Representation of the most abundant metabolites accumulated in the chilli pepper fruit throughout ripening.	186
Figure 4.11. PCA analysis of polar and non-polar compounds throughout ripening in selected lines.	188
Figure 4.12. Heat map of metabolite levels during ripening in selected lines.	190
Figure 4.13. Pathway display of metabolite changes over ripening in chilli pepper fruit at (a) mature green, (b) turning and (c) ripe stages.	195
Figure 4.14. Subchromoplast fractionation of red chilli pepper from a medium and a high intensity line.	197
Figure 4.15. Total amount of carotenoids.	199
Figure 4.16. A comparison of the amount of each carotenoid analysed in R4 and R7.	201
Figure 4.17. Percentage of carotenoids and α -tocopherol per fraction.	203
Figure 4.18. Summary of the location of carotenoids; a comparison of R4 and R7.	205
Figure 4.19. The percentage distribution of the total pool of each carotenoid in subplastidial fractions.	206
Figure 4.20. Representation of PG and fibril formation in chilli pepper.	223
Figure 5.1. Representation of the trend over time for the lightness of chilli powder.	230
Figure 5.2. Representation of the trend in red colour of chilli powder over time.	232

Figure 5.3. Representation of the trend in colour saturation of chilli powder over time.	234
Figure 5.4. Representation of the trend in hue angle of chilli powder over time.	236
Figure 5.5. A representation of the total colour change in chilli powder over time.	237
Figure 5.6. Total colour change (ΔE) for chilli pepper lines stored for 9 months.	239
Figure 5.7. Percentage change of total capsanthin over storage.	240
Figure 5.8. Percentage change of ASTA colour during storage.	241
Figure 5.9. Representation of the change in volatile compositions from fresh to dry.	243
Figure 5.10. PCA of volatile compounds detected in fresh and dry chilli pepper.	244
Figure 5.11 Heat map displaying the change in volatile compounds in dry fruit when compared to fresh fruit.	245
Figure 5.12. PCA of volatile compounds identified in fresh ripe fruit.	247
Figure 5.13. OPLS-DA of volatile compounds identified in fresh chilli pepper in high and low retention lines.	249
Figure 5.14. Heat map visualising the differences in volatile compounds between high and low retention lines in fresh fruit.	250
Figure 5.15. OPLS-DA on volatile compounds identified in the fresh fruit of high and low intensity lines.	252
Figure 5.16. PCA of volatile compounds identified in dry fruit.	254
Figure 5.17. OPLS-DA of volatile compounds identified in dry chilli pepper in high and low retention lines.	256
Figure 5.18. Heat map displaying the changes in volatile compounds in between high and low retention lines in dry fruit.	257
Figure 5.19. OPLS-DA of volatile compounds identified in dry chilli pepper in high and low intensity lines.	259
Figure 5.20. Superoxide dismutase (SOD) activity in fresh and dry chilli pepper.	261
Figure 5.21. Superoxide dismutase (SOD) activity in dried chilli pepper.	262
Figure 5.22. Schematic illustration of the hypothesis of the relationship of lipid peroxidation and carotenoid degradation present in high and low retention lines.	281
Figure 6.1. Colour intensity in red chilli pepper.	288
Figure 6.2. Regulatory mechanisms associated with the expression of the capsanthin capsorubin synthase (CCS) gene in red chilli pepper.	290

Table of tables

Table 1.1.1. Genetic determination of ripe fruit colour of pepper.	46
Table 2.1. Primers used to sequence PSY1.	88
Table 2.2. Primers used to sequence PSY2.	89
Table 2.3. Primers used to sequence DXS.	89
Table 2.4. Primers designed for qPCR on carotenoid biosynthesis related genes.	92
Table 2.5. Remote camera settings.	95
Table 3.1 Table displaying colour intensity phenotypes of the colour diversity panel supplied by Syngenta	103
Table 3.2. Carotenoid and carotenoid esters identified from non-polar extracts in red ripe chilli pepper fruit using HPLC-PDA and LC-MS.	108
Table 3.3. Carotenoid content throughout ripening in 8 selected lines.	116
Table 3.4. Comparison of ripening series in selected lines.	126
Table 3.5. Putative transcriptional regulatory elements identified in PSY1; corresponds to Figure 3.11.	136
Table 3.6. Putative transcriptional regulatory elements identified in PYS2 promoter. Corresponds to Figure 3.14.	143
Table 3.7. Putative regulatory elements identified in the DXS promoter region. Table corresponds to Figure 3.17.	149
Table 4.1. The ratio of esters: free carotenoids in sub-plastidial fractions (expressed as a percentage).	207

List of abbreviations

ABA	Abscisic acid
ACL	acyl carrier protein
AO	Aldehyde oxidase
AMP	Adenosine monophosphate
ATP	Adenosine triphosphate
B	Breaker stage
B+3	Breaker plus three days
B+7	Breaker plus seven days
B+10	Breaker plus ten days
B+14	Breaker plus fourteen days
BCAT	Branched-chain amino-acid aminotransferase
C3H	p-Coumarate 3-hydroxylase
C4H	Cinnamate 4-hydroxylase
CAB	Chlorophyll a/b binding protein
CCD	Carotenoid cleavage dioxygenase
CCoOMT	Caffeoyl-CoA O-methyltransferase
CDP-ME	4-diphosphocytidyl-2C-methyl-D-erythritol
CDP-ME2P	4-diphosphocytidyl-2C-erythritol-2-phosphate
CHD	Coronary heart disease
CHS	Chalcone synthase
CMK	4-diphosphocytidyl-2C-methyl-D-erythritol kinase
COMT	Caffeic acid O-methyltransferase
CTP	Cytidyl triphosphate
DMAPP	Dimethylallyl diphosphate
DPA	Days post anthesis
DXR	1- deoxy-D-xylulose 5-phosphate reductoisomerase

DXS	1- deoxy-D-xylulose 5-phosphate synthase
EIC	Extracted ion chromatogram
FATA	acyl-ACP thioesterase
FPS	Farnesylpyrophospahte synthase
GAPA	Glyceraldehyde 3-phosphate dehydrogenase
GAPF	Glyceraldehyde 3-phosphate dehydrogenase binding factor
GGPS	Geranylgeranylpyrophosphate synthase
HDR	4-hydroxy-3-methyl-2-(E)-butenyl-4-diphospahte reductase
HDS	1-hydroxy-2-methyl-2-(E)-butenyl-4-phosphate synthase
HMBP	1-hydroxy-2-methyl-2-(E)-butenyl-4-phosphate
HMBPP	4-hydroxy-3-methyl-2-(E)-butenyl-4-diphospahte
HPLC	High pressure liquid chromatography
IDI	IPP isomerase
IDS	IPP/ DMAPP synthase
ILE	Isoleucine
Isocit	Isocitric acid
KAS1	3-oxoacyl-(acyl-carrier-protein) synthase
LCMS	Liquid chromatography mass spectrometry
Man	Mannose
MCS	2C-methyl-D-erythritol-2,4-cyclodiphosphate synthase
MCT	4-diphosphocytidyl-2C-erythritol cytidyltransferase
MEP	2-C-methyl-D-erythritol 4-phosphate
MET	Methionine
MG	Mature green stage
MYA	Million years ago
NBT	Nitroblue tetrazolium
NCED	9- <i>cis</i> -epoxycarotenoid dioxygenase
NSY	Neoxanthin synthase
OPLS-DA	Orthogonal projections of latent structures with discriminant analysis

PAL	Phenylalanine ammonia-lyase
PAMT	putative aminotransferase
PHE	Phenylalanine
PG	Plastoglobule
PRO	Proline
PSY1	Phytoene synthase -1; fruit specific
PSY2	Phytoene synthase -2; leaf specific
PTOX	Plastid terminal oxidase
RE	Regulatory element
ROS	Reactive oxygen species
RT-PCR	Real time polymerase chain reaction
SQS	Squalene synthase
TPP	Thiamine pyrophosphate
TRP	Tryptophan
TYR	Tyrosine
VAD	Vitamin A deficiency
VTE1	vitamin E deficient 1

Chapter 1. Introduction

1.1. *Capsicum annuum*

1.1.1. Genus

Chilli peppers (*Capsicum annuum* L.) are members of the *Solanaceae* family which is one of the largest and most economically important families of flowering plants. The family consists of around 90 genera including 3000-4000 species (Knapp et al., 2004). The *Solanaceae* family includes major crop species, such as tomato (*Solanum lycopersicum*), potato (*Solanum tuberosum*), and aubergine (*Solanum melongena*). In addition to other well-known plants such as tobacco (*Nicotiana tabacum*) and petunia (*Petunia* spp.). The *Capsicum* genus forms a clade with the *Lycianthes* genus which is a sister clade to *Solanum* (Figure 1.1) (Bohs and Olmstead, 1997). There are around 30 species of *Capsicum* present today; the most economically notable species of chilli pepper which have been domesticated are *C. annuum*, *C. baccatum*, *C. chinense*, *C. frutescens*, and *C. pubescens*.

1.1.2. Origins

Chilli peppers were first cultivated in the Americas over 6000 years ago and it is generally believed that the *Capsicum* genus originated in Bolivia (Figure 1.2a). The domestication of *C. annuum* is thought to have originated in Mexico or Northern Central America, *C. baccatum* from lowland Bolivia, *C. chinense* from northern lowland Amazonia, *C. frutescens* from the Caribbean, and *C. pubescens* from mid-elevation Southern Andes (Perry et al., 2007). The species *C. annuum*, *C. chinense*, and *C. frutescens* have been described as a species complex and so are more similar to each other than to *C. baccatum* and *C. pubescens*. The domestication and dispersal of chilli pepper has been studied using microfossils. The unique shape of the chilli pepper starch grain allowed identification and discovery of early agricultural systems which were using chilli pepper.

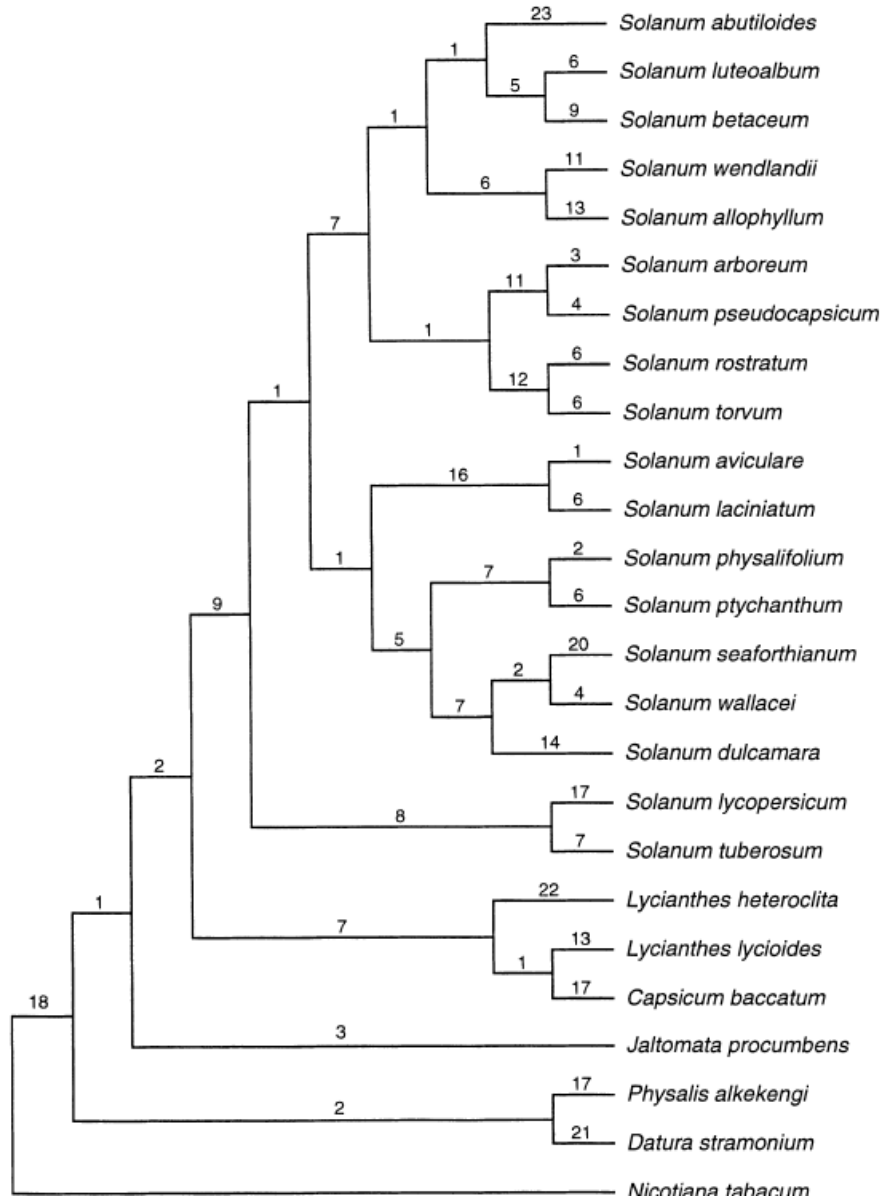


Figure 1.1. A phylogenetic tree of Solanaceae.

Phylogenetic tree based on nucleotide changes on a chloroplastic gene (a subunit of NADH dehydrogenase) (branch numbers) (Bohs and Olmstead, 1997).

Some of the earliest evidence of domesticated chilli pepper was identified in Ecuador around 6100 years ago where starch grains unique to chilli were found in milling stones and cooking vessels often with maize. The fact that Ecuador is not considered to be a central site for domestication suggests that agricultural systems were already in place at this time thus showing the domestication of chilli happened at an earlier time point still (Perry et al., 2007). Other studies have implied that central-east Mexico is the most likely site where the domestication of

chilli originated (Figure 1.2b) (Kraft et al., 2014). Once the Americas were visited by Columbus in the 15th century the chilli pepper spread to the rest of the world, particularly in India and Southeast Asia where it now features as an essential ingredient in many traditional recipes.

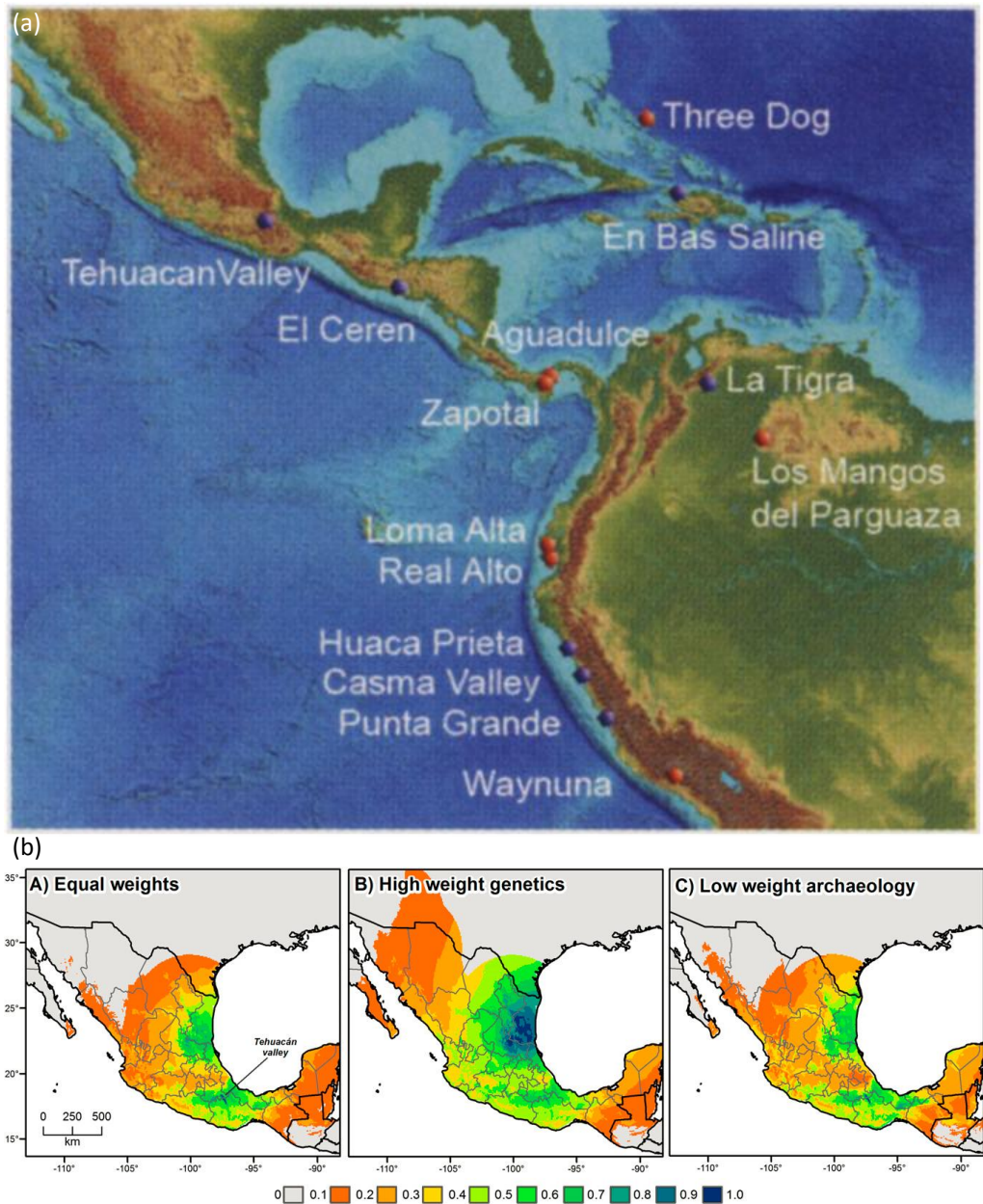


Figure 1.2. Origin of the chilli pepper.

(a) Geographical origin of chilli pepper. The red dots represent archaeological sites which yielded starch grains of chilli pepper and the blue dots represent sites which yielded all other remains of chilli pepper. (b) Consensus models for cultivated chilli pepper and the areas in Mexico in which it was likely domestication originated. These models were obtained by combining data

based on studies of archaeology, ecology, linguistics, and genetics. The values obtained were scaled so 1.0 (dark blue) is the most probable area of first domestication and 0 (grey) is the least probable (adapted from Perry et al., 2007; Kraft et al., 2014).

Peppers have a wide variety of shapes, sizes, colours, and taste. Domestication of *C. annuum* species has resulted in larger fruit, leaves, seeds, and flowers in addition to the traits mentioned previously. Specifically, larger fruit weight and loss of pungency were major aspects which were shaped by domestication of the crop (Paran and Van Der Knaap, 2007). Peppers are considered a vegetable but botanically they are in fact berries. There is a large variation witnessed within species and so the pepper pod-types are used to distinguish between cultivars. Bell peppers, pimiento, sweet yellow wax, Cuban, and squash pod-types are often non-pungent and are prevalent in the United States. Paprika is the name of the ground powder made from the non-pungent varieties (Figure 1.3).

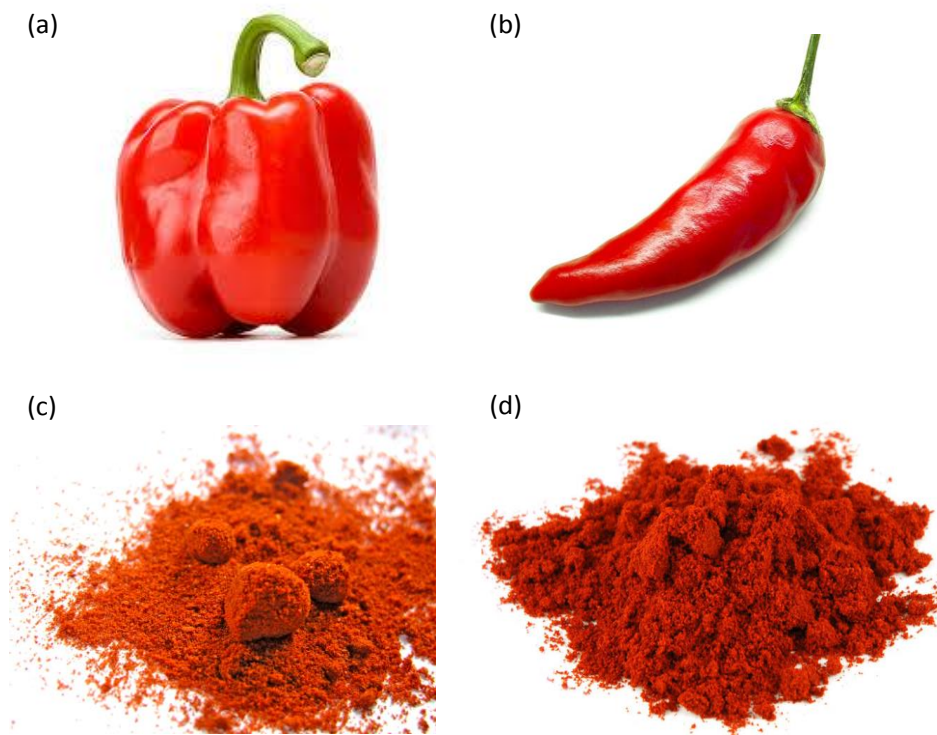


Figure 1.3. Examples of pungent and non-pungent pepper.

(a) Non-pungent bell pepper, (b) Pungent chilli pepper, (c) paprika, ground non-pungent pepper and (d) chilli powder, ground pungent pepper.

However, the pungent pod-types are separated into two sub groups, this is usually based on whether the cultivar is processed or dehydrated. Examples of the most common pod-types are: the cayenne pepper is red and characteristically wrinkly. It is highly pungent and used as powder in sauces and culinary dishes. The New Mexican can be yellow, orange, brown, or red, and the powder is used in many sauces. The Jalapeño is dark green at immature stage and red at mature and is commonly used on nachos, or is canned, pickled, or made into salsa. The mature dried form of this known as chipotle. Other pod-types include ancho, pasilla, mirasol, serrano, de arbol, and piquin (Bosland, 1996). The ground powder of pungent varieties is known as chilli powder (Figure 1.3).

1.1.3. Pungency

Chilli peppers are known for their spicy flavour and the group of compounds responsible for this are the capsaicinoids. The predominant capsaicinoids found in chilli pepper are capsaicin and dihydrocapsaicin (Figure 1.4), but others are present at lower levels, such as nordihydrocapsaicin, homodihydrocapsaicin, and homocapsaicin. These compounds are colourless, odourless alkaloids which are synthesised in the epidermal cells of the placenta of the fruit (Fujiwake et al., 1980). The biosynthesis of the capsaicinoids is conducted by two pathways. The phenylpropanoid pathway is responsible for the synthesis of the phenolic part of the molecule and the fatty acid metabolism determines the branched chain fatty acid. Condensation of vanillylamine, from phenylalanine, and a branched chain fatty acid from either valine or leucine, results in the formation of dihydrocapsaicin (Blum et al., 2003).

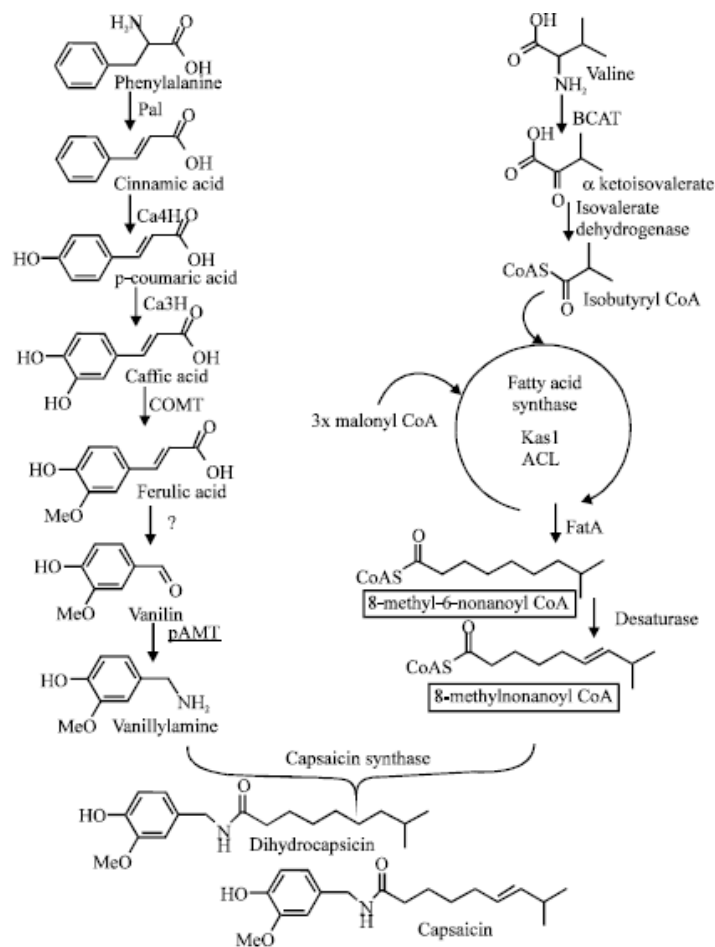


Figure 1.4. Proposed capsaicinoid biosynthesis pathway.

The capsaicin biosynthesis pathway combines the phenylpropanoid biosynthesis pathway (left) with the fatty acid synthesis (right). Abbreviations: Pal, Phenylalanine ammonia-lyase; C3H, p-Coumarate 3-hydroxylase; C4H, Cinnamate 4-hydroxylase; COMT, Caffeic acid *O*-methyltransferase; pAMT, putative aminotransferase; BCAT, Branched-chain amino-acid aminotransferase; Kas1, 3-oxoacyl-(acyl-carrier-protein) synthase; ACL, acyl carrier protein; FatA, acyl-ACP thioesterase (Blum et al., 2003).

The capsaicinoids elicit a sensation of burning pain through the depolarisation of nociceptors which are specialised neurons which detect noxious chemicals. Pungency is expressed as Scoville Heat Units (SHU) and is actually a concentration measurement of capsaicinoids. This organoleptic test is based on diluting the chilli pepper extract with sugar water until taste panellists can no longer detect any heat (Bosland and Baral, 2007).

1.1.4. Pepper and tomato

Pepper and tomato share similar geographical locations in terms of their wild relatives and also have similar domestication history. Tomato is thought to have originated in Peru. Comparison of genome sequences suggest that pepper separated from potato around 36 Mya, and diverged from tomato at around 20 Mya based on whole genome duplication events (Qin et al., 2014). Due to its relation to tomato and considering that the tomato is a model organism in terms of study of the fruit, as well as containing a vast collection of knowledge gathered from transgenic studies, chilli pepper will be compared to tomato where appropriate.

1.2. Colour

Chilli pepper is the world's most widely grown and consumed spice, and is mainly consumed in the form of a powder when utilised in cooking. However, although paprika is ground, non-pungent pepper, this can sometimes be referring to ground, pungent pepper too. Predominantly, it is called chilli powder and is the term used in this study (Figure 1.3).

The colour of chilli powder is important because it is the indicator for fruit quality. Consumers associate colour with the flavour, maturity, and nutritional value. This initial first impression influences whether the consumer will accept or reject the fruit. Therefore, desirable deep red colour of chilli powder is directly responsible for how much the material can be sold for. Consequently, it is paramount that the chilli peppers can maintain their red colour throughout the storage season. In the past attempts to artificially enhance the red colour of chilli powder was a problem with the use of Sudan dyes. The Sudan dyes are known for their colour fastness and low cost but have been classified as a carcinogen resulting in their ban for human consumption (Liu et al., 2014).

In 2011 the global production of pepper reached 34.6 million tons of fresh fruit and 3.5 million dried pepper pods. This was harvested from land accumulating to 3.9 million hectares (Qin et al., 2014).

The red colour of chilli pepper is predominantly caused by the accumulation of carotenoids in the ripe fruit. However, other compounds which can affect the colour are the chlorophylls,

tocopherols (vitamin E), and anthocyanins. Carotenoid concentration levels in chilli pepper fruit are among the highest in plant organs.

1.3. Carotenoids

The carotenoids are a distinctive group of natural pigments which cannot be synthesised *de novo* in animals, excluding some aphids (Moran and Jarvik, 2010). Their unique properties enable them to perform a wide range of functions in living organisms. They are responsible for the striking colour seen in many fruits and vegetables, flowers, fish, birds, insects, and crustaceans (Figure 1.5).

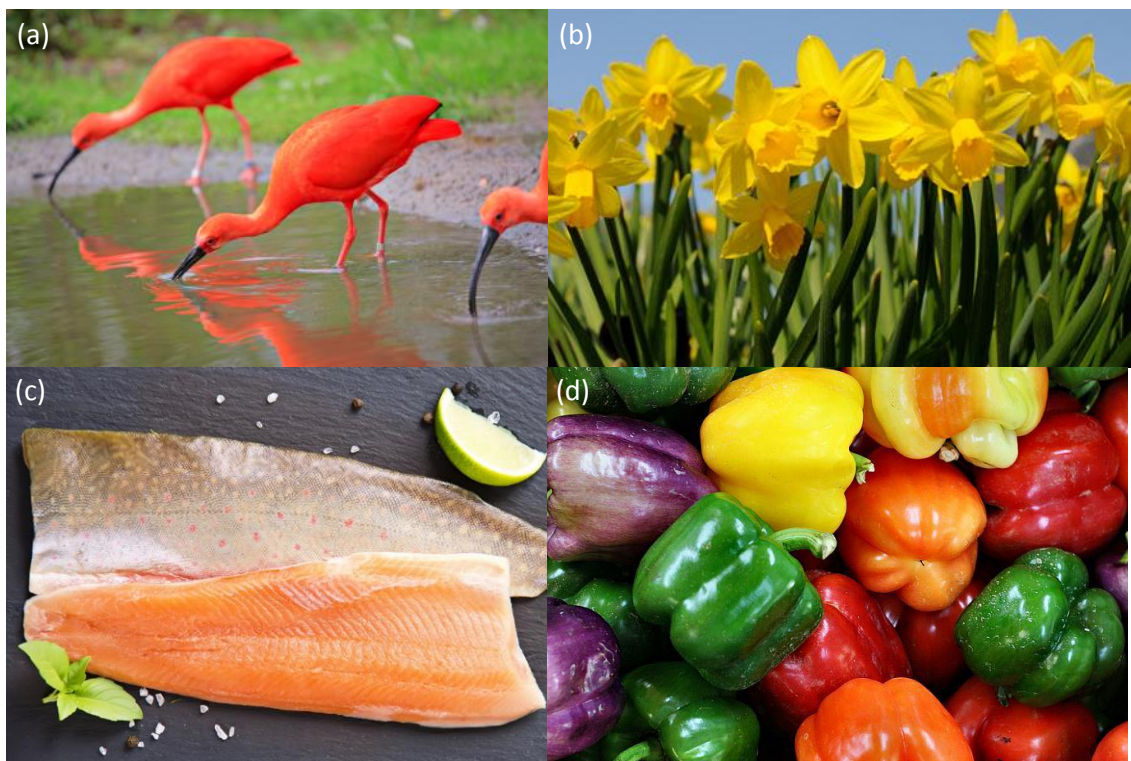


Figure 1.5. Carotenoids in nature.

Examples of carotenoids in nature (a) birds, (b) flowers, (c) fish, and (d) fruits and vegetables.

In the animal kingdom accumulation of carotenoids is often related to sexual behaviour. The vibrant colours of the accumulated carotenoids act as an attractant for potential mates and

could be a direct indication of how healthy the individual is. It has been suggested that the accumulation of carotenoids in birds is related to the oxidative stress present in the individual. Therefore, a female would preferentially select a mate with decreased risk of disease or a good immune system as this would increase the wellbeing and survival rates of her offspring (Von Schantz et al., 1999). This is also the same in fish and there is evidence to suggest that dietary carotenoids are responsible for these variations in colour (Baron et al., 2008). The carotenoids also play a role in social signalling. In plants, the carotenoids are accumulated in fruit and flowers as method of attracting animals for seed dispersal or as a method to attract pollinators, respectively.

Carotenoids such as astaxanthin and canthaxanthin have been used in fish feed in the gold fish and salmon industry. The ketocarotenoids added to the feed are either synthetic or produced by algae (Baron et al., 2008). Hence, there has been an effort in manipulating the ketocarotenoids of crop plants, such as tomato, to provide a more economic source of astaxanthin. This highlights one of the major roles of carotenoids as a colourant in the food industry whereby the carotenoids are used as natural food dyes to add to foods when the colour has been lost due to processing. Chilli powder can be used to modify the colour of many food products, such as soup, sausage, and beverages to name but a few (Arimboor et al., 2014).

The accumulation of carotenoids is not primarily based on reproductive needs. They predominantly have protective functions which provide antioxidant roles against the free radicals produced in photo-oxidation which help to protect against disease states. This will be expanded later in section 1.3.2.

1.3.1. Structure and function

1.3.1.1. Function

Carotenoids are synthesised by plants, bacteria, and algae. There are more than 600 different carotenoids which have been isolated from natural sources (Fraser and Bramley, 2004). In plants, the biosynthesis and accumulation is essential in photosynthesis and plants are therefore unable to survive without them. The carotenoids are located in the plastids. In the chloroplasts they are essential for the assembly of photosystems and act as light-harvesting pigments which transfer energy to chlorophyll initiating photosynthesis (Cazzonelli, 2011). The carotenoids

lutein, violaxanthin, and zeaxanthin are typical of the harvesting complex and allow a larger absorption range of light within the antenna.

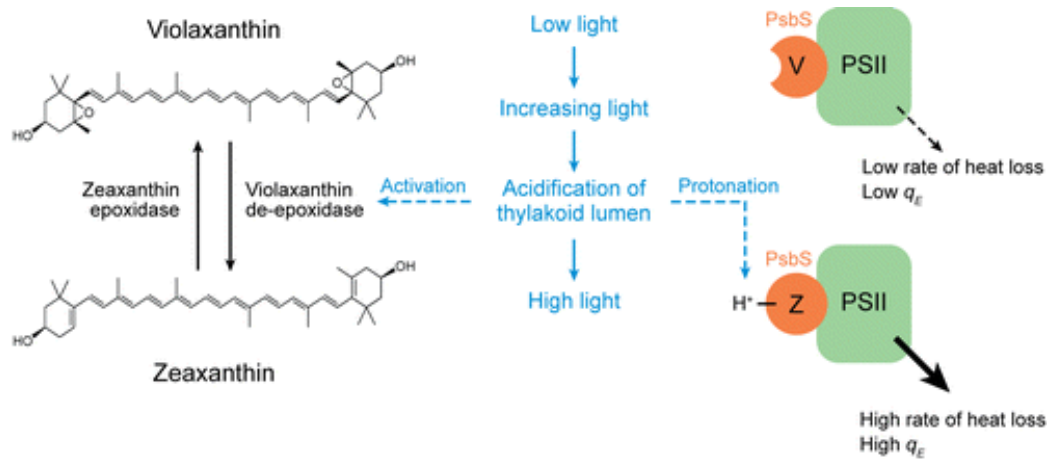


Figure 1.6. Mechanism of the xanthophyll cycle in plants.

At low light violaxanthin (V) is associated with photosystem II (PSII) and functions as a component in nonchemical quenching. At higher light intensities violaxanthin de-epoxidase is activated and converts violaxanthin to zeaxanthin (Z) and this pigment acts to dissipate excess light energy. Abbreviations: q_E , energy-dependent quenching; PsbS, photosystem II b subunit (Baker, 2008).

These compounds are partly responsible, together with anthocyanins, for the yellow and red colours of leaves in autumn once the chlorophyll has been degraded. During the presence of excess light the xanthophyll cycle is activated (Figure 1.6). This occurs when violaxanthin is converted to antheraxanthin then to zeaxanthin by the action of the enzyme violaxanthin de-epoxidase (VDE). This enzyme becomes activated at low pH levels in the thylakoid lumen. Here the excess energy is dissipated as carotenoids are able to quench triplet excited chlorophyll, which can be harmful for the cell by going on to produce reactive oxygen species (ROS), damaging proteins, lipids, and pigments present in the photosynthetic machinery (Li et al., 2009). The transfer of energy from triplet state chlorophyll to carotenoids occurs more readily than to oxygen (Figure 1.7). The carotenoid molecule can transform into a higher-level excited state by the action of one of the bonding π -electrons of the conjugated double bond system, characteristic of carotenoids (1.3.1.2), being promoted to an unoccupied π antibonding orbital (Britton, 1995a). The electrons are delocalised in the double bond system and so this results in

lower energy required to reach the excited state. The energy required corresponds to the range of 400-500nm in the visible region of light (Britton, 1995a).

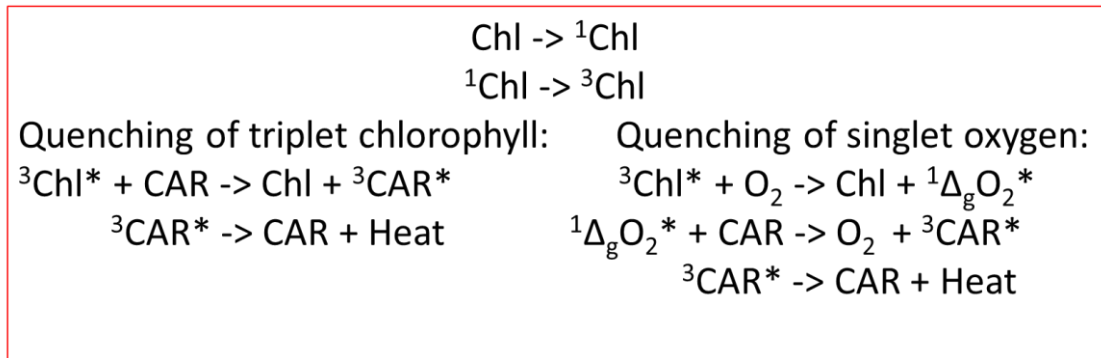


Figure 1.7. Photochemical quenching of triplet chlorophyll and singlet oxygen by carotenoids.

Key: Chl, chlorophyll; ${}^3\text{Chl}^*$, triplet chlorophyll, CAR, carotenoids; O_2 , oxygen; ${}^1\Delta_g\text{O}_2^*$, singlet oxygen; *, excited state (adapted from Frank and Cogdell, 1993).

Carotenoids can also accept excited electrons from singlet oxygen. This ion is highly destructive and can lead to the formation of ROS and other free radicals but this is prevented when the energy is transferred to a carotenoid. Due to the low energy requirement of the excited state the carotenoid is unable to go on to transfer energy to other molecules and the excitation from the singlet oxygen is dissipated to the surroundings (Britton, 1995a). This therefore emphasises the importance of the role of carotenoids in light harvesting and photo-protection during photosynthesis.

In addition to the photo-protective role in the chloroplasts, the carotenoids can act as antioxidants. In low oxygen conditions the carotenoid molecule can consume free radicals breaking autooxidation chains. When the carotenoids are reacting with free radicals hydrogen abstraction, electron transfer, or addition reactions ensue (Figure 1.8). Once the reaction has taken place the conjugated bond system is disrupted leading to the bleaching of the chromophore. It is thought that addition reactions do not take place with molecular O_2 but only with acylperoxyl radicals (Krinsky and Yeum, 2003). Once the carotenoids have reacted with the radicals this leads to the production of apocarotenoids and volatile carbonyls. These will be discussed later (1.4.3).



Figure 1.8. Carotenoid reactions with radicals.

Carotenoids can react with radicals through (a) hydrogen abstraction, (b) electron transfer, and (c) addition. Key: R, radical and CAR, carotenoid.

Although carotenoids have the ability to quench a wide range of free radicals the most efficient reactions are observed with the peroxy radicals which are generated during lipid peroxidation. Based on the carotenoids highly hydrophobic properties and their preference for products of lipid peroxidation it has been suggested that one of the key roles of the carotenoids is to protect lipophilic compartments, such as cellular membranes and lipoproteins, from damage caused by oxidation (Stahl and Sies, 2003).

However, it has been shown that in high oxygen environments carotenoids can act as pro-oxidants and carry on the free radical chain via autooxidation. These carotenoid radicals can go on to oxidise unsaturated fatty acids thus intensifying the damage. However, high oxygen environments are not characteristic of the physiological conditions within most tissues of the plant (Stahl and Sies, 2003).

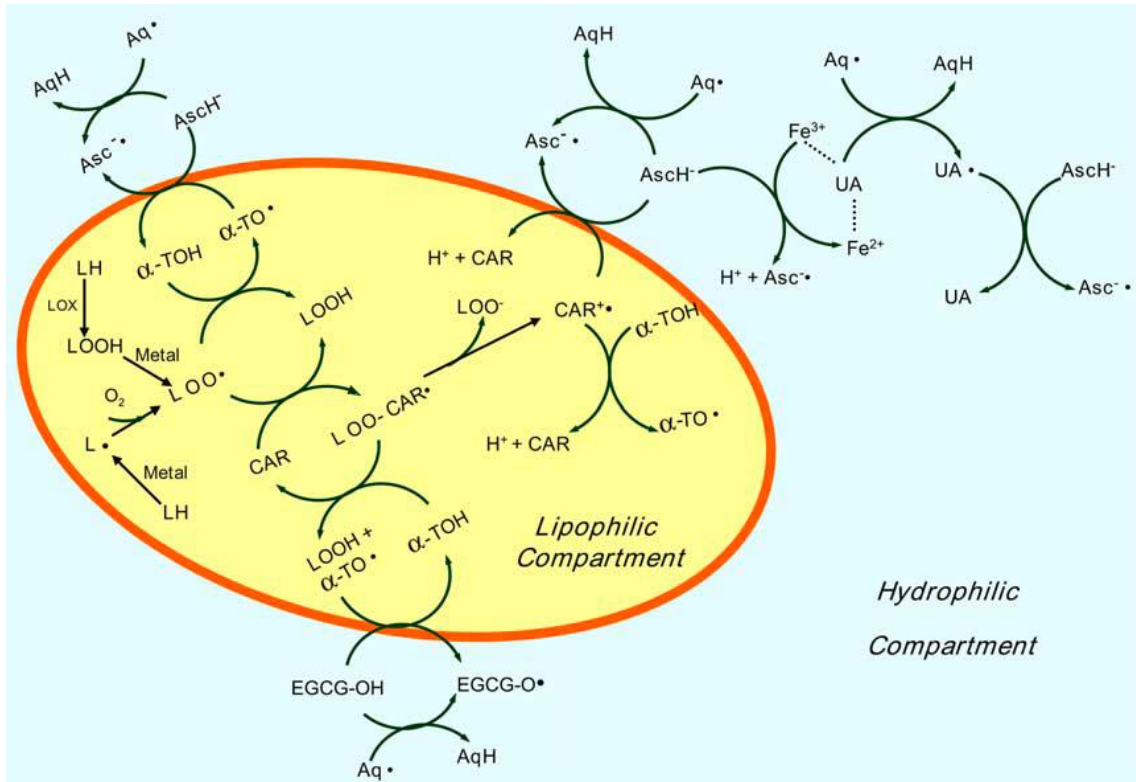


Figure 1.9. Interaction between carotenoids and other antioxidants.

The interaction between lipid peroxyl radicals (LOO^{*}) produced during lipid peroxidation with carotenoids (CAR), α -tocopherols (α -TOH), and ascorbic acid (AscH⁻). Abbreviations: Asc⁻, ascorbyl radical; Aq^{*}, aqueous radical; AqH, aqueous hydrogen donor; L^{*}, lipid alkyl radical; LOX, lipoxygenase; CAR⁺, carotenoid radical cation; α -TO^{*}, α -tocoperoxyl radical; EGCG-OH, (-)-epigallocatechin gallate; EGCG-O^{*}, (-)-epigallocatechin gallate radical; UA, uric acid (Krinsky and Johnson, 2005).

Carotenoids can also use their antioxidant properties to interact and protect other antioxidants. It was found that when feeding α -tocopherol deficient chicks with canthaxanthin, the chicks experienced increased levels of α -tocopherol in the membranes and reduced lipid peroxidation. This suggested that the carotenoids can protect or repair α -tocopherol (Mayne and Parker, 1989). There has also been evidence to suggest that β -carotene, α -tocopherol, and ascorbic acid participate in synergistic interactions (Stahl and Sies, 2003). Studies in frozen trout have shown that astaxanthin degradation was not affected by α -tocopherol concentration, but α -tocopherol degradation was affected by astaxanthin concentration; thus, indicating a potential protective role of astaxanthin (Mortensen et al., 2001). This therefore suggests there are interactions between the carotenoids and other known antioxidants. Krinsky and Yeum (2005) propose a

schematic of how these interactions take place, shown in Figure 1.9. It has been suggested that the hydrophobic radical cation of tocopherol formed within the lipid membranes can be generated by carotenoids such as zeaxanthin. This forms a radical cation of carotenoid which would be reduced by an external ascorbic acid at the surface of the inner membrane (Krinsky and Yeum, 2003).

1.3.1.2. Structure

The carotenoids are isoprenoids which are C₄₀ molecules containing conjugated double bonds. The parent C₄₀ carbon skeleton is where all carotenoids are derived from. The ends of the carbon skeleton can be modified by three ways: cyclisation, hydrogenation, and oxygen-containing groups. Carotenoids containing oxygen groups are known as xanthophylls, and preceding them consisting of only carbon and hydrogen, are the carotenes (Britton, 1995b). Examples of these carotenoids can be seen in Figure 1.10.

The polyene chain which creates the backbone of the carotenoid molecule is highly reactive and electron-rich. This property therefore makes carotenoids highly sensitive to oxidation by attack from electrophilic reagents. This can be seen when the carotenoids are stored in conditions with heat and light, the oxidative processes acting on the carotenoids will result in the bleaching of colour caused by the breaking of the chromophore.

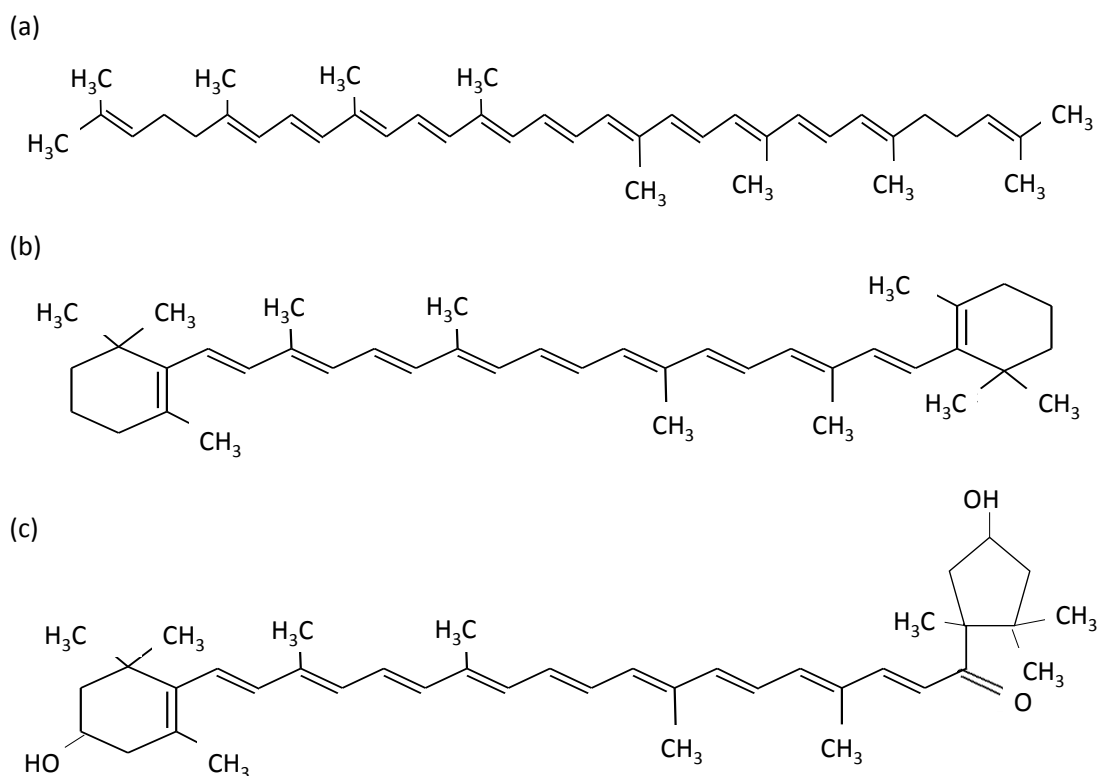


Figure 1.10. Examples of carotenoids with different end group structures.

(a) Lycopene is a linear carotene, (b) β -carotene is a cyclic carotene, and (c) capsanthin is a xanthophyll (due to oxygenation of the cyclic groups) with one cyclohexane end group (left hand side like β -carotene) and one cyclopentane end group (right hand side).

As the number of double bonds increase, then the energy of the excited state is lower. Therefore the ability of to quench singlet oxygen or other free radicals increases too (Edge et al., 1997). The functional groups at the ends of the carotenoid molecules are also thought to influence quenching abilities. It has also been proposed that carotenoids with epoxide groups increase singlet oxygen quenching. This was elucidated when β -carotene, zeaxanthin, and isozeaxanthin reaction rates were compared. Although these molecules all contained the same nine conjugated double bond system only the β -carotene and zeaxanthin had similar reaction rates, and isozeaxanthin had a much slower reaction rate therefore highlighting the significance of the change of hydroxyl group on the oxidation performance (Woodall et al., 1997b). However, it has also been shown that that lycopene has the faster reaction rate when exposed to a free radical. This was followed by β -carotene and then astaxanthin. It was proposed that lycopene could more easily undergo the addition of free radical due to its longer chromophore (Woodall et al., 1997b). Faster reaction rates are favourable in biological systems as this reduces the damage

that the free radicals can inflict within the cell. However, these experiments were carried out *in vitro* and this may not extrapolate to biological environments. This is noteworthy as the pepper fruit predominantly accumulate xanthophylls with epoxide groups and tomato fruit accumulate high levels of lycopene. Thus, these crops are important to study to enhance human health benefits (Edge et al., 1997).

1.3.2. Health and nutrition

The role of carotenoids as potent antioxidants is of prominent interest in many studies on human health. This is because many of the diseases prevalent in the western world are caused by exposure to free radicals and many diseases present in the developing world can be related to nutritional deficiencies. It has been strongly suggested that the antioxidant properties of the carotenoids can be utilised to reduce the risk of certain disease states. The human DNA receives an estimated 10,000 'oxidative hits' per cell per day. This is therefore the reason for degenerative diseases (Ames et al., 1993). The longer the lifespan of the individual, the more oxidation the DNA is exposed to and although the cell contains numerous repair mechanisms and protective compounds this can eventually lead to the accumulation of mutated genes which manifest as disease (Figure 1.11).

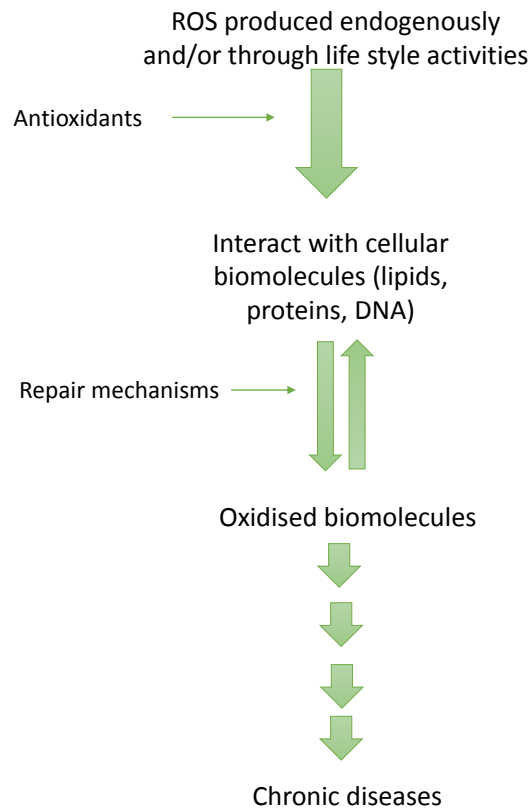


Figure 1.11. Oxidative stress, antioxidants, and chronic diseases (adapted from Rao and Rao, 2007).

Peppers are rich in beneficial phytochemicals such as vitamin E, vitamin C, and flavonoids. The carotenoids provide protection against potential disease states by lowering the amount of harmful radicals that are present in the cells.

The most established function of carotenoids in terms of human health is the provitamin A activity which is possessed by carotenoids which contain β -ring end groups. Once ingested the carotenoid molecule is cleaved by a dioxygenase to form retinal (vitamin A) (Fraser and Bramley, 2004). It is thought that β -carotene has the highest provitamin A activity. In a study looking at the β -carotene content of multiple fruit and vegetables it was found that carrots, mangos, and sweet potatoes, have the highest β -carotene content, and peppers (raw and cooked) contained double the β -carotene levels when compared to tomato paste (Krinsky and Johnson, 2005). There has been evidence to suggest that vitamin A deficiency (VAD) can be alleviated with the supplementation of carotenoids, particularly lutein and zeaxanthin. Vitamin A has an essential role in many biological processes, such as the visual system, growth and development, maintenance of epithelial cells, reproduction, and immune function (Ahmed, 1999). This causes

a range of symptoms spanning from night blindness to xerophthalmia, which could lead to total blindness (Ye et al., 2000). The fact that 124 million children worldwide are estimated to be deficient in Vitamin A, and that VAD is the leading cause of childhood blindness, led to the development of rice which accumulates β -carotene to try to improve eye health in children in many developing countries (Humphrey et al., 1992; Ye et al., 2000).

Lutein and zeaxanthin have been linked with protecting against eye diseases. These carotenoids are the only ones found in the retina of the eye at the *macula lutea* and carry out a protective role against light induced oxidation of the retina which is often the cause of macular degeneration. There has been found to be linear correlation between the intake of dietary carotenoids and the macular degeneration (Congdon and West, 1999). It has also been shown that men and women with a higher intake of lutein and zeaxanthin have decreased risk of cataract extraction by approximately 20% (Krinsky and Johnson, 2005).

An interesting property of carotenoids is their ability to inhibit the growth of tumour cells. The carotenoids lycopene and β -carotene, as well as retinal, were found to reduce growth rates in C-6 glioma cells in inoculated rats (Wang et al., 1989). β -Carotene was demonstrated to inhibit proliferation in human squamous cells, by perhaps inducing the appearance of a heat shock protein (Schwartz et al., 1990). The main source of lycopene is from tomato based products. However, lycopene is not found to accumulate in pepper fruits. In other cell lines there have been reports of carotenoids inducing apoptosis, inhibiting malignant transformation, promotion of cellular gap junctions (Krinsky and Johnson, 2005). Due to the ability of carotenoids to affect cell growth there has therefore been a lot of evidence to suggest that carotenoids are associated with reducing the risk of some cancers. Although results can be variable, studies on reducing the risk of lung and colon cancer have been the most consistent (Krinsky and Johnson, 2005). Lycopene has proven to be of particular interest as it has shown links with reducing the risk of prostate cancer (Giovannucci et al., 1995). While the precise mechanism by which lycopene exerts its effects remains elusive, there is intense research focus on oxidative metabolites of lycopene (lycopenoids) which may modulate gene expression (Erdman et al., 2009). There is evidence to suggest that supplementation with β -carotene can be harmful and act as a pro-oxidant when given to heavy smokers (Omenn et al., 1996).

The carotenoids have also been associated with reducing the risk of coronary heart disease (CHD). A causation of CHD is the oxidation of low density lipoproteins (LDLs) in the blood vessels. The uptake of these oxidised LDLs by foam cells causes vascular lesions associated with the disease. Once the carotenoids have entered the bloodstream from the gut they are transported

by these LDLs, therefore a diet rich in carotenoids can prevent the oxidation of LDLs by quenching ROS. However, there has been mixed results in studies into carotenoid intake and CHD (Krinsky and Johnson, 2005).

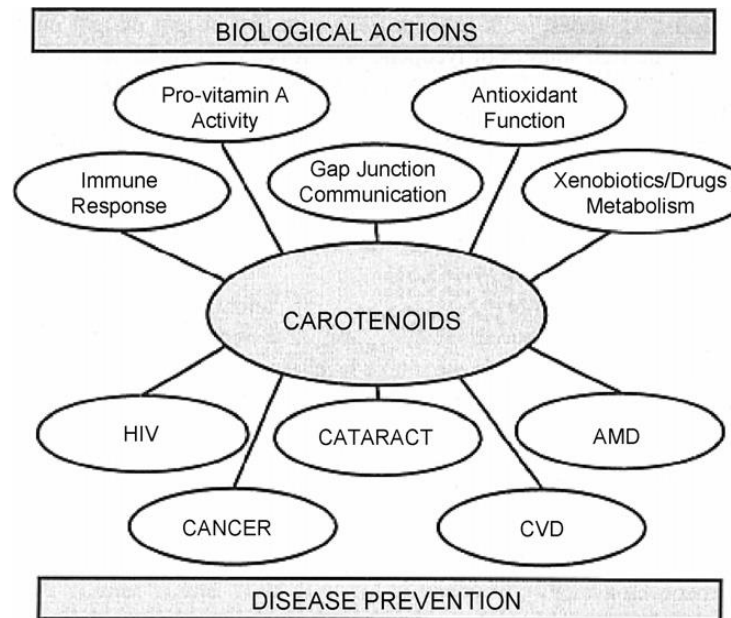


Figure 1.12. Roles of carotenoids in the prevention of chronic diseases. Abbreviations: AMD, age-related macular degeneration; CVD, cardiovascular disease (Adapted from Rao and Rao, 2007).

The lowering of risk of other diseases such as HIV, hypertension, osteoporosis, infertility in men, and possibly Alzheimer's has been linked to a high dietary intake of carotenoids also (Rao and Rao, 2007). A diagram adapted from Rao and Rao illustrates the connection between the properties of carotenoids and their connection to disease (Figure 1.12).

1.3.3. Biosynthesis

1.3.3.1. MEP pathway

The isoprenoids, also known as terpenoids, are composed of C₅ isoprene units called isopentenyl diphosphate (IPP). This group of compounds is one of the most diverse families of natural products with around 20000-35000 members (Cordoba et al., 2009). The compounds

synthesised are classified as hemi- (C_5), mono- (C_{10}), sesqui- (C_{15}), di- (C_{20}), tri- (C_{30}), and tetraterpenes (C_{40}) (Lichtenthaler et al., 1997). The carotenoids are synthesised from eight isoprene units (C_{40}) which are supplied by the deoxy-D-xylulose 5-phosphate/ 2-C-methyl-D-erythritol 4-phosphate (DOXP/ MEP) pathway. IPP can be synthesised from two separate pathways present in plants. The mevalonate pathway was originally thought to be the precursor to all isoprenoids but studies using radio labelled precursors of this pathway revealed that there was a mevalonate independent pathway in bacteria (Rohmer et al., 1993), green algae (Schwender et al., 1996), and higher plants (Lichtenthaler et al., 1997). This pathway gives rise to many other isoprenoids (Figure 1.13). These include photosynthesis related compounds such as chlorophylls and plastoquinones, in addition to sterols, gibberellic acid, abscisic acid, brassinosterols, cytokinins, and dolichols (Wanke et al., 2001). The cytoplasmic isoprenoids are mainly the sterols, the plastidic isoprenoids are the carotenoids, chlorophylls and plastoquinones, and the mitochondrial are the ubiquinones.

The MEP pathway consists of eight reactions catalysed by nine enzymes. The first step in the pathway is the condensation of pyruvate and glyceraldehyde 3-phosphate (GAP). This proceeds via the thiamine dependent transketolase type reaction whereby the C_2 unit (from pyruvate) is condensed with the C_1 aldehyde group of GAP (Fraser and Bramley, 2004). Thiamine pyrophosphate (TPP) is required as a cofactor (Hunter, 2007). The resulting compound is 1-deoxy-D-xylulose 5-phosphate (DXP) and the reaction is catalysed by the enzyme DXP synthase (DXS). DXS was the first gene to be identified from the MEP pathway. The substrate DXP is also used in the synthesis of thiamine and pyridoxal. Characterisation of the DXS gene was achieved by knockout studies in *Arabidopsis* known as *DXS/CLA1* giving rise to the albino phenotype. The expression of DXS is required for proper chloroplast development (Estévez et al., 2000).

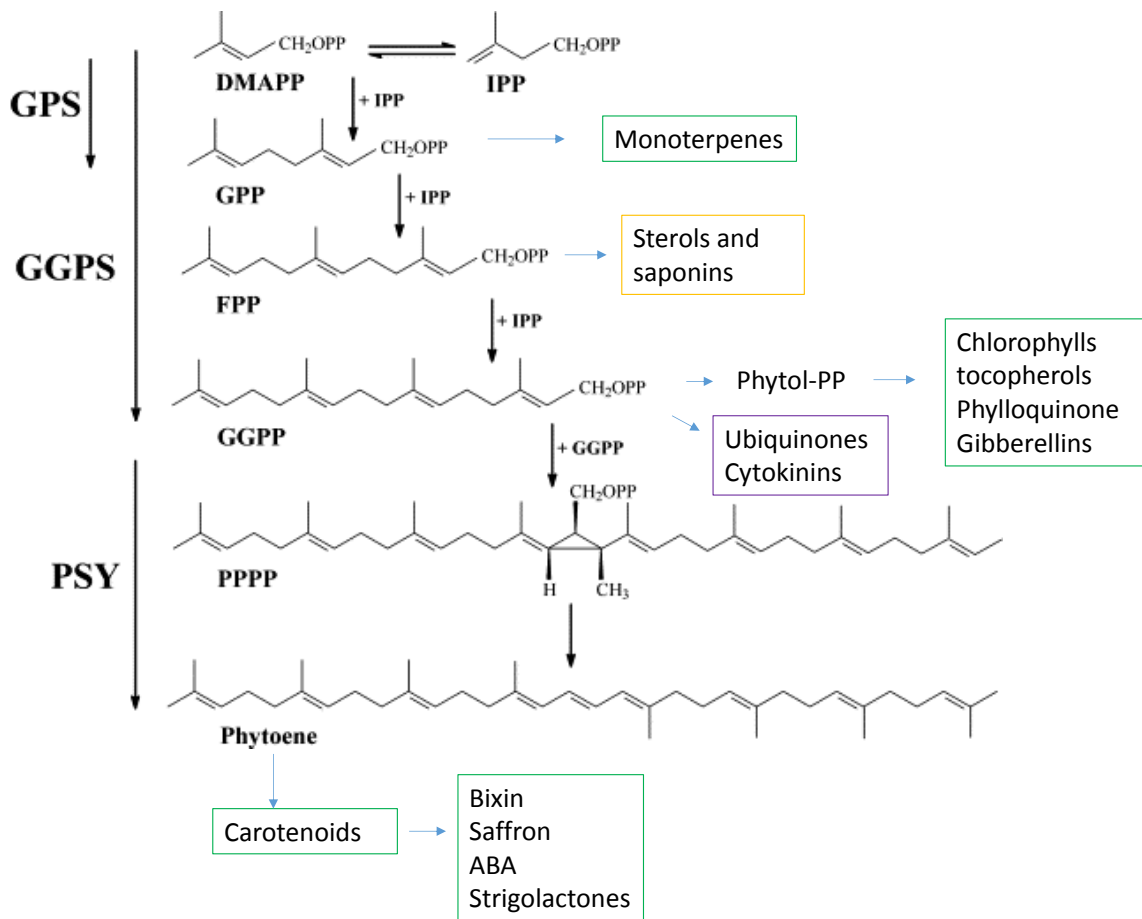


Figure 1.13. Isoprenoid biosynthesis in plants.

An overview of the isoprenoid biosynthesis pathway and the potential end products associated. The sterols and saponins are generally synthesised from substrates from the mevalonate pathway in the cytoplasm (yellow box) and ubiquinones are synthesised in the mitochondria (purple box). The remaining products are generally synthesised from the MEP pathway in the plastids (green box). Abbreviations: DMAPP, dimethylallyl diphosphate; GPP, geranylpyrophosphate; GPS, geranylpyrophosphate synthase; GGPS, geranylgeranylpyrophosphate synthase; FPP, farnesylpyrophosphate; PPPP, prephytoenepyrophosphate; PSY, phytoene synthase; ABA, abscisic acid (adapted from Fraser and Bramley, 2004).

The next enzyme in the pathway catalyses the formation of MEP from DXP via the action of DXP reductoisomerase (DXR) whereby DXP undergoes a rearrangement and reduction reaction. NADPH and Mn^{+2} are cofactors which are required for the reaction to take place (Hunter, 2007).

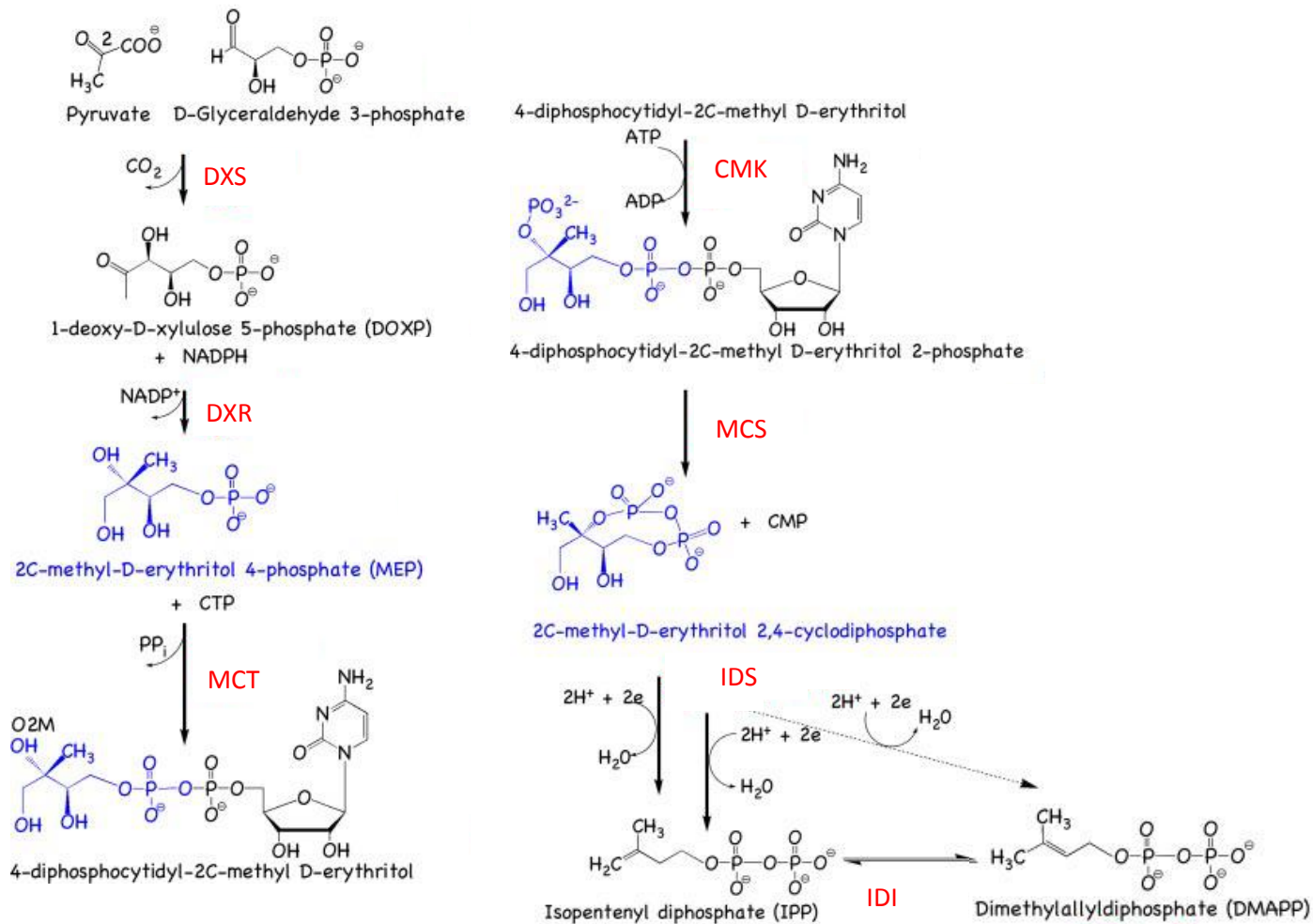


Figure 1.14. The MEP pathway.

Reactions of the MEP pathway. Abbreviations: DXS, 1-deoxy-D-xylulose 5-phosphate; DXR, DOXP reductoisomerase; MCT 4-diphosphocytidyl-2C-erythritol cytidyltransferase; CMK, 4-diphosphocytidyl-2C-methyl-D-erythritol kinase; MCS, 2C-methyl-D-erythritol-2,4-cyclodiphosphate synthase; IDS, IPP/DMAPP synthase; IDI, IPP isomerase (adapted from Hunter, 2007).

The divalent cation binds first to orient the substrate allowing the following rearrangement reaction can be carried out. The methylerythrose intermediate formed from the rearrangement is then reduced by hydride (Hunter, 2007).

MEP reacts with the nucleotide cytidine triphosphate (CTP) to form the compound 4-diphosphocytidyl-2C-methyl-D-erythritol (CDP-ME) by the action of 4-diphosphocytidyl-2C-erythritol cytidyltransferase (MCT) and the release of pyrophosphate. The MEP phosphate carries out a nucleophilic attack on the α -phosphate of the CTP (Hunter, 2007). The next stage of the pathway involves a CDP-ME kinase (CMK) which catalyses the transfer of the γ -phosphoryl moiety of ATP to CDP-ME. The resulting structure is known as 4-diphosphocytidyl-2C-erythritol-2-phosphate (CDP-ME2P) and ADP is released. The binding of the cofactor results in the γ -phosphoryl moiety of ATP undergoing nucleophilic attack from the polarised (O₂M) hydroxyl group (Miallau et al., 2003).

The CDP-ME2P is then transformed into 2C-methyl-D-erythritol-2,4-cyclodiphosphate (MECP) and AMP via the action of 2C-methyl-D-erythritol-2,4-cyclodiphosphate synthase (MCS). The MCS enzyme uses two divalent cations, Zn⁺² and Mn⁺², the reaction is thought to be carried out with the nucleophilic attack by the terminal phosphate moiety on CDP-ME2P on the β -phosphate.

In the last stages of the MEP pathway MECP undergoes reduction and elimination to form 1-hydroxy-2-methyl-2-(E)-butenyl-4-phosphate (HMBP) by HMBP synthase (HDS) and then 4-hydroxy-3-methyl-2-(E)-butenyl-4-diphosphate (HMBPP) catalysed by HMBPP reductase (HDR). HMBPP finally goes on to create IPP and dimethylallyl diphosphate (DMAPP) which is catalysed by the enzyme IPP/DMAPP synthase (IDS). These compounds are created in a 5:1 ratio (Fraser and Bramley, 2004; Hunter, 2007).

The IPP isomerase (IDI) is responsible for the conversion of IPP into DMAPP. IPP and DMAPP undergo a head to tail condensation to create a C₁₀ molecule geranyl diphosphate (GPP) catalysed by GPP synthase (GPS), another IPP is added to form a C₁₅ molecule farnesyl diphosphate (FPP) and then a final IPP is added to form geranylgeranyl diphosphate (GGPP) catalysed by GGPP synthase (GGPS). GGPP is the direct substrate to the carotenoid biosynthesis pathway. The FPP molecule is a precursor to the biosynthesis of sterols and saponins and the GGPP molecule goes on to form phytyl-PP which is the precursor to chlorophylls, tocopherols, tocotrienols, and phyloquinones (Figure 1.13) (Lichtenthaler et al., 1997). The IPI and GGPS were both found to be located in the chromoplast stroma in chilli pepper, and were found to be associated together along with PSY1 enzyme (Gómez-García and Ochoa-Alejo, 2013).

Many of the enzymes present in the MEP pathway are encoded by small gene families. Multiple *DXS* genes have been found in many higher plants such as Arabidopsis, maize, and rice. In most of these plants the *DXS* genes tended to cluster into independent clades suggesting these genes have specific functions which have been maintained through evolution (Cordoba et al., 2009). Type-1 *DXS* accumulates at high levels in photosynthetic tissues, type-2 *DXS* is involved in the accumulation of isoprenoid secondary metabolites such as carotenoids and type-3 *DXS* has a role which is yet to be elucidated (Cordoba et al., 2009). In tomato, there was a single *DXS* gene which was targeted to the plastid. However, in pepper there were two *DXS*-like genes identified, but only one had an involvement in the MEP pathway (*CapTKT2*) and the other was involved in the pentose pathway and glycolysis (Bouvier et al., 1998b). The *GGPS* gene has one copy in the pepper on chromosome 4 and tomato has two copies on chromosome 4 (Thorup et al., 2000; Ament et al., 2006).

1.3.3.2. Carotenoid biosynthesis pathway

The carotenoid biosynthesis pathway commences with the condensation of two GGPP molecules to form phytoene and the first enzyme in the pathway is phytoene synthase (PSY) (Figure 1.14). Phytoene is formed as a 15-*cis* isomer and is then converted to all-*trans* isomer derivatives (Dellapenna and Pogson, 2006). The pepper PSY requires a Mn^{+2} cofactor but the tomato PSY enzymes require ATP and a divalent cation to function, which could be Mn^{+2} or Mg^{+2} . In pepper, PSY is found to be associated with chloroplastic membranes but not integral and this is consistent with the results found in tomato too (Dogbo et al., 1988; Fraser et al., 1994, 2000). It has been suggested that there are at least two homologs of the *PSY* gene in the pepper genome, similar to tomato. However, only one has been characterised.

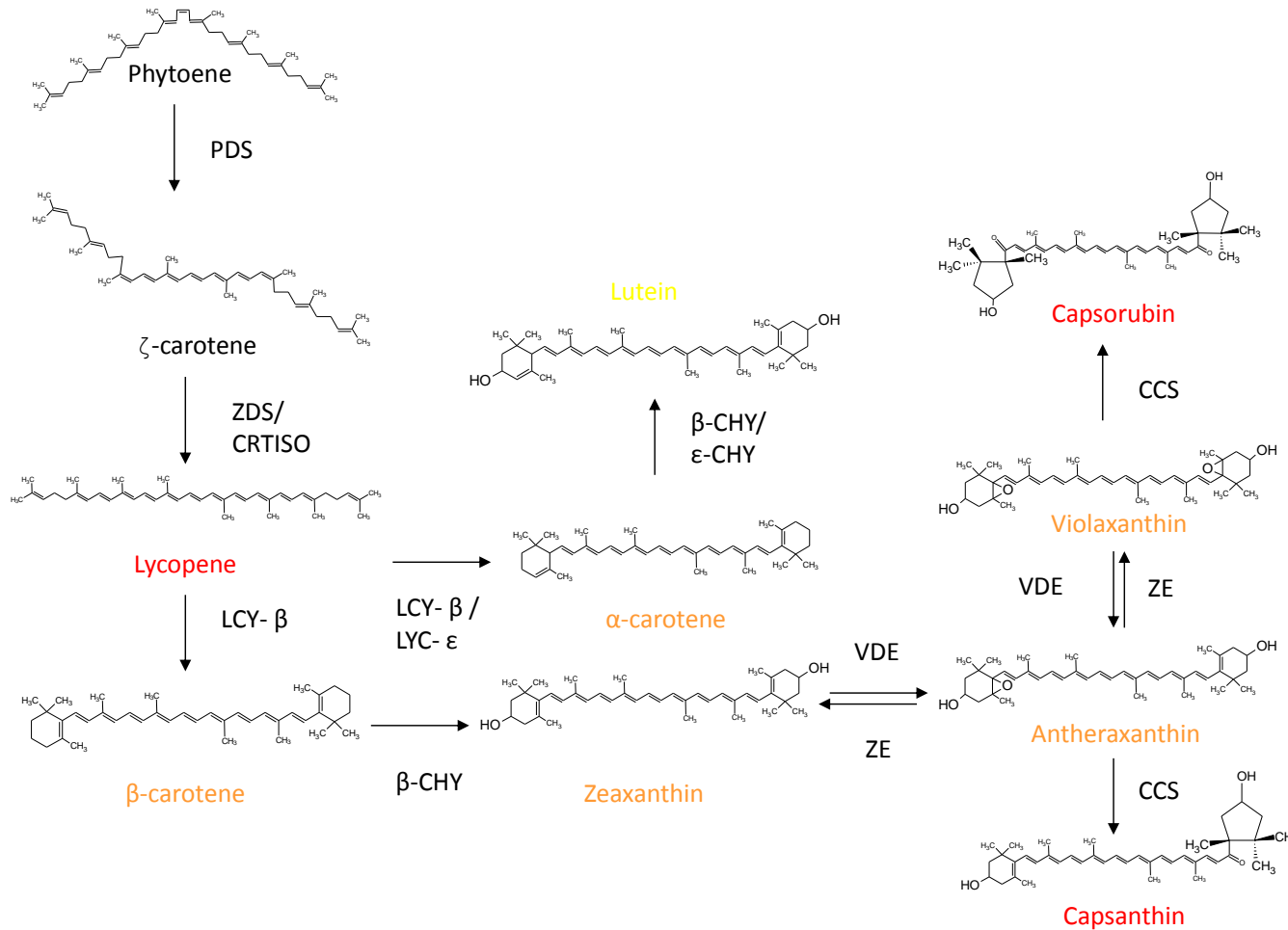


Figure 1.15. The carotenoid biosynthesis pathway in pepper.

Abbreviations: PDS, phytoene desaturase; ZDS, ζ-carotene desaturase; CRTISO, carotenoid isomerase; LCY-β, lycopene β-cyclase; LCY-ε, lycopene ε-cyclase; β-CHY, β-carotene hydroxylase; ε-CHY, ε-carotene hydroxylase; ZE, zeaxanthin epoxidase; VDE, violaxanthin de-epoxidase; CCS, capsanthin capsorubin synthase.

The pepper *PSY* was located on chromosome 4 whereas the tomato *PSY* homologs are found on chromosomes 2 and 3 (Thorup et al., 2000).

Desaturation and isomerisation

Phytoene then undergoes a series of desaturation reactions in order to introduce the conjugated double bond system. This produces phytofluene, ζ -carotene, neurosporene, and lycopene; thus, resulting in a red coloured compound based on the extension of the chromophore. The desaturation reactions are catalysed by phytoene desaturase (PDS) and ζ -carotene desaturase (ZDS). The PDS enzyme catalysed the first two desaturation reactions and is suspected to be a bifunctional flavoprotein. This enzyme has phytoene and phytofluene desaturation activity, binds FAD and is membrane bound. The *PDS* gene has a single copy in the pepper and tomato genomes and is located on chromosome 3 (Thorup et al., 2000). Desaturation of phytoene is carried out by the removal of two hydrogen atoms during each saturation step, PDS therefore requires plastid terminal oxidase (PTOX) and plastoquinone to regenerate reductants (Dellapenna and Pogson, 2006). Mutants with a deficient PTOX do not accumulate carotenoids and accumulate phytoene (Gómez-García and Ochoa-Alejo, 2013). The ZDS enzyme catalyses the formation of neurosporene and lycopene. This gene has been identified in numerous plants including pepper and tomato (Albrecht et al., 1995; Bartley et al., 1999). It appears to be a single copy gene on chromosome 1 for both plants (Thorup et al., 2000).

The desaturation reactions resulted in the formation of all-*trans* lycopene from 15-*cis* phytoene, but there are also isomerisation reactions occurring within the sequence. This was supported by the discovery of prolycopene which accumulates in the tomato *tangerine* mutant. This mutant was found to have a mutation in the carotenoid isomerase (*CRTISO*) gene. This enzyme appears to enable isomerisation of lycopene in dark and in non-photosynthetic tissues. In photosynthetic tissues photoisomerisation can occur substituting for a mutant *CRTISO*. Interestingly, in bacteria only one enzyme is needed for the desaturation and isomerisation reactions present from phytoene to lycopene. This is known as CRTI. The presence of two desaturation enzymes in plants suggests a gene duplication event resulting in a specialised reaction perhaps a method of optimising the efficiency of the production of lycopene (Albrecht et al., 1995).

Cyclisation

After the synthesis of lycopene the carotenoid pathway branches in two and the cyclisation of the ends of the molecule is achieved via the formation of a six-membered ring. The first branch, known as the beta branch, is characterised by the formation of two β -rings and thus β -carotene is formed from lycopene. The second branch, known as the alpha branch, is characterised by the formation of α -carotene which consists of one β -ring and one ϵ -ring. The β - and ϵ -rings are catalysed by the lycopene β -cyclase (LCY- β) and lycopene ϵ -cyclase (LCY- ϵ), respectively. The difference between the end rings formed is due to the position of the double bond within the ring structure. Lycopene cyclisation occurs via a carbonium ion intermediate whereby the C2 and C2' undergo proton attack. The intermediate formed is then stabilised by loss of a proton at the C1 or C4 position giving rise to a β -ring and an ϵ -ring, respectively with the assistance of an unbound FAD, and NADPH (Beyer et al., 1991; Sandmann, 1994). The expression profiles of the two pathways mentioned above suggests they are differentially regulated when the chloroplast transitions into a chromoplast. This development sees a shift from expressing alpha branch biosynthetic genes to the beta branch biosynthetic genes. The LCY- ϵ enzyme catalyses the conversion of lycopene into α -carotene and lutein. This gene is found as a single copy in both the pepper and tomato genomes and is located in chromosome 9 and 12, respectively (Thorup et al., 2000).

The LCY- β was found to operate in chromoplast membranes in pepper and so far there has been only one isoform identified (Camara et al., 1982). In tomato, there are two LCY- β isoforms which are tissue specific. One isoform is present in the green tissue, like other plants, and one which is specific to the chromoplast (*CYC-b*). This has been found to be expressed in fruits and flowers. One of the *LCY- β* genes in tomato maps to chromosome 10 which is analogous to the pepper *LCY- β* . Although the position has not yet been detected it is also assumed that there is a second *LCY- β* in pepper (Thorup et al., 2000).

At the onset of ripening the *LCY- β* gene in pepper does not become induced like other carotenoid biosynthetic genes such as *PSY1* and *CCS* (Huguency et al., 1995). However, in tomato the *CYC-b* gene becomes down-regulated at the onset of ripening to allow the accumulation of lycopene.

The *LCY- β* gene in pepper was found to share more sequence similarity with cyanobacteria as opposed to non-photosynthetic bacteria. This same gene also shares 55% identity with the capsanthin capsorubin synthase (*CCS*), which also possesses lycopene β -cyclase activity. This sequence homology is likely to be due to the similarities in the type of reactions these enzymes catalyse leading to the formation of β -rings present in β -carotene and the κ -rings present

capsanthin and capsorubin (Hugueney et al., 1995). It is evident that the CCS enzyme does not act as the sole cyclase enzyme as there are examples of CCS mutants which do not produce capsanthin or capsorubin but still retain their lycopene β -cyclase activity. The sequence similarity between these two genes therefore suggests that perhaps they originated from the same ancestral gene. Most likely a gene duplication of lycopene β -cyclase took place and further mutations led to the formation of the CCS gene (Hugueney et al., 1995). Interestingly, in tomato although the two *LCY- β* genes only shared around 53% identity to each other the chromoplast specific isoform is 86% identical to the pepper *CCS* gene. Therefore, the gene duplication probably took place before the divergence of *Capsicum* from *Lycopersicon* (Ronen et al., 2000).

Xanthophyll formation

After the cyclisation reactions have taken place oxygenation of the end groups occurs to give rise to the formation of the xanthophylls. The oxygenation of α - and β -carotene occurs via addition of a hydroxyl molecule at the C3 and C3' positions which led to the creation of α - and β -cryptoxanthin, respectively. These two compounds then go on to form lutein and zeaxanthin, respectively. These reactions are catalysed by the carotene hydroxylases. The β -ring hydroxylases are ferredoxin dependent, nonheme dioxygenases that require iron. The ϵ -ring hydroxylase is a member of the cytochrome P450- type monooxygenases (Dellapenna and Pogson, 2006). Mechanistically activated molecular oxygen is used to break the carbon-hydrogen bond resulting in the retention of a hydroxyl group (Bouvier et al., 1998c). There is thought to be two copies of the β -carotene hydroxylase in pepper and tomato which map to chromosomes 3 and 6, respectively (Thorup et al., 2000).

Once zeaxanthin has been formed a 5,6-epoxy group is added to the β -rings. The addition of one epoxy group gives rise to antheraxanthin and the addition of two epoxy groups forms violaxanthin. These reactions are catalysed by the zeaxanthin epoxidase (ZEP) and are collectively known as the xanthophyll cycle as mentioned previously (1.3.1.1) (Hugueney et al., 1996). Therefore, the formation of violaxanthin from zeaxanthin is a reversible reaction and the formation of zeaxanthin from violaxanthin is catalysed by violaxanthin de-epoxidase (VDE). ZEP showed the presence of FAD binding domain as well as requiring NADPH for activity (Gómez-García and Ochoa-Alejo, 2013).

Finally, the last step in the carotenoid biosynthesis pathway which is typical of most other higher plants, including tomato, is the conversion of violaxanthin into neoxanthin by the action of the

neoxanthin synthase (NSY). This enzyme carries out a similar reaction as the LCY- β and CCS enzymes whereby a transient carbocation is formed during the opening of the 5,6-epoxides suggesting a strong phylogenetic relationship (Bouvier et al., 2000). NSY carries out a ring opening reaction and stabilises the carbocation intermediate followed by a molecular rearrangement. The mechanism proposed is that the C6 oxygen of the cyclohexenyl ring is attacked by a proton from the active site of the NSY enzyme (Bouvier et al., 2000).

Capsicum has a unique step after the synthesis of violaxanthin and antheraxanthin which results in the formation of red pigments, capsorubin and capsanthin, respectively. These compounds contain an unusual cyclopentane ring or κ -ring. This step is unique to the *Capsicum* genus in terms of the *Solanaceae* family but has been identified in other organisms such as tiger lily and asparagus (Jeknić et al., 2012; Simpson et al., 1977). The bi-functional CCS enzyme was found to have activity in the membrane fractions of the chromoplast with less than 2% associated with the fibrils (Bouvier et al., 1994). It has been suggested that the mechanism of this enzyme is that C5 oxygen of the cyclohexenyl ring is attacked by an exchangeable proton from the active site (Bouvier et al., 2000). It is noted that although the CCS enzyme is capable of synthesising both capsanthin and capsorubin, the CCS gene is found to have a single copy in the pepper genome which maps to chromosome 6. Interestingly, this position corresponds to the chromoplast specific *CYC- β* , or *B* gene in tomato further supporting an evolutionary ancestor (Thorup et al., 2000).

Neoxanthin can be converted to xanthoxin by 9-*cis*-epoxycarotenoid dioxygenase (NCED) and then subsequently abscisic acid (ABA) by aldehyde oxidase (AO) (Gómez-García and Ochoa-Alejo, 2013).

Esterification

Xanthophylls which are produced in excess are esterified to allow more efficient storage within the plastoglobuli. They can either be mono- or diesterified depending on whether one or two fatty acids are added to the oxygen-containing moieties present on the cyclic end groups. The fatty acids for esterification in pepper are C12:0, C14:0, and C16:0 (Schweiggert et al., 2005).

1.3.4. Genetics

The inheritance of mature fruit colour in pepper has been proposed in a study with Hurtado-Hernandez and Smith (1985). In this study a white and a deep red pepper were crossed and the colour of the mature fruit of pepper was to be attributed by the interaction of three independent pairs of genes now known as *y*, *c1*, and *c2*. The F₂ population identified eight phenotypes from the cross which included: red, light red, orange, orange-yellow, pale orange, pale orange-yellow, lemon yellow, and ivory or white. The red colour of ripe fruit is dominant over orange-yellow fruit, and orange-yellow is dominant over the yellow and white fruit. The gene pairs attributing to fruit colour are summarised in Table 1.1. The *y* locus has been identified as being the *CCS* gene (Lefebvre et al., 1998; Popovsky and Paran, 2000) and the *c2* locus has been identified as the *PSY* gene (Thorup et al., 2000; Huh et al., 2001). The *c1* locus has yet to be identified. These different pepper varieties therefore offer a good opportunity to study the regulation of the carotenoid biosynthesis.

Tomato also has natural occurring variants which result in the alteration of carotenoid composition and fruit colour. The genes involved in the manifestation of red, orange, yellow and white fruit are discussed below. Examples of the natural colour mutant in pepper and tomato are displayed in Figure 1.16.

Table 1.1.1. Genetic determination of ripe fruit colour of pepper.

(adapted from Hurtado-Hernandez and Smith, 1985).

Genotype	Fruit colour
<i>y+</i> , <i>c1+</i> , <i>c2+</i>	Red
<i>y+</i> , <i>c1</i> , <i>c2+</i>	Light red
<i>y+</i> , <i>c1+</i> , <i>c2</i>	Orange
<i>y+</i> , <i>c1</i> , <i>c2</i>	Pale orange
<i>y</i> , <i>c1+</i> , <i>c2+</i>	Orange-yellow
<i>y</i> , <i>c1+</i> , <i>c2</i>	Pale orange-yellow
<i>y</i> , <i>c1</i> , <i>c2+</i>	Lemon-yellow
<i>y</i> , <i>c1</i> , <i>c2</i>	White

1.3.4.1. Red Fruit

Pepper

Based on the three independent gene pairs identified by Hurtado-Hernandez and Smith the red fruit of pepper is carrying the dominant *y*, *c1*, and *c2* alleles. Therefore the *PSY1*, *CCS*, and the unknown *c1* gene must be present and functional for the red fruit colour to occur.

Tomato

The red colour of wild-type tomato is due to the accumulation of lycopene which accounts for about 90% of total carotenoid content. The remaining carotenoids β -carotene, lutein, and phytoene are accumulated in small amounts. The red fruited *old gold* mutant lacks β -carotene. This mutation also manifests in the flowers which accumulate lycopene and is caused by a lack of function mutation in the lycopene β -cyclase gene (Ronen et al., 2000).

There are a number of high pigment (*hp*) mutants present in tomato which give rise to a deep red phenotype. The high pigment phenotype is caused by a number of mutations in genes including the UV damaged DNA binding protein 1 (*DDB1*), de-etiolated 1 (*DET1*) and *ZEP* (Lieberman et al., 2004; Mustilli, 1999; Galpaz et al., 2008).

1.3.4.2. Yellow fruit

Pepper

The *CCS* gene was discovered to be deleted in some yellow fruited varieties (Lefebvre et al., 1998). In addition to this some yellow varieties have been found to possess a *CCS* gene, but they were found to have a frame-shift mutation resulting in early translation termination or single base-pair mutation resulting in an early stop codon. Accumulation of α -ring carotenoids such as α -carotene and lutein are a common feature of yellow fruited peppers and carotenoid content does not increase during ripening (Popovsky and Paran, 2000; Ha et al., 2007a).

Tomato

The *rr* mutant in tomato which has pale yellow fruit flesh is similar to the orange fruit phenotype described in Huh et al (2001). The lack of carotenoids present in the ripe fruit is caused by an aberrant transcript with no PSY1 activity (Fray and Grierson, 1993). The resulting yellow fruit phenotype is therefore caused by a low total carotenoid content.

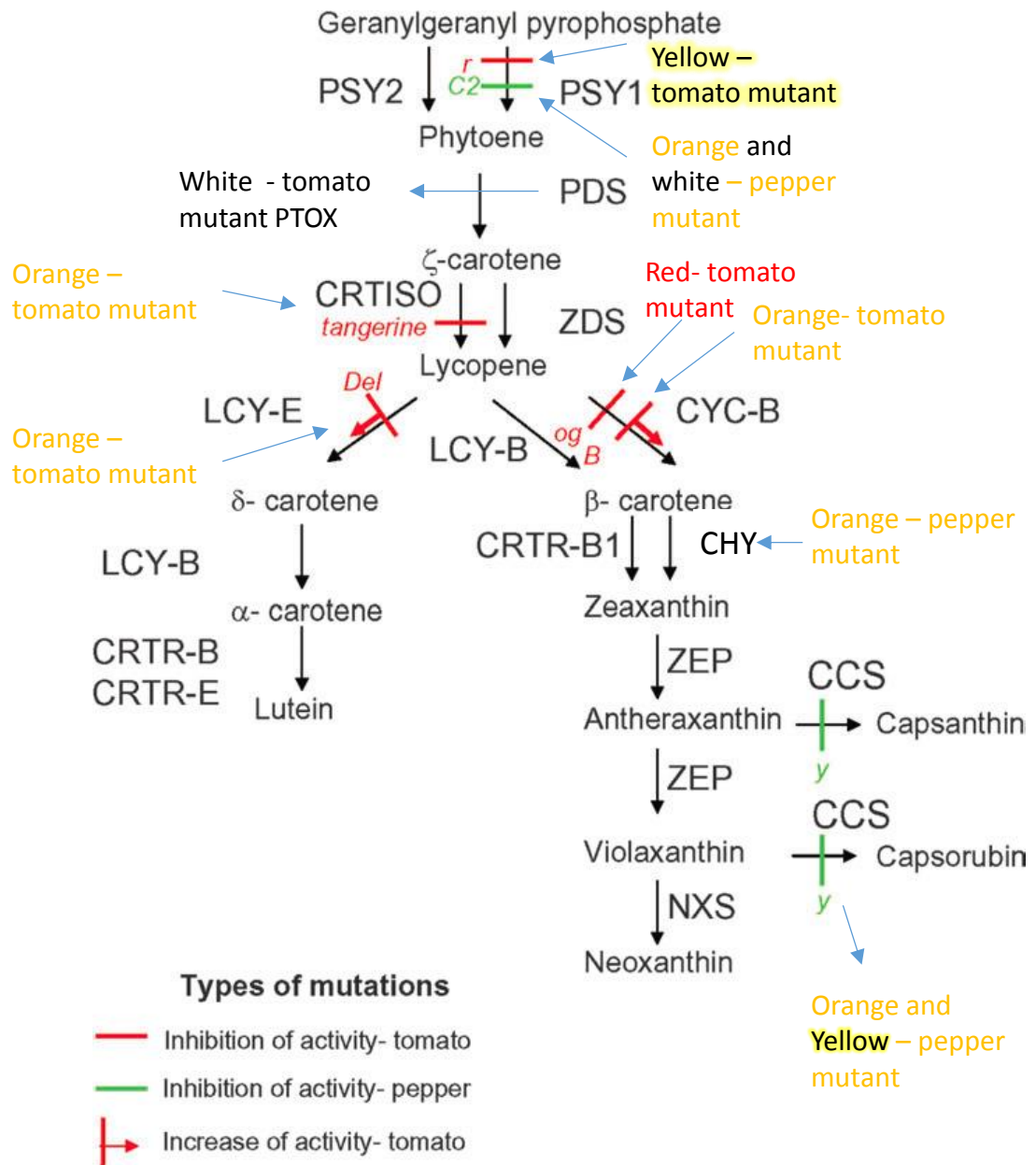


Figure 1.16. Comparison of natural colour mutants in tomato and pepper.

The carotenoid biosynthesis pathway in pepper and tomato was annotated to identify which genes were down/ up-regulated in order manifest a change in fruit colour. The colour of the

mutant is also annotated. Abbreviations: B, Beta; Del, Delta (Adapted from Paran and Van Der Knaap, 2007).

1.3.4.3. Orange fruit

Pepper

Orange fruited pepper can arise from many different carotenoid biosynthetic gene mutations. This can result in lowered gene expression creating lower levels of total carotenoids formed or result in complete loss of expression of the gene causing a block in the biosynthesis pathway. Accumulation of α -carotenoids has been seen in orange varieties like that seen in yellow fruit (Ha et al., 2007a). Borovsky et al (2013) showed that the orange fruit phenotype could be caused by a mutation in the β -carotene hydroxylase (*CHY2*) gene. This results in a decrease in the overall total carotenoid content, in addition to causing a block in the pathway that leads to the accumulation of β -carotene. Orange can also arise from accumulating very low levels of carotenoids occurring based on impaired catalytic activity from the PSY enzyme. In these fruit capsanthin is detected at very low levels. This study found that aberrant *PSY* transcripts were produced by abnormal splicing events thus causing the low PSY activity resulting in low levels of substrate supplied into the carotenoid pathway (Huh et al., 2001). Finally, orange mutations can occur by the deletion of an upstream region of the *CCS* gene resulting in no transcript levels being detectable, similar to the yellow varieties (Lang et al., 2004).

Tomato

As seen in pepper there are also many circumstances which can lead to the orange colouration of tomato fruit. The orange fruited *Beta* mutant in tomato is a result of the accumulation of β -carotene, at around 45% total carotenoid content. However, this phenotype is caused by the high expression of the lycopene β -cyclase gene. This gene is usually down-regulated at the onset of ripening in red tomatoes facilitating the accumulation of lycopene the red pigment by restricting its conversion to β -carotene. In the *Beta* mutant β -carotene accumulates at the expense of lycopene (Ronen et al., 2000).

Another naturally occurring orange tomato led to the discovery of CRTISO from *tangerine* as mentioned earlier. This results in the accumulation of the polycopene resulting in orange fruit (Isaacson et al., 2002).

Orange tomatoes can also arise by an increase in *LCY-ε* expression during ripening. In wild-type red tomatoes this gene normally undergoes down-regulation at breaker stage but this *Delta* mutant showed increased *LCY-ε* transcripts levels resulting in the accumulation of δ -carotene at the expense of lycopene (Ronen et al., 1999).

1.3.4.4. Non-pigmented fruit

Pepper

In pepper, white fruit is a result of complete lack of carotenoids including phytoene. This variety has no expression of *PSY*, *PDS*, *CHY* or *CCS* (Ha et al., 2007a). This is a result from containing recessive alleles for all colour trait loci (*y*, *c1* and *c2*).

Tomato

The *ghost* tomato mutant which has white fruit accumulates phytoene instead of any coloured carotenoids, this is a result of non-functional *PTOX* gene. This enzyme is required in the desaturation of phytoene and acts as a terminal oxidase in the plastid. Carotenoid biosynthesis past this point cannot occur with a non-functional *PTOX* (Josse et al., 2000).

1.3.5. Regulation of carotenoid biosynthesis

The biosynthesis and accumulation of carotenoids during fruit ripening is concurrent with the differentiation of chloroplasts to chromoplasts. During this transition the thylakoid membranes become disorganised and an achlorophyll lamellae system forms. Complex regulatory mechanisms act in this process. Besides fruit development there are many other processes which can also modulate carotenoid biosynthesis such as stress and light. There have been multiple levels of regulation identified in the past which shall be explained below and are summarised in Figure 1.17.

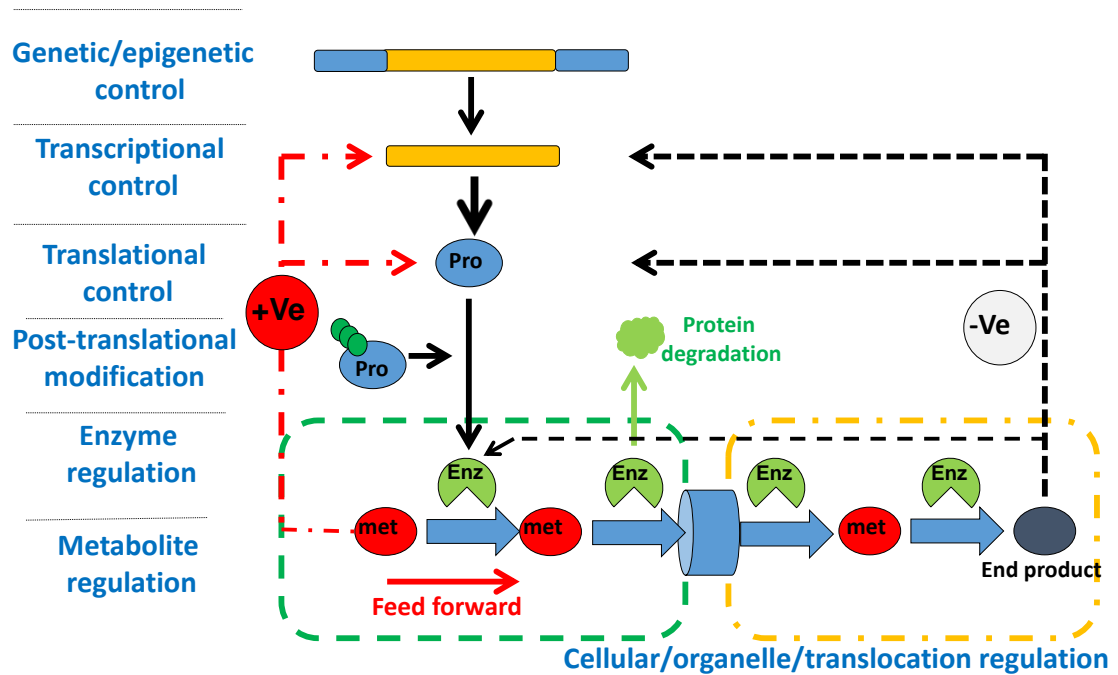


Figure 1.17. Different mechanisms associated with the regulation of biochemical pathways.

Key: Pro, protein; Enz, enzyme; Met, metabolite (Paul Fraser, personal communication).

1.3.5.1. Transcriptional regulation

The regulation of the carotenoid biosynthesis pathway is controlled predominantly by transcriptional means. Pepper and tomato fruit experience temporal and developmental regulation during fruit ripening when the beta branch is up-regulated and the alpha branch is effectively down-regulated. This is obtained by an induction in gene expression for many genes in the pathway including *PSY1*, *PDS*, *CHY*, and *CCS* during ripening. There is evidence to suggest that expression levels of key carotenoid biosynthetic genes are regulators of the pathway. The *PSY* gene in pepper has been proposed to have a key role in carotenoid accumulation by featuring as a rate limiting step in the pathway (Huh et al., 2001). This is also found to be the case in tomato (Fraser et al., 2002). Flux control coefficients are a means of calculating the contribution of an individual enzyme(s) to the overall pathway flux through a pathway (Stitt and Sonnewald, 1995). To date tomato represents the only example where flux control coefficients have been calculated. This study found that *PSY1* had the greatest influence on carotenoid biosynthesis (Fraser et al., 2002). These data showed a similar trend to that obtained from transcript analysis, which proposed the steps in the pathway with the greatest influence over the pathways flux. It is also true that with the advent of systems biology pathway and global

correlation between transcripts are informative in inferring the regulatory control points; however, as shown in Figure 1.17 there are multiple levels of cellular regulation and to fully decipher the underlying regulatory mechanisms detailed analysis is required. The *DXS* gene has also been considered as a rate limiting step in isoprenoid biosynthesis (Lois et al., 2000). The expression pattern and activities throughout ripening were analysed in pepper and tomato fruit and it was found that the expression pattern was in agreement with the enzyme activity, whereby when the expression of the *PSY* gene was up-regulated there were increases in enzyme activities at this stage (Romer et al, 1993). However, although this is true for *PSY* it should not automatically be assumed that all enzyme activities mirror gene expression. It is also thought that the pepper *PSY* is not induced as strongly as the tomato *PSY1*. This could be a result of the tomato *PSY* being directly regulated by ethylene whereas pepper is not (Romer et al, 1993).

In addition to transcriptional up-regulation during the ripening process, carotenoid biosynthesis genes can be up-regulated in response to oxidative stress and light (Bouvier et al., 1998a). The induction of carotenoid genes has been studied extensively using carotenoid biosynthesis inhibitors.

When pepper discs were incubated with the metflurozon, an inhibitor of *PDS*, the *GGPS*, *PSY*, *PDS*, and *LCY-β* genes were found to have increased transcript levels. There was also found to be an increase in *ZEP* and *CCS* transcript levels (Bouvier et al., 1998a), therefore, showing the blocking of carotenoid biosynthesis stimulates carotenoid biosynthetic gene expression both prior to and after the point of inhibition. This phenomenon could be described in two ways. Firstly, the lack of end products in the carotenoid biosynthesis pathway could feed back to up-regulate necessary genes or secondly, the loss of carotenoids could result in the production of high levels of ROS which then signal to increase gene expression. It is entirely possible that both these mechanisms can regulate carotenoid biosynthesis. In the same study the authors showed that incubating pepper discs with the hydroperoxides induced *GGPS* and *CCS* transcript accumulation (Bouvier et al., 1998a). Similarly, it has been shown that inhibition of catalase activity with amitrole can result in lycopene accumulation in wheat, maize, barley, and radish seedlings (Bouvier et al., 1998a). This is because the inhibition of catalase results in ROS formation which then induces carotenoid biosynthesis. This was further supported by studies carried out using the *CCS* gene promoter fused to a reporter gene. Expression of the reporter gene was induced by ROS (Bouvier et al., 1998a). This study therefore illustrates the regulation of the carotenoid biosynthesis genes modulated in response to oxidative stress, perhaps by ROS signalling. Mechanical injury was also found to induce *GGPS* and *PSY* transcript levels (Huguency

et al., 1996). These results are also seen in tomato when cupric ions induced the formation of hydroxyl radicals stimulating lycopene synthesis (Rushing and Huber, 1985).

The response of carotenoid genes to light was studied in pepper leaves. When pepper leaves were treated with just norflurazon in the dark there was no accumulation of phytoene present. This herbicide inhibits PDS. The transcript levels of *PSY* were increased when subjecting the plant to light. When the leaves are in dark conditions the risk of photo-oxidation is not an issue and so the carotenoid biosynthesis genes such *PSY*, *PDS*, *PTOX*, and *LCY-β* are down-regulated (Simkin et al., 2003). This is also concurrent with tomato whereby an increase in *PSY* transcripts occurred when the plant was exposed to light. The decrease in transcript levels was also observed in the dark (Giuliano et al., 1993a).

Tissue specific regulation using differential gene expression is another way in which carotenoid biosynthesis is regulated. There are two *PSY* genes in tomato *PSY1* and *PSY2* which correspond to fruit and green tissue, respectively. In tomato, these two genes are under tissue specific regulation and so although the *PSY2* can be seen to be expressed at a very low level in tomato it does not contribute to fruit carotenogenesis (Fraser et al., 1999). It has been speculated that there are two *PSYs* in pepper also, but until this present study, only the fruit specific *PSY1* has been cloned (Romer et al, 1993; Kim et al., 2010).

In *Arabidopsis* it has been shown that isoprenoid end products, such as chlorophyll, carotenoids, tocopherols, and ABA are increased or decreased accordingly in transgenic lines which increase or decrease expression (Cordoba et al., 2009). This has also been seen in tomato (Lois et al., 2000).

Sucrose has the ability to increase the accumulation of several MEP pathway genes. This is more than likely to do with the first substrates of the MEP pathway, pyruvate and GAP, being derived directly from photosynthesis or glycolysis (Cordoba et al., 2009).

Epigenetic regulation

Epigenetics is the study of inherited cellular or physiological phenotypes, caused by alterations in gene expression, that occur without a change in the sequence of the DNA (Wolffe, 1999). An example of this phenomenon is seen in the tomato Colourless Non-ripening (*Cnr*) mutant. This mutant was found to have altered levels of transcripts of the candidate gene but no nucleotide sequence differences were present. On investigation it was found to contain a more heavily methylated promoter region when compared to the wild type. Hypermethylation is associated

with gene silencing and so suggests that the *Cnr* mutant is caused by the silencing of the candidate gene which is then inherited unchanged over many generations (Manning et al., 2006).

There have also been discoveries that the *CRTISO* gene can be regulated by chromatin remodelling enzymes. This gene accommodates sequences which are similar to a protein called SDG8 which is a histone lysine methyltransferase. Trimethylation of the nucleosome histone tails induces permissive gene expression through an open chromatin configuration (Cazzonelli et al., 2010). These effects, however, are probably global and not for individual enzymes.

1.3.5.2. Translational regulation

Control of the synthesis of proteins can be implemented at a translational level. This can be achieved by altering the rate of protein synthesis from mRNA. Ethylene signalling provides an example of this, whereby a study found that ethylene insensitive 2 (EIN2) represses translation of the ethylene insensitive F-box binding proteins (EBF1/2). The mRNA EBF1/2 are recognised by sequences in the 3'UTR. This study illustrated that translational control is a key step in ethylene signalling (Li et al., 2015).

1.3.5.3. Post-translational regulation

Transcriptional/ translational regulation is not the sole regulatory control acting on the pathway and with further studies utilising modern techniques it is emerging that the pathway is regulated at multiple levels which warrant discussion below.

Metabolite regulation

Many of the genes in the isoprenoid biosynthesis are nuclear encoded. However, the biochemical reactions that take place are compartmentalised into the plastid. For this reason the expression and activity of the enzymes must be regulated for metabolism to operate efficiently and adapt to changes in the plant's development and environment, thus, allowing the development of the cell and the correct response of the cell to certain stimuli to be monitored. Ideally, when the plastid starts to accumulate more protein than is needed then the

accumulation of the product acts to deactivate the synthesis of further products. Alternatively, plastid encoded genes can be switched off resulting in a block in the synthesis (Pogson et al., 2008).

There is some evidence to suggest that carotenoid biosynthesis enzymes can be regulated by metabolites' levels which alter the activity state of the enzyme. In the MEP pathway there was evidence of the influence of post-translational regulation. This is illustrated by Arabidopsis mutants which show high levels of DXS and HDR proteins despite dramatic decreases in transcript levels, thus suggesting a method of inactivating enzyme activity (Guevara-Garcı et al., 2005).

Evidence for post-translational regulation is also present in the carotenoid biosynthesis pathway. When the tomato PSY1 protein was incubated with β -carotene or chlorophyll there was a twofold reduction in activity. In contrast to phytoene, ζ -carotene and lycopene which had no effect (Fraser et al., 2000).

Plants, like other organisms, have shown other methods of regulation too. Mutants in the MEP pathway have shown that the MEP pathway genes may be regulated by a retrograde chloroplast to nuclear signalling response. This is shown in mutants with arrested chloroplast development which contained very low transcript levels of the MEP pathway genes (Guevara-garcı et al., 2005). Products of the carotenoid pathway have also been shown to modulate the expression of the DXS gene in tomato. This was witnessed when the tomato *rr* mutant, which has a non-functional PSY1, was shown to stay expressed at the end of ripening when usually it becomes down-regulated. This therefore suggested that products from the carotenoid pathway can down-regulate the expression of the DXS gene, which is nuclear encoded, when levels have reached a sufficient level (Lois et al., 2000). This study also showed that injecting tomato halves with DXP could up-regulate the *PSY1* gene, further suggesting that the metabolites present in the MEP pathway can modulate expression of carotenoids biosynthesis genes (Figure 1.18).

A study in orange fruited pepper revealed that the orange mutant displayed higher expression of carotenoid pathway genes. This mutant was characterised by having low total carotenoid content and a mutated β -carotene hydroxylase. It was evident that the up-regulated genes could be caused by the lack of negative feedback signal from end products. This mutant also showed high CCS expression despite very low levels of capsanthin produced (Borovsky et al., 2013).

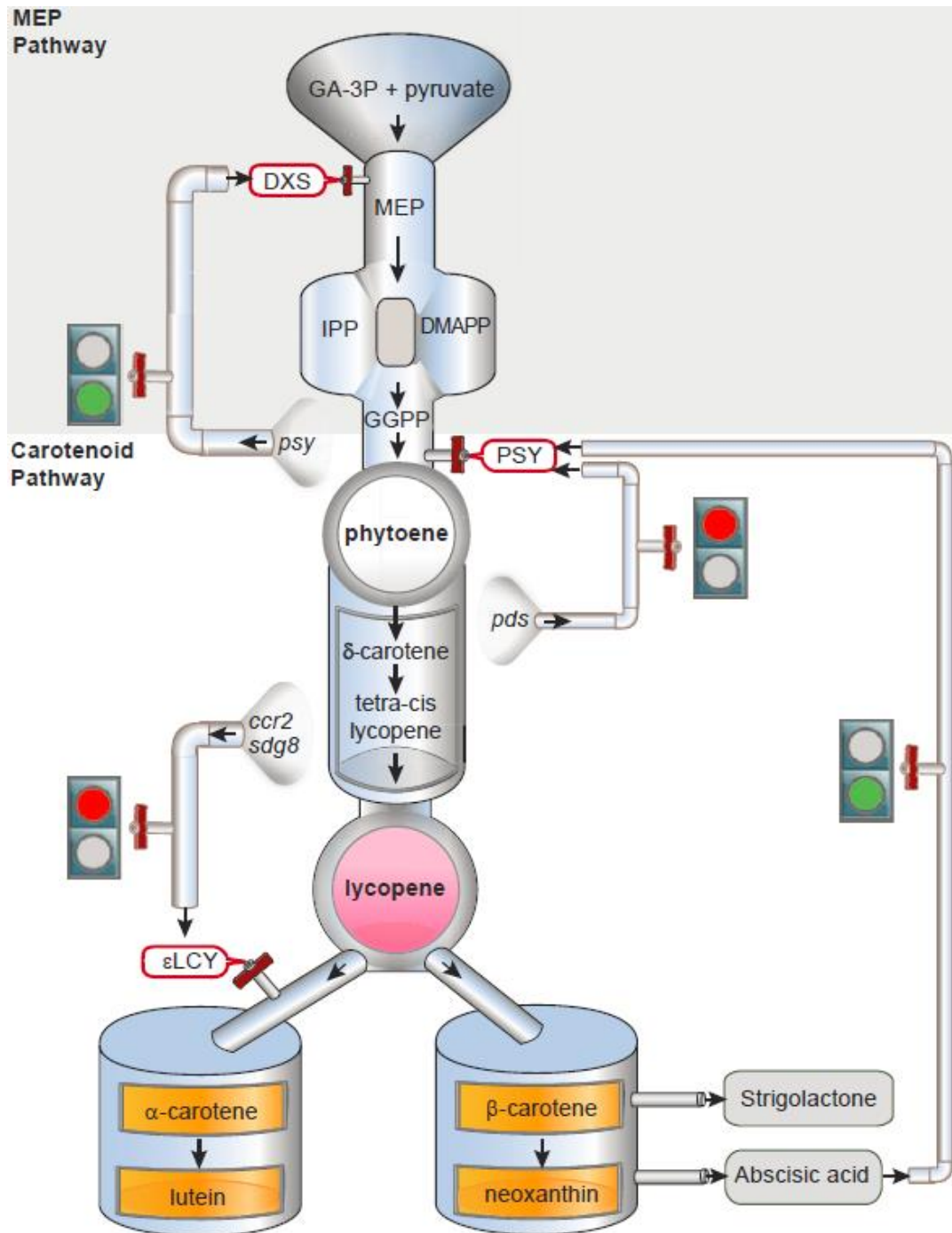


Figure 1.18. A model for carotenoid metabolic feedback in plants.

Positive (green lights) and negative (red lights) feedback is present within the carotenoid and MEP pathways. Transcriptional and post-translational mechanisms modulate gene expression (Cazzonelli, 2011).

Addition of the bacterial *crtB* gene in tomato results in elevated levels of β-carotene, this in turn feeds back to down-regulate the endogenous *PSY1* (Fraser et al., 2009). In tomato feedforward mechanisms are also at play. This can be seen by overexpressing the *DXS* gene; the resultant

elevation of phytoene levels causes the *PDS* gene to become down-regulated (Fraser et al., 2009).

A summary of these feedback processes has been illustrated in Figure 1.18 by Cazzonelli, 2011.

Metabolite channelling

Metabolites in the carotenoid biosynthesis pathway are thought to form a metabolon whereby sequential steps are structurally held together to form a complex to aid metabolite channelling. This places each enzyme in the pathway in the most efficient location to interact with its corresponding substrate (Dogbo et al., 1988). It has been suggested that metabolite channelling can regulate carotenoid biosynthesis; when investigating PSY1 mutants, although the PSY2 gene is expressed and the protein is present, it cannot compensate for the loss of PSY1. One reason for this could be because PSY2 is not part of the metabolon that forms in plastids of the ripe fruit and so inefficient metabolite channelling results in reduced total carotenoid content (Fraser et al., 1999). Additionally, the flux coefficient for PSY1 is found to be significantly reduced in transgenic tomato expressing *crtB*; thus reducing the influence PSY1 has on the pathway. This can explain why the increase in gene expression is not reflected by the small increases in carotenoid content analysed (Fraser et al., 2002). It has been postulated that the reason for this is that the PDS enzyme is unable to efficiently access the phytoene produced by *crtB* due to the metabolites produced in the pathway being channelled to optimise access for endogenous enzymes.

PSY was also found to co-immunoprecipitate with OR family proteins which may promote proper folding of PSY. When OR genes were overexpressed, interactions did not affect gene expression but positively mediated carotenoid content and protein levels (Zhou et al., 2015). This suggests that OR can regulate PSY post-translation. PSY is thought to be located in the stroma when inactive; therefore, OR might be involved in associating the soluble, inactive PSY to the membrane for activation and interaction with other enzymes in a protein complex containing IDI and GGPPS, thus allowing efficient metabolite channelling to occur (Fraser et al., 2000).

Carotenoid degradation and turnover

There are specific cleavage enzymes which act on the carotenoids. It is generally thought that the total content of carotenoids is the sum of carotenoid biosynthesis, storage, and degradation. The enzymes involved in the degradation are carotenoid cleavage dioxygenases (CCDs). Members of this family include NCED which is involved in the biosynthesis of ABA. Cleavage of

carotenoids result in the formation of ketone and aldehyde products, known as apocarotenoids. The apocarotenoids formed can go on to be plant hormones and produce signalling molecules, as well as carotenoid derived volatiles, which will be discussed later (1.4.3). In plants, it has been discovered that the CCD1 enzymes catalyse the cleavage of β -carotene. However, there have been others which also act on β -carotene. CCD4 is a plastid localised enzyme and is thought to be the first step in the formation of crocin. Other known apocarotenoids include β -ionone, retinal, ABA, and strigolactone (Harrison and Bugg, 2014). There are five CCD4 enzymes and they can all use β -carotene as a substrate generating β -ionone (Campbell et al., 2010). However, although they cleave their substrates with a similar mechanism they are thought to have different biochemical functions. There was an interesting CDD4a mutant identified in chrysanthemum which resulted in a change in petal colour from white to yellow (Ohmiya et al., 2006). It would appear that the presence of CCD4 did not allow accumulation of carotenoids under normal circumstances. Analysis of CCD4 gene expression in potato revealed that the yellow-fleshed Phureja tubers exhibited considerably lower expression of CCD4 when compared to the white-fleshed Tuberosum. When this same gene was down-regulated in a white-fleshed variety there was found to be fivefold increase in total carotenoid content, particularly violaxanthin (Campbell et al., 2010).

1.3.5.4. Compartmentalisation, sequestration, and storage

Isoprenoid biosynthesis is regulated in part by the compartmentalisation of metabolites into different cellular locations, such as the plastid, the cytosol, and the peroxisomes. This is so different isoenzymes have access to the substrates produced in the compartments they are located in, allowing the metabolites to be transformed efficiently. An example of this is the presence of FPS and GGPPS in the cytosol and plastid to synthesise different branches of the isoprenoid biosynthesis pathway for the production of sterols and carotenoids, respectively.

The sequestration of carotenoids into storage structures is a form of regulation in the plastids. This involves the partitioning of carotenoids into compartmentalised structures physically separating them from biosynthetic enzymes. There are a variety of mechanisms present in plants which allow the efficient storage of large amounts of carotenoids. It is possible that the type of storage structure is determined by the abundant carotenoids accumulated. It is evident that the sequestration of the carotenoids into storage structures firstly prevents the biosynthesis membranes becoming saturated with carotenoids and disrupting the balance, and secondly

stops accumulation of end products in active cellular structures which could cause negative feedback.

The *OR* gene mutant identified in cauliflower was found to accumulate β -carotene. The wild-type *OR* gene product contains two transmembrane domains and a cysteine-rich zinc finger domain. This zinc finger domain is highly specific to DnaJ co-chaperones. These co-chaperones are involved in protein folding, protein translocation, and protein assembly and disassembly. However, the mutant *OR* gene contains an insertion mutation leading to the formation of three splice variants of the OR protein. This mutant appears to be able to induce differentiation of proplastids into chromoplasts and when expressed in potato results in the enhancement of carotenoid production. This therefore shows that it works by creating metabolic sinks for carotenoid storage by creating more chromoplasts (Lu et al., 2006).

Another example of altering the sequestration mechanism to enhance carotenoid production is in experiments with the tomato *DET1* mutant. This gene is a negative regulator of light signalling. Down-regulation of this gene gave rise to the high pigment phenotype (*hp-2*). A characteristic of this mutant, as well as increased carotenoid content, was increased plastid size and number. This therefore suggests that the plastid compartment size can regulate the amount of carotenoids produced (Enfissi et al., 2010). This is also seen in the other tomato high pigment mutants such as the *hp-3* mutant. This is caused by a blockage in the carotenoid biosynthesis pathway at ZEP and leads to increased plastid compartment size and number as a response to elevated carotenoid content (Galpaz et al., 2008). A similar story was also true for the *hp-1* mutant (Cookson et al., 2003).

Overexpression of bacterial genes *CrtB+I* in tomato fruit revealed that the increases in the carotenoid content in transgenic lines were simultaneous with an up-regulation in carotenoid sequestration mechanisms. This was characterised by the increased number of membraneous sacs present in the transgenic line (Nogueira et al., 2013). This operates to partition the carotenoid precursors from their subsequent biosynthetic enzymes as a means of regulation through compartmentalisation, thus resulting in control of the flux of carotenoids through the biosynthetic pathway.

The negative feedback regulation of carotenoid end products and the plastid's ability to store them efficiently has been shown to exert regulatory effects on the storage of carotenoids. It is therefore paramount to understand the biochemical and molecular feedback mechanisms associated with carotenoid sequestration processes.

1.3.6. Carotenoid storage and deposition

Plastids are intracellular organelles which are present in plants. These organelles are thought to have originated as the result of an endosymbiotic event whereby eukaryotic algae incorporated a photosynthetic prokaryote, cyanobacteria, into their cell system, thus, forming a mutualistic relationship based on the trade of safety for food. Plastids have evolved to carry out a variety of specialised functions. Chloroplasts are the plant's main food source which enable the plant to harvest and store the sun's energy by the action of photosynthesis. In pepper, when the fruit is at mature green stage of development, chloroplasts are the predominant plastid located in the cells. The chlorophyll associated with the photosynthetic machinery in the thylakoid membranes causes the green colour of fruit. However, as the fruit begins to ripen profound biochemical and morphological changes occur and the chloroplast differentiates into a chromoplast which is a non-photosynthetic plastid (Figure 1.19).

The differentiation from chloroplast to chromoplast is characterised by the breakdown of chlorophyll and the disorganisation of the thylakoid membranes (Figure 1.19). Simultaneously new membrane systems are constructed into organised membrane complexes (Egea et al., 2010). The chromoplast membranes are different from the chloroplast membranes and do not rely on the materials produced from the breakdown of the thylakoid membranes. This is seen in chlorophyll retaining peppers where the thylakoids remain present after the fruit has started the accumulation of carotenoids. This results in a brown colour of the fruit (Deruère et al., 1994).

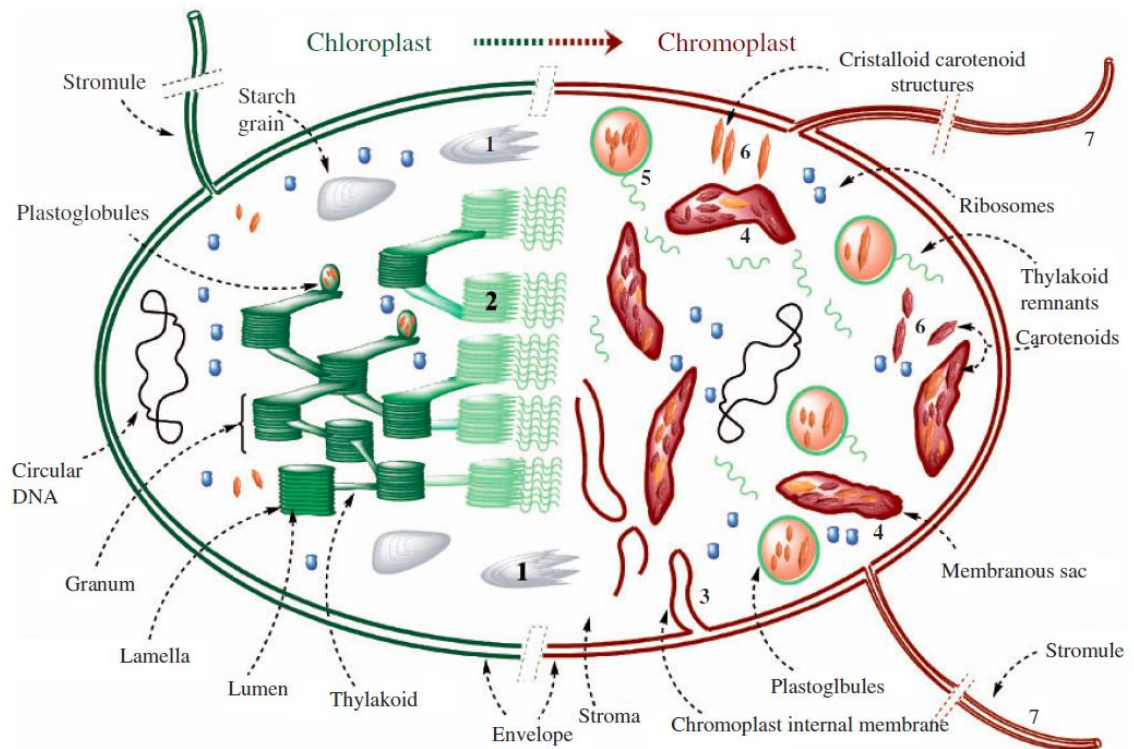


Figure 1.19. The transition from chloroplast to chromoplast.

The differentiation of the chloroplast into chromoplast experiences the breakdown of the starch granules, grana, and thylakoids (1 and 2). The synthesis of new membrane structures from the inner membrane (3) leading to the formation of carotenoid-rich membrane sacs (4) and plastoglobuli (fibrillar type in pepper) (5). The appearance of carotenoid-containing crystalloids (common in tomato) (6). There is also an increase in protrusions from the plastid envelope (7) (Egea et al., 2010).

1.3.6.1. Plastoglobuli

The carotenoids are extremely hydrophobic and so are generally located within hydrophobic environments, such as the inner cores of lipid membranes. Specialised structures which store the carotenoids away from polar environments are known as plastoglobuli (PGs). Therefore, the increase in size and number of PGs is concurrent with chromoplast differentiation (Egea et al., 2010). These structures are thought to form when the accumulation of carotenoids reach a certain concentration acting as a sink for excess compounds formed. This phenomenon is common and has been witnessed in the storage of excess lipids and excess esterified cholesterol (Kovanen et al., 1975). Studies have shown that the type of PGs accumulated in chromoplasts in

plants can differ greatly. There have been reports of globular, crystalline, membraneous, fibrillar and tubular PGs (Vishnevetsky et al., 1999; Camara et al., 1995). Globular PGs, as seen in tomato chromoplasts, are thought to be in evolutionary terms the most primitive, whereby proteins with hydrophobic regions and polar lipids form the surface of the PG structure and the carotenoids are found in the interior of the structure, which is non-polar (Vishnevetsky, 1999; Camara et al., 1995). *Capsicum*, however, have been shown to contain fibrillar PGs. A characteristic trait of these structures when compared to globular type structures is that there is a much lower ratio of apolar to polar components. Therefore, there is a much larger ratio of protein to lipid in fibrillar PGs (Vishnevetsky, 1999; Camara et al., 1995).

Fibrillar PGs, or fibrils, have been elucidated as elongated, threadlike structures which tend to pack in parallel fashion. These threadlike structures form bundles of microfibrils. In pepper, electron microscopy has suggested that the microfibrils present in the fibrils are organised in a hexagonal fashion but they can also appear on their own too (Simpson and Lee, 1976; Deruère et al., 1994). Some studies suggest that there are cross-bridges between individual microfibrils (Deruère et al., 1994).

The carotenoids are thought to be stored in parallel to the long axis of the fibrils in the interior of the fibril which is surrounded by a sheath of protein and lipid. The pigments were also found to be difficult to extract with lipophilic solvents suggesting that they were bound structurally to a non-lipid component (Frey-Wyssling and Kreuzer, 1958; Simpson and Lee, 1976). The most abundant protein associated with the fibrils is fibrillin and the lipids associated are galactolipids (monogalactosyldiacylglycerol (MGDG) and digalactosyldiacylglycerol (DGDG)) and phospholipids. The differentiation from chloroplast to chromoplast is concurrent with a change in lipid composition. In pepper, there were less total phospholipids but more galactolipids present in the chromoplast fibrils when compared to the thylakoid membranes (Deruère et al., 1994). This was supported by another study which found in both field and greenhouse conditions the amount of galactolipids was higher in the chromoplasts when compared to the chloroplasts (Whitaker, 1991). However, another study found that during ripening there was an increase in phospholipid and a decrease in galactolipid when looking at total lipid content in plastids (Camara and Brangeon, 1981). The phospholipids and galactolipids orient themselves so their hydrophobic tails interact with the carotenoids and their polar heads interact with polar regions of fibrillin (Deruère et al., 1994).

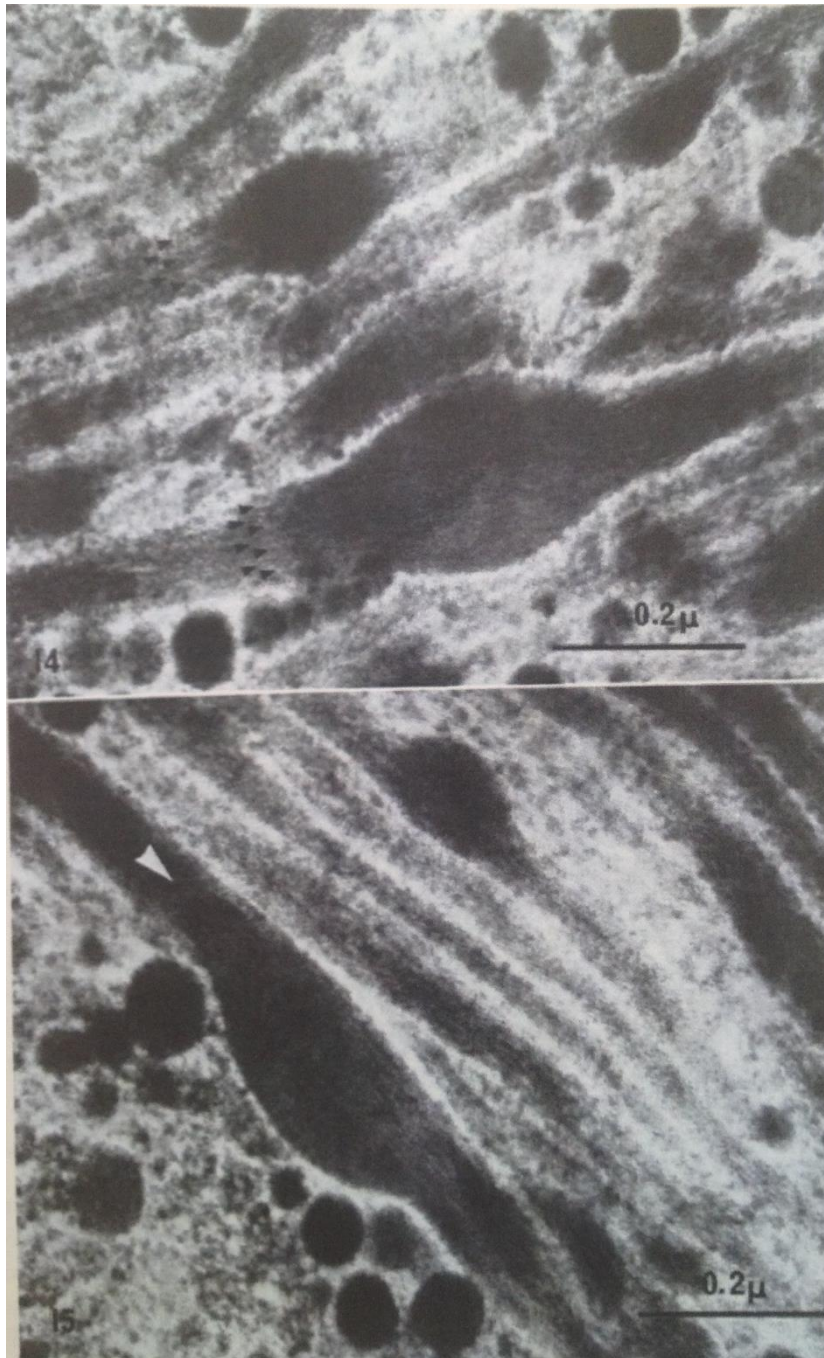


Figure 1.20. Longitudinal sections of globular plastoglobuli transforming into fibrillar plastoglobuli found in *Capsicum annuum* (Simpson and Lee, 1976).

Fibrillar PGs are fairly common in plant chromoplasts. Other examples of plants which possess fibrillar PGs include plants such as winter cherry, cucumber, greater celandine, Japanese rose, and asparagus to name a few (Wrischer et al., 2007; Prebeg et al., 2006b, 2006a; Wuttke, 1976; Simpson et al., 1977). There is evidence to suggest that the fibrillar PGs arise from globular PGs (Figure 1.20). This has been seen in pepper, cucumber, and greater celandine. It has been

proposed that fibrils form from the addition of material from the stroma to elongate the globular PG (Simpson and Lee, 1976). However, a study in *Capsicum* disagrees with this idea as when staining with osmium the fibrils and the PGs have different densities and are not homogenous. This study proposes that the fibrils arise from the lamellae (Frey-Wyssling and Kreutzer, 1958). It is possible, however, that this is a staining artefact and the difference in densities is due to the recruitment of fibrillin decreasing the lipid to protein ratio.

Although PGs are generally considered to be storage structures there is some evidence suggesting that metabolism may also be occurring here (Figure 1.21). Enzymes involved in carotenoid cleavage, tocopherol biosynthesis, and jasmonate synthesis have been located there when carrying out proteomics on PGs (Bréhélin et al., 2007). This included the presence of the vitamin E deficient 1 (VTE1) involved in tocopherol biosynthesis. The other enzymes for this pathway are localised to the envelope membrane thus suggesting synthesis, storage and trafficking roles (Vidi et al., 2006). The carotenoid cleavage dioxygenase (CCD4) has been identified in PGs and has been shown to increase in response to darkness, thus suggesting a role in carotenoid degradation in response to dark (Ytterberg et al., 2006).

In pepper, evidence of carotenoid biosynthesis enzymes in the plastid has been discovered. These included ZDS, LYC- β , and CHY, therefore, again suggesting synthesis and storage roles (Ytterberg et al., 2006).

There has also been evidence to suggest that PGs are involved in stress response. This is particularly relevant in terms of the globular PGs accumulated in the chloroplasts. In oxidative conditions the numbers of PGs are seen to increase to provide protection to the thylakoid membranes (Bréhélin and Kessler, 2008).

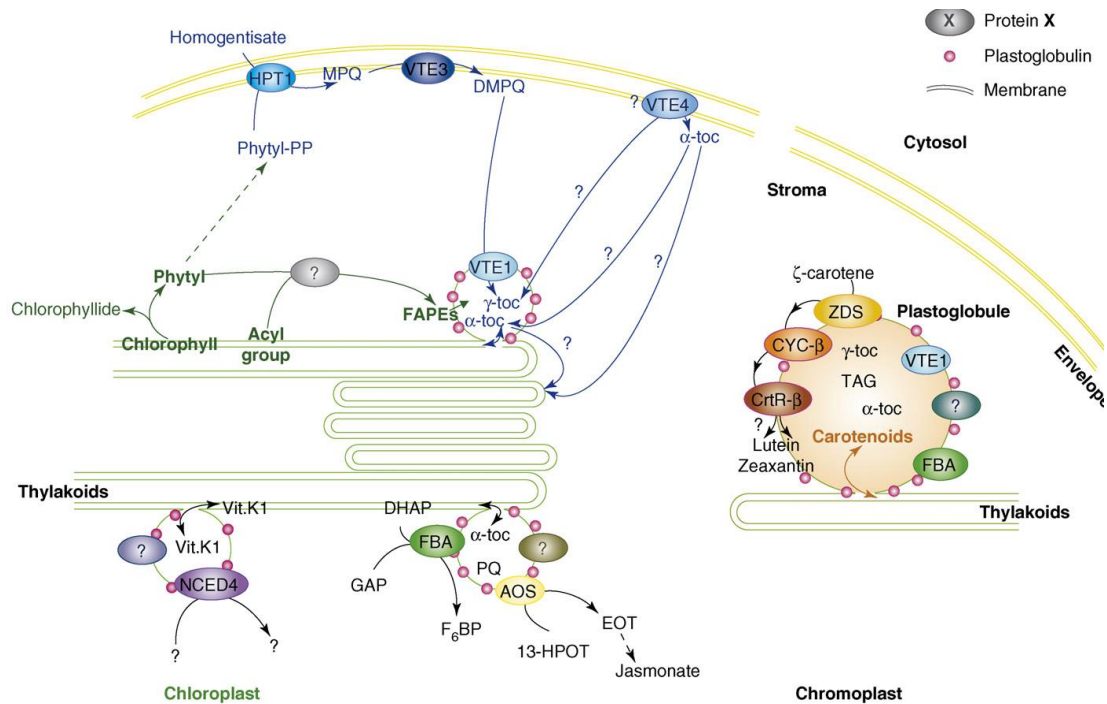


Figure 1.21. Metabolic processes present in plastoglobuli (PGs).

PGs have been shown to be associated with metabolic enzymes in chloroplasts and chromoplasts. The vitamin E deficient 1 (VTE1) enzyme is involved in the tocopherol biosynthesis pathway. Allene oxide synthase (AOS) is involved in jasmonate biosynthesis, NCED4 is a carotenoid cleavage enzyme and ζ -carotene desaturase (ZDS), lycopene β -cyclase (CYC- β), and β -carotene hydroxylases (CrtR- β) are carotenoid biosynthesis genes. Abbreviations: HPT1, homogentisate phytyltransferase; MPQ, 2-methyl-6-phytyl-1,4-hydroquinol; DMPQ, 2,3-dimethyl-5-phytyl-1,4-hydroquinol; VTE4, vitamin E deficient 4; FAPes, fatty acid phytyl esters; 13-HPOT, 13-hydroperoxylinolenic acid; EOT, 12,13-epoxyoctadecatrienoic acid; FBA, fructose-1,6-bisphosphate aldolase; DHAP, dihydroxyacetone-phosphate; GAP, glyceraldehyde 3-phosphate; PQ, plastoquinone; Vit.K1, phylloquinone; TAG, triacyl glycerol (Bréhélin et al., 2007).

1.3.6.2. Fibrillin

Plant plastoglobulins are proteins which are known to be associated with lipids in the plastid. These proteins are assumed to play a predominantly structural role which regulates the size and type of PGs accumulated within the plastid.

A member of the plastoglobulin family, fibrillin, was discovered in red peppers and is the main protein which is associated with the fibrillar PGs. This protein has also been referred to as plastid-lipid-associated protein (PAP) and ChrB in other studies. Fibrillin is a nuclear encoded protein which is thought to be transported into the plastid in a soluble, inactive form. Fibrillin gene expression seems to be highly regulated by many processes including growth and development, hormones, biotic and abiotic stress.

The formation of fibrils can be reconstituted by adding fibrillin to polar and isoprenoid lipids analogous to those found in fibrils. This study by Deruère et al (1994) found that fibril formation was dependent on fibrillin concentration and the ratio of lipid to protein reflected conditions *in vivo*. The type of carotenoids present also affected fibril formation whereby the presence of acyclic carotenoids, such as lycopene, was unsuccessful in forming fibrils but cyclic carotenoids could. The xanthophylls were more efficient than β -carotene, and xanthophyll esters were most efficient at forming fibrils when compared to all other forms of carotenoids. Therefore, it was proposed that fibril formation relied on the presence of cyclic carotenoids to reach a critical concentration. This was further supported by blocking the synthesis of β -carotene using CPTA. The result was that lycopene was accumulated and no fibrils were detected (Deruère et al., 1994).

In pepper, fibrillin transcripts were not present in leaves and were found at low levels in mature green fruit. The transcript levels were found to increase throughout ripening and were at the highest levels in mature ripe fruit.

Although the fibrillar PGs are where the fibrillin protein is most abundant in pepper, in tomato fibrillin is found in other locations within the plastid. For example, it has been found to be associated with the thylakoid membranes (not found in pepper chloroplasts from leaves or green fruit) as well as globular PGs. It has been proposed that fibrillin may have a structural role in maintaining thylakoid membranes under stress conditions. When fibrillin was constitutively expressed in tomato fruit there was a 95% increase in total carotenoid, particularly lycopene and β -carotene. An important point of this study is that although fibrillin was over-expressed in tomato, the only effect on the PGs was that they formed grape-like clusters. There was,

however, no formation of fibrillar PGs (Simkin et al., 2007). This suggests that the expression of fibrillin alone is not capable of inducing fibrillar formation in pepper. Fibrillar formation is likely to be initiated by the presence of esterified carotenoids which are prevalent in pepper. Expression of fibrillin in tobacco also suggested that fibrillin has structural roles for protection of membranes under stress conditions. These transgenic plants contained more thylakoid-associated fibril when exposed to drought or high light conditions (Rey et al., 2000).

The sequestration and storage of carotenoids accumulated in fruit during ripening is intimately linked with lipid biosynthesis. The carotenoids are first esterified with saturated fatty acids and it has been shown that lipid concentration is crucial in the formation of globular and fibrillar PG.

1.4. Lipids

Lipids are essential components of plant cells. The membranes are responsible for the majority of the total lipid content. Epidermal cells produce cuticular lipids which are present in the surface of the plant, provide a physical barrier from pathogens, and prevent water loss. Lipids are also used in the synthesis of hormones and used in the acylation of some proteins and other compounds, such as the carotenoids. The most abundant types of lipids are derived from fatty acids and glycerolipid biosynthesis pathway (Ohlrogge and Browse, 1995). Free fatty acids are generally not found within the cell; most fatty acids are esterified to glycerol. Membrane lipids are glycerolipids with two fatty acids attached to the sn1 and sn2 positions of glycerol, sn3 is occupied by a polar head group. The hydrophobic tails and the polar heads allow the formation of the lipid bilayers. The plastids are the major site for fatty acid synthesis (Ohlrogge and Browse, 1995). However, fatty acids can also be synthesised in the ER via a eukaryotic pathway. Fatty acids synthesised inside the plastid have sn1 C18 and sn2 C16 distribution whereas fatty acids synthesised outside the plastid have C16 or C18 at sn1 and sn2 is C18 (Whitaker, 1991). The major substrate for fatty acid synthesis located within the plastid is acetyl-coenzyme A (CoA). It is thought that the elongation of C18 to C22 occurs outside the plastid and this typically supplies the long chain fatty acids needed in the cuticular wax.

In plants tissues the most predominant saturated fatty acids are palmitic (C16:0) and stearic acid (C18:0). The most abundant unsaturated fatty acids are oleic (C18:1), linoleic (C18:2), and linolenic acid (C18:3). It has long been established that the fatty acid composition of the cell membranes allow the plant to adapt to different temperature environments. It has been seen

in nature that increasing the percentage of poly unsaturated fatty acids allows the membrane to maintain integrity under cold conditions. This is because the unsaturated fatty acids are not packed as tightly as saturated fatty acids and this results in the membrane having more fluidity (Murata and Los, 1997).

1.4.1. Lipid composition

Plant plastid membranes contain specific lipids when compared to other membranes outside the plastid. Most of the glycerolipids in chloroplasts are glycolipids, galactolipids and sulfolipids. This is in contrast to other cell membranes which generally consist of phospholipids. Galactolipids have poly-unsaturated fatty acids attached at the sn1 and sn2 positions on the glycerol. As the thylakoids are the most highly developed membranes in plant systems it is thought that the galactolipid, MGDG, is the most abundant lipid on earth (Marechal et al., 1997).

In pepper pulp, the predominant fatty acids have been described as palmitic (C16:0), oleic acid (C18:1), linoleic acid (C18:2), and linolenic acid (C18:3) with linoleic and linolenic acid as the major fatty acids constituting 45% and 10% to the total lipid content, respectively (Bekker and Asilbekova, 2003; Pérez-Gálvez et al., 1999). When looking at the overall lipid content of the fruit pulp neutral lipids constituted around 80% of the total lipids with glycolipids, phospholipids, and surface lipids contributing around 14, 3, and 3% respectively. The glycolipid fraction gave rise to the highest content of unsaturated fatty acids, particularly linolenic acid (Asilbekova, 2003). The ratio of MGDG to DGDG was found to increase by eightfold during ripening in pepper fruit (Whitaker, 1991). The carotenoids are esterified with saturated fatty acids as these are not as prone to oxidation as the unsaturated fatty acids, thus stabilising the carotenoids for storage. Tomato fruits predominantly accumulated linoleic acid at around 60%. This was followed by oleic, palmitic, linolenic, and stearic acid (Cook et al., 2002). Transgenic tomato lines expressing higher levels of carotenoids were found to have increased levels of MGDG. Since it has been shown that MGDG has a high tendency for interfacial curvature, it appears that the membrane adapts to the increase in carotenoids by increasing plasticity. This has been proposed as a response to the formation of more PGs which form from areas of high curvature (Nogueira et al., 2013).

1.4.1.1. Cuticle lipids

The cuticle of pepper fruit has a different lipid composition when compared to the pulp. Cutin is a lipid polymer and is the main constituent of the cuticle (Figure 1.22). Pepper fruit cuticle differs from tomato fruit cuticle because it contains epoxy acids in the cutin. The wax profile typical of pepper consists of very long chain fatty acids (C20-C32), aldehydes (C24, C26, C29 and C32), alkanes (C20-C35), cyclic triterpenes and sterols. The alkanes are usually the most abundant component of the wax, but ranged from 13-74% of the total waxes thus showing the variability within the pepper lines analysed. Pepper was found to vary over 14-fold in wax composition which was double that of wax composition variability in tomato (Parsons et al., 2013; Yeats et al., 2012). Studies into the relationship between water loss and wax composition showed that varieties with low water loss had the highest amounts of alkanes. Water loss rates were also higher in varieties containing high free fatty acids (Parsons et al., 2013).

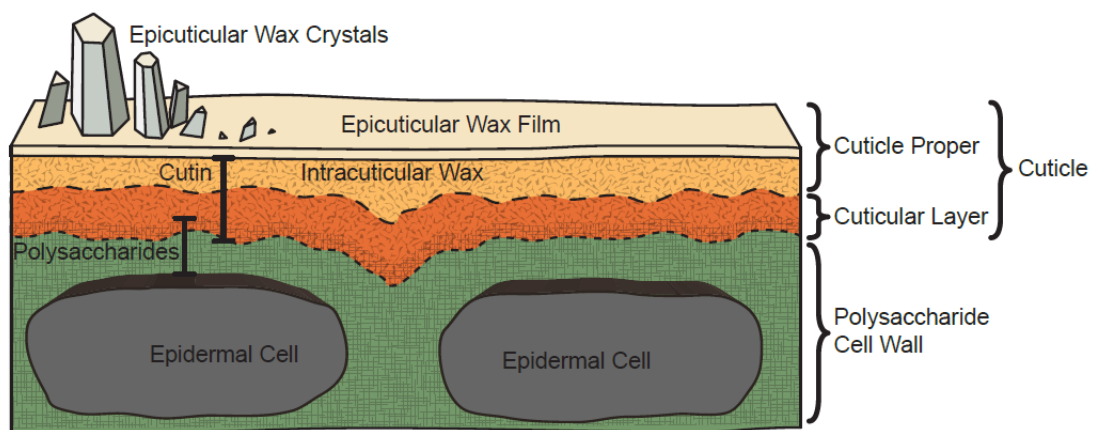


Figure 1.22. Plant cuticle structure (adapted from Yeats and Rose, 2013).

Variation in cuticle composition is common among pepper varieties. This is due to the many biotic and abiotic stressors which have influenced the adaptation of the lipid composition. Circumstances such as pathogens and animal predation, drought, sun, and freezing tolerance, requirement for seed dispersal, and domestication all play a role in cuticle diversity (Parsons et al., 2013).

1.4.2. Lipid peroxidation

As mentioned previously the carotenoids protect against lipid peroxidation. Lipid peroxidation is undesirable as it leads to the formation of ROS which damages cell membranes resulting in compromised membrane integrity. Different carotenoids can protect the membranes in different ways depending on their biochemical properties. Lycopene and β -carotene are restricted to the hydrophobic core of the membranes and therefore scavenge radicals present there. Zeaxanthin and other xanthophylls can span across the bilayer and position their hydroxyl groups towards the hydrophobic-hydrophilic interface of the bilayer and act to scavenge radicals entering from the aqueous phase (Woodall et al., 1997a).

The carotenoids' role in protecting the lipids from oxidation is commonly thought to be the reason for their degradation during storage. Therefore, it is important to understand the oxidative processes leading to the production of ROS via lipid peroxidation which can present in the cell.

The lipoxygenase (LOX) enzyme is a source of ROS production. It catalyses the hydroperoxidation of poly-unsaturated fatty acids (Figure 1.23). The hydroperoxyl derivatives produced can then go on to produce more radicals resulting in an initiation of lipid peroxidation chain reaction. However, the action of LOX is not the only instigator of lipid peroxidation as other ROS produced through alternative cellular processes such as photosynthesis and the electron transfer chain can create ROS too. Either way lipid peroxidation leads to the production of lipid peroxy and hydroperoxides radicals. The highly reactive peroxy radicals formed can go on to produce hydroperoxide radicals thus initiating a chain reaction. Although lipid peroxidation is a destructive process there has been reason to suggest that it has a role in signal transduction too (Blokhina et al., 2003). For example, when β -carotene becomes oxidised through light stress in *Arabidopsis*, the β -cyclocitral volatile compound formed goes on to induce changes in genes related to single oxygen response (Ramel et al., 2012).

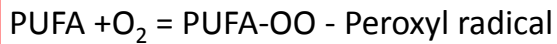
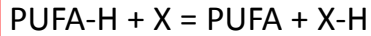


Figure 1.23. Lipid peroxidation reactions.

Key: PUFA, poly unsaturated fatty acid; X, oxidising agent (adapted from Blokhina et al., 2003).

The lipid derived peroxide molecules produced by the action of LOX can go on to produce a vast repertoire of derivatives as seen in Figure 1.23. The levels and compositions of the lipid derived volatiles produced in these reactions can be studied to assess what predominant reactions are taking place, thus, giving a reflection of the oxidative conditions of the plant.

Although there are enzymatic antioxidant defences to aid carotenoids with the scavenging of ROS, there have been some instances where imbalances in the coordination of these enzymatic antioxidants can perpetuate ROS production. In terms of the superoxide anion the enzymes superoxide dismutase (SOD) and catalase work together to neutralise the radical. The SOD enzyme converts the superoxide radical to hydrogen peroxide, and the catalase enzyme converts hydrogen peroxide into hydrogen and water (Beauchamp and Fridovich, 1971). However, when disparities occur within the expression/activities of these enzymes problems can ensue. For example, the postharvest physiological deterioration of cassava is caused by production of ROS from an oxidative burst postharvest. In the first 24hrs after harvest the hydrogen peroxide produced by SOD is immediately neutralised; however, after this there is not sufficient catalase to scavenge the hydrogen peroxide produced (Xu et al., 2013). This therefore leads to the accumulation of hydrogen peroxide which in turn generates more ROS.

1.4.3. Volatile compounds

Plant volatiles are generally low molecular weight lipophilic molecules. Non-conjugated volatiles can cross membranes and evaporate into the atmosphere. In nature, plants use the release of volatiles as a way to communicate in a species-specific manner to signal, attract pollinators or react in response to predators. This can be by releasing volatiles toxic to the herbivore or

releasing volatiles to attract the herbivores' predator (Pichersky et al., 2006). Plant volatiles are usually produced in the epidermal cells of flowers, and at the surface glandular trichomes of the vegetative organs. In some plants volatiles can be synthesised and stored in specialised cells which release when the plant becomes physically disrupted. Volatiles can also be synthesised at specific developmental stages such as flowering, ripening, and maturation.

Commercially, the volatiles released from a fruit are responsible for the aroma. The volatile composition is therefore an important factor to consider in plant breeding strategies as it is the aroma and taste which lead to the perception of flavour. Therefore, the flavour of a fruit communicates to the brain a perception of the nutritional quality of the fruit, thus, enabling a preference to be constructed. For example, fatty acid derived volatiles can signal the presence of essential poly-unsaturated fatty acids and it has been shown previously that there is an association between carotenoid content and carotenoid derived volatiles produced (Goff and Klee, 2006; Borovsky et al., 2013). There was an increase in the accumulation of the norisoprenoid β -carotene cleavage aroma compounds in an orange pepper mutant which accumulated β -carotene. Therefore the carotenoid content can positively influence preference by using volatiles to signal high levels in fruits (Borovsky et al., 2013).

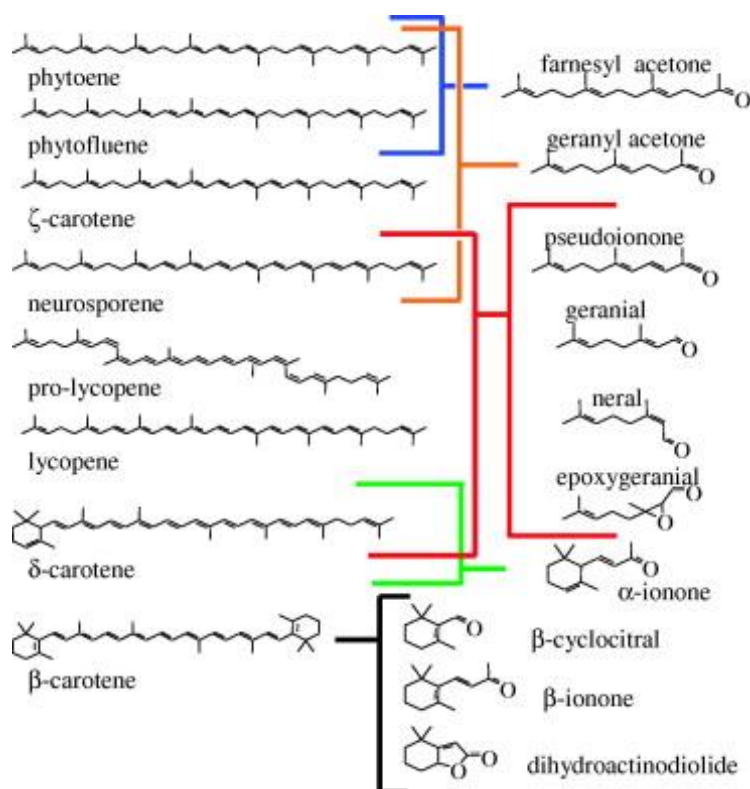


Figure 1.24. Carotenoid derived volatiles and their potential precursors (Lewinsohn et al., 2005).

Volatile compounds can be synthesised from a wide range of primary and secondary metabolites. To date, there have been over 7000 flavour compounds identified (Goff and Klee, 2006). The isoprenoids are responsible for the largest group of volatiles produced. Enzymes known as terpene synthases use compounds from the MEP pathway such as GPP, FPP, GGPP and DMAPP to produce terpene volatiles. Monoterpenes and sesquiterpenes are the most abundant. These reactions start with the removal of the pyrophosphate group, forming a carbocation. Stereochemical rearrangements then lead to the production of one of two major products (Pichersky et al., 2006). The carotenoids can also undergo cleavage reactions by CCDs to produce apocarotene volatiles (Figure 1.24). Another group of volatiles are produced during the oxidation of fatty acids, whereby decarboxylation results in the formation of aldehyde and ketone molecules. Other groups of volatiles can be produced from compounds containing aromatic rings and amino acids. A diagram from Pichersky et al (2006) illustrates the substrates which can go on to form volatile compounds (Figure 1.25).

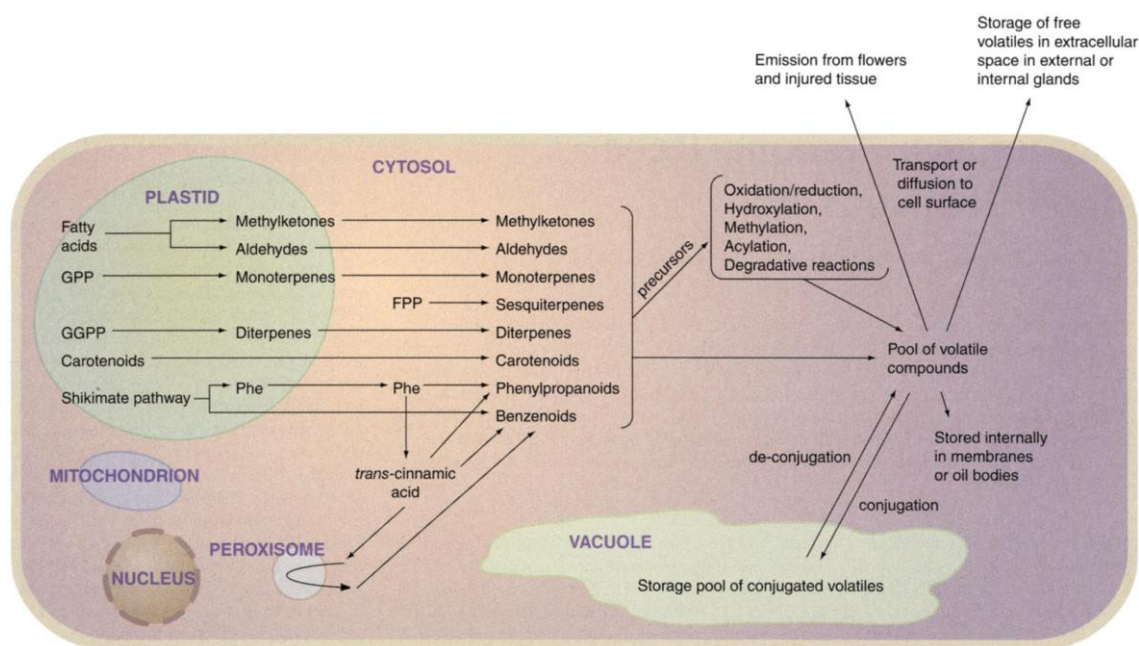


Figure 1.25. Summary of the cellular processes which can result in the production of volatiles in plants.

Most modification reactions occur in the cytosol and the majority of precursors originate from the plastid. Other subcellular structures which give rise to volatiles include the peroxisome and vacuole (Pichersky et al., 2006).

Volatile compounds are produced enzymatically by the action of peroxidases, lipoxygenases, and dioxygenases. They can also be produced non-enzymatically by the action of ROS. In the case of carotenoids, it has been discovered that lycopene can give rise to the formation of geranial and other norisprenoids. While volatile compounds such as β -ionone, β -cyclocitral, and dihydroactinoidine are derived from β -carotene (Lewinsohn et al., 2005).

1.5. Plant breeding: Strategies of genetic intervention for improved traits

1.5.1. Conventional breeding

Conventional breeding strategies were highly successful in the 1960s when they were employed to greatly enhance rice and wheat yield, becoming known as 'the green revolution'. Since then strategies have been progressing towards a more genetic approach. Conventional breeding is achieved primarily with the creation of homozygous lines. These are often inbred lines. These lines are then crossed and plants containing all desirable traits are selected for further breeding. Sometimes, one of the parents is a wild relative conveying a desirable trait such as disease resistance. This approach does have its limitations when the incorporation of this desirable trait is accompanied by undesirable traits, such an occurrence is known as linkage drag. The undesirable traits in most cases can be removed by repetitive backcrossing which is time consuming. This traditional approach is also fundamentally restricted by the sexual compatibility of the parent lines. Hybridisation is a type of conventional breeding. This method exploits the desirable traits from two parent varieties, usually homozygous, and combines these genotypes by cross pollination, thus, creating a heterozygous F1 population with alleles from each parent. In some cases, the offspring produced can be stronger than the either parent resulting in hybrid vigour, or heterosis.

1.5.2. Doubled haploids (DH) populations

This method allows the production of a homozygous plant from a heterozygous plant. This is achieved by artificially doubling the chromosome number of haploid cells, creating doubled

haploids (DH). Conventional breeding can take up to six generations to reach homozygosity, whereas DH populations achieve it in one generation. DH populations are convenient to use to study QTL effects.

1.5.3. Mutagenesis and TILLING

Mutagenesis has been utilised in conventional breeding strategies. This method uses chemicals or radiation to introduce mutations into the DNA of plants. This facilitates the development of new or desired traits. This approach, however, is not favourable as the site of mutagenesis cannot be controlled and undesirable traits are often a result. However, an approach known as Targeted In Local Lesions IN Genomes (TILLING) allowed incorporation of mutations into a plant genome using ethyl methanesulfonate (EMS) mutagenesis. This technique has been used to create a tomato mutant reference collection which specifically generated three tomato colour mutants (Minoia et al., 2010). This population was used to identify mutations in the tomato *B*-gene which led to increased levels of lycopene through a loss of function mutation (Silletti et al., 2013). TILLING was also used to identify mutations present in the *PSY1* gene in tomato whereby mutagenesis introduced a premature stop codon into the gene displaying similar characteristics to the yellow flesh *r* mutant (Gady et al., 2012). Unfortunately, there is no available literature for TILLING studies in *Capsicum*.

1.5.4. Marker assisted selection (MAS)

Colour, and traits such as yield, quality, disease resistance and flavour are considered important traits in agriculture. These traits are controlled by genes within a defined genomic region. Polymorphisms within these genes can be associated with desirable traits. The location in the genome which these gene combinations are found are known as quantitative trait loci (QTL) (Fridman et al., 2004). There are a number of ways in which the genes of known desirable traits can be utilised in breeding strategies to improve crop colour, quality, yield, etc.

Marker assisted selection (MAS) utilises the identification of molecular markers for specific regions that delineate sections responsible for the trait. Molecular markers can be used to locate the presence or absence of polymorphisms present in genes with desirable traits. This is achieved by selecting a molecular marker which is closely linked to the polymorphism causing

the desirable trait. This allows the traits from each parent in a segregating population to be identified on a molecular level whereby the phenotype is selected on the genotype of a marker. Furthermore, this allows selection of genotypes at seedling stage. MAS is thought to be more effective, efficient, cost-effective, and reliable than conventional breeding methods (Collard et al., 2005).

In pepper, MAS was utilised for breeding pepper varieties with different fruit colours. Analysis of six carotenoid biosynthetic genes was carried out. It found a polymorphism in PCR pattern of the *CCS* gene in a segregation population from a red and an orange parent. This was attributed to a deletion upstream of the *CCS* gene thus identifying an allele for orange fruit colour (Lang et al., 2004). Restriction fragment length polymorphism (RFLP) and specific-PCR polymorphisms derived from the *CCS* gene have also been utilised to distinguish between red and yellow fruit varieties and has therefore been utilised in MAS breeding (Lefebvre et al., 1998). In tomato, MAS breeding was utilised to select for tomatoes with a deep red colour caused by a high lycopene content. This was achieved using molecular markers associated with the *B*-gene in the tomato mutant *old gold crimson* (1.3.4.1) (Park et al., 2009).

1.5.5. Genetic engineering

Conventional breeding strategies, such as hybridisation, and strategies such as mutagenesis are often time consuming, unpredictable, and restricted to sexually compatible individuals. These limitations have led to the development of more targeted approaches such as genetic engineering. Genetic engineering refers to the manipulation of genes either by the transfer of genetic material to another organism or by changing the sequence of a gene. Genetic material can be transferred into a plant via the aid of a plant specific bacteria. Typically, *Agrobacterium tumefaciens* mediated gene transfer, or alternatively direct DNA transfer using particle bombardment and electroporation approach. There has been a vast wealth of studies carried out that have focussed on the use of genetic engineering strategies to manipulate the carotenoid biosynthesis genes in plants, specifically tomato.

The *DXS* gene has been targeted for genetic manipulation in the past due to its influence on isoprenoid biosynthesis. In tomato, a bacterial *DXS* under the control of the *Capsicum* fibrillin promoter led to a 1.6fold increase in carotenoid content. Phytoene and β -carotene were the most affected, each with a 2.4fold increase (Enfissi et al., 2005). Similar results were also

achieved in potato when a bacterial *DXS* was expressed, a 2fold increase in total carotenoid content was obtained, including a 6-7fold increase in phytoene (Morris et al., 2006).

The phytoene synthase gene has been the most extensively targeted gene in the carotenoid biosynthesis pathway. It has been overexpressed in *Arabidopsis*, canola, carrot, maize, potato, rice, tomato, and wheat. In *Arabidopsis*, the *PSY* gene was expressed under a seed-specific promoter which led to a 45 fold increase in β -carotene (Lindgren et al., 2003). Alternatively, constitutive expression of *PSY* did not affect green tissue but non-photosynthetic calli and roots experienced 10 and 100-fold increases in carotenoid content. Furthermore, expression of *PSY* under a storage root-specific promoter cloned from yam resulted in carotenoid accumulation in white carrots, although not to the same extent as the orange phenotype (Maass et al., 2009b). In canola, seed-specific over expression of a bacterial *PSY* resulted in 50-fold increase in carotenoids in the seeds (Shewmaker et al., 1999). Transgenic potatoes expressing the bacterial *PSY* displayed just over 6-fold increases in carotenoid content, again, with β -carotene becoming more predominant when compared to wild-types, as well as, lutein (Ducreux et al., 2005). The early stages of the development of 'golden rice' utilised the constitutive expression of a daffodil *PSY* to produce phytoene (Burkhardt et al., 1997). However, there has been better success when using constructs expressing additional carotenoid biosynthesis genes such as lycopene cyclase and lycopene desaturase (Ye et al., 2000).

In tomato, the first attempts to express a transgenic *PSY* under a constitutive promoter resulted in high expressers with elevated carotenoid content that displayed dwarfism. This was due to the diversion of substrates away from GA (Fray et al., 1995). This problem was rectified when the a bacterial *PSY1* gene (*crtB*) was expressed under the fruit-specific polygalacturonase promoter region resulting in 2-4-fold increases in fruit carotenoid content (Fraser et al., 2002).

Pepper is far behind in the world of plant biotechnology due to its severe recalcitrant morphogenic nature and genotypic dependence. While other members of the *Solanaceae* family like tomato, potato, tobacco, and petunia have proved very cooperative in tissue culture, pepper is very difficult to regenerate. The most success in plant regeneration has been achieved through organogenesis. In addition to this, sexual incompatibilities have been observed in domesticated and wild-type varieties. This therefore further decreases the gene pool available to plant breeders hindering genetic exchange. In addition, pepper plants are highly heterozygotic and thus lack the ability to propagate in a vegetative or asexual fashion, this results in cross-pollination (Kothari et al.). Despite these drawbacks there has been progress in the development of transgenic pepper plants. A study by Liu et al (1990) showed transformation of seedlings

which were expressing a GUS reporter gene. This was achieved using an *Agrobacterium* mediated gene transfer method (Liu et al., 1990). Presently, *Agrobacterium* mediated transformation was utilised to express an antisense aminotransferase gene present in the capsaicin biosynthesis pathway. This resulted in the reduction of vanillylamine production in *C. frutescens* (Gururaj et al., 2012). This therefore illustrates the slow but sure progression in pepper transgenesis.

1.5.6. Recent advances in breeding strategies: CRISPR CAS

The CRISPR-cas system of genome targeted modification represents a recent development in plant breeding. This technique utilises the prokaryotic adaptive immune system involving Clustered, Regularly Interspaced, Short Palindromic Repeats (CRISPR) which are widespread in bacteria. This function is to protect themselves against invading viral and plasmid DNAs. This works by a CRISPR associated protein with endonuclease activity, cas9, which binds synthetic RNA and can be used as an RNA-guided endonuclease genome editing tool (Shan et al., 2013). This technique was employed in rice to target the PDS gene and attempts produced efficient and targeted mutagenesis. The knockout in the PDS gene was achieved and minimal off target effects were found (Shan et al., 2013). A schematic outlining the action of this strategy can be seen in Figure 1.26.

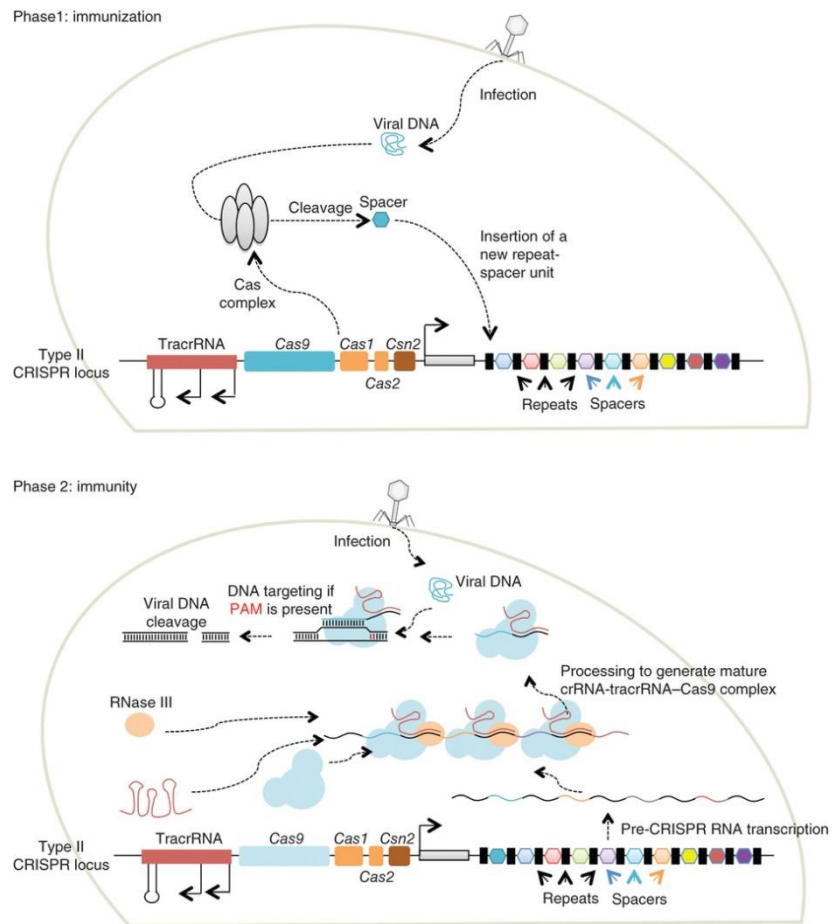


Figure 1.26. Functioning of the type II CRISPR-Cas systems in bacteria.

Phase 1 is the immunisation phase where the CRISPR stores the molecular sequence of a previous infection by the integration of invading DNA into the CRISPR locus as spacers. Phase 2 is the immunity phase where the bacterium uses this stored information to defend against the invading DNA. This is carried out by transcribing CRISPR RNAs (crRNAs) that find DNA complementary to the spacers and cleave up the nucleic acids (adapted from Mali et al., 2013).

1.6. Aims and objectives of this study

The aim of this project was the elucidation of underlying molecular and biochemical mechanisms associated with colour intensity and colour retention in fresh and dried chilli pepper (*Capsicum annuum*).

Objective 1: To characterise colour intensity among a colour diversity panel.

The pigment profile was analysed in a commercially-supplied colour diversity panel throughout ripening. This activity will enable association of colour intensity phenotypes with amounts and/or compositions of pigments accumulated in chilli pepper fruit (Chapter III).

Objective 2: To identify components responsible for the colour intensity phenotype.

Lines were selected from a colour diversity panel based on perturbed carotenoid content. These lines were then analysed at a gene, transcript and metabolite level to gain a deeper understanding of the regulatory mechanisms occurring in the carotenoid biosynthesis pathway (Chapter IV). Sequestration mechanisms were also examined using subchromoplast fractionation.

Objective 3: To characterise colour retention phenotype among a colour diversity panel.

Lines from a colour diversity panel were used to design a protocol which would speed up colour loss in chilli pepper during storage thus allowing colour retention to be analysed more rapidly (Chapter V).

Objective 4: To identify mechanisms responsible for colour retention phenotype.

Oxidative and degradative mechanisms were investigated to understand processes present which were protecting or degrading the carotenoid pigments. This was carried out using volatile analysis (Chapter V).

Chapter 2. Materials and Methods

2.1. Plant material

All chilli lines were grown in a light and temperature controlled greenhouse. Supplementary lighting was used with an intensity of $110\mu\text{mol. m}^{-2}. \text{sec}^{-1}$ on a 16/8 hour light/ dark cycle. The temperature during the day was 25°C and during the night 18°C.

2.2. Harvesting/ sampling

2.2.1. Fruit material

Ripe fruit were selected based on showing characteristics of optimal ripeness. This was represented by fully red colour fruit which had not experienced any drying out of the bottom of the fruit or skin. Seeds were sown in September 2012 and harvested March –May 2013.

Flowers were tagged at anthesis and mature green stage was around 55 days post anthesis (dpa). The fruit were then tagged again at breaker. This was characterised by the first sign of red colour appearing. Seeds were sown in June 2013 and harvested November 2013-January 2014.

2.2.2. Leaf material

Three leaves per plant were collected and pooled. Typically, unless stated, a minimum of three plants per line were used. Thus this constituted at least three biological replicates. The leaves were collected at the expanding leaf stage of development, frozen in liquid nitrogen, and stored at -80.

2.2.3. Storage

A sample set of four fruits from each plant were pooled and a minimum of three different plants were used as biological replicates. All fruits were harvested, deseeded, frozen in liquid nitrogen, and stored at -80°C. The samples were freeze dried and stored at -20°C. Ground powder was

obtained using a tissue lyser (Qiagen), with two metal balls (3mm). The microcentrifuge tube holder and tubes (2ml) were chilled on dry ice (30 min). The tissue lyser ground the material at 50Hz (2 min), three times, or until samples were ground into a fine, homogenous powder. This material was used for LC-MS and HPLC analysis.

Material used for RNA and DNA extraction was ground to powder, using the tissue lyser method, from fruit stored at -80°C.

2.3. Extraction of carotenoids

Ground chilli powder (10mg) was added to a microcentrifuge tube (2ml). Methanol (200µl), chloroform (500µl), and distilled water (200µl) were added, vortexed, and incubated on ice (20 min). The samples were centrifuged at 12000 rpm (5 min). The chloroform layer (bottom) was removed and added to a fresh tube (2ml). Chloroform was added to the original tube (500µl) and the sample was vortexed and incubated on ice (20 min). Again, the chloroform layer was removed and pooled with the previous chloroform fraction. The chloroform was evaporated using a rotary evaporator (GeneVac Ez-2 plus; 30 min) and the dried carotenoid extract was stored at -20 until ready to run on the HPLC.

2.4. Separation of carotenoids

Quantification of the carotenoids and α -tocopherol was achieved by High Pressure Liquid Chromatography with a photodiode array (HPLC-PDA). HPLC grade acetate (100µl) was used to resuspend the dried carotenoid extract. The sample was centrifuged at 12000 (5 min) and added to a glass insert (50µl) in a glass vial with a screw cap.

HPLC was carried out on a Waters Alliance system (2695) with a photodiode array detector (Waters 996). A reverse-phase C₃₀, 5µm column (250 x 4.6mm) with accompanying guard (YMC Inc., USA) was used and the temperature of the column was maintained at 25°C with a column chiller (Jones Chromatography 7955).

Solvents used were: solvent A-methanol, solvent B-0.2% ammonium acetate, and solvent C-*tert*-methyl butyl ether (MTBE). The elution gradient used was 95% A, 5% B, isocratically (12 min),

80% A, 5% B (12 min), followed by a linear gradient to 30% A, 5% B, and 65% C (30 min). The extract (5 μ l) was injected at a flow rate of 1ml/ min (Fraser et al., 2000).

2.5. Identification and quantification of carotenoids

The data were collected and analysed using Empower software (version 2). The area of the peak obtained from the samples was compared to the area of a known amount of standard carotenoid to allow quantification from linear dose response curves.

2.6. Identification of carotenoids and their esters

To complement the UV/vis and carotenoid spectra, mass spectrometry (MS) was employed to facilitate improved identification and quantification of the carotenoid esters. Carotenoids were extracted and ran on the HPLC-PDA using the above method (2.3 and 2.4) and 1ml fractions were collected from the 10 to 40 min during the 60 min run. Thus collecting the main peaks from the carotenoid profile. Samples were run in triplicate. The fractions were dried down and resuspended with ethyl acetate (50 μ l) and the three replicates were pooled and added to a glass insert within a glass vial with a screw cap. The samples underwent HPLC with an ultimate 3000 with DAD (Dionex) before an on-line MS as described (Perez-Fons et al., 2011). The column used was C₃₀, 3 μ m (150 x 2.1mm) with a guard. The mobile phase was altered to help ionisation (by addition of formic acid) and consisted of: solvent A-methanol (0.1% formic acid) and solvent B-MBTE (0.1% formic acid). The elution gradient used 100% A (5 min), 95% A (4 min), followed by a linear gradient to 25% A (30 min). The gradient then went to 10% A (10 min). The extract (20 μ l) was injected at a flow rate of 0.2ml/min. The ionisation mode used was Atmospheric Pressure Chemical Ionisation (APCI) Maxis (Bruker) operating in a positive ion polarity (Thermo Scientific, San Jose, California, USA). The capillary and the vapourisation temperatures were set to 200°C and 400°C, respectively. A mass scan from 100-1600 *m/z* was performed. Quantification was carried out in with the same method as HPLC-PDA (2.5).

2.7. Metabolite profiling

The material used in this experiment was mature green, turning, and ripe stages of ripening for the R1, R3, and R7 lines. Ground chilli powder (10mg) was added to a microcentrifuge tube (2ml). Methanol (400 μ l) and distilled water (400 μ l) were added and vortexed. The samples were then inverted at room temperature (1 hr). Chloroform was added (800 μ l) and the samples were vortexed and centrifuged at 12000 rpm (5 min). Both phases, polar (top) and non-polar (bottom), were collected.

The polar extract (20 μ l) was transferred to a glass vial (Agilent) and ribitol standard (10 μ l; 1mg/ml in methanol) was added. The methanol was evaporated using a rotary evaporator (GeneVac Ez-2 plus; 1-2 hr) on HPLC fraction setting. Myristic-d₂₇ acid (1mg/ml in chloroform; 10 μ l) was added to the non-polar phase and the rotary evaporator was used to dry down (40 min). Samples were stored at -20°C until derivatisation.

Methoxyamine-HCL (MEOX; 30 μ l; 20mg/ml in pyridine anhydrous) was added to the samples and incubated at 40°C (1 hr), then N-methyl trimethylsilyl trifluoroacetamide (MSTFA; 70 μ l) was added and incubated at 40°C (2 hr).

Gas chromatography-mass spectrometry was accomplished using an Agilent 7890B gas chromatograph system with a 5977A MSD. Samples were injected (1 μ l) with a split/ splitless injector at 290°C with a 20:1 split as previously described in (Enfissi et al., 2010). The internal standard was used to retention time lock the samples. The gas chromatography oven was kept at 70°C (4 min) before ramping at 5°C/min to 310°C. This final temperature was maintained (10 min) making a total of 60 min. The GC-MS interface was set (290°C) and the MS ran in full scan mode using 70 eV EI+ and scanned from 50-800 D. To identify the compounds in the chilli pepper profile an MS library was constructed from in-house standards, in addition to the NIST 11 MS library. To facilitate the determination of retention indices (RIs) a retention time calibration on all standards was carried out. Thus RIs and MS allowed identified by comparison with the MS library. AMDIS V2.71 was used to identify peaks and create a report. The reports generated by AMDIS were combined with ID align and transferred to Excel (Microsoft Office 2013) to normalise the data using the internal standards.

2.7.1. Statistical analysis and data visualisation

The normalised data was then analysed using PCA (principle component analysis) in SIMPCA P V13 (Umetrics AB). PCA is a statistical tool to visualise the variance within a data set according to its principle components. The two graphs produced show the distribution of samples according to their similarities/differences (score plot) and the variables causing the separation (loading plot). The axis on both graphs is a statistical score awarded during the analysis. One-way ANOVA with Dunnett's post-hoc test was carried out using SPSS 19 (IBM). Statistical differences ($P \leq 0.05$) were determined for the metabolites and plotted in a heat map using excel. These data were then overlaid on a pathway diagram using BioSynLab (Royal Holloway, University of London).

2.8. Extraction and analysis of nucleic acids

2.8.1. Optimised DNA extraction

The Qiagen DNeasy plant mini kit was used to extract and purify genomic DNA from chilli pepper. The material used were expanding leaves which were collected as mentioned previously (2.2.2). The leaves had been stored at -80 and were ground using a tissue lyser (50Hz; 2 min). The tube holder and the tubes has been cooled on dry ice (30 min). Plant material remained frozen throughout the grinding and weighing procedures and 100mg of tissue was used for extraction. This was to ensure high yields as well as minimal degradation. The plant material is first lysed in AP1 buffer (400 μ l) and the RNA present was degraded using RNase A (4 μ l). The samples were incubated at 65°C (10 min) and inverted several times to ensure all cells were lysed. Buffer P3 (130 μ l) was added and the samples were incubated on ice (5 min). This step is to precipitate detergent, proteins, and polysaccharides. The samples were centrifuged at 12000 rpm (5 min) and the supernatant was added to the QIAshredder mini spin column and centrifuged at 12000 rpm (2 min). This removes precipitates and cell debris. The flow-through was transferred to a new tube with care not to disrupt the pellet. Buffer AW1 (1.5 x volume of lysate collected) was added to the lysate and mixed thoroughly. A proportion of the lysate was then added a DNeasy mini spin column and was centrifuged at 8000 rpm (1 min). The flow-through was discarded and the remaining lysate was added and centrifuged again. The flow-through was discarded and the column was placed into a new microcentrifuge tube. Buffer AW2 (500 μ l) was added to the

column and centrifuged at 8000 rpm (1 min), the flow-through was discarded and AW2 was added again (500µl) and centrifuged at 8000 rpm (2 min). These steps are carried out to wash the DNA extracted. The column was then transferred to a new microcentrifuge tube and centrifuged at 8000 rpm (2 min) to ensure there was no ethanol left. The AE elution buffer (40µl) was added to the column and centrifuged at 8000 rpm (1 min). This step was repeated giving a final total of 80µl. Samples were measured on the nanodrop for concentration and purity, and stored at -20°C. Purity was given based on the 260/280 ratio.

2.8.2. Optimised RNA extraction

The Qiagen RNeasy plant mini kit with RNase-free DNase was used to carry out extraction of RNA from fruit tissue. The fruit material used was harvested as described in section 2.2. 100 mg of fresh material was used and care was taken to ensure material stayed frozen throughout the grinding and weighing procedure. RLT buffer (450µl; containing 14.3M β-mercaptoethanol (10µl)) was added to the ground fruit material and vortexed. This causes the cells to lyse. The lysate is then transferred to the cells to a QIAshredder spin column and centrifuged at 12000 rpm (2 min). The flow-through was transferred to a new microcentrifuge tube taking care not to disturb the pellet. Ethanol (0.5 x volume of lysate collected) was added and mixed. A proportion (650µl) was added to an RNeasy spin column and centrifuged at 8000 rpm (15 sec). The flow-through was discarded and the remaining lysate was added and centrifuged at 8000 rpm (15 sec) and the flow-through was discarded. The RW1 buffer (350µl) was added to the column to wash the membrane. The column was centrifuged at 8000 rpm (15 sec). The flow-through was discarded and then RDD buffer (80µl; containing RNase-free DNase I (10µl)) was added to the membrane and incubated at room temperature (15 min) to ensure degradation of any contaminating DNA. RW1 buffer (350µl) was then added again and centrifuged at 8000 rpm (15 sec). The flow-through was discarded. RPE buffer (500µl) was added to the column and centrifuged at 8000 rpm (15 sec) to wash the membrane. The flow-through was discarded and more RPE buffer was added (500µl) the centrifugation step was repeated. If the column membrane was still very discoloured (red or green) then the column was washed with pure ethanol (500µl) and centrifuged at 8000 rpm (1 min). This was repeated until the membrane had returned to a more neutral colour. The column was transferred to a new microcentrifuge tube and centrifuged at 8000 rpm (1 min) and then left to sit on the bench at room temperature (5 min). This was to ensure all ethanol had evaporated. The column was transferred to a new

microcentrifuge tube and RNase-free water was added (50µl). The column was centrifuged at 8000 rpm (1 min) and the flow-through was re-added to the column and centrifuged again. Total amount collected was 40µl. The concentration and purity was measured on a nanodrop, samples with a 260/230 and a 260/280 ratio as close to 2 were selected. The integrity of the RNA was assessed by performing electrophoresis on an agarose gel (1%).

2.9. Sequencing of isoprenoid biosynthesis genes

In order to sequence the *PSY1*, *PSY2* and *DXS* genes in lines R3 and R7 primers were designed to create overlapping fragments. These primers were designed on sequences available on National Centre for Biotechnology (NCBI) for sweet pepper (*PSY* and *DXS*) and tomato (*PSY2*).

2.9.1. Primer design

Primers were designed using NCBI/ Primer-BLAST and Primer3Plus (<http://www.bioinformatics.nl/cgi-bin/primer3plus/primer3plus.cgi/>). Primer design specifications: primer melting temperatures (T_m) were between 50-60°C, maximum 5°C difference in primer T_m, 500-3000bps for fragment length, 10-30bp primer length, and 40-60% GC content. Primers were supplied by Eurofins MWG Operon, UK. Amplicons with a length over 1000bps had a higher concentration of MgSO₄ added to reactions. The primer pairs used to sequence the *PSY2* gene are displayed below (Table 2.1, Table 2.2, and Table 2.3).

Table 2.1. Primers used to sequence *PSY1*.

Name	Forward	Reverse	Annealing T _m
P1	TCTTTGACATTCTTTGCGGC	ACACTTTCTGGAGGTAATGGGA	50
P2	GTGTGTGTTGGTCTACTGGG	AGGCCACTCTCAAATTCTATTCT	53
P3	TCTTTGACATTCTTTGCGGC	AGGCCACTCTCAAATTCTATTCT	53
P4	CACTACAGCTCCCGCTATGC	ACACTTTCTGGAGGTAATGGGA	53
P5	TGCAGAGTACGCAAAGACGT	AGCTGATTTGCGATCCCCAA	53
P6	CTCAGGAAGTCTATAATGCTGGT	CCCAAGCAAGAACCAAACTCC	53
P7	GATGCTGCTTTGTCCGACAC	AGCAAATGACGACACCCAGT	53
P8	CTCAGGAAGTCTATAATGCTGGT	ATGTCAAATGGCCGTCCACT	53
P9	GGCAGGTCTATCCGACGAAG	AGCAAATGACGACACCCAGT	53
P10	GGCAGGTCTATCCGACGAAG	CCAGTTTTCGTGCCCATAGC	53
P11	TACCGCAGGATACTGGACGA	CCAGTTTTCGTGCCCATAGC	53

Table 2.2. Primers used to sequence *PSY2*.

Name	Forward	Reverse	Annealing Tm
F1	ACCAGTCTGACCTCAACCTT	CCAACCTGCGAATAGCAACG	56
F2	GGTGGAAACTACAAGAGAAGAGA	CCAAGAACCAAATCAGCAAACAG	57
F3	ACCCTTTTCCTTTCTAGACAGT	ACATCACCGTATATTGCCAG	56
F4	ACCCTGCTAATGACTCCAGAC	CCGCCCGCTGAAAATATCTT	56
F5	TCCTGTTTCGTTTGGCAGTC	GCAAATATGTCTTCGCCGGA	56
F6	CAGGGCTCTCCGGCGAAG	AACAGCAACGATGCCAACAC	56

Table 2.3. Primers used to sequence *DXS*.

Name	Forward	Reverse	Annealing Tm
D1	ACACCACTTACCATTGAGGGG	CACTGCCACTGTCCTGTTC	55
D2	AGTGACAGTAGCACCAGCAC	AGAACTACATGTGGGAGAACTGT	55
D3	TTGTAGAATGCTCATGTTGAACCA	TCCGACCGCTTAGTAAATCCA	55
D4	TGTTGCAGTCATATCCTCACA	TGCGACTTCTCTTAGTTCTCTGA	55
D5	CCAGTTCCTCCTGTTGGAGC	TTTAAGGCGGTCTAGTGGCG	55
D6	AGGTCCTGTAAGTATCCATGT	TGCACAGAAAGGTTTGAGGC	55
D7	AGCAGATAAAGACATTGTTGCAA	ACTGCTGAGCCGTATCCCAA	
D8	ACTTTCATGGCATGTCTCCC	ATTCTTTACAGTTCTTGCATCT	

Amplification was performed on Techgene thermocycler (Techne, UK). The tubes were incubated at 95°C (2 min) to activate the DNA polymerase and denature the DNA template. There was then 30 cycles of: denaturing (95°C; 20 sec), annealing (approximately 55-60 depending on Tm of primers used; 10 sec), and extension (72°C; 15 sec for fragments with 500-1000bps and 20 sec for fragments with 1000-3000bps). PCR reactions were carried out using Illustra puReTaq Ready-to-go PCR beads (GE Healthcare). The bead contains 200mM dNTP (dATP, dCTP, dGTP, and dTTP) in 10mM Tris-HCl buffer (pH 9.0) with 50mM KCl and 1.5mM MgCl₂. In addition to, 2.5 units of puReTaq DNA polymerase. Genomic DNA (50ng) was added to the PCR along with a forward and reverse primer (25pg) as well as sterilised water up to 25µl.

2.9.2. Nucleic acid analysis

The PCR products were then subjected to gel electrophoresis. The gel (1% w/v) consisted of agarose gel (0.4g) in TAE (50ml; Tris, acetic acid, and EDTA), and GelRed (5µl; Biotium, UK). A DNA hyperladder (1kb; Promega) was used to identify the length of the amplicon. Samples were loaded in the wells of the gel with Blue/orange Loading Dye (X6; Promega, UK). The gels were run at 100V (20 min). The bands were visualised using an imaging system (Syngene, UK).

2.9.3. Cloning of PCR amplicons

The PCR products were ligated into vectors to allow the amplicons to be cloned. The vectors used were pCR 2.1 TOPO cloning vectors. The PCR product (2µl), salt solution (1µl), TOPO vector (1µl), and sterile water (2µl) were added to an autoclaved microcentrifuge tube (0.5ml) and incubated at room temperature (5 min). This was to allow the amplicon to become ligated with the vector. The TOPO cloning reaction (2µl) was added to a vial of One Shot TOPO10 chemically competent cells. *E. coli* cells, mixed gently and incubated on ice (20 min). The cells were then heat shocked at 42°C (30 sec) and transferred immediately back to ice. S.O.C medium (250µl) was added to the cells and the cells were incubated horizontally at 200 rpm at 37°C (1 hr).

Two aliquots of the transformed cells were then spread on LB agar plates (50µl and 100µl). The plates contained kanamycin (50µg/ml), 5-bromo-4-chloro-3-indolyl-β-D-galactopyranoside (X-gal; 100mg in 2ml dimethylformadine), and Isopropyl β-D-1-thiogalactopyranoside (IPTG; 240mg in 10ml filter sterilised dH₂O). Each plate (20ml) contained 100µl of IPTG and 40µl of X-gal. The plates were incubated overnight at 37°C.

White colonies (positive) were picked from the plates and used to inoculate LB media (5ml) which contained kanamycin (50µg/ml) and were again incubated over night at 200rpm (37°C). Glycerol stocks of the transformed cells were produced in order allow long-term storage. The bacteria culture (1.5ml) was added to sterilised glycerol (0.5ml), frozen in liquid nitrogen and stored at -80°C.

The remaining liquid culture was subjected to a miniprep to isolate the plasmid DNA from the bacterial cells. This was carried out using the Wizard *Plus* SV Minipreps DNA purification system kit (Promega, UK). The liquid culture was centrifuged at 5000 rpm (5 min) with Eppendorf centrifuge 5810R. The supernatant was discarded and the pellet was resuspended into a microcentrifuge tube (1.5ml) with cell resuspension solution (250µl). Cell lysis solution (250µl) was then added, the tubes were inverted to mix causing the cells to lyse and incubated at room temperature (5 min). Alkaline protease solution (10µl) was added to inactivate any endonucleases and other proteins released during cell lysis. This was followed by neutralisation solution (350µl) and the samples were inverted 4 times. The samples were then centrifuged at 12000 rpm (15 min). The cleared lysate (supernatant) was transferred to a spin column by

decanting and care was used not to disturb the pellet. The column was centrifuged at 12000 rpm (1 min), and again the flow-through was discarded. Column wash (750µl) was added and centrifuged at 12000 rpm (1 min), and the flow-through was discarded. This was repeated with 250µl and centrifuged for 2 min. The column was placed into a new microcentrifuge tube, centrifuged (1 min), and placed into another new microcentrifuge tube. Nuclease-free water was added (50µl) was to the column and centrifugation at 12000 rpm (1 min) allowed elution of the plasmid DNA from the column. This was repeated so a total of 100µl of plasmid DNA was eluted. The DNA was stored at -20°C. Sequencing of the PCR products was carried out by Eurofins MWG Operon, UK. Construction of the contigs and gene sequence were carried out using SeqMan Pro and Seqbuilder (Lasergene, DNASTar, UK). Sequencing of the genes were carried out in duplicate whereby the DNA material was extracted from different plants and any areas of discrepancy carried out in triplet.

Construction of the 3-D protein models was performed using an online program SWISS-MODEL (<http://swissmodel.expasy.org/>, Basel, Switzerland) (Biasini et al., 2014).

2.10. Transcription factor analysis

Transcription factor analysis was carried out by Syngenta (personal communication, Syngenta, UK).

2.11. Gene expression analysis

Quantitative real-time PCR was used to measure the transcript levels of key carotenoid related genes. This was performed in an effort to characterise gene expression profiles. The RNA material used was extracted as described previously (2.8.2). Primers were designed to span amplicons of 100-150bps in length. These primers were around 10-30bps in length, had 40-60% GC content, and Tms of 50-60°C. They were provided by Eurofins MWG Operon, UK. The primers employed for each of the carotenoid biosynthesis related genes mentioned in this study can be found below (Table 2.4).

Table 2.4. Primers designed for qPCR on carotenoid biosynthesis related genes.

Gene	Forward	Reverse
PSY1	TACCGCAGGATACTGGACGA	CTGATTTTCATGTTCTTGTAGAAGGC
PSY2	AGGAGTCGCAGAATTGAGCTCT	GTGAAGAAGAAGTTAACTTGGGGG
DXS	GTTGAAGGGGAGAGAGTGCC	CAGAAGCAGCAGCCAAACAG
CCS	TACTGGCACGGGTTCCCTTC	TGCTAGATTGCCAGCAGTT
CHY2	GGATGGCCTACATGTTTGTTTAC	TCCGAGTGATGAAGCTGATGTG
rsAct	TGATTTGGCCTGATCAACAA	AAAGGCCCGGGATATACAAC

The amplicons created were cloned in to a plasmid using the TOPO TA cloning system previously described in section 2.9.3. These plasmids were then utilised to create calibration curves which were run concurrently with each qPCR reaction. This was achieved by measuring the concentration of the plasmid and creating a curve which had 5 points of known concentration that covered the range of transcript concentration present in the samples. cDNA was generated using Illustra Ready-to-go RT-PCR Taq beads (0.5 ml; GE Healthcare, UK). The PCR reaction contained RNA (200ng), 25 μ M oligo (dT)₁₅ (Promega), and sterile dH₂O. The tubes were transferred to the thermocycler and incubated at 42°C (30 min) and then denatured at 95°C (5 min). The cDNA (15-25ng) created were added to a qPCR reaction which used Quantifast SYBR Green PCR kit (Qiagen, UK), in addition to forward and reverse primers (10 μ M), and the SYBR Green Master Mix (10 μ l), and the qPCR was carried out using a Research Rotor-Gene RG-3000 thermocycler (Corbett Life Sciences, UK). The thermocycler began with 95°C (15 min), and then carried out 40 cycles of 94°C (15 sec), 50°C (30 sec), and 72°C (15 sec). All samples were carried out in triplet. A melt curve was generated for every reaction to ensure specific binding of the primers. The efficiency of the standard curve was between 0.95-1.05 and the R² value was above 0.985. The reference gene, ATP synthase subunit alpha F1 complex, used in these studies was selected and tested using a geNorm kit (Primer design, UK).

Data analysis was carried using the delta delta Ct ($\Delta\Delta$ Ct) method. The Ct value provides a number for the amount of copies of the transcript present. Calculations were carried out as seen below (Equation 2.1). Thus giving results based on relative amounts.

$$\Delta Ct = Ct \text{ target} - Ct \text{ reference gene}$$

$$\Delta\Delta Ct = \Delta Ct \text{ calibrator} - \Delta Ct \text{ sample}$$

$$2^{-\Delta\Delta Ct}$$

Equation 2.1. Calculations for the delta delta Ct method.

2.12. Subchromoplast fractionation

Subchromoplast fractionation was utilised to allow the locations of carotenoid storage to be elucidated. This method was adapted from Nogueira et al., 2013.

Fresh chilli pepper (30g) from a medium (R4) and a high intensity (R7) line were cut into small pieces, covered with foil, and left overnight (4°C). The chilli pepper was homogenised with extraction buffer (0.4M sucrose, 50mM Tris, 1mM EDTA, and 1mM DTT) at pH 7.8 in a blender (Waring products, UK). This was carried out three times (2 sec). The resulting mixture was filtered through 4 layers of muslin. The filtrate was then transferred to two large centrifuge pots (500ml), one for each line. The pots were then filled up to around 350ml with extraction buffer and balanced ($\pm 1g$). The pots were centrifuged at 5000 g (4°C; 10 min) using a Sorval RC5C centrifuge (Thermo scientific, UK) with a GSA-3 rotor which had been precooled. The supernatant was removed and the pellet was resuspended in extraction buffer and placed into two small centrifuge tubes (500ml). The tubes were then centrifuged at 9000 g (10 min) using the same Sorval RC5C centrifuge with a precooled GSA-5 rotor. The supernatant was discarded and the pellet was resuspended in 3ml of 45% sucrose gradient buffer (sucrose 45% (w/v), 50mM Tricine, 2mM EDTA, 5mM sodium bisulphate, and 2mM DTT). The tubes were vortexed and homogenised with a hand held potter homogeniser (VWR, UK).

The sucrose gradients were constructed whereby chilli pepper extract in 45% sucrose (8ml) was added to the bottom of a Ultra-Clear centrifuge tube (38.5 ml; Beckman Coulter, UK), this was then followed by 35% sucrose gradient buffer (6ml), 20% sucrose gradient buffer (6ml), 15% sucrose gradient buffer (4ml), and 5% sucrose gradient buffer (8ml). Three tubes were used for each line so approximately 10g of fresh material was present in each tube. The tubes were then centrifuged at 100000 g (18hr $\pm 1hr$; 4°C) using a L7 ultracentrifuge with a SW28 swing out rotor (Beckman Coulter, UK). Fractions (1ml) were then collected from the top using a Minipuls 3

peristaltic pump and FC203B fraction collector (Gilson, UK). Carotenoids were extracted and analysed using methods described in sections 2.3 and 2.4.

2.13. Image analysis

The image analysis method was based on the use of computer visions systems (CVS) to obtain L^* , a^* , and b^* coordinates from RGB coordinates from a digital image as a quantitative measurement of colour. The image analysis system was designed by Syngenta. Algorithms correct for image variables due to source distance, camera own characteristics, fruit glossiness, and fruit curvature. The CVS consists of a suspended digital camera (Canon EOS Digital Rebel XT with lens: Canon 10-12mm Zoom Macro and Canon 50mm Macro) above an imaging igloo. The igloo has two fluorescent lamps (Westcott Spiderlite TD5 Location Kit with Westcott 27W/ 100V Daylt FLOU lamps), the angle between the axis of the lens and the sources of illumination are 45° (Figure 2.1).

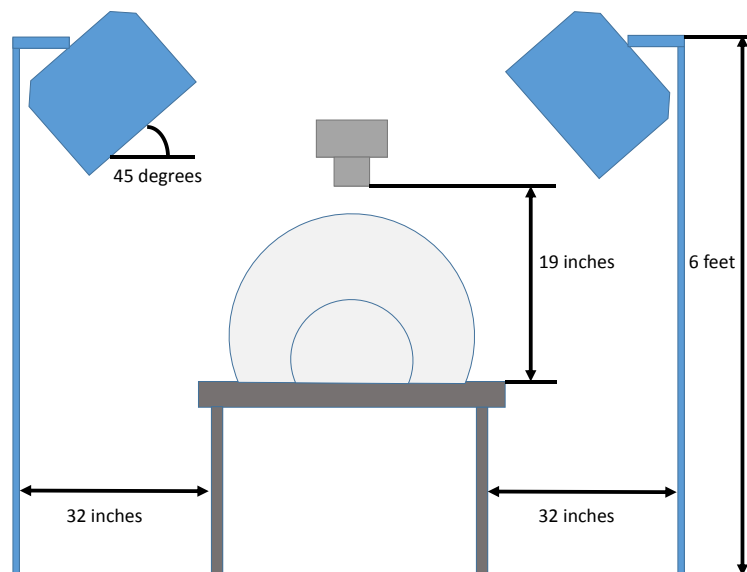


Figure 2.1. Image analysis system.

The camera is connected to the computer via a USB connector where it is operated remotely. The software used for the camera-to-computer communication is EOS Utility and the software used for image viewing and editing is Digital Photo Professional version 3.8.1.

Image analysis relies on keeping the variables constant. Therefore the light has to be the same intensity at every session otherwise the images cannot be compared from session to session. The images were taken in a blacked out room and the lights are switched on for 20 minutes to keep the light intensity constant.

2.13.1. Camera settings

The camera was set to autofocus on the lens and manual on the dial. The lens was set to 50mm and the computer was used to set up the following variables (

Table 2.5).

Table 2.5. Remote camera settings.

Variable	Setting
Mode	Manual (M)
Shutter speed	1/6
Aperture	F14 (whole chillies) F20 (chilli powder)
ISO	100
White balance	Custom ()
Metering mode	Evaluating ()
Lens focus mode	Automatic Focus <AF>
Image quality	Large Fine ()
Image type to save as	JPEG (.JPG)

2.13.2. Camera calibration

The camera was calibrated to a white balance (Photoflex EZY grey balance) and colour card (X-Rite Digital Colour Checker) (Figure 2.2). The white balance measured the RGB saturation at the

inside and the outside of the image to ensure the colour saturation was uniform throughout the image.

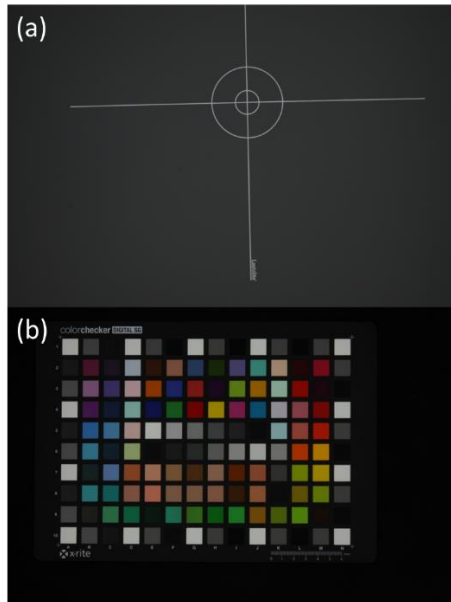


Figure 2.2. Image calibration.

(a) White balance and (b) colour card.

2.13.3. Whole fruit and powder imaging

The images of whole chilli peppers were taken using a white background and chilli powder images were taken using a black background (Figure 2.3). This is because the shiny surface of the whole chilli peppers reflected the black background causing the colour to be perceived to be darker than it was. This was not an issue with the chilli powder.

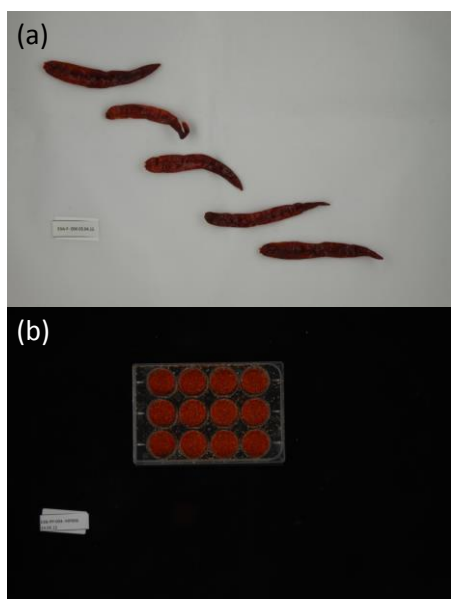


Figure 2.3. Examples of images containing (a) whole chilli peppers and (b) chilli powder.

2.13.4. Analysis

A macro was used to convert the RGB coordinates of the pixels present in the image to L^* , a^* , b^* , chroma and hue colour space coordinates. The macro was run using ImageJ and written and supplied by Rob Lind, Syngenta.

2.14. Colour loss during storage

2.14.1. Optimisation of colour loss

Chilli powder was stored for 6 weeks under different temperature and light conditions. The conditions were 15°C, 20°C, 30°C, and 40°C in a 12/ 12 light/ dark cycle. 30°C under UV (constant) and 30°C under black light. Images were taken at the start of the experiment and then every week to monitor colour change using the method described above (2.13).

2.14.2. Long storage

Whole chilli peppers were stored for 7.5 months and images were taken at the start of the experiment and then every 180 days until the end of the experiment to allow the change in colour to be monitored as described above (2.13).

2.14.2.1. Pigment analysis

HPLC-PDA was carried out on the samples that had been imaged at the start, end, and every 180 days. This was to quantify the change in carotenoids. This was carried out using the method described in sections 2.3 and 2.4.

2.14.2.2. ASTA

ASTA measurement was carried out as an alternative measurement of colour. The method used was the ASTA 20.1 for determining extractable colour of paprika (American Spice Trade Association, 1987). This is a spectrophotometer (460nm) based assay whereby ground pepper material (100mg; obtained from the long storage experiment) was added to a volumetric flask containing acetone (100ml). The ground material was passed through an 850 μm sieve. The volumetric flask was stoppered, shaken, and left in dark (16 ± 1 hr). Three replicates were carried out for each sample. The flask was shaken and left to settle (2 min). The absorbance of a standard glass filter from the National Bureau of Standards (NBS) was measured at wavelength 465nm. The extracted chilli powder samples were measured at 460nm and acetone was used a blank.

The ASTA value was calculated by first determining the instrument correction fraction (I_f) which is an indication of instrument reliability. Then, ASTA colour can be calculated using the formula below in Equation 2.2. If the sample possessed an absorbance higher than 0.7 then the sample was diluted with acetone by factor of 2.

$$I_f = \frac{\text{NBS absorbance at } 465\text{nm}}{\text{Laboratory absorbance at } 465\text{nm}}$$

$$\text{ASTA colour} = \frac{\text{Absorbance of acetone extract} \times 16.4 \times I_f}{\text{Sample mass (g)}}$$

Equation 2.2. Equation for calculation of ASTA colour.

2.15. Volatile analysis

Chilli pepper juice extract was produced by adding water (150ml) to fresh fruit (50g) and homogenising in a blender until the seeds were no longer present (4 min). 1.5 ml was added to Cryo. S freezing tubes (4ml; Greiner Bio-One, UK) and frozen in liquid nitrogen. Six replicates from each plant were frozen and four plants per line were sampled. Two of the frozen samples were freeze dried and the dry weight to water ratio was calculated. Chilli peppers (50g) dried for three weeks in an incubator (35°C) had the same ratio of dry weight to water added to them and they were homogenised in a blender (4 min). Aliquots (1.5ml) were made and samples were immediately frozen in liquid Nitrogen.

Volatile analysis was carried out on the chilli pepper juice samples for fresh and dry fruit by Syngenta. The volatiles and semi-volatile components were extracted using a solid phase matrix approach. Then were introduced into a GC-MS via thermal desorption. This procedure was carried out at Syngenta following internal SOPs (collaborative contribution, personal communication, Aniko Kende, Syngenta).

2.16. Superoxide dismutase (SOD) assay

The superoxide dismutase (SOD) isoenzymes were visualised using a native-PAGE protein gel. The proteins were extracted from chilli pepper material from two different experiments. First batch of material came from fresh (freeze-dried), dry (incubated for 3 weeks at 35°C), and stored (90 days at 10°C) chilli peppers. The second batch of material come from chilli peppers which had been stored at 20°C for 6 weeks and the material used was from day 0 and week 6.

The proteins from dry, ground pepper powder (20mg) were extracted with sample buffer (200 μ l; 1.5M Tris-HCl (pH 6.8), glycerol (25% v/v), and bromophenol blue (0.01% w/v)), incubated on ice (10 min), and centrifuged at 12000 rpm (2 min). The protein extract (10-20 μ l) was run on a 10% running gel (Total volume 10ml; 1.5M Tris-HCl (pH 8.8), Bis-acrylamide (30% w/v), APS (10% w/v), and TEMED (5 μ l)) and a 4% stacking gel (Total volume 10ml; 0.5M Tris-HCl (pH 6.8), Bis-acrylamide (30% w/v), APS (10% w/v), and TEMED (5 μ l)). The protein extracts were run alongside high range molecular weight rainbow protein marker (GE Healthcare). This was performed at 100V through the stacking gel (20 min) and 120V through the running gel (1-2 hr). The gel was incubated with nitroblue tetrazolium (NBT (0.1% w/v); 15 min), and washed with dH₂O, and incubated with potassium phosphate buffer (100mM potassium phosphate, 0.028mM riboflavin, and 28mM TEMED; 15 min), washed again briefly with dH₂O and placed on a light box to allow photo-oxidation of the NBT.

Chapter 3. Characterisation of colour
intensity throughout ripening in red
chilli pepper lines

3.1. Introduction

Carotenoids are the abundant pigments in ripe chilli peppers, the biosynthesis and accumulation of carotenoids occurring during the ripening process are responsible for the deep red colour of the fruit. In industry, the deep red colour at the point of harvest is a highly desirable trait.

In this study the carotenoids present in the ripe fruit of a colour diversity panel were identified using HPLC and LC-MS, in order to determine whether the composition or amount of these pigments could account for the differences in colour intensity. Selected lines were studied over 6 stages of ripening to provide valuable insights into the biosynthesis and accumulation of the carotenoids identified and their association with fruit ripening. The ratio of red to yellow carotenoids was determined throughout ripening to see if there were any differences between lines with different colour intensities.

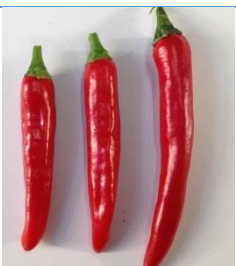
In addition, three genes, which from previous studies on fruit crops are known to have key roles in the formation of the carotenoids, *PSY1*, *PSY2* and *DXS*, were sequenced. Lines selected for having perturbed carotenoid accumulation were analysed to see if any allelic variation between lines could be attributable to colour intensity phenotypes.

3.2. Results

3.2.1. Characterisation of colour intensity phenotypes found in the chilli pepper discovery panel

The 12 chilli lines studied were part of a colour diversity panel, which were supplied by Syngenta, and were selected on the basis of their different colour intensity and colour retention phenotypes; this section will address the differences in colour intensity phenotypes. The 12 chilli lines have been characterised below in Table 3.1.

Table 3.1 Table displaying colour intensity phenotypes of the colour diversity panel supplied by Syngenta

Line	Colour intensity phenotype	Description of ripe fruit	
R1	High	Small; thick walled; smooth skin	
R2	High	Long; thin walled; wrinkled skin	
R3	Low	Small; thin walled; smooth skin	
R4	Medium	Long; thick walled; smooth skin	
R5	Medium	Medium; thick walled; smooth skin	

R6	Medium	Medium; thick walled; smooth skin	
R7	High	Long, medium walled, wrinkled skin	
R8	Medium	Small; thin walled; smooth skin	
R9	Medium	Long, thin walled, smooth skin	
R10	Medium	Medium, thin walled, smooth skin	
R11	Medium	Long; thick walled; smooth skin	

R12	Medium	Small, thin walled; smooth skin	
------------	--------	------------------------------------	---

3.2.2. Identification and quantification of free and esterified carotenoids present in red chilli pepper fruit

3.2.2.1. Identification of free and esterified carotenoids present in the ripe fruit

In this study 12 red chilli lines were subjected to HPLC-PDA to identify and quantify the carotenoids and carotenoid esters present in the fruit. LC-MS allowed elucidation of the fatty acid moieties of the esters. This was because identification of compounds, solely using co-chromatography and UV//Vis spectrometric data, can be difficult due to the complexity of the carotenoid extracts and similarities among the *Capsicum* carotenoid profiles. The extracts were not saponified to allow the carotenoid and carotenoid esters to be studied simultaneously in detail. This decision was reached based on saponification studies conducted. Saponification of extracts resulted in simplified chromatograms with the complexity of the carotenoid esters being lost. Given that the most predominant carotenoids accumulating in red pepper are capsanthin diesters this information is crucial to the characterisation of the colour intensity phenotype. Saponification also resulted in the degradation of carotenoids. For example, β -carotene levels were threefold less when saponification with 6% potassium hydroxide (w/v) was carried out at 60°C for 5 hours. Such conditions did not even achieve complete eradication of the esters present. Thus, extraction methods using saponification resulted in an underestimation of the carotenoids quantities accumulating. Therefore, non-saponified extracts provided more valuable information into the formation of carotenoid esters as a means of accumulation in the ripe fruit where colour intensity differed.

The free carotenoids being more polar than their esters eluted first, followed by the monoesters, β -carotene, and then the diesters (Figure 3.1). Peak 17 and 18 show that in some lines the first and most abundant β -carotene isomer coelutes with a capsanthin C16:0 monoester. The line used as representative chromatogram in Figure 3.1 displays peak 17 and 18 as the most predominant peak. This, however, varies between lines.

The peaks 27, 29, 30, 31 and 32 correspond to the capsanthin diesters which are typically the most abundant of all the carotenoids and esters examined (Figure 3.1). The fragmentation experienced during MS by the parent carotenoid molecule is related to the loss of fatty acids, which is how the degree of acylation was determined. Identification of the capsanthin esters is represented in Figure 3.2 as an example. The method used positive ionisation resulting in the molar mass of the compound plus a hydrogen ion $[M+H]^+$. For example, the identification of capsanthin C12:0, C14:0 produces 5 ion fragments (Figure 3.2e). The molecular weight of free capsanthin is 584.871 Da, plus H^+ resulting in identification on the MS at m/z 585 $[M+H]^+$. The dehydration of fragment ions from protonated molecules occurs in hydroxylated carotenoids resulting in parent molecule of a capsanthin diester having an m/z of 549 (Schweiggert et al., 2005). The m/z of lauric acid and myristic acid are 200.3178 and 228.3709, respectively. These lose a hydrogen when they form a bond with capsanthin and gain a hydrogen ion in the MS so they will be identified as the same mass. The total mass of the capsanthin diester had m/z 977.7948. When lauric acid is lost the m/z becomes 777.7644 due to the loss of 200.3178 and when myristic acid is lost the parent capsanthin molecule becomes 549.4081. Concurrently, when myristic acid is lost from the diesters, and lauric acid is still attached, the mass can be identified as the total mass of the diester minus myristic acid which is 749.5860 (Figure 3.2e).

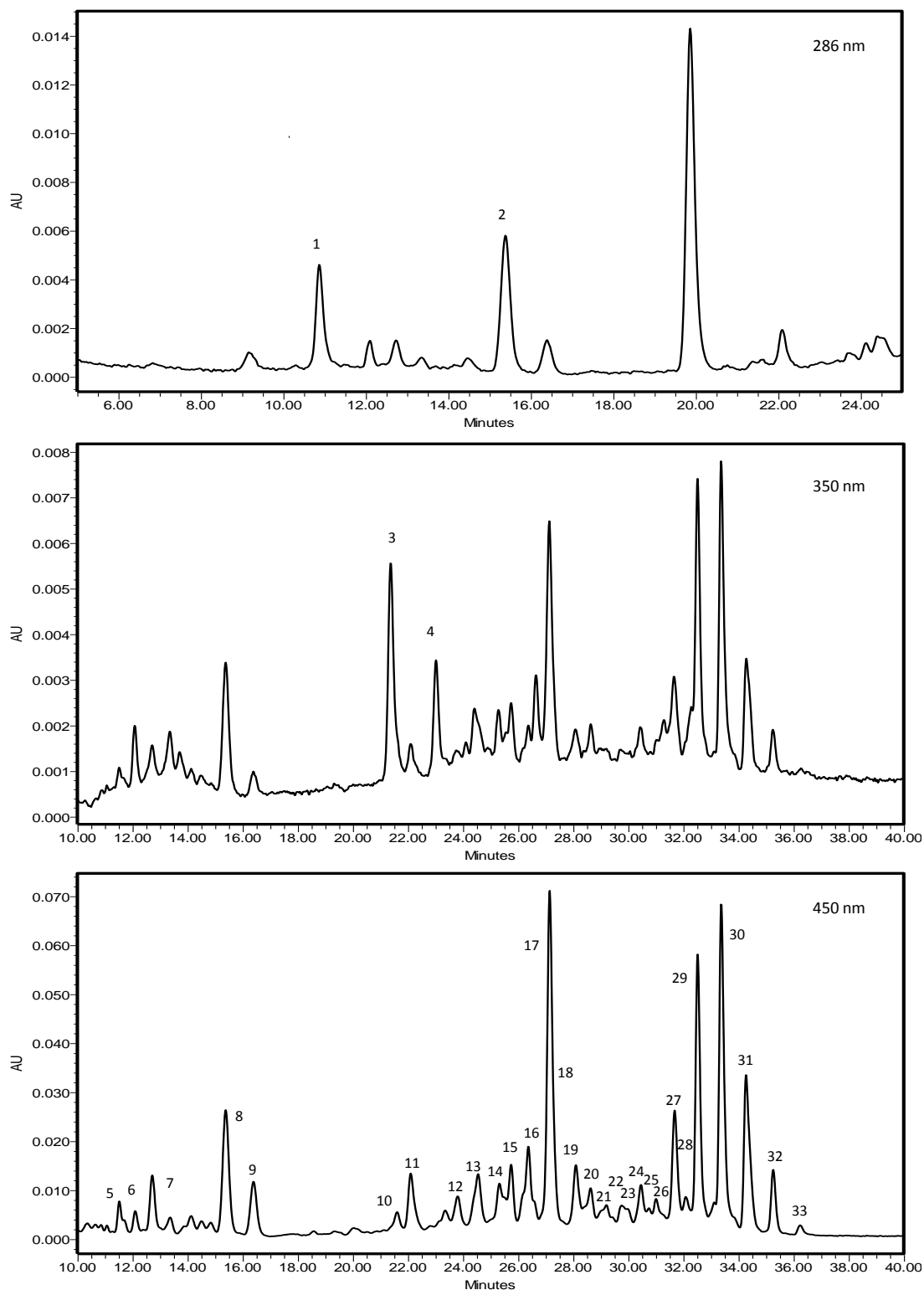


Figure 3.1. Typical HPLC-PDA profile of carotenoids and their esters in a red ripe chilli pepper.

HPLC-PDA analysis was performed in order to identify and quantify the carotenoids present in the ripe fruit of red chilli pepper. See table 3.2 for assignment of peaks. Identification of esterified carotenoids and their corresponding fatty acids was carried out using LC-MS.

Table 3.2. Carotenoid and carotenoid esters identified from non-polar extracts in red ripe chilli pepper fruit using HPLC-PDA and LC-MS.

Peak No.	RT	λ_{\max} (nm)	[M+H] ⁺	MS/MS	$\Delta m/z$	Compound
1	11.1	286	-	-	-	α -Tocopherol
2	20.1	286	-	-	-	Phytoene
3	21.6	350	-	-	-	Phytofluene-1
4	23.3	350	-	-	-	Phytofluene-2
5	10.5	439, 468	601.4242	-	-	Violaxanthin
6	10.8	436.7, 464.5	-	-	-	Neoxanthin
7	13.1	445.1, 472.9	-	-	-	Antheraxanthin
8	16.2	475.3	585.4295 567.4195	-	18(OH)	Capsanthin
9	17.1	450, 479	-	-	-	Zeaxanthin
10	22.1	442.7, 479	-	-	-	Antheraxanthin (monoester)
11	22.6	453, 481	-	-	-	β -Cryptoxanthin
12	24.4	448.8, 472.9	-	-	-	Antheraxanthin (monoester)
13	25.1	447.5, 474.1	-	-	-	Antheraxanthin (monoester)
14	25.9	469.3	767.5960 567.4184	-	200.1776 (C12:0)	Capsanthin- C12:0 (monoester)
15	26.3	471.7	795.6285 567.4196	-	228.2089 (C14:0)	Capsanthin- C14:0 (monoester)
16	26.9	446.3, 475.3	-	-	-	Antheraxanthin (monoester)
17	27.6	453.6, 479	-	-	-	β -carotene-1
18	28.2	474.3	-	-	-	Capsanthin- C16:0 (monoester)
19	28.6	453.6, 472.9	-	-	-	β -carotene-2
20	29	445.1, 474.1	-	-	-	Antheraxanthin (diester)

21	29.2	494.7	965.7600 565.4035	-	400.3565 (2xC12:0)	Capsorubin- C12:0-C12:0 (diester)
22	29.7	466.9	993.7906 793.6125 765.5815 565.4031	-	200.1782 (C12:0); 228.2043 (C14:0)	Capsorubin- C12:0-C14:0 (diester)
23	30.5	457.2, 481.4	961.8004 761.6233 733.5926 533.414	-	200.1781 (C12:0) 228.2078 (C14:0) 428.3862 (C12+C14)	Zeaxanthin- C12:0-C14:0 (diester)
24	30.5	457.2	-	989.8313 761.6226 533.4147	228.2087 (C14:0) 446.4166 (2xC14:0)	Zeaxanthin- C14:0-C14:0 (diester)
25	31	451.2	-	-	-	Zeaxanthin (diester)
26	31.5	448.8, 471.7	-	-	-	Antheraxanthin (diester)
27	32.1	476.6	949.7634 749.5860 549.4116	MS ² (749.5860) 549.5753 MS ² (949.7634) 549.4105	200.0107 (C12:0) 400.3529 (2xC12:0)	Capsanthin- C12:0-C12:0 (diester)
28	32.8	440.3, 471.7	-	-	-	Antheraxanthin (diester)
29	33	480.2	977.7948 777.7644 749.5860 549.4081	MS ² (977.9441) 777.6167 MS ² (777.6172) 549.4093 MS ² (749.5864) 549.4081	200.3274 (C12:0) 228.2079 (C14:0) 200.1783 (C12:0)	Capsanthin- C12:0-C14:0 (diester)
30	33.9	474.1	1005.8266 777.6176 749.5863 549.4093	MS ² (1006.0266) 778.6251 MS ² (1006.0266) 549.4047	227.4015 (C14:0) 456.6219 (2xC14:0)	Capsanthin- C14:0-C14:0 (diester)

				MS ² (777.6176) 549.4080	228.2096 (C14:0)	
31	34.9	475.3	1033.8576 805.7760 777.7598 549.4087	MS ² (1034.0387) 549.4125 MS ² (805.6504) 549.4058 MS ² (777.6182) 549.4101	484.6416 (C14:0, C16:0) 256.2446 (C16:0)	Capsanthin- C14:0-C16:0 (diester)
32	35.8	475.3	1061.8897 805.6498 549.409	MS ² (1062.4010) 805.6547 MS ² (805.6475) 549.409	256.7463 (C16:0) 256.2389 (C16:0)	Capsanthin- C16:0-C16:0 (diester)
33	36.4	449, 475	1045.8943 789.6546 533.4140	MS ² (1045.8943) 533.4401 MS ² (789.6546) 533.4219	256.2327 (C16:0) 256.2327 (C16:0)	Zeaxanthin- C16:0-C16:0 (diester)

The LC-MS data revealed that the fatty acids used to esterify the carotenoids present in chilli pepper were saturated fatty acids such as lauric acid (C12:0), myristic acid (C14:0), and stearic acid (C16:0). Capsanthin was found in free, mono- and diesterified forms, as was antheraxanthin. Capsorubin was only in diesterified form and zeaxanthin was found in both the free and diesterified form. Violaxanthin was identified on the LC-MS but not in an esterified form.

The remaining carotenoids present were identified from the comparison between characteristic carotenoid spectra displayed by authentic standards and co-chromatography. In addition reference spectra found in the literature were consulted (Britton et al., 2004).

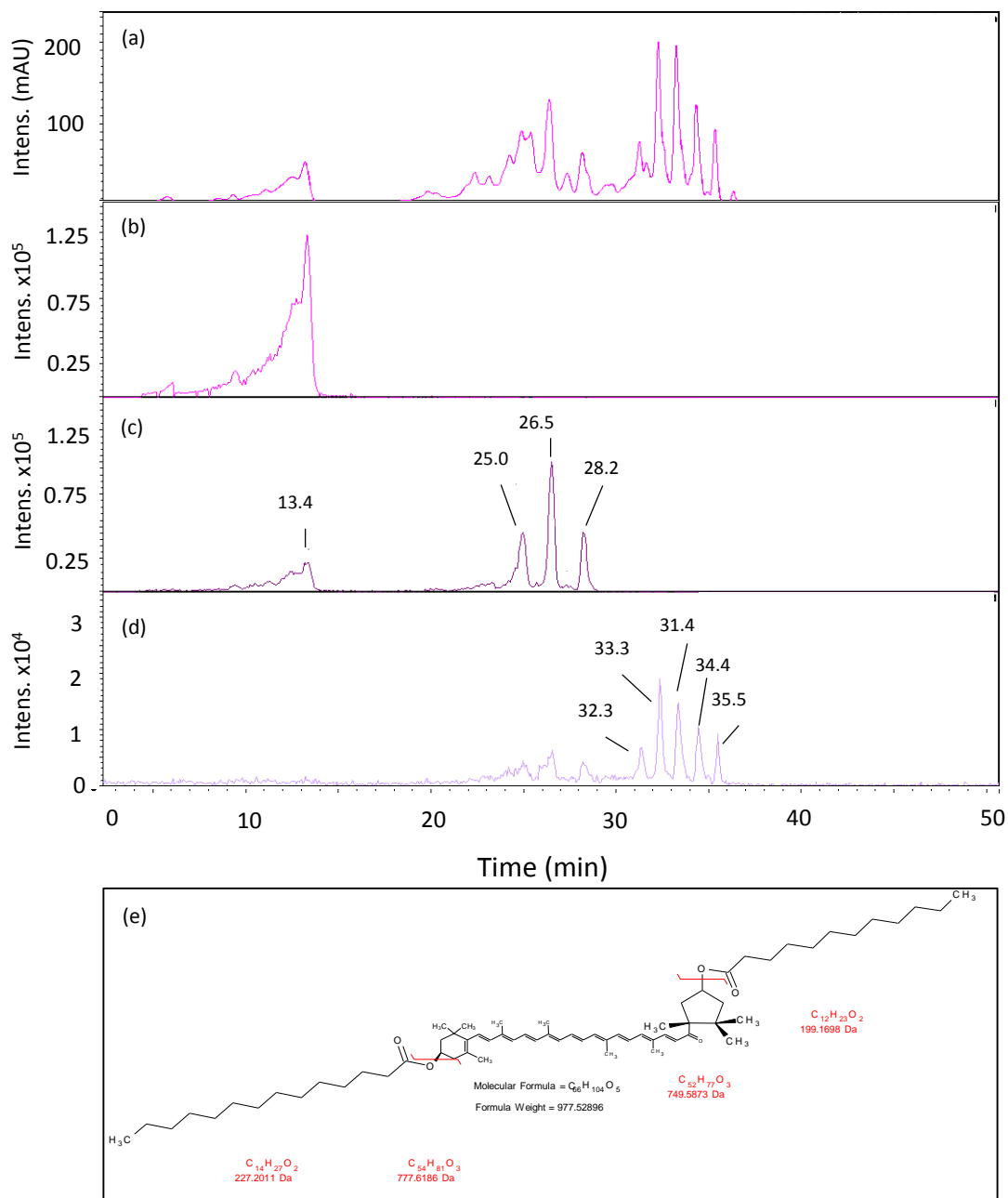


Figure 3.2. Example of capsanthin and capsanthin esters identified on the LCMS.

(a) UV chromatogram at 450nm. Extracted ion chromatogram (EIC) (b) at 585.4303±0.002 representing free capsanthin, (c) at 567.4200±0.005 representing capsanthin monoesters, and (d) at 449.4000±0.005 representing capsanthin diesters. (e) Structure of capsanthin diester C12:0, C14:0 with molecular weights to illustrate the identification of carotenoid esters on the LC-MS.

3.2.2.2. Quantification of free and esterified carotenoids in the ripe fruit

Once the carotenoids had been identified by various chromatographic and spectrometric procedures, the carotenoid content present in the red fruit of the 12 lines constituting the diversity panel were determined. These lines were all grown at the same time, the fruit were not tagged but were harvested at an optimal stage of ripeness. The amounts of each carotenoid and carotenoid ester were calculated and are summarised in Figure 3.3, and it was apparent that there were significant differences and similarities between lines. The main pigments accumulated were capsanthin, β -carotene, antheraxanthin, phytoene, β -cryptoxanthin, zeaxanthin, and α -tocopherol. Phytofluene, capsorubin, violaxanthin, and neoxanthin were found to be accumulated at lower amounts.

The amount of free carotenoids accumulated was investigated. Carotenoids such as capsanthin, zeaxanthin, and antheraxanthin (which eventually become esterified), were found at high levels in the high colour intensity lines R1, R2, and R7 high (Figure 3.3a-c). This was most evident in the accumulation of capsanthin where around 550-650 $\mu\text{g}/\text{gDW}$ accumulated. R4 also accumulated high levels of antheraxanthin.

The lines R2, R4, and R7 accumulated the highest total coloured carotenoids in ripe fruit (Figure 3.3o), with R2 and R4 accumulating approximately 7500-7700 $\mu\text{g}/\text{gDW}$ and R7 accumulating up to nearly 9000 $\mu\text{g}/\text{gDW}$. This was reflected in many of the carotenoids analysed, as concurrently, zeaxanthin esters, antheraxanthin esters, and β -cryptoxanthin showed the same trend. Two of the high intensity lines, R2 and R7, displayed similar amounts and composition of accumulated carotenoids, such as free capsanthin, free zeaxanthin and its esterified form, free antheraxanthin and its esterified form, and as previously mentioned β -carotene and β -cryptoxanthin.

The low intensity line, R3, was consistently low in carotenoid content when compared to the other lines, with a total coloured carotenoid content of 3500 $\mu\text{g}/\text{gDW}$. This line was grouped significantly lower in all pigments analysed, except capsorubin diesters and α -tocopherol (Figure 3.3g and l).

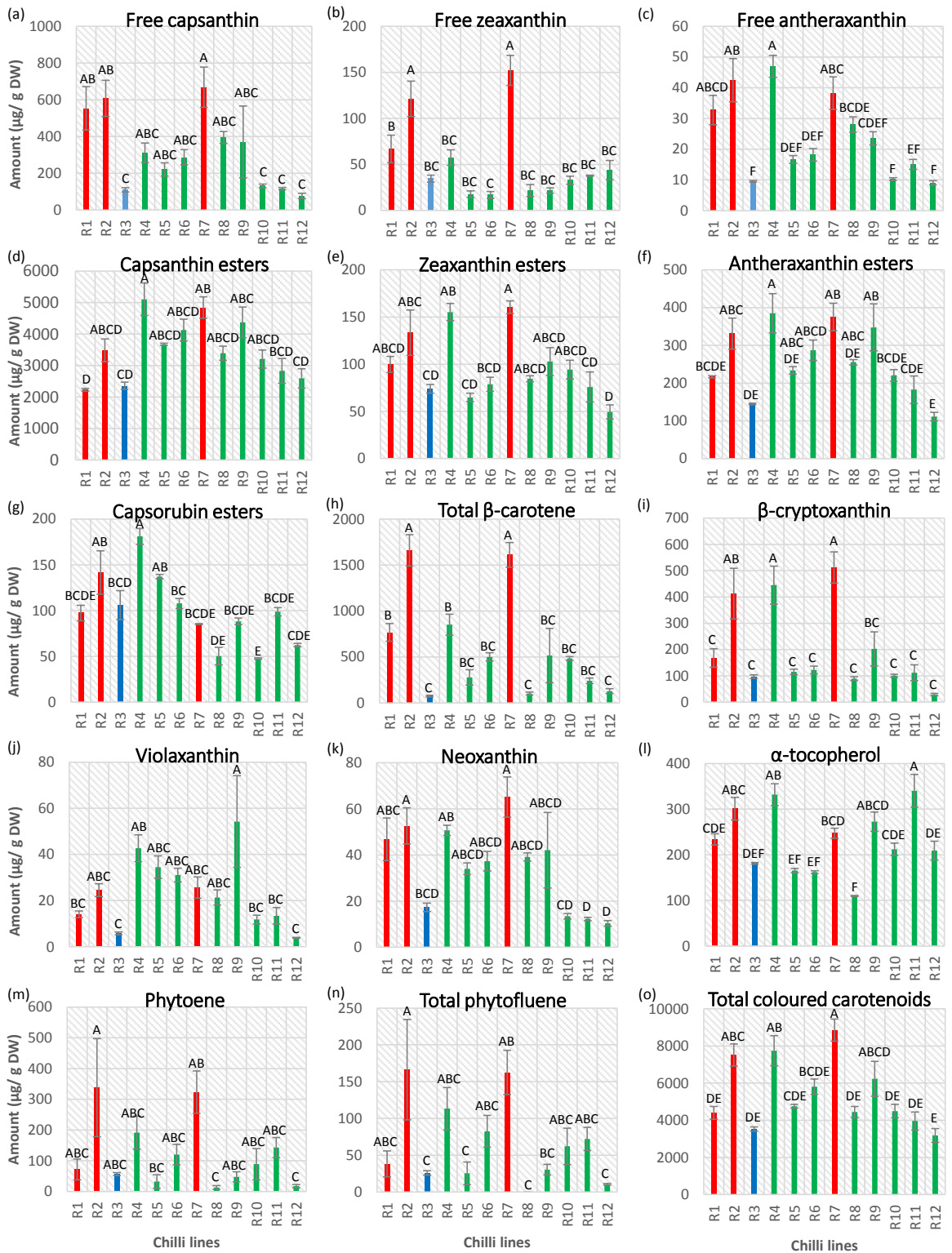


Figure 3.3. Summary of coloured carotenoid content in ripe fruit.

12 lines were subjected to HPLC-PDA and the carotenoids identified were quantified based on carotenoid standards. One way ANOVA with tukey post-hoc statistical analysis was carried out and lines grouped based on their significance within the panel of lines ($P \leq 0.05$). Error bars represent \pm SE ($n=3$). Bar colour represents: red, high intensity; green, medium intensity; blue,

low intensity. Total coloured carotenoids represents the sum of all carotenoids identified (neoxanthin, violaxanthin, antheraxanthin, capsanthin, zeaxanthin, β -cryptoxanthin, β -carotene, and capsorubin) excluding phytoene and phytofluene.

R12, although phenotyped as a medium intensity line, showed similar amounts and was grouped statistically with R3 for all carotenoids analysed as well total carotenoid content.

The remaining lines, R5, R6, R10, and R11 did not stand out significantly when compared to the other lines. These medium intensity lines could be sub-categorised into low-medium and medium phenotypes. R10 and R11, based on the fact that these lines are grouped lower when looking at significant changes in free capsanthin, free antheraxanthin, violaxanthin and neoxanthin present when compared to R5 and R6 could be assigned to a low-medium phenotype. Whereas R5 and R6 lines can stay in the medium phenotype category. R12 should be reclassified as low intensity based on the quantitation data determined in this study. R9 was found to have a high violaxanthin content but the variance witnessed in this line was large, thus making the results less robust.

Further analysis into capsanthin content was carried out to investigate the percentage of the most abundant compounds in terms of total carotenoid content present (Figure 3.4). For the majority of carotenoids analysed the percentage accumulation showed similar trends to their contents; however, there were differences when investigating capsanthin. The percentage of free capsanthin was similar to amounts, with respect to the high intensity lines R1 and R2 accumulating the largest free capsanthin levels (8-12%) and to a lesser extent R7 (7%). When examining the percentage of capsanthin esters and total capsanthin it was evident that there was a lower percentage of capsanthin diesters accumulated, as well as total capsanthin, when compared to the total carotenoid content.

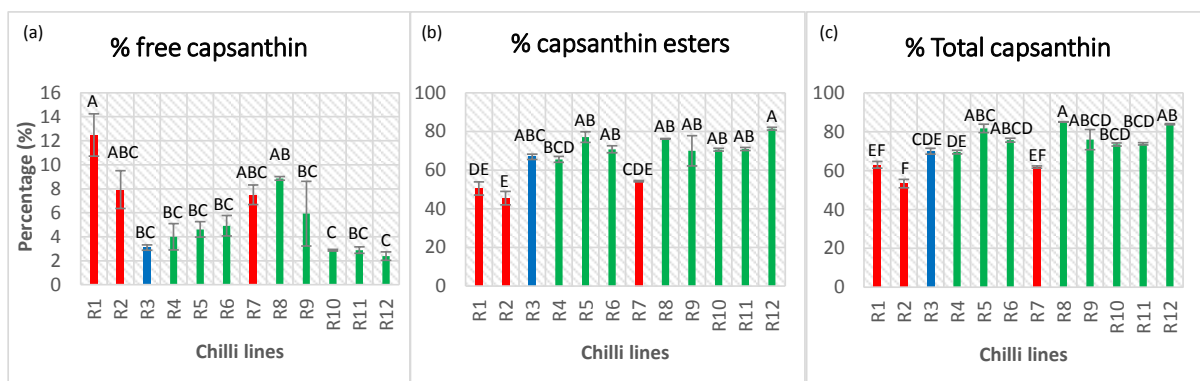


Figure 3.4. The percentage of capsanthin and corresponding esters of the total carotenoid content.

The percentage of (a) free capsanthin, (b) total capsanthin esters, and (c) total capsanthin was calculated. One one-way ANOVA with tukey post-hoc statistical analysis was carried out and the lines were grouped based on their significance within the panel of lines ($P \leq 0.05$). Error bars represent \pm SE (n=3).

3.2.3. Characterisation of carotenoid biosynthesis throughout ripening

To gain a further understanding of the biosynthesis and accumulation of carotenoids in red chilli pepper the pigments were measured throughout ripening. The plants were tagged at anthesis, the mature green (MG) stage was determined as 55 days post anthesis (dpa), breaker (B) was then tagged by the first appearance of red colour on the green fruit and the stages analysed after breaker were breaker plus three days (B+3), breaker plus seven days (B+7), breaker plus 10 days (B+10), and breaker plus 14 days (B+14). Eight lines were selected from the panel previously analysed (3.2.2.2) based on perturbed carotenoid content as summarised in Table 3.3.

Table 3.3. Carotenoid content throughout ripening in 8 selected lines.

The carotenoid content ($\mu\text{g}/\text{gDW}$) for selected lines was analysed in 6 stages of ripening to observe biosynthesis and accumulation over the ripening process. The stages were (a) mature green (MG), (b) breaker (B), (c) breaker plus 3 days (B+3), (d) breaker plus 7 days (B+7), (e) breaker plus 10 days (B+10), and (f) breaker plus 14 (B+14). The ripening length within the colour diversity varied thus resulting in some lines displaying longer ripening lengths than others. Values discussed in the text are shown in bold. Statistical analysis was carried out using ANOVA ($P \leq 0.05$). The $\pm\text{SE}$ was calculated ($n=3$). Key: -, not detected.

(a) MG

Carotenoids	R1	R2	R3	R4	R7	R8	R11	R12
Violaxanthin	40.76 \pm 16.42	86.73 \pm 15.70	46.91 \pm 2.81	160.27 \pm 24.32	62.27 \pm 5.19	84.49 \pm 20.56	128.03 \pm 20.52	44.78 \pm 8.07
Neoxanthin	15.88 \pm 4.76	13.49 \pm 3.61	6.66 \pm 0.75	52.91 \pm 8.15	11.71 \pm 1.68	27.11 \pm 2.50	55.85 \pm 7.98	37.83 \pm 4.73
Antheraxanthin	17.33 \pm 0.88	17.60 \pm 3.15	10.36 \pm 0.39	35.52 \pm 2.46	13.87 \pm 2.54	18.37 \pm 1.70	22.96 \pm 3.00	16.97 \pm 3.21
Chlorophyll b	412.42 \pm 57.8	646.13 \pm 139.87	253.04 \pm 24.08	1066.73 \pm 103.31	310.91 \pm 26.88	704.43 \pm 38.80	960.06 \pm 150.20	740.12 \pm 64.91
Lutein	463.85\pm44.86	856.08\pm181.35	399.90\pm51.48	1079.31\pm82.33	357.51\pm37.75	756.68\pm44.45	1120.54\pm136.65	825.00\pm64.07
Zeaxanthin	14.21\pm1.72	3.72 \pm 0.93	2.70 \pm 1.11	17.90 \pm 4.79	3.30 \pm 0.85	13.31 \pm 4.09	4.98 \pm 2.17	4.29 \pm 0.60
Chlorophyll a	256.50 \pm 215.47	183.62 \pm 15.70	344.92\pm108.61	-	102.54 \pm 11.07	641.86\pm57.30	1436.05\pm470.20	1354.50\pm132.68
β -carotene	69.34 \pm 35.85	119.80 \pm 24.87	53.27 \pm 5.64	149.03 \pm 14.37	40.08 \pm 3.30	122.57 \pm 7.11	88.95 \pm 11.08	77.36 \pm 5.55
α -tocopherol	59.10 \pm 10.60	88.35 \pm 10.23	84.99 \pm 7.18	140.11 \pm 22.62	61.60 \pm 5.40	134.02 \pm 14.70	144.73 \pm 10.35	63.12 \pm 11.45
Total carotenoid	621.36 \pm 94.26	1097.41 \pm 220.59	519.79 \pm 58.14	1494.94 \pm 122.16	488.74 \pm 41.73	1022.53 \pm 73.40	1421.30 \pm 173.77	1006.22 \pm 83.39

(b) B

Carotenoids	R1	R2	R3	R4	R7	R8	R11	R12
Violaxanthin	11.47±0.24	33.35±3.28	22.45±6.60	47.97±1.58	18.81±2.95	25.52±6.43	39.10±7.11	22.09±1.93
Neoxanthin	7.35±1.02	33.44±10.39	8.26±1.77	81.74±2.33	10.36±3.18	24.87±3.78	33.11±2.90	6.80±1.92
Antheraxanthin	15.36±0.77	19.96±3.14	7.33±2.38	36.82±4.44	14.05±1.21	26.09±1.27	26.68±0.66	26.28±0.86
Chlorophyll b	293.32±36.09	441.06±40.98	136.58±33.23	706.85±21.39	198.60±25.39	554.76±59.80	557.84±69.20	226.61±7.41
Lutein	-	472.07±33.76	251.59±41.31	877.27±56.42	176.99±28.66	636.19±88.32	897.55±70.59	396.81±42.87
Capsanthin	48.11±11.42	34.82±9.74	25.07±13.54	23.21±8.19	56.86±15.62	60.47±21.01	8.41±1.75	40.37±13.70
Zeaxanthin	78.26±4.19	36.74±21.25	26.32±15.19	77.80±18.35	18.03±3.07	155.57±30.27	42.64±15.49	180.41±21.12
Chlorophyll a	79.11±0.31	129.55±11.32	64.30±20.38	-	33.79±6.00	337.96±78.36	112.73±14.58	82.59±14.23
β-cryptoxanthin	32.67±3.47	22.47±5.68	18.72±9.85	30.60±4.32	13.71±3.96	21.69±3.88	-	49.68±8.04
β-carotene	159.90±6.54	108.61±16.42	73.08±16.51	134.77±3.74	52.86±8.24	108.40±37.91	77.77±4.42	101.57±15.63
Capsanthin esters	37.28±6.31	20.60±3.93	-	-	46.17±15.69	-	-	-
Zeaxanthin esters	40.66±7.71	-	104.88±32.18	-	-	44.31±23.82	-	53.22±20.56
α-tocopherol	59.58±1.31	77.19±7.94	64.96±9.69	143.74±11.40	58.19±4.11	225.11±27.00	152.54±6.88	83.47±9.80
Total carotenoid	431.05±23.90	798.16±109.58	472.74±67.12	1310.18±52.04	403.28±53.80	1114.78±107.42	1135.56±66.71	860.66±101.39

(c) B+3

Carotenoids	R1	R2	R3	R4	R7	R8	R11	R12
Violaxanthin	9.14±0.29	21.72±7.42	-	25.95±6.99	50.16±3.42	15.25±8.07	11.18±0.92	-
Neoxanthin	5.58±3.36	80.46±32.14	-	17.01±2.24	19.22±1.86	23.48±11.02	19.98±2.98	13.05±2.07
Antheraxanthin	25.81±6.24	43.55±3.79	3.19±1.62	50.08±0.46	27.41±4.22	23.55±3.56	27.72±0.97	32.43±4.82
Chlorophyll b	202.14±76.45	430.66±143.51	11.20±2.65	220.49±27.95	275.48±16.47	340.81±170.90	191.42±17.05	83.55±55.65
Lutein	-	272.55±97.05	16.98±4.18	222.86±23.34	129.08±2.52	515.19±209.54	417.59±58.02	181.73±91.12
Capsanthin	209.76±29.32	265.35±96.09	89.08±34.50	227.66±25.64	96.52±30.75	113.00±34.67	62.85±7.42	104.14±13.36

Zeaxanthin	136.23±28.61	97.74±40.09	54.64±14.95	159.48±26.48	30.16±14.45	190.83±38.70	98.33±16.54	213.53±35.44
Chlorophyll a	264.22±166.75	435.15±208.21	-	-	-	492.90±254.83	-	-
β-cryptoxanthin	114.16±14.80	144.72±30.38	61.85±10.28	113.17±6.92	35.81±11.19	34.36±7.05	31.27±5.33	48.51±11.72
β-carotene	394.32±22.35	312.87±68.43	197.18±32.37	160.05±24.26	66.60±26.66	117.74±3.13	60.02±3.58	127.57±32.30
Anther esters	37.20±3.43	95.78±19.11	30.91±3.63	41.31±6.62	-	12.53±3.36	10.58±0.25	28.71±6.50
Capsorubin esters	34.64±6.40	-	28.15±3.54	-	-	-	-	-
Capsanthin esters	544.49±38.63	607.89±179.70	765.93±127.59	475.27±42.46	115.74±53.07	202.01±94.13	141.64±10.61	428.37±89.69
Zeaxanthin esters	159.21±6.72	48.58±18.81	84.54±12.58	19.88±7.48	-	288.96±170.31	12.15±6.15	54.00±17.64
α-tocopherol	114.98±2.37	139.89±9.08	90.87±2.04	198.17±12.26	67.34±11.06	271.94±33.17	217.73±22.54	162.33±15.25
Phytoene	35.98±4.90	58.18±42.36	93.07±25.47	61.55±8.51	-	-	44.84±9.51	99.92±5.23
Phytofluene	-	-	39.55±9.38	24.44±5.47	-	-	10.25±2.82	7.91±0.79
Total carotenoid	1624±72.88	2028.98±362.08	1482.33±108.93	1598.71±83.75	558.77±136.80	1556.79±73.63	989.43±38.84	1259.18±145.11

(d) B+7

Carotenoids	R1	R2	R3	R4	R7	R8	R11	R12
Violaxanthin	15.59±0.56	40.02±6.38	10.98±1.90	-	35.92±10.51	33.21±9.63	3.26±3.25	19.22±5.56
Neoxanthin	12.09±8.03	90.91±9.50	-	36.06±8.84	23.86±2.26	4.49±0.89	3.54±0.78	-
Antheraxanthin	30.15±2.97	58.98±3.27	11.17±3.12	57.94±3.48	60.66±2.48	39.56±1.14	25.62±4.17	22.50±1.05
Chlorophyll b	60.02±17.08	217.39±7.69	-	92.42±7.82	257.92±32.18	77.79±1.76	45.07±7.59	19.51±1.72
Lutein	-	-	-	41.12±6.08	98.67±25.71	30.06±11.09	60.94±32.97	-
Capsanthin	403.61±58.30	506.54±65.45	92.38±26.96	345.80±14.42	490.84±63.26	454.47±65.09	110.87±13.43	225.07±9.41
Zeaxanthin	72.85±6.43	111.75±6.66	42.85±17.97	113.01±6.21	99.00±17.37	132.70±8.36	73.36±6.73	132.81±24.90
Chlorophyll a	-	329.56±34.01	-	-	-	-	-	-
β-cryptoxanthin	225.85±38.14	527.63±33.98	119.88±15.24	228.49±31.82	322.03±73.47	101.50±7.62	25.25±3.91	99.04±20.27
β-carotene	891.20±98.50	1179.96±92.91	352.06±51.80	323.23±15.31	472.10±119.77	171.76±41.82	176.36±12.56	328.80±46.36
Anther esters	176.67±24.03	375.12±41.13	64.30±10.89	129.34±17.56	198.43±44.58	123.99±24.00	93.84±11.61	80.31±5.93

Capsorubin esters	176.10±39.42	39.69±6.35	114.03±28.34	32.64±9.79	-	-	38.84±11.61	158.60±44.20
Capsanthin esters	1899.79±192.45	2650.24±199.40	2072.84±293.56	1276.82±158.49	1738.28±422.79	1725.83±365.21	1204.36±213.81	1957.70±14.67
Zeaxanthin esters	124.17±8.45	204.87±26.73	224.92±28.60	36.89±2.84	26.41±3.01	48.51±12.39	73.19±15.74	113.90±21.40
α-tocopherol	172.49±5.57	188.49±15.37	167.06±21.28	253.83±39.10	172.39±15.75	374.14±7.98	271.11±24.25	176.58±20.65
Phytoene	108.10±28.60	85.97±17.87	154.48±12.78	240.86±57.75	79.27±47.85	60.24±5.88	560.91±98.78	108.39±20.18
Phytofluene	49.50±12.86	15.49±3.52	60.19±6.71	99.46±18.19	33.69±22.58	33.61±3.35	74.91±7.52	39.37±7.56
Total carotenoid	4209.01±392.07	6048.70±278.58	3502.99±453.04	3106.87±321.49	3759.12±769.10	3045.11±473.27	2586.20±192.55	3324.31±75.68

(e) B+10

Carotenoids	R1	R2	R3	R4	R7	R8	R11	R12
Violaxanthin	26.43±0.61	65.54±8.16	16.15±0.26	10.86±1.87	57.54±13.97	14.62±2.23	10.41±1.96	10.13±1.12
Neoxanthin	18.33±1.68	32.01±11.37	4.81±0.63	7.99±0.43	32.90±1.83	14.18±1.10	4.51±1.36	-
Antheraxanthin	25.97±2.51	41.68±5.84	9.10±1.31	45.01±1.91	53.39±5.04	38.77±1.17	21.07±3.04	22.62±3.21
Chlorophyll b	26.26±2.10	68.65±21.64	7.66±0.08	49.38±4.85	76.42±7.73	67.69±1.74	31.17±14.59	20.84±3.32
Capsanthin	287.20±20.11	507.08±67.69	56.16±9.03	297.55±24.89	664.60±37.74	391.93±17.15	96.99±8.01	178.50±36.27
Zeaxanthin	56.10±1.93	81.18±3.78	21.86±4.10	77.03±8.84	109.19±20.01	131.78±17.89	62.17±7.56	95.87±26.22
β-cryptoxanthin	180.10±8.31	758.83±50.49	135.82±7.51	296.35±27.62	595.56±36.05	155.75±32.84	96.19±14.84	103.83±29.30
β-carotene	720.54±72.36	1954.77±100.36	320.06±105.59	636.82±63.59	1940.70±88.09	417.02±107.01	229.08±22.90	424.55±79.86
Anther esters	181.65±12.09	461.57±38.49	62.68±2.31	203.30±28.83	510.05±47.84	187.87±17.29	135.53±31.07	127.12±2.95
Capsorubin esters	213.72±21.01	25.77±6.41	118.38±6.58	86.88±8.85	43.14±2.55	-	50.46±13.21	179.10±22.02
Capsanthin esters	2356.79±119.44	4528.57±318.89	2299.42±409.41	1849.04±211.28	4228.99±451.64	2335.33±136.05	1492.85±215.95	2760.57±206.19
Zeaxanthin esters	98.90±7.47	73.28±5.71	278.26±51.36	41.01±5.78	90.14±0.19	91.49±3.04	59.95±12.08	127.45±35.15
α-tocopherol	194.79±2.83	303.67±47.15	177.67±19.24	301.36±8.16	271.15±24.95	485.78±28.63	307.72±9.85	208.16±8.69
Phytoene	97.37±37.60	468.47±197.02	103.22±47.14	336.74±24.25	377.75±82.24	129.46±13.01	872.43±277.96	108.39±44.31
Phytofluene	47.76±15.79	220.10±73.27	37.17±18.96	155.78±15.46	192.17±39.35	70.23±7.25	132.42±35.66	40.18±15.11
Total carotenoid	4348.50±148.22	9390.80±587.34	3834.77±451.32	4163.71±355.76	9090.61±511.14	4114.24±56.71	3332.75±218.99	3324.31±75.68

(f) B+14

Carotenoids	R1	R2	R4	R7
Violaxanthin	68.05±17.60	67.18±7.39	26.92±3.32	71.74±3.02
Neoxanthin	14.13±1.36	26.28±3.05	16.14±1.50	33.47±5.40
Antheraxanthin	20.44±0.36	49.69±1.63	52.21±3.51	48.53±4.82
Chlorophyll b	16.48±4.21	58.35±9.31	39.35±1.26	45.70±6.18
Capsanthin	202.45±0.01	561.50±55.20	232.55±27.80	617.69±52.97
Zeaxanthin	35.39±5.72	112.38±5.93	71.33±9.65	133.55±5.64
β-cryptoxanthin	285.65±22.06	710.21±7.85	353.46±39.79	846.39±45.91
β-carotene	1018.29±59.09	2523.91±82.72	400.45±83.31	2874.48±281.86
Anther est	324.85±23.68	555.49±20.36	193.60±16.21	534.24±43.56
Capsorubin est	154.55±19.39	123.42±12.89	102.88±18.82	-
Capsanthin est	3290.89±179.33	4686.36±237.43	2666.10±194.28	5653.29±432.50
Zeaxanthin est	100.54±25.95	77.20±7.67	20.82±6.76	115.20±16.51
α-tocopherol	274.92±11.07	389.19±19.76	420.79±21.76	376.30±47.18
Phytoene	127.02±10.99	727.21±85.99	378.16±31.49	672.72±242.63
Phytofluene	70.18±6.70	376.89±27.37	159.40±8.44	331.84±107.44
Total carotenoid	5848.308±156.9984	11164.78±366.6623	4776.358±181.2221	12126.56±1128.216

As the ripening process progressed the total carotenoid content increased in all lines. The medium intensity lines R4, R8, R10 and R11 increased around 2-4 fold, whereas the high and low intensity lines experienced an approx. 9-10 fold increase for R1, R2 and R3. The high intensity line, R7, underwent an approx. 25 fold increase in the total carotenoid content throughout ripening.

At the mature green stage of fruit development the carotenoids that occur are involved in the protection of the photosynthetic apparatus, as well as the chlorophylls which give the fruit the green colour. Lutein is the most predominant carotenoid accumulated in MG fruit, followed by β -carotene, violaxanthin, and α -tocopherol. Neoxanthin, free antheraxanthin, and free zeaxanthin were present at low levels (Table 3.3a). Chlorophyll a was the more abundant chlorophyll analysed, there was more chlorophyll a present in the medium and low intensity lines when compared the high intensity lines. R4 and R11 accumulated the highest amounts of chlorophyll in green fruit, with around 1400-500 $\mu\text{g}/\text{gDW}$ in comparison to R1, R2 and R7, 100-250 $\mu\text{g}/\text{gDW}$. A similar trend is seen with chlorophyll b, but in this case the differences were less significant and the lowest content was seen in R3. R4 and R11 accumulated the highest amounts at around 1000 $\mu\text{g}/\text{gDW}$ compared to R3 which was around 150 $\mu\text{g}/\text{gDW}$. Interestingly, when examining the ratio of chlorophyll a to b in the MG fruit, the low and medium lines show a higher ratio of a: b; whereas, the high intensity lines and R8 have a higher ratio of b to a (Figure 3.5). However, only the extremes are significant. In terms of the other carotenoids analysed there were no real differences between lines in amounts of β -carotene accumulated, and α -tocopherol was found to be more prevalent in R4, R8 and R11 and was significantly higher than R1, R7 and R12. Violaxanthin again showed a similar trend with R4 and R11 possessing the highest amounts but only R4 was significantly higher.

At the onset of ripening at the breaker stage there was a visible decrease in lutein and the chlorophylls whereas capsanthin, β -carotene, zeaxanthin, capsorubin and antheraxanthin esters start to accumulate (Table 3.3b). It was observed that different lines accumulated different esters first. At the breaker stage there is a clear decrease in chlorophylls, while lutein accumulated, although chlorophylls remained the most abundant pigments at this stage. Chlorophyll a decreased at a faster rate than chlorophyll b, with chlorophyll b being more predominant compared to chlorophyll a at this breaker stage. The trend between lines was similar to MG whereby R4 and R11 were significantly high at 600-70 $\mu\text{g}/\text{gDW}$ but R3, R7 and R12 were significantly low at around 30-60 $\mu\text{g}/\text{gDW}$, and chlorophyll a accumulates at significantly higher levels in R8 and R11. α -Tocopherol is the next predominant pigment at breaker stage; and again R4, R8 and R11 are significantly higher than the other lines. Among

levels with lower intensity R4 was found to have significantly more violaxanthin, neoxanthin, antheraxanthin, and capsanthin. There was some evidence of the early accumulation of esters at this stage too. The zeaxanthin diesters were found in 4 lines analysed at this stage R1, R8, and R12 at about 40-50 $\mu\text{g/gDW}$ and in R3 at 100 $\mu\text{g/gDW}$. Interestingly, capsanthin diesters were only found present in the three high intensity lines R1, R2 and R7 at around 20-50 $\mu\text{g/gDW}$, and R8 at 30 $\mu\text{g/gDW}$.

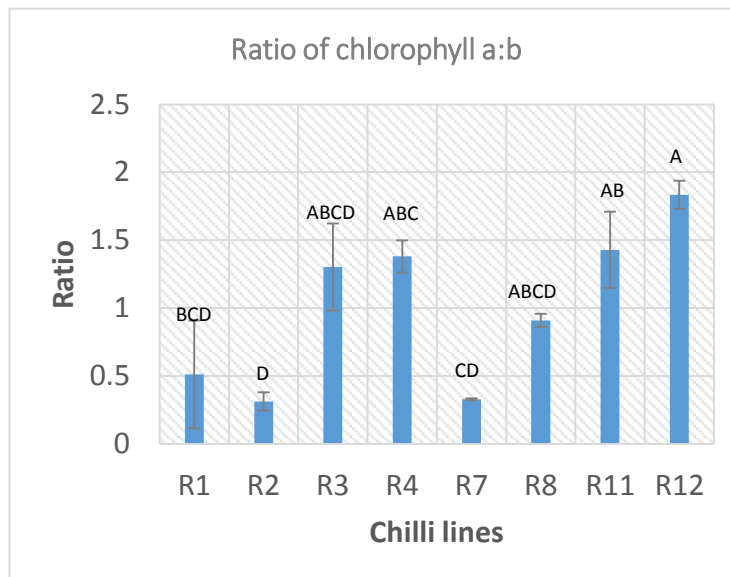


Figure 3.5. Ratio of chlorophyll a to b.

The ratio of chlorophyll a to b in ripe fruit was calculated to see if there were differences displayed between lines. Error bars represent $\pm\text{SE}$ ($n=3$). One-way ANOVA with post-hoc tukey was carried out and the lines were grouped based on significance ($P \leq 0.05$).

The next stage of ripening examined was breaker plus three days (B+3). For all lines lutein is still the predominant carotenoid accumulated, and chlorophyll b is the next abundant pigment. However, at this stage the significant accumulation of capsanthin diesters was initiated. Free capsanthin, free and esterified zeaxanthin, α -tocopherol, and β -carotene also accumulated at higher levels in all lines (Table 3.3c). When comparing the amounts of capsanthin diesters, capsorubin diesters, phytoene, and phytofluene the low intensity line, R3, had significantly higher amounts accumulated but accumulated significantly less violaxanthin, antheraxanthin, and α -tocopherol. Similarly, the high intensity line, R2, is significantly higher than the other lines in neoxanthin, free and esterified antheraxanthin, chlorophyll a, β -cryptoxanthin, and β -

carotene. The other high intensity line, R1, is also significantly high in antheraxanthin esters, chlorophyll a, β -cryptoxanthin, and β -carotene. Another line accumulating high carotenoids at this stage is R8, with high levels of neoxanthin, chlorophyll a and α -tocopherol. Lines which were found to have low levels included the high intensity line R7, which was significantly low in capsanthin and antheraxanthin esters, β -carotene, zeaxanthin, phytoene, phytofluene, and α -tocopherol. R8 was also significantly low in carotenoids similar to R7, excluding zeaxanthin and capsanthin diesters. There were no significant differences found between lines for free capsanthin, chlorophyll b, lutein, and zeaxanthin diesters. Also, capsorubin diesters were only present in R1 and R3 lines and chlorophyll a was only present in R1, R2 and R8.

Next, the stage designated as breaker plus 7 days (B+7) was analysed, the fruit are predominantly red in most lines analysed at this point. This becomes evident in the lines which have a high total carotenoid content and high intensity phenotype, which is reflected as capsanthin diesters becoming the predominant carotenoid present. Interestingly, at this stage there are no significant differences between lines when analysing the amounts (Table 3.3d). The next most abundant compound is β -carotene which was found to have significantly high levels in the two high intensity lines, R1 and R2, at around 890 and 1180 $\mu\text{g}/\text{gDW}$, respectively. The high intensity line, R2, was also found to accumulate significantly higher amounts of violxanthin, neoxanthin, free and esterified antheraxanthin, chlorophyll b and a, zeaxanthin diesters, and β -cryptoxanthin. R7 also shared high levels in the neoxanthin, antheraxanthin, chlorophyll b, and lutein. The low intensity line, R3, as well as R12, was found to accumulate significantly low levels of neoxanthin, antheraxanthin and chlorophyll b. R3 was also found to have low levels of α -tocopherol and R12 also had low antheraxanthin diesters and phytofluene. Lutein had almost completely diminished and low levels are only found in R4, R7, R8, R11. There were no significant differences found between lines in the accumulation of zeaxanthin.

Breaker plus 10 days is the ripening stage which corresponds to ripe for most fruit as this is when the fruit is most red before senescence begins. There are, however, specific lines which have a longer ripening period which will be discussed later. The profile of carotenoids accumulated at this stage is similar to B+7, but the carotenoids are present at higher levels. Capsanthin, free and esterified, as well as β -carotene predominate. Lutein and chlorophyll a have completely diminished, and chlorophyll b is still present (Table 3.3e). The high intensity line, R7, dominates over the other lines displaying significantly higher levels in the majority of carotenoids examined, excluding free and esterified zeaxanthin, α -tocopherol, capsorubin diesters, and phytofluene. R2 is also a high intensity line and shows a similar pattern of highly accumulated carotenoids as R7, but not to the same extent; it did not accumulate high levels of free

antheraxanthin and chlorophyll b, but it did accumulate more phytofluene. These two lines contained higher levels of the most abundant carotenoids, free capsanthin, esterified capsanthin, and β -carotene with levels reaching approximately 500, 4500 and 2000 $\mu\text{g}/\text{gDW}$, respectively in R2 and 660, 4200 and 2000 $\mu\text{g}/\text{gDW}$ in R7. On the opposite end of the scale the low intensity line R3 was significantly low in the majority of compounds analysed, excluding β -carotene, and is significantly high in zeaxanthin esters and capsorubin diesters.

Finally, the last stage of the ripening series analysed was breaker plus 14 days. Analysis was only carried out in lines which showed a longer period of ripening as the fruit were not experiencing senescence at this stage. The three high intensity lines R1, R2 and R7 showed these characteristics as well as R4, a medium intensity line, which has displayed high levels of total carotenoid content. The most predominant carotenoids seen at this stage were those associated with ripe fruit, such as capsanthin and β -carotene (Table 3.3f). When looking at capsanthin diesters the four lines separated into two groups based on their significance whereby R2 and R7 have higher levels of capsanthin diesters, when compared to R1 and R4. However, all these lines display high levels at approximately 4600, 5700, 3300 and 2700 $\mu\text{g}/\text{gDW}$, respectively. When you compare these lines at their last stage of ripening to the lines which finished ripening at stage B+10, it was observed that the high intensity lines accumulated more capsanthin diesters compared to other lines analysed. Statistical analysis on the pigment contents present group R7 and R2, into a group designated A, R1 was in group B, and all the remaining lines were in group BC. The same trend was seen for β -carotene. All three high lines were found to be significantly higher in violaxanthin and antheraxanthin diesters.

The biosynthesis and accumulation of capsanthin and its corresponding esters were studied further to aid definition of the differing colour intensity phenotypes displayed between selected lines; three lines were chosen based on the ripening series data previously shown (Table 3.3). These were R1, R3 and R7. R1 and R7 were chosen because they were high intensity lines which display different characteristics of carotenoid accumulation, as opposed to R2 which was very similar to R7 in terms of carotenoid content. R1 and R7 also appear to have differing rates of ripening. R3 was chosen based on its consistently low accumulation of most carotenoids analysed (Figure 3.6).

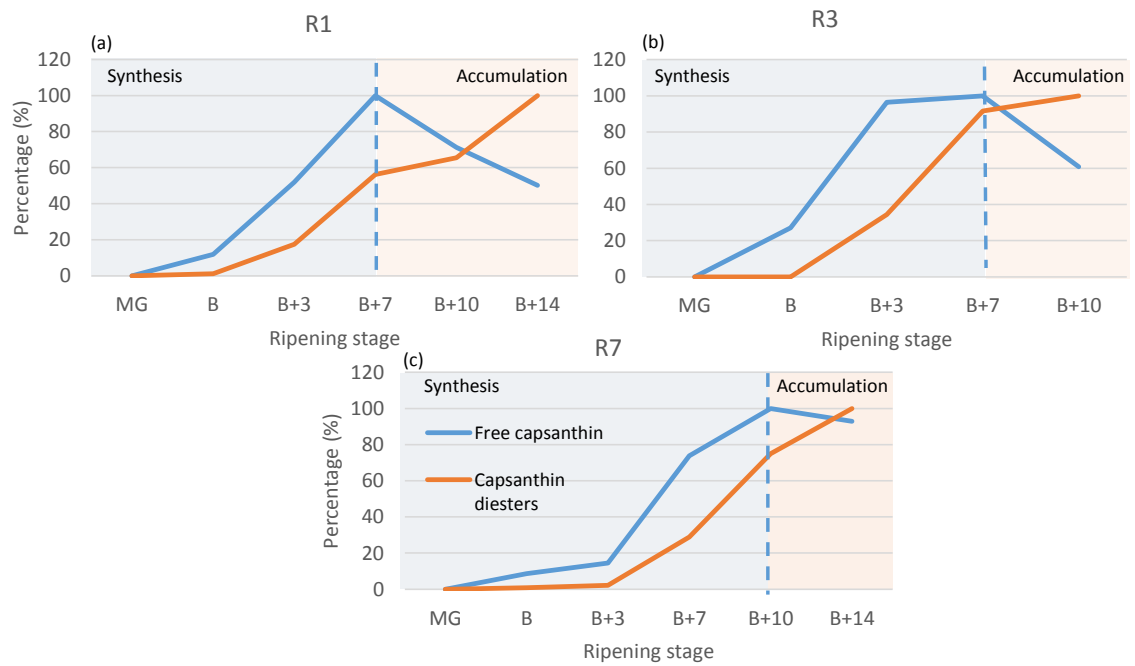


Figure 3.6. The determination of capsanthin and its corresponding esters during ripening, showing the transition between synthesis and accumulation.

The amount of free and esterified capsanthin was calculated as a percentage, whereby the highest amount throughout ripening was 100%, allowing the transition between biosynthesis and accumulation to be visualised.

Comparison of the lines selected to analyse the biosynthesis and accumulation of capsanthin firstly allowed visualisation of the transition between the biosynthesis of free capsanthin and the accumulation of capsanthin esters throughout ripening. When comparing the high intensity lines (R1 and R7) it was revealed that the accumulation of capsanthin esters were linear throughout ripening; however, in the low intensity line (R3) the accumulation of capsanthin esters begins to plateau at the end of the ripening process, around B+7. Finally, the differing ripening rates experienced between the lines analysed was also illustrated. The R1 and R3 lines displayed a faster rate of ripening than the R7 line when the fruits were tagged. This is apparent when comparing the transition between biosynthesis and accumulation as R1 and R3 experienced a transition around the B+7 stage. In contrast the R7 line took longer to reach this point, at B+10.

3.2.3.1. Comparison of rate of ripening in selected lines

After the pigment analysis was carried out over ripening it became clear that some of the lines ripened at a much slower rate. For example, the R2 and R7 line took longer to reach a red stage from breaker and had a much longer ripening time frame. This can be seen in Table 3.4 whereby the R7 line stays green a lot longer than the R1 and R3.

This was investigated by examining the pigments accumulated throughout ripening in each line using principle component analysis to see if the pigments at specific stages clustered together. The mature green stages separated based on photosynthesis related carotenoids and chlorophylls, and the ripe separated based on the ripening related pigments, such as capsanthin and its esters, β -carotene, β -cryptoxanthin, antheraxanthin and its esters, phytoene, phytofluene, and α -tocopherol, whereas the more intermediate stages of ripening separated based on zeaxanthin and its esters and capsorubin.

Table 3.4. Comparison of ripening series in selected lines.

Ripening stage	R1 (High intensity; fast ripening)	R3 (Low intensity; fast ripening)	R7 (High intensity; slow ripening)
MG			
B			
B+3			

B+7			
B+10			
B+14			

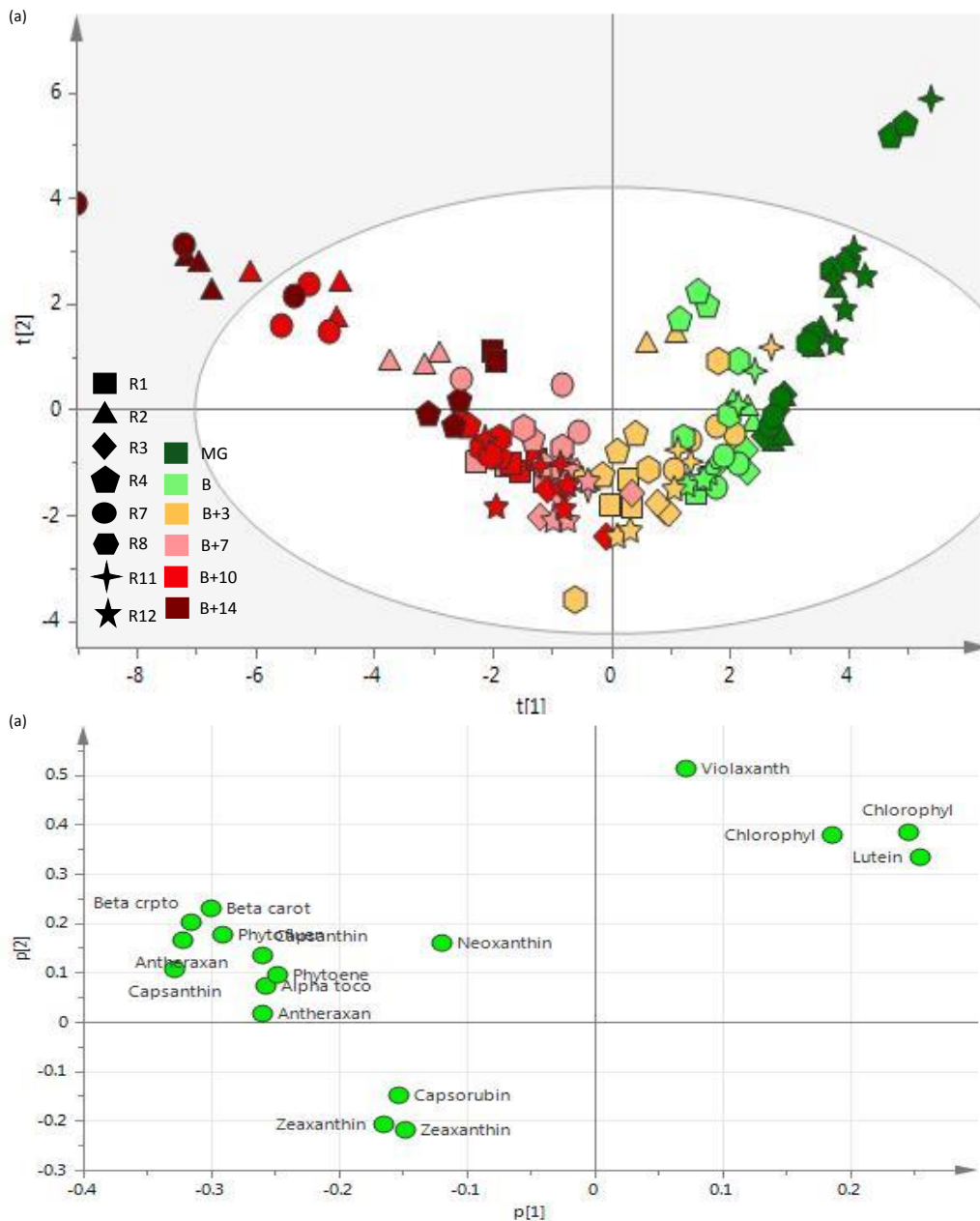


Figure 3.7. PCA of carotenoid pigments throughout ripening in selected lines.

PCA was carried out on all the pigments identified throughout the ripening stages in the selected lines to allow visualisation of the pigment accumulation throughout ripening. (a) PCA scores and (b) PCA loadings.

Interestingly, the ripe stages of the high intensity lines were all found in the top left quartile of the PCA separating from the others with the ripening related pigments, previously mentioned.

The low and medium intensity lines were located in the bottom left quartile of the PCA separating based on zeaxanthin and capsorubin (Figure 3.7).

PCA analysis carried out on the data revealed that the slow ripening lines, R2 and R7, separated away from all the other lines at B+10 and B+14 stages for ripening related carotenoids. It was found that the B+7 stages of R2 and R7 clustered with B+14 stages for fast ripening lines R1 and R4. It was also discovered that the R3 lines B+10 stage clustered with B+7 of the other lines shown.

3.2.3.2. Ratio of red to yellow carotenoids accumulated throughout ripening

As an alternative method of evaluating the carotenoid content and composition of carotenoids, the ratio of red to yellow coloured carotenoids was calculated. The red carotenoids included capsanthin and capsorubin, whereas the 'yellow' carotenoids were all those that were yellow-orange in colour, such as zeaxanthin, antheraxanthin, β -carotene, β -cryptoxanthin, violaxanthin, and neoxanthin (Figure 3.8).

The red to yellow ratio analysis was carried out as it was hypothesised that the high intensity phenotype lines would have a high red to yellow ratio, as this has been seen previously (Hornero-Méndez et al., 2000). However, it was discovered that the opposite was true. The high intensity phenotype lines had a much lower ratio of red to yellow carotenoids than the remaining low and medium intensity lines. The ratio of red to yellow carotenoids was then examined throughout ripening to gain insight in the accumulation of these compounds throughout ripening. It was revealed that the ratio of red to yellow carotenoids increased as ripening progressed until B+10 in the R1 line, and earlier at B+7 in the R7 line, and then started to decline (Figure 3.8b and d). However, the low intensity line, R3, did not experience a decrease in ratio, the ratio increased throughout ripening and then plateaued at B+7. This showed that once the high intensity lines reached a certain stage of ripening the red carotenoids did not continue to be synthesised at the same rate and the yellow carotenoids stayed at a similar rate of synthesis; thus, resulting in the accumulation of yellow carotenoids in the later stages of ripening. This was not experienced in the R3 line, this line continued to synthesise the red carotenoids at the same rate it was producing the yellow precursors.

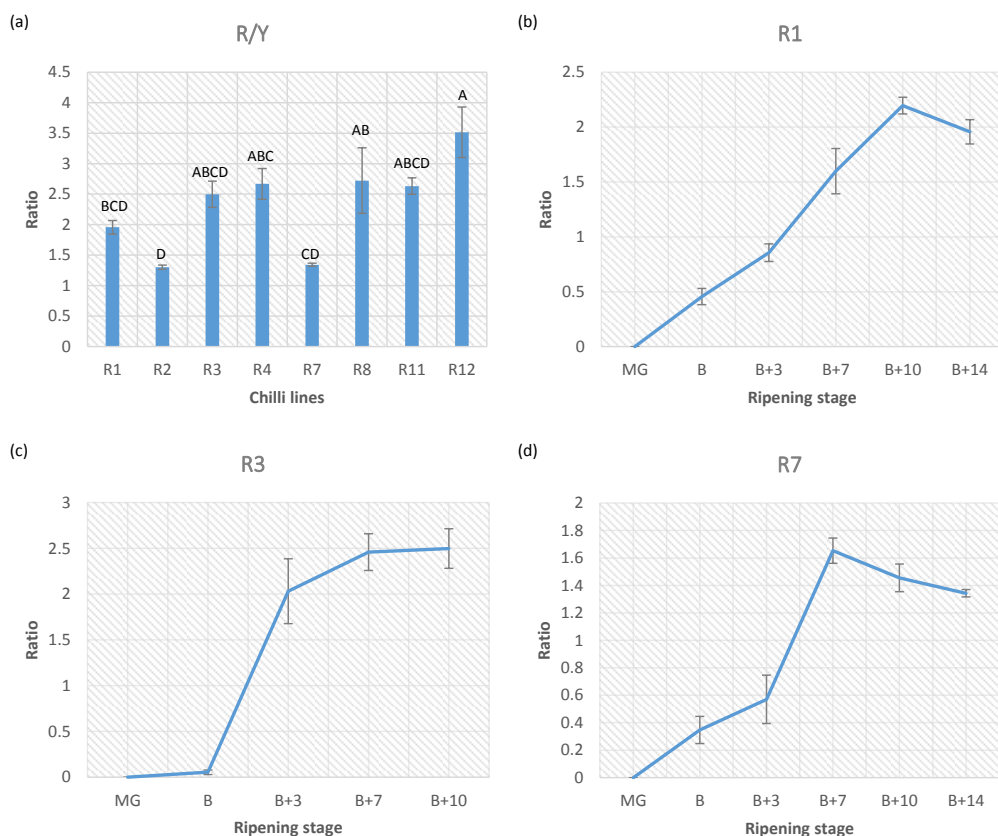


Figure 3.8. Ratio of red to yellow carotenoids.

The ratio of red to yellow carotenoids was calculated in (a) selected lines and throughout ripening, in (b) R1, a high intensity line, (c) R3, a low intensity line and (d) R7, a high intensity line. Error bars represent \pm SE ($n=3$). One-way ANOVA with post-hoc tukey was carried out and the lines were grouped based on significance ($P \leq 0.05$).

3.2.4. Sequencing of *PSY1*, *PSY2* and *DXS* in selected lines

Keys genes encoding biosynthetic enzymes in the pathways known to have the most influence over carotenoid formation were sequenced to ascertain the presence of allelic differences. Correlating these allelic differences to altered carotenoid content, could potentially reveal underlying mechanisms associated with increased colour intensity traits in the lines R3 and R7. These lines were chosen on the basis of their carotenoid content; for example, R3, is a low intensity phenotype line which displayed consistently low amounts of carotenoids when

compared to the other lines. R7, on the other hand, was shown to accumulate consistently high amounts of carotenoids when compared to the other lines and has a high colour intensity phenotype.

The fruit and leaf specific phytoene synthase 1 and 2 (*PSY1* and 2), respectively, were chosen to study as the fruit specific *PSY1* is known to have the most influence over the carotenoid biosynthesis pathway in tomato, and based on flux coefficients, shown that under standard environmental conditions it is the enzyme with the most influence over the pathway (Fraser et al., 2002). The leaf specific isoform was identified and characterised to see if this gene had any influence on the accumulation of carotenoids in the fruit. Finally, a gene from the MEP pathway, *DXS*, was selected to sequence because this pathway is present immediately upstream from the carotenoid biosynthesis pathway, and is postulated to be the rate limiting step in isoprenoid biosynthesis in tomato and *Arabidopsis* (Lois et al., 2000). The genes were cloned from genomic DNA to allow comparison of promoter and coding regions.

3.2.4.1. Fruit specific phytoene synthase

The *PSY1* gene in lines R3 and R7 were sequenced using overlapping fragments with primers designed from a *Capsicum PSY1* from NCBI (EU753855). *PSY1* was located on chromosome 4 of the pepper genome database 2.0. The *PSY1* gene consists of a 1260 bp coding region which encodes a 419 amino acid protein. This gene contains 6 exons and 5 introns. The start codon was located in the first exon. The R3 line had an identical amino acid sequence to NCBI entries with accessions GU085273 (Guzman et al., 2010), EU753855 (Huo et al, 2008), and X68017 (Romer et al, 1993). However, R7 had a base pair substitution creating a tyrosine to cysteine change at amino acid 59 (Cys⁵⁹) (Figure 3.9). This is present in the first exon of the coding sequence. When comparing the introns and exons there is very little variability between the two sequences. Apart from the base pair substitution previously mentioned there were only 4 other differences throughout the sequence and these were found in the introns. Therefore, the mRNA of the two lines analysed were highly conserved within chilli pepper of differing colour intensities, as well as others characterised from the *Capsicum* genus.

Modelling of the *PSY1* protein structure was carried out in SWISS-PROT. This program used squalene synthase to build a model as they catalyse a very similar reaction. The first 125 amino acids were not present in SQS suggesting the presence of a signal peptide (Figure 3.10). Predotar

was used to predict the sequence contains a plastid transit peptide with a probability score of 0.82.

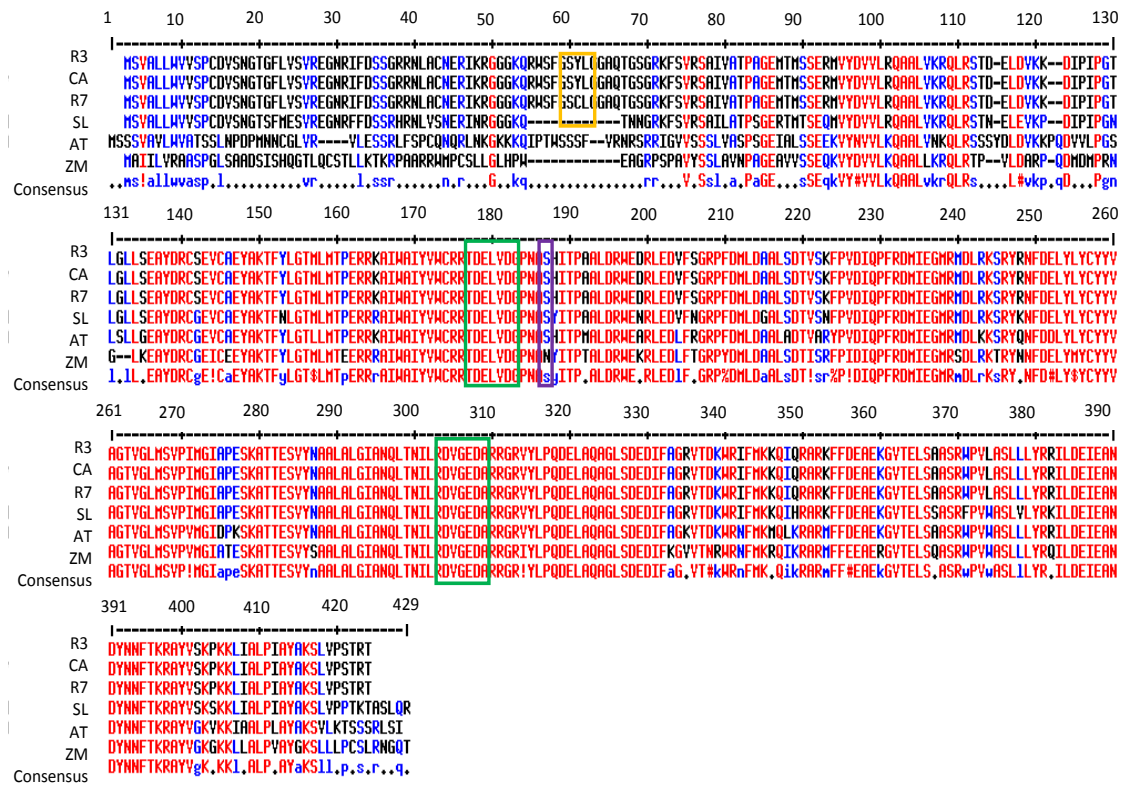


Figure 3.9. Comparison of amino acid sequence of PSY1 between different higher plants.

The coding regions of the *PSY1* gene in selected lines R3 and R7 were converted into an amino acid sequence and compared to other plant species available on NCBI: CA, *Capsicum annuum* (ACE78189); SL, *Solanum lycopersicum* (ABM45873); AT, *Arabidopsis thaliana* (AT5G17230) and ZM, *Zea mays* (AAR08445). This revealed the presence of a base pair substitution in R7 resulting in a tyrosine replaced by a cysteine (Cys⁵⁹) in the transit peptide (orange box) and showed the highly conserved regions in the putative active site (green box) (Shumskaya et al., 2012). Alignment carried out using Multalin (Corbet, 1988).

Interestingly, the *Capsicum* varieties analysed and the tomato sequence all started with the sequence MSVALLWVVS. Generally the *Capsicum* and tomato were more similar than the maize and *Arabidopsis* at the N-terminus, with the signal peptide showing the most variation. There is also variation found at the C-terminus.

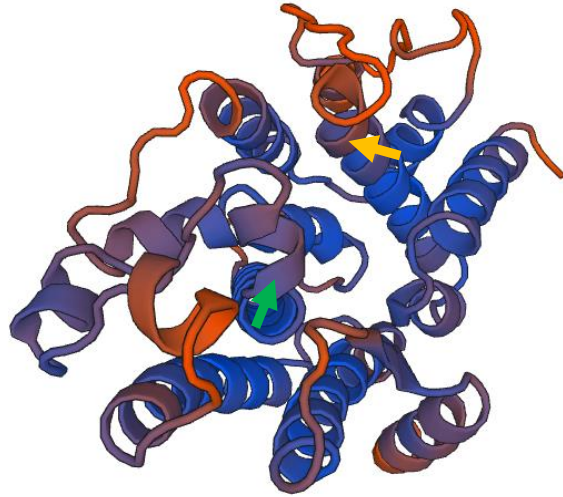


Figure 3.10. Predicted protein structure of the PSY1 protein in chilli pepper.

The PSY1 gene sequences of chilli lines R3 and R7 were elucidated and the structure of the PSY1 protein (excluding the transit peptide) was modelled using SWISSPROT.

The PSY1 enzyme belongs to a family of trans-isoprenyl diphosphate synthases, such as farnesylpyrophosphate synthase (FPS), geranylgeranylpyrophosphate synthase (GGPS) and squalene synthase (SQS). The enzyme is a monomer and the entire structure is predominantly α -helices. The active site comprises a central cavity of anti-parallel α -helices with aspartate rich regions (DXXXD) which formed the first layer of helices. The active sites are indicated by arrows on Figure 3.10 and both contain negatively charged aspartate and glutamate which face into the central cavity. Glycine and valine are also present in both sites. The first site is at ¹³⁷DELVD¹⁷⁷ and the second site is at ²⁹⁹DVGED³⁰³.

The promoter sequences were analysed for transcription factor binding motifs in order to evaluate whether there were any differences in transcription factor binding sites, and so regulatory mechanisms, between the high and low intensity lines which could alter gene expression. It is important to stress at the outset the regulatory elements identified are only putative and are described as leads for further experimental work. There were no differences observed between the R3 and R7 lines, and also no differences when compared to the *Capsicum*

phytoene synthase promoter from the Sol Genomics Network suggesting the promoter sequence is highly conserved in the *Capsicum* genus. Although there were no differences between the lines, putative regulatory elements (REs) were identified to give an insight into the regulatory mechanisms involved in *PSY1* expression.

-2022 GTTGGTCTACTGGGCGGAGCTAGAGTATCAGTTACGGATTAGTTGAATTTAGTAGCTTAG
(a) -1961 CTTAACCTGTAAACATAGTAACTTAAAAATATTGTAAAATTTAGAACTCATAAACTTCAAAT
-1899 TTTGACTCATTACATTTCTTGATATACAAAGTTGCAATCTTTGACATTCTGTGTGGCTTTTAA
-1836 TTGCTATGGTTGTGCGCTTGTGCTATACATGGGCGGATCTAGAGTGTTAGTTACGGGTTT
-1775 AGTTGAATTCAGTAACTTTAGTTCAAACCCCGTAATGTGTTTACTTAGAAAATTAGAATTT
-1713 AGAACTCATAAATTTCAAATTTTGGTTCGTTACATTTCTTGATATATAAAATTGCAATCTTTG
-1650 ACATTCTCTGTGGCTCTTTATTGCTATGGTAGTGTGCTTGTGCTATACTAGGGGTGGAGCT
(b) -1588 AGAGTGTCAATTATGGGTTTGGTTGAATTCAGTAACTTTAGTTCAAACCCATAACGTGTTA
-1526 AACTTAGAAATATTAGATTTTAGAACTCATAAACTTCAAATTTTACTGCTTACATTTTCTTG
-1463 ATATACGAAGTTGCAATCTTTGACATTCTGTGTAACCTTCTATTGCTATTGTAGTGTGTTGT
-1400 TGCTATACTAGGGGCAGAGCTACAGTGTGAGTTATGTATTAGTTGAATTCAGTAGCTTTG
(c) -1339 GTTCAAACCCATAACATAGTAACTTAAAAATGTTAAAAATTTAGAACTCATAAACTTCAA
-1277 TGTTGACTCGTTACATTTCTTGATATACAAAGTTGCAATCTTTGACATTCTTTGCGGCTTTT
-1214 ATTGCTATGGTTGTGTGCTTGTGCTATACATGGGCGGAGCTAGAGTGTTAGTTACGGGTT
-1153 TAGTTGAATTTAGTAGTTTGTGCTCAGACCCGTAATTTGTAACCTAAAAACATTAGAATT
(d) -1091 CTGAACCCATAAAGTTCAAATTTTACTCGGTTGACTTCTAGATGTATAAAGTTTCAATCT
-1029 TTAACATTCTTTGTAACCTTTTATTGCTATAGTAATGTTCTTTTGTATACTAGGGGCGGAA
-966 CTAGAGTGTAAGTCGAATTCAGTAACTTTAGTTCAAACCATGTAACCTAGTATCTAAAAAT
-904 ATTAATAATTCGGAACCCATAAACTTCAAATTTTACTCCGACTATACAAGAATAGAATTTG
-842 AGAGTGGCCTAAAATTTAGTGTCCATTGTTAGTGGAGAACCAATTATCAAGGTTTGTTC
-780 CTTCACTTCTTGATATACAAGTTGCAATGCTTAACATTCCCTGTAACCTTTCTATTCCACTGGT
(e) -717 AGTGTGCTTGTGCTATACCGGGGCGGAGCTAGAGTGTTAGTTACGGGTTTGGTCTGACTTT
-656 AGTAGGGCAGCCCGTCACTACAGCTCCCGCTATGCGCAGGGTGGCGGGAAGGGGCGGA
(f) -597 CCACAAGAGTCTTTTAAACATTTTGCAAGGAGCTGTTCCACGCTTGAACCGGGGACCTCCT
-535 AGTCACTAGAATTCAGTAGCTTTAGTTGAGAATCCACAACTTCAAATTCTAGCTCCGCCTA
(g) -473 CTAGTGAATAAAATAATAGAAAATGAGCACTTGCCTTATGAATATAGCTTCTACGTGTA
(h) -412 CCAAATAGAAAGTGAGGTGCTTATTATAATCTAGTTGACTAAATATAGAAAATGATCCCAT
(i) -351 TACCTCAGAAAGTGTGATTCCACTTTGTGCTTTCAATAGTGTAATAATAGTTTCTCAAACAT
(j) -289 CCTTTCTTTGTGCCATTGGTAGGTAAGTTGCTGTTTGTCTTGTGGAGATGTTTTTAA
-226 AGTTAAAATGTTTATACTCAGGAAGTCTATAATGCTGGTACGAGTTCATGTGAACTCAGT
(k) -164 AGTTTTCGTAAGCAATCCACTAATACTATAAATTTGACCGTGAACCTCGCTTGTATCA

TTTCATTAACTTGAGGTCGCTATAGGAGCCGATAAACTTCCAACTTCTGAATCAGTTTTTGT
 102 TTATACTCAAGTATGATGTTTGGTTTATCTCATATTGCAG
 -40 AAGCCAAGAAATAGGTTATTTCTTTGTTTGATAGTGGAAGTATACTCTAGTGGGAATCTACT
 +1 AGGAGTTACTTATTTTCTATAAAGAAGACAAAAACCTTGGAGTTGCTTTAGACAACCAAGG
 +63 TTTTTCTTGTTTCAGAATG +141
 +124

Figure 3.11. Putative regulatory elements present in the PSY1 promoter.

In silico transcription factor analysis was carried on the promoter of the *PSY1* gene and putative regulatory elements (REs) were elucidated. The blue ATG represents the start of the coding region, the red nucleotides represent the 5'UTR, and the green nucleotides represent the promoter region. The yellow highlighted sequences are potential light-regulated elements, the red highlighted sequences represent putative REs found in the phenylpropanoid biosynthesis pathway, light blue highlighted regions represent putative REs which are activated in response to stress, dark green represents predicted CarG motifs, and dark blue represents a region which has the most homology with other promoters and possible key regulatory site. The light blue ATCTA motifs are also found in PSY of Arabidopsis (Welsch et al., 2003). Green indicates a possible TATA-rich motif as well as the purple TATA box. The letters a-k are described in Table 3.5.

The *in silico* transcription factor analysis on the promoter region revealed some putative regulatory elements. Firstly, the dark blue highlighted area, spanning -260 to -273, was found to have homology with many other species in terms of regulation (Figure 3.11j). For example, this sequence is found in the promoter region of the flavonoid biosynthesis gene, flavanone 3-hydroxylase (*F3H*) and is involved in the activation of the gene in response to light (Hartmann et al., 2005). This same element is also found to be light regulated in other flavonoid and phenylpropanoid biosynthesis genes, such as chalcone synthase (*CHS*) and phenylalanine ammonia-lyase (*PAL*) (Logemann et al., 1995), as well as being related to stress response in tobacco and soybean. There were also other regulatory elements present in the promoter sequence which were present in flavonoid and phenylpropanoid biosynthesis genes which were involved in activation as a response to stress (Figure 3.11d and f; Table 3.5) (Ito et al., 1997; Grimmig and Matern, 1997).

Other possible stress related REs identified were homologous to the binding site for WRKY28 which activates members of the salicylic acid biosynthetic pathway in response to pathogens (van Verk et al., 2011), and JAMYC which binds a G-box and activates amino acid hydrolysis in response to pathogens (Boter et al., 2004). Potential motifs homologous to MYC transcription factor REs found in aubergine and tobacco were also predicted (Chen et al., 2011).

Light-regulated motifs were prevalent in the *PSY1* promoter. REs homologous to the box I motif which binds GT-1, a light regulated transcription factor, were predicted, as well as motifs also present in the promoter region of the chlorophyll a/b binding (*CAB*) gene. The *CAB* motif was found twice in the promoter sequence of *PSY1*, in addition to similar regulatory elements involved in the light regulation of the *CAB1R* in rice (Figure 3.1c, g and i)(Schindler and Cashmore, 1990; Luan and Bogorad, 1992). A possible ACE1 transcription factor binding site was predicted which also binds a phytochrome a regulatory gene (Li et al., 2010).

There were a number of potential CarG box REs predicted which bind MADs box transcription factors. These tended to have roles in the plant development, such as plant embryo development, ripening, and flowering (Tang and Perry, 2003; Fujisawa et al., 2011).

The nucleotides containing the ATCTA motif were highlighted blue as this motif was also found in the *PSY* promoter of *Arabidopsis*. Putative TATA rich regions were identified and represented by purple nucleotides (Figure 3.11).

Table 3.5. Putative transcriptional regulatory elements identified in *PSY1*; corresponds to Figure 3.11.

Ref	Regulatory element	Regulatory element; binding factor	Gene	Plant	Gene function; Response
(a)	ATtTGACTCAT	WRKY28 BS; WRKY28	ICS1	<i>Arabidopsis thaliana</i>	SA biosynthesis; Biotic stress response (van Verk et al., 2011).
(b)	AtAACGTGTTaA	T/G box; JAMYC2 and JAMYC10	LAP	<i>Lycopersicon esculentum</i>	Amino acid hydrolysis; Wounding

					response (Boter et al., 2004).
(c)	AAAAtGTTAAAA	Box I; GT-1	Cab-E	<i>Nicotiana plumbaginifolia</i>	Chlorophyll a binding; Light regulated (Schindler and Cashmore, 1990).
(d)	GaACCCATaAAG	Box E; unknown	CCoAOMT	<i>Petroselinum crispum</i>	Phenylpropanoid biosynthesis; Stress response (Grimmig and Matern, 1997).
(e)	CGgGTTGGTCG	Box II; unknown	psCHS1	<i>Pisum sativum</i>	Flavonoid biosynthesis; Stress response (UV and elicitor) (Ito et al., 1997).
(f)	TTTTAACaTTTT	Box I; GT-1	Cab-E	<i>Nicotiana plumbaginifolia</i>	Chlorophyll a binding; Light regulated (Schindler and Cashmore, 1990).
(g)	CTACGTGTA	ACE1; HY5	FHY1	<i>Arabidopsis thaliana</i>	Phytochrome a regulation; light regulated (Li et al., 2010).
	CTACGTGT	GBF1 BS7; GBF1		<i>Arabidopsis thaliana</i>	Stress regulated
(h)	CCAAAATTaG	CarG (016); RIN	TBG4	<i>Lycopersicon esculentum</i>	Cell wall modification; Ripening regulated (Fujisawa et al., 2011).
	CCAAAATTAG	CarG; FLC	SOC1	<i>Arabidopsis thaliana</i>	TF;

					Flowering (Hepworth et al., 2002).
	TGACTAAATATAGAAA	CarG3 (DTA4)	AGL15	<i>Arabidopsis thaliana</i>	TF; Plant development (Tang and Perry, 2003).
(i)	AGTGTAAAAT	Box III*; unknown	Cab1R	<i>Oryza sativa</i>	Chlorophyll a binding; Light regulated (Luan and Bogorad, 1992).
(j)	TGGTAGGTAag	MRE-core; R2R3-type MRE	F3H	<i>Arabidopsis thaliana</i>	Flavonoid biosynthesis; Light regulated (Hartmann et al., 2005).
	TGGTAGGTAAG	Box I; unknown	chsA	Various plants	Flavonoid biosynthesis; Light regulated
	GGTAGGTAAG	Box L; unknown	PAL-1	<i>Petroselinum crispum</i>	Phenylpropanoid Biosynthesis; Unknown (Logemann et al., 1995).
	TGGTAGGTAAGAT	13bp - box	LTR-Tto1	<i>Nicotiana tabacum</i>	LTR- retrotransposon; Stress response
	GGTAGGTAAG	MYB92 BS3; MYB92		<i>Glycine max</i>	Unknown; Stress response
	TGTCTGTTtT	MYCS (PT3); MYC	PT3	<i>Solanum melongena</i> <i>Nicotiana tabacum</i>	Mycorrhizal induced (Chen et al., 2011).

3.2.4.2. Leaf specific phytoene synthase

The chilli pepper *PSY2* gene sequences in R3 and R7 were elucidated with overlapping fragments using primers designed from the tomato *PSY2*, as they are very similar. The *PSY2* gene consists of a 1299 bp coding sequence with 6 exons and 5 introns and comprises a 438 amino acid protein. The chloroplast transit peptide recognition program Predotar predicted the presence of a plastid signal peptide with a probability of 0.61. This was the same for both sequences. The *PSY2* sequence is located on chromosome 2 of the pepper genome database 2.0.

When comparing the R3 and R7 amino acid sequences they are 99.8% similar with two amino acid differences. The first is at residue 149 and contains a serine in R3 (Ser¹⁴⁹) and a tyrosine in R7 (Tyr¹⁴⁹). The second difference is at 257 and contains a histidine in R3 (His²⁵⁷) and tyrosine in R7 (Tyr²⁵⁷). In both cases the substituted amino acids are polar. However, when protein modelling was carried out the position of the substitutions may affect the structure of the protein as the 257 substitution is close the putative active site proposed by Shumskaya et al., 2012 (Figure 3.12). Additionally, when alignment of chilli pepper *PSY1* and 2, tomato *PSY1* and 2, Arabidopsis *PSY*, and maize *PSY2* was carried these amino acids were conserved throughout all plants analysed and so the substitutions were unique to the R3 line (Figure 3.13).

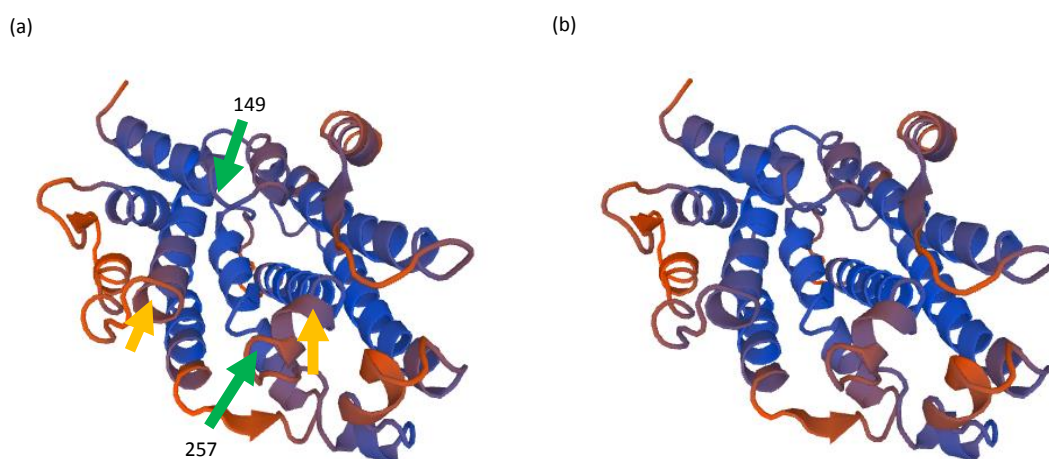


Figure 3.12. Comparison of the predicted structure of the PSY2 protein.

The *PSY2* gene was sequenced in a low and high intensity phenotype line (a) R3 and (b) R7, respectively. The structure of the *PSY2* protein was predicted using SWISSPROT. The top green

arrow on present amino acid substitution 149 (Ser¹⁴⁹) and the bottom green arrow represents substitution 257 (His²⁵⁷) which are unique to R3 and the orange arrows represent putative active sites as proposed by Shumskaya et al., 2012.

The PSY1 and PSY2 amino acid sequences share 89% similarity in R3 and R7. There is an 8 amino acid insertion in PSY2 coding region in the proposed chloroplast transit peptide which is the most variable part of the coding sequence, as found previously in PSY1. This insertion was also present in the tomato PSY2, 20 amino acids missing when compared to the tomato PSY1, and the insertion was absent from *Arabidopsis* and maize (Figure 3.13).

The structure of the PSY2 enzyme is very similar to the PSY1 enzyme. As previously mentioned for PSY1 the protein consists of a central cavity surrounded by α -helices. The first layer of helices closest to the central cavity is where the active sites are located. These aspartate-rich regions are essential for the binding of the GGPP substrates via a Mn²⁺ salt bridge.

A smaller insert (4 AAs in PSY1, chilli and tomato; 6 AAs in PSY2, chilli and 9AAs in PSY in *Arabidopsis*) was located in tomato PSY2 and maize slightly upstream from the insert previously mentioned.

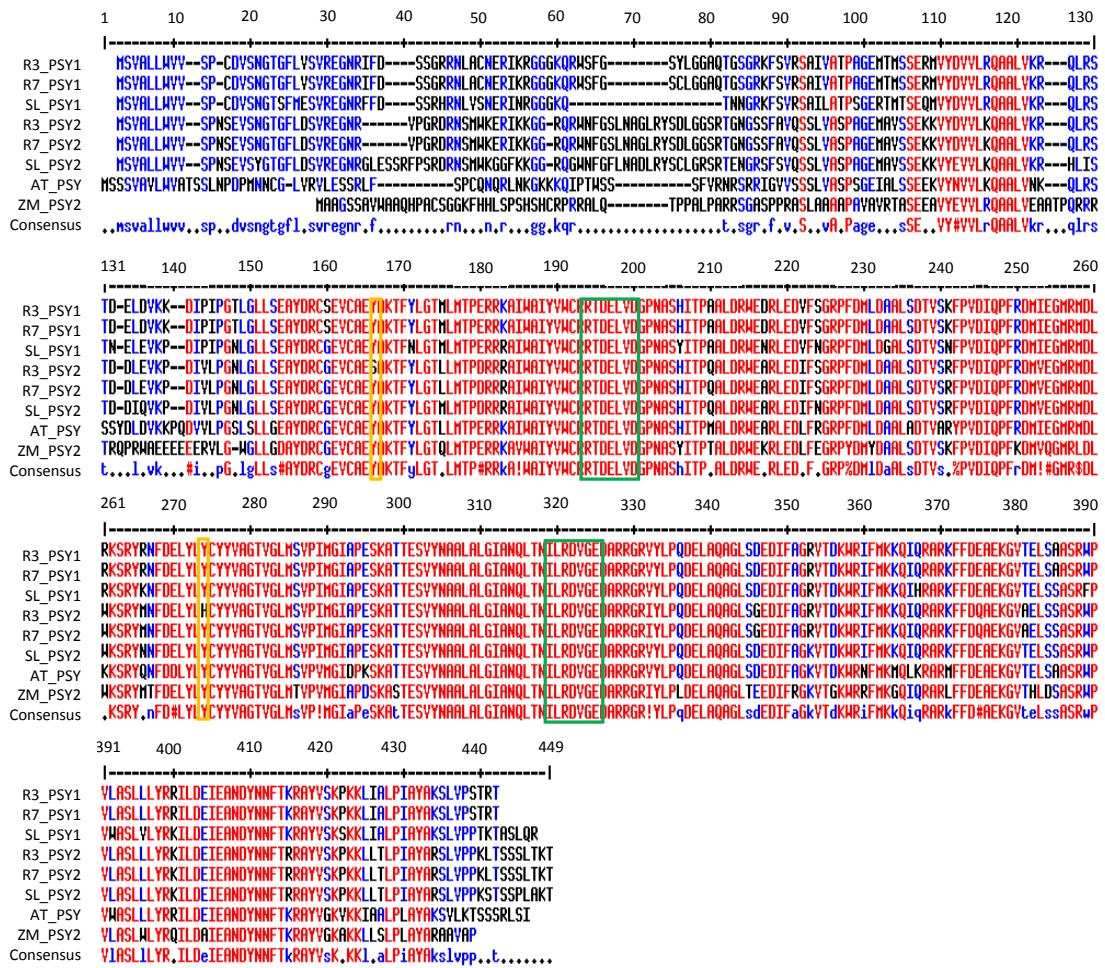


Figure 3.13. Comparison of amino acids in PSY1 and PSY2 between different higher plants.

Amino acid alignments of PSY1 chilli pepper and tomato; PSY2 chilli pepper, tomato and maize and PSY *Arabidopsis* was carried out to analyse the homology between PSY1 and PSY2 proteins within a species and over different plants. The amino acid sequences of the three species were obtained from NCBI: PSY1: SL, *Solanum lycopersum* (ABM45873); AT, *Arabidopsis thaliana* (AT5G17230); PSY2: SL, *Solanum lycopersum* (NM_001247742) and ZM, *Zea mays* (AAX13807). The green boxes represent putative active sites and the orange boxes represent differences in amino acid sequence unique to the R3 PSY2 protein. Alignment was carried out using Multalin (Corbet, 1988)

The promoter regions of the *PSY1* and *PSY2* chilli pepper genes were aligned and this revealed that there was only 44.2% similarity between them. This is unsurprising as there is little similarity between the tomato *PSY1* and *PSY2* promoter sequences.

In silico transcription factor analysis was carried out on the *PSY2* promoter region. The R3 and R7 promoter regions of *PSY2* had 99.6% similarity when aligned. This included 6 bp substitutions

and one bp deletion in the R3 line. The 5'UTR region was predicted based on its homology to the tomato *PSY2* 5'UTR. However, sequencing of the mature protein, using peptide mass fingerprinting, would allow the UTRs to be annotated more accurately. When the sequences were scanned in the regRNA 2.0 database, the software predicted the presence of splice sites in the 5'UTR. This suggested there may be an intron present here and the additional translational start sites (TSS) present could be removed in an intron.

```

-2655 ACCAGTCTGACCTCAACCTTTGTCTACTTATATACTATATTAAGGAGCATTGGAAA
(a)-1299 ATAAATGTAGCCATAACTTATTAGAGACTAGCTTAATGGGTCTTTTGTGTAATCA
(b)-1490 TCAATTTCTCGAAAGTTAAAATTGGAATCAGGTC AATTTCCAACCA AACTTCTG
-1434 ATACGAAATAATGTTAGGTCTCGTCAGAAATAATAATGTGGGCTTTTACATAAAAA
-1378 GAGTAATCCTTAGAATTTGATTTAAATATATTGTCATCTGTCCTTGTACTAGAATT
-1321 TTTTCTTTTGGTGAACAGGCAAGGATTTATTATAATATAATAACAAAAATATTTA
-1264 CAAGTCTTGTCCTTGTACTAGAACTTACACATACGGCATCTAATACTAACTAG
(c)-1207 TGGCGGACAGTGTGtA AATTTACGTGTATCTGTTACGACCAGAGGTCACAAATGGA
-1152 CTCATTCAACTTAATTTCAAGGGATAAAGTAAAGTTAAAGTTAATAAATAAATTAT
-1096 TGATTCGCTCAAAGTTATAAGAGTTAAAATAGATTGGACCATCTGCCTAGTTCT
-1040 TGCTAAATTTTAGTTGCTTTATTTGATTTTAAATAATCTCTCGATTAA GTCTCTCA
-982 ATAATGAGTTAATTTGATTGATAATCAATTTAATTTTAAATAGATTAAAACAGTTTG
(d)-925 GA CCGAAATAAG CCGAACTAATAAATAGATGAATTACTAATCCTTCCAAATTTCCA
-869 ATACTTGAAAGAATTAGGGGGCGTTGATTGGGAGCAAGTTATTAGCTATCTGAGA
-814 AAAAAATTATCTCATAATATAAGTTATGCAATCACTATGATATAAATAAACCAATA
-757 AGATTGACTAATACTCCAACCAATACTAAATAAAATAATTTATATTTTATCCTGAA
(e)-700 ATTA TTTATTATTATTATTATTATA CCTTACAG CTCAAACCGAACAA CTTTCTTAGAAG
(f)-642 AAATACTTTTACACCTCTCA TTCTGACCAG GTGTTAGTGTGGGA AAAAGGTTAAAA
(g)-586 GGTGGAAACTACAAGAGAAGAGAATAGAGATAGAATCTGAACCACTT AATTATAA
-641 TCA GCACAACCTCGTGTACACAGGTGAACAAAAAATTTGAATGGTCTAAAAGCTA
-586 TTCAAAAATATATAGGAAGTATAATTCAAACAAGTAAATGCTGCTGAAATTGTTGA
-357 GATCAGTAGCAAGAAGTGGCACTTCTTTACTTTATTTCAACTAACGTTGCTATTCTG
-300 CAGGTTGGTTATTTTAATCCCCCTGTAGCTTTCATTATTAATCTGGTTTTCCATT
-242 ATATAATCATATTTTATACTATTAAGATATGAATACCCTTTTCCTTTTCTAGACAG
(h)-184 TTTCTACGTGTAAATCAAAGTTAGAAAGGGAgCTTATTATAATACAAT TAACTATAT
-127 ATAGTAA TCTCCATTACTTAAAATATAGTGTGAACCATGTTCAATTTGGGGGTTTTT

```

-70 CTATTTGTGAGTTGAGTAATTTTTAAAGATTCTTGCATTTTGCTGTTTGCTGATTTG
 -12 GTTCTTGGTATT
 +1 GGGATACTTTATTTTATTAATTCACAACAAAAGTTTGAATTTTATGCTTTTTGAGT
 +288 GGTATAACTGTATCAGTTGTATGATATATAAAGTATATTTGGTTTATCTCATTGTG
 (i) +345 CAGAAACTCAGAAAGACCAAGGTTTGGCTTCTTGTGATGAGTGGTGCAttATAAG
 (j) +402 TCTGCTTGTGTAAGCCAAAGTTGGTCACTTTCTCATCATGCGATTTTTATAATCGT
 +457 TGATATTGCTTCAAATTTGGTGGATAGACTCTAGTGGATATCTACTAGTAGAATTT
 +512 TTTTAATTATTTGGGATAAACTAGGCTGAGGTGAGGTGAGAAGGTAACATAAAG
 +523 GACAGACAAAACTTGGGAATTGTTTTAGACTACCAAGGTCTCTTGTTTAAGCATG
 +532

Figure 3.14 Putative regulatory elements present in the PSY2 promoter.

In silico transcription factor analysis was carried out on the PSY2 promoter regions of R3 and R7 to elucidate putative regulatory elements (REs). The blue ATG represents the start of the coding region, the red nucleotides represent the 5'UTR and the green nucleotides represent the promoter region. The red highlighted regions represent possible REs found in phenylpropanoid biosynthesis related genes; the pink regions are potential REs found to be hormonally regulated; the light blue regions represent putative stress regulated REs; the dark green regions represent CarG box REs and the dark blue region is an element which has the most homology with other promoters and a possible key regulatory site. The above sequence is the R7 promoter region and the differences between R3 and R7 are displayed as red characters and the grey region corresponds to a RE only present in R7. See Table 3.6 for description of REs.

Table 3.6. Putative transcriptional regulatory elements identified in PYS2 promoter. Corresponds to Figure 3.14.

Ref	Motif	Regulatory element; binding factor	Gene	Plant	Gene function; Response	In PSY1
(a)	CTTAATGGGTCT	Box E	CCoAOMT	<i>Petroselinum crispum</i>	Phenylpropanoid biosynthesis; Stress response (Grimmig and Matern, 1997).	Y

(b)	AATtCCAACCA	Box-L4; DcMYB1	DcPAL1	<i>Daucus carota</i>	Phenylpropanoid biosynthesis; Stress response (Maeda et al., 2005).	N
(c)	tGGCGGaCAGTG	GRA; unknown	Rab17	<i>Zea mays</i>	ABA regulated	N
	aTTACGTGTAT	C/A box; HY5	PIN1	<i>Arabidopsis thaliana</i>	Auxin carrier proteins; cytokinin regulated	N
	TTACGTGT	GBF1 BS8; GBF1		<i>Arabidopsis thaliana</i>	Stress regulated	Y
(d)	CCGAAATAAG	CarG; FLC	SOC1	<i>Arabidopsis thaliana</i>	Transcription factor; Flowering (Hepworth et al., 2002).	Y
(e)	TtaATTATTATTATT ATTATa	C2; unknown	GmAux28	<i>Glycine max</i>	Auxin regulated	N
	CTCAAACCGAaCAA	P box 4; unknown	C4H	<i>Arabidopsis thaliana</i>	Phenylpropanoid biosynthesis; Stress response (Bell-Lelong et al., 1997).	N
(f)	TTCTGACCAG	W-box; bhWRKY1	bhGOLS1	<i>Boea hygrometrica</i>	Sugar biosynthesis; Stress response (Wang et al., 2009).	N
	AAAAGGTTAAAA	Box I; GT-1	Cab-E	<i>Nicotiana plumbaginifolia</i>	Chlorophyll a binding; Light regulated (Schindler and Cashmore, 1990).	Y
(g)	AATTATAATCA	C-DP BS2; cytokinin	POR	<i>Cucumis sativus</i>	Plastid development;	N

		dependent protein			cytokinin regulated (Fusada et al., 2005).	
(h)	TCTACGTGTA	UV LRE; unknown	CHS	<i>Arabidopsis thaliana</i>	Flavonoid biosynthesis; Light regulated (Wade et al., 2001).	Y
	TTcTACGTGTAA	G/ A box; FY5	IAA3/	<i>Arabidopsis thaliana</i>	Auxin regulation; cytokinin regulated	N
	CTACGTGT	ACE1; FY5	FHY1	<i>Arabidopsis thaliana</i>	Phytochrome a regulation; light regulated (Li et al., 2010).	Y
	CTACGTGT	GBF1 BS7; GBF1		<i>Arabidopsis thaliana</i>	Stress regulated	Y
	TACGTGTAAATC	ABRE3a.3b; unknown	Sbdhn2	<i>Sorghum bicolor;</i> <i>Sorghum vulgare</i>	ABA regulated (Buchanan et al., 2004).	N
	TaACTATATATAGTA	CarG3 (DTA4)	AGL15	<i>Arabidopsis thaliana</i>	Transcription factor; Plant development	Y
(i)	TTGcTtCTGTtG ATGA	Motif d; epicotyl-specific	PSPAL2	<i>Pisum sativum</i>	Phenylpropanoid biosynthesis; Unknown (Kato et al., 1995).	N
(j)	CCAAAGTTGG	CarG (016); RIN		<i>Lycopersicon esculentum</i>	Cell wall modification; Ripening regulated (Tang and Perry, 2003).	Y

The *in silico* transcription factor analysis revealed a putative RE in the *PSY2* promoter in Figure 3.14h. This was a G-box motif which was present in flavonoid biosynthesis gene, *CHS*, and the phytochrome a promoter region, and was regulated in response to light (Wade et al., 2001; Li et al., 2010). This motif also shared with various genes involved in stress response and hormone regulation (Buchanan et al., 2004). Another possible G-box motif, homologous to one found in a *CAB* protein and regulated in response to light, was also predicted (Schindler and Cashmore, 1990). Plus, other motifs which were also identified in numerous phenylpropanoid biosynthesis genes, such as caffeoyl-CoA O-methyltransferase (*CCoAOMT*), cinnamate 4-hydroxylase (*C4H*), and *PAL*. These were binding factors which had a role in stress response (Grimmig and Matern, 1997; Bell-Lelong et al., 1997; Kato et al., 1995; Maeda et al., 2005).

Putative REs which were regulated by auxin and ABA were present, sharing homology with motifs located in the promoters of genes associated with plant and chloroplast development (Fusada et al., 2005).

Finally, the CarG box motif which binds RIN was identified and is involved in cell wall modification is regulated by ripening. This was also found in *PSY1* in R3 and R7 (Fujisawa et al., 2011).

When the R3 and R7 transcriptional analysis was carried out there was found to be a W-box motif which binds WRKY1 (Figure 3.14f) which was present in the R7 line but absent in the R3 line due to a bp deletion of a cytosine (Wang et al., 2009).

3.2.4.3. 1-Deoxy-D-xylulose 5-phosphate synthase (DXS)

The coding and promoter region of *DXS* was sequenced. The *DXS* coding region was 4135bps in length and comprises of 10 exons and 9 introns. This gives rise to a 719 amino acid protein. The *DXS* protein is a homodimer which is part of a subfamily which belongs to the thiamine pyrophosphate (TPP) family. It consists of a TPP binding domain and a pyrimidine (PYR) binding domain represented by orange arrows in Figure 3.15. The C-terminus of the *DXS* protein has homology with the other transketolases. There are two active sites each of which is the interface of the domains.

There were 5 amino acid substitutions when comparing the R3 and R7 lines; in R3 at residue 77 there was a valine instead of an aspartic acid (Val⁷⁷), an alanine in place of a valine (Ala¹²¹), and

a cysteine substituted by an arginine (Cys⁶¹⁰). All three substitutions were unique to R3 when compared to R7, sweet pepper (CAA75778), tomato (NM_001247743), *Arabidopsis* (CP002688), and maize (EF507248). R7 contained two amino acid substitutions, with valine replacing alanine at residue 232 (Val²³²) and phenylalanine in place of a leucine (Phe²⁵¹), thus, giving the amino acid sequences 99.3% similarity. On comparison of the conserved regions of the DXS proteins described previously in Bouvier et al., 1998b the Val²³² substitution in R7 was located within a conserved domain for thiamine-dependent enzymes (Figure 3.16). Modelling of the protein structure of DXS was carried out (Figure 3.15) and 71 amino acids from the N-terminus were not included implying the presence of a chloroplast transit peptide; however, this could not be identified using prediction programmes such as Predotar.

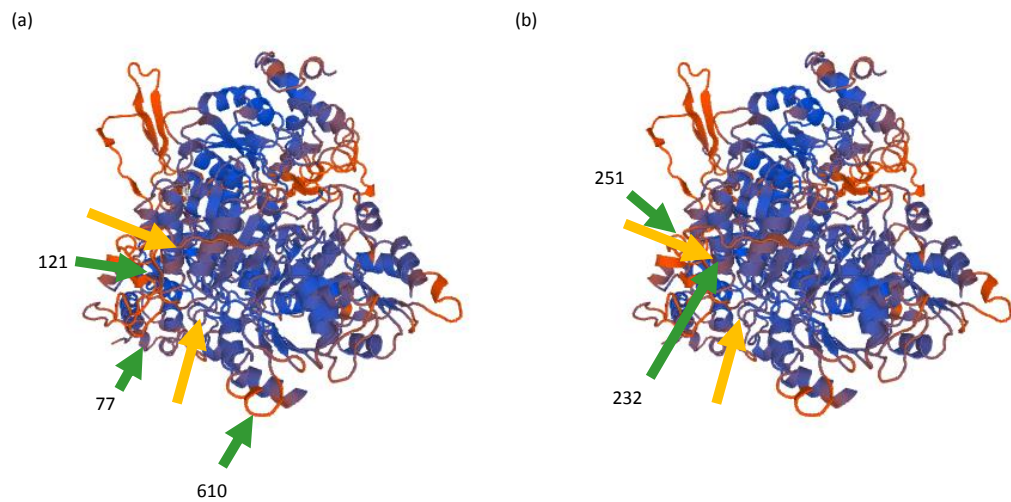


Figure 3.15. Comparison of the predicted structure of the DXS protein.

The DXS gene was sequenced in a low and high intensity line (a) R3 and (b) R7, respectively. A predicted structure of the protein was created using SWISSPROT (excluding the possible chloroplast transit peptide). The green arrows represent amino acid substitutions and the orange arrows represent conserved domains in thiamine-dependent enzymes and transketolase motifs characterised in (Bouvier et al., 1998b).

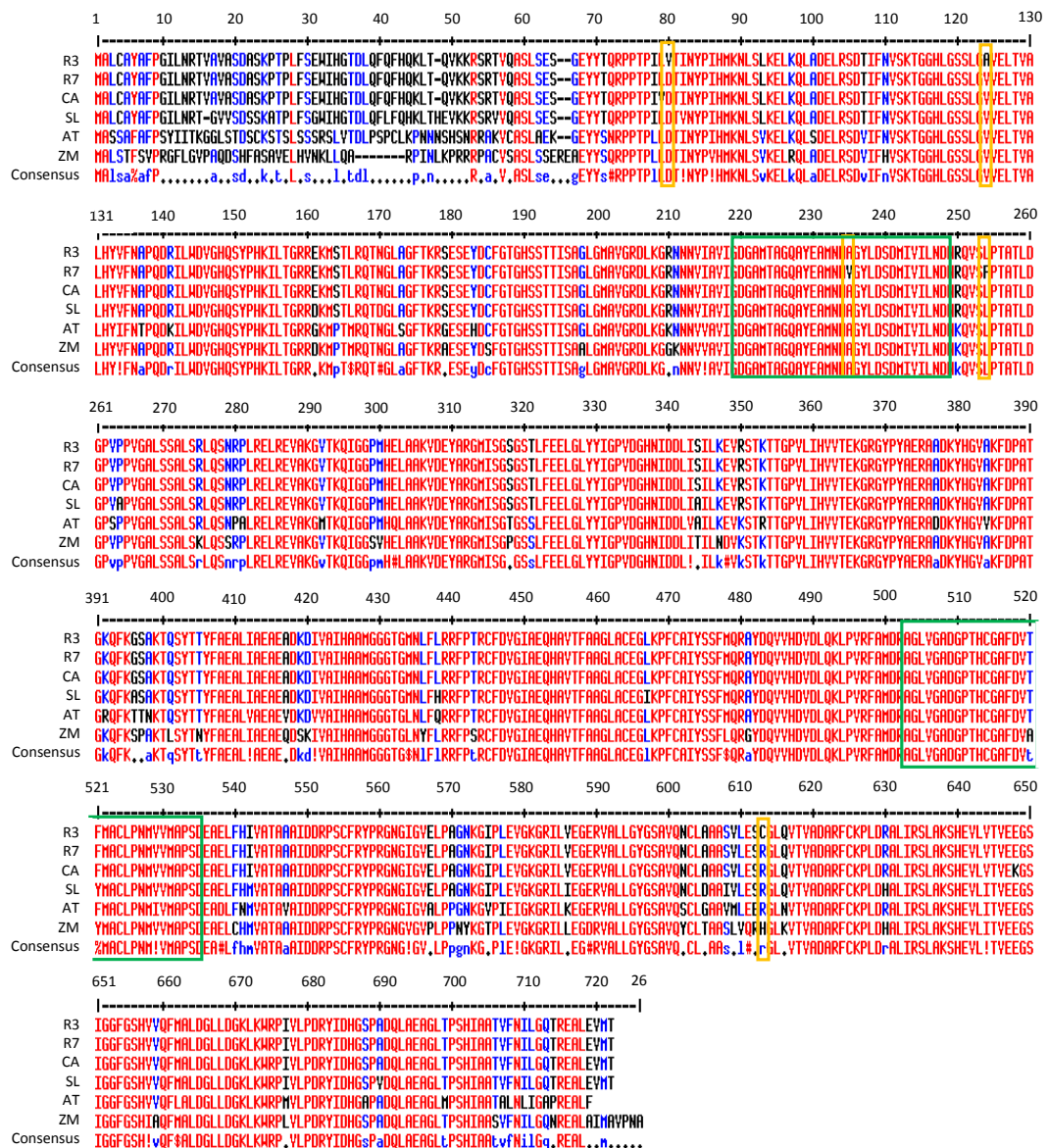


Figure 3.16. Comparison of the DXS amino acid sequences in different higher plants.

The chilli pepper *DXS* gene was sequenced and the amino acid sequence was aligned with other plant species to investigate conserved regions. These sequences were obtained from NCBI: CA, *Capsicum annuum* (CAA75778); SL, *Solanum lycopersicum* (NM_001247743); AT, *Arabidopsis thaliana* (CP002688) and ZM, *Zea mays* (EF507248). The orange boxes represent amino acid substitutions unique to R3 and R7 and the green boxes represent thiamine diphosphate binding site (first) and a conserved domain in thiamine-dependent enzymes (second) (Bouvier et al., 1998b). Alignment carried out using Multalin (Corbet, 1988).

-493 CACCATTCCCATTCTTTCCACCCCAATCAAAAAGATACATTATCATATCTTTCTA
(a) -435 TCTATTTGTGATTTTCTGACGTGGCCCAATAGAAAGTAGTGCAACTTTTTCAAGA
-378 TTTCAATTCATATCCTAGCTTATTCAATGCTATAACAACACCAGTGATATATTCATAC
-320 AAGTGTCTTTCACATCACTTTGCTCTTGGTTTAGAGCATTGATCCTTTCATAAAG
(b) -263 ATTCAGTTTCTTCTCCATTCTCATCCCTCCAATCACACCCTAATTTCTGGGTTATT
(c) -204 CAGGTACAGAAGTAAACAGAAAAAAAAAAAAAGAAAAGAAAGAAAAACA
(d) -150 GCATTTAGTGACAGTAGCACAGCACACCCCACTAGATTTTCTTGAAAGAATTTTG
-94 AATTAATCCCCTTTATCAAGAAAACCCAGTTAGGATTTGGAAGTTAGGCACATT
(e) -38 ATTGGGTGGTTGGGTCTCTGAAAACCTGCATAAATTC
+1 TTGGTATATACATACAAAACACTCTTTATCATG +33

Figure 3.17. Putative regulatory elements present in the DXS promoter.

In silico transcription factor analysis was carried out on the promoter region of DXS in R3 and R7 and putative regulatory elements (REs) were elucidated. The highlighted sequences correspond to Table 3.7. Yellow represents possible light REs; light green represents plastid specific RE; purple represents potential REs found in the promoters of genes involved in primary metabolism and red represents putative REs found in phenylpropanoid biosynthesis genes. The red bps indicate the differences between the R3 and R7 line and grey represents a G-box RE that is only present in R3. This above sequence is taken from the R3 line.

Table 3.7. Putative regulatory elements identified in the DXS promoter region. Table corresponds to Figure 3.17.

Ref	Motif	Regulatory element; Binding factor	Gene	Plant	Gene function; Response
(a)	TCTGACGTGGC	G-box; CG-1	CAB	<i>Nicotiana plumbaginifolia</i>	Chlorophyll binding; light regulated (Schindler and Cashmore, 1990).
	CTGACGTGGC	CUF-1 BS;CUF-1	CAB2	<i>Arabidopsis thaliana</i>	Chlorophyll binding; light regulated

	TGACGTGGC	TAGA2	GH3	<i>Glycine max</i>	Auxin regulated
	tGACGTGG	G-box; GBF	gPAL2	<i>Antirrhinum majus</i>	Phenylpropanoid biosynthesis; flowering related (Liang et al., 1989).
	ACGTGGC	ABRE1/2; ABI3; ABI5; AREB1	RD29B	<i>Arabidopsis thaliana</i>	Drought response; ABA regulated (Uno et al., 2000).
	TGACGTGG	GBF1 BS4; GBF		<i>Arabidopsis thaliana</i>	Stress regulated
	TGACGTGG	Hex; HBP-11(17); HBP-1b(c38)	H3	<i>Triticum aestivum</i>	Histones (Mikami et al., 1994).
(b)	TCTCCATTTC	Gap box 1; GAPF	GapA	<i>Arabidopsis thaliana</i>	Glycolysis; light regulated
	TCGCTATTCTT	CII; S2F	RPL21	<i>Spinacia oleracea</i>	Plastid development; developmental regulated (Lagrange et al., 1997).
(c)	ACAgAAAAaAAAAAAA GaaA		SBEI	<i>Zea mays</i>	Starch branching; Sugar regulated (Kim and Gultinan, 1999).
	AAAAAAAAAAGAAA AA	UN U2; unknown	rbcS3C	<i>Lycopersicon esculentum</i>	Carbon fixation; light regulated (Manzara et al., 1991).
	AAA AAAGAAAGAAA	Box d; DOF1	cyPPDK1	<i>Zea mays</i>	Photosynthesis; Photosynthesis regulated (Yanagisawa, 2000).

(d)	CCAgCAcACCCC	Box 2; unknown	chsA	<i>Petunia hybrida</i>	Phenylpropanoid biosynthesis; flowering regulated (van der Meer et al., 1990).
(e)	TGGGTGGTTGGG	Box L3; DcMYB1	DcPAL1	<i>Daucus carota</i>	Phenylpropanoid biosynthesis; Stress response (Maeda et al., 2005).
	GGGTGGT	GS1B AC box 1; PtMYB1 and 4	PtGS1b	<i>Pinus sylvestris</i>	Nitrogen metabolism (Cánovas et al., 2007).

The R3 and R7 promoter regions were aligned and they shared 99% similarity, with 7 base pair substitutions and a 7 base pair insert. The *DXS* promoter was predicted to have a common G-box RE seen in Figure 3.17a, which was also found in various other plants and numerous functions postulated. This element was present in *CAB* gene promoter in tobacco and *Arabidopsis* (Schindler and Cashmore, 1990). Although a motif from the same gene was also found in *PSY1* and *PSY2*, it differed from the one present in *DXS*. This motif has also been found in genes related to phenylpropanoid biosynthesis, stress response, and genes which are regulated by hormones such as auxin and ABA (Liang et al., 1989; Uno et al., 2000; Mikami et al., 1994).

Further downstream of the putative light regulated G-box was another homologous motif found to bind the S2F factor in spinach, this motif has also been found in the promoters of nuclear genes encoding plastid genes, the gene in which it was identified in spinach was a plastid ribosomal protein induced by plastid development (Lagrange et al., 1997).

A second key putative regulatory motif identified in the *DXS* promoter was a long GAAA repeat (Figure 3.17c). This motif was recognised from numerous genes with more of a primary metabolism role, this motif was also found in genes involved in starch branching and carbon fixation (Kim and Guiltinan, 1999; Yanagisawa, 2000), as well as another light regulated *rbcS3C* in tomato (Manzara et al., 1991).

Lastly, a motif homologous to a MYB binding RE was identified which was also identified in the promoter regions of phenylpropanoid biosynthetic genes, such as *PAL* and *CHS*, and phenylpropanoid related genes which were involved in nitrogen metabolism and have previously been identified as having links to lignin biosynthesis (Maeda et al., 2005; Cánovas et al., 2007; van der Meer et al., 1990).

The R3 and R7 promoter regions were compared to see if there were any differences in putative regulatory elements which could be responsible for altering the regulation of the *DXS* gene. There was a putative G-box motif found to bind GAP binding factor (GAPF), which was also found in the promoter region of glyceraldehyde 3-phosphate dehydrogenase (*GapA*), which was identified in R3 but not present in R7 due to a thymine to adenine substitution (Jeong and Shih, 2003). There were three other substitutions identified in the promoter regions but these were not located in putative REs.

3.3. Discussion

In the chilli powder industry, it is important for the growers to have deep red chilli pepper fruit which will keep this trait at the point of harvest and throughout post-harvest storage. However, because there is no correlation between the intensity of a red chilli at the point of harvest and its ability to retain its colour when stored, the development of new lines wastes time and money during the storage period (8 months) to see if these chillies will be high retention varieties. So, in terms of this project it was important to define 'colour' in the chilli pepper fruit to allow a deeper insight of the biochemical and molecular mechanisms which are operating and ultimately once the colour intensity of the fruit has been fully characterised a better understanding of the degradation processes during storage will be achieved.

3.3.1. Characterisation of carotenoids and carotenoid esters in chilli pepper

3.3.1.1. Identification of the carotenoid and carotenoid esters present in ripe fruit

Firstly, in order to characterise colour intensity in red chilli pepper the coloured compounds accumulating in the fruit need to be defined. This study involved the characterisation of the pigment content of 12 lines, which were part of a colour diversity panel, to determine whether

the amount of pigment accumulated, or the composition of pigments accumulated, is attributable to colour intensity phenotype.

The compounds which are mainly responsible for the red colour of ripe fruit are the carotenoid pigments and similar GGPP derived isoprenoids, the tocopherols. HPLC-PDA was carried out to identify the carotenoids present, and because the carotenoid profile in chilli pepper is very complex due to the presence of carotenoid esters, LC-MS allowed identification of the esters and fatty acids associated with these esters. The LC-MS results revealed that the carotenoid esters exclusively contained the fatty acids lauric acid, myristic acid, and stearic acid. This agrees with reports in the literature (Breithaupt and Schwack, 2000; Schweiggert et al., 2005). Free, mono- and diesterified capsanthin were identified, whereas capsorubin was only found in the diesterified form on the HPLC-PDA. However, the mass for free capsorubin was detected on the LC-MS suggesting very low levels. Previous studies have reported the presence of monoacylated derivatives of capsorubin but they did not detect free capsorubin further supporting that free capsorubin is present in very low levels (Breithaupt and Schwack, 2000; Schweiggert et al., 2005; Giuffrida et al., 2013). Zeaxanthin and antheraxanthin were found in free, mono- and diesterified form. The most abundant capsanthin monoester was myristic acid (C14:0) and the most abundant capsanthin diester was C14:0, C14:0 (Breithaupt and Schwack, 2000; Schweiggert et al., 2005; Giuffrida et al., 2013).

There were approximately 31 carotenoid and carotenoid esters identified using this method; however, the amounts varied between lines. The most abundant carotenoid accumulated in ripe fruit were the capsanthin diesters which contributes to around 40-80% of total carotenoid content, depending on the line investigated. This is typical of red pepper and has been described in the literature that the red in colour of capsanthin is responsible for the red colour of the ripe fruit (Gregory et al., 1987; Ittah et al., 1993; Weissenberg et al., 1997; Deli et al., 2001). The amount of capsanthin diesters accumulated also varied, where the range was 2200–5800 µg/ g DW. The other main pigments accumulated in ripe fruit were β-carotene (1-20%), antheraxanthin (4-5%), β-cryptoxanthin (1-6%), α-tocopherol (3-9%), zeaxanthin (1-4%) and phytoene (0.3-4%). This is concurrent with other studies of red pepper (Minguez-Mosquera and Hornero-Mendez, 1994). The other red carotenoid capsorubin was accumulated at much lower levels when compared to capsanthin, at around 1-3% for the total carotenoid content. This suggests a preference for antheraxanthin over violaxanthin by the capsanthin capsorubin synthase (CCS) enzyme. Previous studies have found capsorubin to contribute to 3-20% for the total carotenoid content in sweet red pepper but the compositions and amounts of carotenoids accumulated between lines analysed varied greatly. This highlighted the versatile nature of

carotenoid accumulation seen in peppers demonstrated in their natural colour diversity (Minguez-Mosquera and Hornero-Medez, 1994; Gregory et al., 1987; Deli et al., 2001).

The R7 line accumulated the highest amount of total coloured carotenoids at approximately 9000 µg/ gDW. Most carotenoids particularly capsanthin, antheraxanthin and zeaxanthin esters, β-carotene, β-cryptoxanthin, phytoene, and phytofluene accumulated at significantly high levels in this R7 line when compared to the others analysed. Other high carotenoid lines were R2 and R4. R2 was very similar to R7 in terms of carotenoid composition. The R3 and R12 lines were found to accumulate the lowest amounts, with a total colour carotenoid content of 3000-3500 µg/ gDW. Almost threefold lower than that of R7. Based on the R12 line having a very similar carotenoid composition to R3 this line should be denoted as a low intensity phenotype. The remaining lines did not significantly stand out during carotenoid analysis as they accumulated a mid-range of all carotenoids when compared to the other lines, based on these results R5, R6 and R10 were not studied further.

Upon comparing the individual carotenoids present between the lines, the first notable result was that high intensity phenotype lines tended to accumulate high levels of free carotenoids which eventually become esterified, such as capsanthin, zeaxanthin, and antheraxanthin (Figure 3.3). In particular, the accumulation of free capsanthin was most significant. This suggests that these high intensity phenotype lines were experiencing a high level of carotenogenesis which may be resulting in the accumulation of the end-product, which is not being esterified efficiently. This can be seen when comparing the percentage capsanthin diesters between lines, the high intensity lines displayed a lower percentage of capsanthin esters in terms of total carotenoid content perhaps due to the increase in free carotenoids accumulated.

3.3.1.2. Characterisation of carotenoid biosynthesis throughout ripening

The lines R1, R2, R3, R4, R7, R8, R11 and R12 were selected based on the results from section 3.2.2.1. The other lines were not studied further due having similar or mid-range colour intensity phenotypes within the diversity panel. These lines were selected to study the carotenoid content of 6 stages of ripening in red chilli pepper, they were tagged from anthesis and breaker stage, and studied for two weeks after. It is known that pepper undergoes profound metabolic and morphological transformations during the ripening process whereby the chloroplast differentiates into a chromoplast, the photosynthetic machinery breaks down, and thylakoids

become more disorganised. During this time there are changes occurring to the carotenoid composition within the plastid and the accumulation of xanthophyll and xanthophyll esters predominate (Deruère et al., 1994; Minguez-Mosquera and Hornero-Medez, 1994; Deli et al., 2001).

At the mature green stage of fruit development lutein is the most abundant carotenoid, residing in the light harvesting complexes, where it aids the dissipation of excitation energy during photosynthesis (Cazzonelli, 2011). This is typical for most green tissue and the other carotenoids seen at this stage are involved in protecting the photosynthetic machinery, such as neoxanthin, β -carotene, violaxanthin and zeaxanthin, although these compounds are found at much lower levels. At the onset of ripening, lutein and the chlorophylls are depleted as the photosynthetic machinery starts to breakdown (Minguez-Mosquera and Hornero-Mendez, 1993). Although previous studies have reported the decrease and disappearance of neoxanthin throughout ripening, this varied in the lines investigated in this present study. In R4, R8, R11 and R12 neoxanthin levels did decrease as ripening progressed but there were lines which experienced no change, such as R1, R3, and R9, and in the high intensity line R7 there was an increase in neoxanthin witnessed, and this line has also been characterised as having low levels of capsorubin accumulated. This was interesting considering that it accumulates high levels of most other carotenoids analysed. If the CCS enzyme had a preference for creating capsanthin from antheraxanthin as opposed from transforming violaxanthin to capsorubin this may lead to the more substrate available for neoxanthin synthase, thus increasing the levels of neoxanthin as ripening progresses (Deli et al., 2001; Minguez-Mosquera and Hornero-Medez, 1994; Hornero-Méndez et al., 2000). The decline of lutein suggests there is a shift in regulation of the α - and β -branches of the biosynthesis pathway, whereby the α -branch becomes down-regulated and the β -branch becomes up-regulated leading to the accumulation of xanthophylls (Ronen et al, 2002) (Figure 1.14). At this stage the chilli starts to turn red as a result of the *de novo* synthesis of capsanthin, zeaxanthin, capsorubin, antheraxanthin and their esters, as well as β -cryptoxanthin, phytoene, and phytofluene. An overview of carotenoid biosynthesis throughout ripening in a high and low intensity line can be seen in Figure 3.18.

It is known that there are two processes involved in carotenoid biosynthesis, firstly the conversion of photosynthetic carotenoids already residing in the green fruit, and secondly the *de novo* synthesis of xanthophylls and ketocarotenoids (Minguez-Mosquera and Hornero-Mendez, 1993). The *de novo* synthesis of carotenoids during ripening can be seen in the net increase in total carotenoid content in the lines analysed throughout ripening (Hornero-Méndez et al., 2000; Hornero-Méndez and Mínguez-Mosquera, 2000; Deli et al., 2001; Gnayfeed et al.,

Finally the remaining high intensity line, R7, increased the total carotenoid content of its fruit by 25 fold during ripening. All lines which had larger increases in total carotenoid content had low levels in MG fruit. The medium intensity lines which experienced a 2-3 fold change throughout ripening may be due to the large amount of carotenoids found in the MG fruit. These medium intensity lines had high levels of around 2500-4000 $\mu\text{g/g}$ DW, whereas the R1, R2, R3 and R7 lines which experienced larger increases in total carotenoid content had much lower levels at around 1000-2000 $\mu\text{g/g}$ DW in MG fruit. The R4 line has a high total carotenoid content in ripe fruit but this line also has a high total carotenoid content in MG fruit. It is known that the accumulation of carotenoids during ripening is a combination of two processes so perhaps this line expresses biosynthetic genes, for the *de novo* synthesis of carotenoids, at lower levels when compared to the other lines because there are already high levels of carotenoids accumulated in the green fruit than can be utilised. Furthermore, the larger increases observed in total carotenoid content in high intensity lines suggests the presence of highly active genes involved in the carotenoid biosynthesis pathway during ripening resulting in larger pool of substrates accumulating (Huh et al., 2001; Lois et al., 2000; Fraser et al., 2002).

Investigation of the chlorophyll a and b ratios in the mature green fruit of chilli pepper revealed that the high intensity lines had a lower ratio, and low and medium lines showed a higher ratio of chlorophyll a to b (Figure 3.5). Additionally, as ripening progressed it was apparent that chlorophyll a degraded much faster than chlorophyll b this could potentially be because of chlorophyllase having a higher affinity to chlorophyll a than b (Minguez-Mosquera and Hornero-Mendez, 1993). So bearing in mind that chlorophyll a degrades more rapidly during ripening this could suggest that the high intensity lines are showing early ripening related metabolism compared with the other lines analysed.

There was a difference in ester accumulation in the early stages of ripening, as previously mentioned one of the main aspects of carotenoid accumulation in pepper is the appearance of carotenoid esters. Differences were seen in the first esters accumulated. Interestingly, the high intensity lines and R8 preferentially accumulated capsanthin esters first, when compared with the remaining low and medium intensity lines which either did not accumulate any at this early stage or accumulated zeaxanthin esters predominantly. This emphasises the possibility of differences in the expression of carotenoid biosynthesis genes or activity of the enzymes, as the low and medium lines appear to be less efficient at producing the end-product at this stage. Perhaps this is because some genes/ enzymes are slower to be up-regulated in response to ripening than others, and thus this supports the previously suggested idea about the high

intensity lines showing earlier signs of ripening-related metabolism due to having a lower chlorophyll a to b ratio.

The rate of ripening varied between lines and so the last stage of ripening differed due to some of the fruit undergoing senescence at B+14 stage, and were too old to analyse. These lines were: R3, R8, R11, and R12, and the last stage of ripening being B+10. The remaining lines were analysed up until B+14 stage. Analysis of the last stage of ripening revealed that in these later stages of ripening the capsanthin diesters were accumulated at higher levels in the three high intensity lines. The abundance of capsanthin diesters in the ripe fruit, and the fact that capsanthin is red in colour, strongly suggests that concentration of capsanthin diesters at the end stages of ripening are responsible for the intensity of the red colour of the fruit. Evaluation of free and diesterified capsanthin over ripening in selected lines illustrated that high levels of free capsanthin accumulated at earlier stages of ripening (as discussed in section 3.3.1.1) in the high intensity lines. This led to a linear increase in capsanthin diesters over ripening, thus resulting in a higher level of capsanthin diesters present at the last stages of ripening, when these high accumulating lines (R1 and R7) were compared to the low intensity line (R3). This line was seen to plateau in the production of free capsanthin before ripening completed inevitably resulting in lower levels of capsanthin diesters accumulating at the later stages (Figure 3.6). This could be because the carotenoid biosynthesis genes start to become down-regulated as ripening finishes and no new precursor substrates are being synthesised. The later stages of ripening are just converting the accumulated substrates, such as free capsanthin, into carotenoid esters.

Examining the accumulation of free capsanthin and capsanthin diesters over time also displayed the biosynthesis to accumulation transition in selected lines thus visualising the differences in ripening rate. The selected lines were R1, a high intensity line with a fast ripening rate, R3 a low intensity line with a fast ripening rate and R7 a high intensity line with a slow ripening rate. Both the fast ripening lines experienced the biosynthesis to accumulation transition at an earlier time, B+7, compared to the slow ripening line, which experienced it at B+10. These results led to a deeper look into ripening rates between lines by carrying out PCA on all the pigments, at all the stages, in all the lines studied in the ripening series. This revealed that the R7, as well as the R2, ripened at a much slower rate when compared to the other lines, whereby stage B+7 of R2 and R7 clustered with the B+14 stages of fast ripening lines R1 and R4. It also showed some clustering at B+10 of R3, another fast ripening line, with the B+7 stage of all the other lines. This was backed up by finding from the pigment data previously mentioned where at B+3 stage R7 accumulated high levels of green tissue related compounds and R3 was high in capsanthin diesters. As ripening progressed, R7 was still found to have high levels of chlorophyll b at B+7 stage.

Additionally, the PCA revealed that the high intensity lines, R1, R2 and R7 all separated with the ripening related carotenoids, such as capsanthin and its esters, antheraxanthin and its esters, β -carotene, β -cryptoxanthin, phytoene, phytofluene, and α -tocopherol, whereas the low and medium intensity lines separated based on the zeaxanthin and its esters and capsorubin.

Another aspect of pigment accumulation investigated, was the ratio of red to yellow compounds. There was found to be a lower ratio of red to yellow carotenoids in the high intensity lines. So, although these lines had a much higher amount of capsanthin accumulated they also had more yellow precursor compounds present too. Especially at the later stages of ripening. This suggests that although these lines may have highly expressed key carotenoid biosynthesis genes at the onset of ripening, at the cessation of ripening genes involved in the production of the red carotenoids become down-regulated (Huh et al., 2001; Lois et al., 2000; Fraser et al., 2002; Guzman et al., 2010). This can be seen when the red to yellow ratio in two high intensity lines was compared to a low intensity line. The high lines decrease in ratio after ripe stage suggesting that the rate of production of red carotenoids is slowing down, but the yellow carotenoids are still being produced at the same rate causing a decrease in red to yellow ratio (Hornero-Méndez et al., 2000). Perhaps this is caused by negative regulation whereby the red carotenoids reach a certain threshold level which feedback to the red carotenoid biosynthesis gene, capsanthin capsorubin synthase, resulting in its down-regulation. The low intensity line is not experiencing a decrease in carotenoid gene expression as it does not produce enough red carotenoids to initiate the negative feedback mechanism.

3.3.2. Sequencing of *PSY1*, *PSY2* and *DXS*

In the previous section (3.3.1) the results implied that the colour intensity phenotype was correlated with the amount of free and esterified capsanthin, whereby the high intensity lines accumulated higher levels than the low and medium intensity lines. As this carotenoid is the last in the carotenoid biosynthesis pathway it was proposed that this was due to highly expressed carotenoid biosynthesis genes. This has been seen frequently in numerous different plants in previous reports that the up-regulation of carotenoid biosynthesis genes result in increased levels of carotenoids (Shewmaker et al., 1999; Fraser et al., 2002, 2007). Key genes already known to have the most influence over the carotenoid biosynthesis pathway were sequenced in a high and low intensity phenotype, R7 and R3, respectively. These were the phytoene synthases and *DXS*. The phytoene synthases were selected to sequence as the fruit specific *PSY1*

is thought to be the rate limiting step in carotenoid biosynthesis in pepper and tomato (Huh et al., 2001; Fraser et al., 2002). The leaf specific *PSY2* gene although known to be present has not been sequenced and characterised before in pepper, therefore sequencing allowed the leaf specific phytoene synthase role in chilli pepper fruit ripening to be determined. Finally, the *DXS* gene was sequenced as this gene is thought to be the rate limiting step in isoprenoid biosynthesis (Lois et al., 2000).

3.3.2.1. Phytoene synthase-1

The ripe fruit of pepper can be classified into 8 classes, ranging from white to deep red, when a red and a white fruited variety are crossed. Other ripe colours include green, purple, and black. Genetic analysis has identified three independent gene loci responsible for the colour variation experienced from the red/ white cross. They are known as *Y*, *C1* and *C2*. *Y* has been identified as corresponding to the *CCS* gene, *C1* is unknown and *C2* corresponds to the *PSY1* gene (Hurtado-Hernandez and Smith, 1985; Lefebvre et al., 1998; Popovsky and Paran, 2000; Thorup et al., 2000; Huh et al., 2001).

PSY1 encodes an enzyme which is responsible for the head to tail condensation of GGPP. This enzyme is membrane associated but not integral. *Capsicum* phytoene synthase is a monomeric protein which is responsible for the conversion of two GGPP molecules to pre-phytoene pyrophosphate then to phytoene using Mn^{2+} as a cofactor (Dogbo et al., 1988). The gene encoding this protein was found to have a coding sequence of 1260 bps with 6 exons and 5 introns, with an amino acid sequence of 419, which was slightly longer than tomato (412) (ABM45873) and maize (410) (AAR08445) but shorter than Arabidopsis (422) (AT5G17230).

The modelling of the protein structure was carried based on previous models of human squalene synthase (SQS) (Pandit et al., 2000). The structure consisted of a central cavity which was surrounded by helices which was similar to SQS. The enzyme contains different layers of helices surrounding the cavity. The first layer contains the two aspartate-rich regions (DXXXD) which have been identified as essential for catalytic activity, the negatively charged aspartate and glutamate face into the cavity and were thought to bind the Mn^{2+} cofactor. Site directed mutagenesis of both aspartate residues results in complete loss of activity in SQS; however, mutagenesis of glutamate residues did not have the same effect therefore suggesting their roles are not functionally equivalent (Gu et al., 1998). These aspartate-rich regions stabilise the diphosphate groups and each site has a specific role in the two-step reaction, whereby it is

thought that one site binds GGPP to aid attack of the carbonium ion and another which binds GGPP to facilitate carbocation insertion (Pandit et al., 2000). The tyrosine residue identified which is also present in SQS is thought to aid stabilisation of the carbon cations through their interaction with the π electrons of aromatic rings, therefore indicating the tyrosine residues role in stabilisation of the carbon cation intermediate (Gu et al., 1998). The first half of the reaction binds two GGPP molecules via salt bridges Mn^{2+} at the diphosphate moieties; one a prenyl acceptor and one prenyl donor, the hydrophobic tails extend to the more hydrophobic end of the channel. There is a nucleophilic attack on the allylic cation by the double bond of the second GGPP, producing an allylic carbocation, pre-phytoene pyrophosphate. This reaction releases a diphosphate group and the intermediate is rearranged to form phytoene with the second elimination of diphosphate (Gu et al., 1998; Pandit et al., 2000).

The *PSY1* gene was found to be highly conserved within the chilli pepper lines that were analysed. The only difference in the amino acid sequences analysed was a tyrosine to cysteine substitution. It was revealed when the chilli pepper *PSY1* was aligned with plants, such as sweet pepper, tomato, *Arabidopsis*, and maize that it was located in an insertion which was unique to the *Capsicum* genus. Therefore, it would be unlikely this affected the enzyme activity of the *PSY1* protein as the substitution was located in the potential chloroplast transit peptide (Gallagher, 2004; Giorio et al., 2008; Shumskaya et al., 2012). This was assumed as when the protein structure of this gene was modelled, the software based its structure on a squalene synthase enzyme, which is known to catalyse a similar reaction, and removed the first 125 amino acids thus suggesting the N-terminus does not affect the enzyme activity of the protein (Dogbo and Camara, 1987). Other evidence that supports this is that in maize there is a potential cleavage site which removes the transit peptide (Shumskaya et al., 2012), and in tomato the predicted chloroplast transit peptide is thought to be around 60 amino acids long with the cleavage site found in the insertion (Giorio et al., 2008). This N-terminal sequence was most variable between all the plants aligned. The identification of the putative chloroplast transit peptide was carried out based on prediction software, protein modelling software and previous work from tomato (Bartley et al., 1992). However, proteomic analysis could provide evidence of transit peptides based on known sequences.

Interestingly, the *PSY1* maize mutant containing the Asn^{168} which gave rise to increased carotenoid production and fibrillar plastoglobuli phenotype was not present in the amino acid sequence of *PSY1* in the chilli pepper lines selected. Even though *Capsicum* is known to accumulate fibrillar plastoglobuli (Deruère et al., 1994; Shumskaya et al., 2012). This suggests that this Asn^{168} amino acid is not responsible for the initiation of fibril formation in *Capsicum*.

However, when the activity of the enzyme with the Asn¹⁶⁸ mutant was removed, and so was no longer a highly expressed *PSY1*, fibrillar formation ceased to occur. Thus, suggesting that the activity of enzyme or the expression of the gene may be signalling fibrillar production.

The promoter regions of the R3 and R7 lines were found to have no differences and thus were highly conserved between these lines. These results suggest that the differences in carotenoid accumulation present in these selected lines is not due the *PSY1* gene as they both have the ability to respond to the same transcriptional signals. This information suggests that perhaps a gene further upstream of the carotenoid biosynthesis pathway may well be responsible. However, it cannot be ruled out that the gene could be regulated differently between lines at an epigenetic level.

The promoter region of *PSY1* contains many putative regulatory elements. One sequence in particular (-260- -270 Figure 3.11j) shared homology with many other plants, and so has been proposed as a key regulatory element in the chilli pepper promoter of *PSY1*. This motif was found in the promoter regions of two flavonoid biosynthesis genes, *F3H* and *CHS*, in *Arabidopsis* and parsley, respectively, and phenylpropanoid biosynthesis gene *PAL*. This motif is thought to be light regulated in these genes. The *F3H* promoter motif was found to bind a MYB regulatory element (Logemann et al., 1995; Hartmann et al., 2005). Other genes which shared homology with this motif were involved in stress response in tobacco and soybean. There were also other REs in the chilli *PSY1* promoter which were found in the promoters of flavonoid and phenylpropanoid biosynthesis genes such as *PAL* and *CCoAOMT* which were activated in response to stress (Ito et al., 1997; Grimmig and Matern, 1997). However, none of the plants which shared this homology were fruit bearing so these REs are likely to involved in the activation of carotenoid biosynthesis in response to stress, as it has been known that fruit ripening can be activated when the plant is under stressful conditions in order to disperse its seeds as a way of survival (Bouvier et al., 1998a; Li et al., 2008). This is further supported by the presence of homologous REs found in the flavonoid and phenylpropanoid biosynthesis genes as these pathways are also activated during fruit ripening. In apple, MYB transcription factors control the regulation of anthocyanin pathway genes (Tacos et al., 2006). Thus, indicating the potential response of carotenoid biosynthesis and phenylpropanoid biosynthesis in response to stress and ripening being regulated by the same transcription factors, which are possibly MYB-like.

Other putative REs located in the *PSY1* promoter were found in the chlorophyll binding (CAB) proteins and a phytochrome a regulatory gene. As well as, some CarG box REs which bind MADS

box transcription factors, which have roles in embryo development and flowering, and specifically one which binds a *RIN* transcription factor in tomato which is thought to regulate fruit ripening in a cell wall modification enzyme (Fujisawa et al., 2011). The presence of these CarG box motifs sharing homology with master regulator transcription factors, which are involved in many developmental processes, provides an insight into the synchronisation of multiple complex signalling pathways involved in the execution of fruit development and ripening and the activation of ripening in response to stress.

In the literature, it has been found in *Arabidopsis* that phytochrome interacting factors (PIF) are involved in the down-regulation of carotenoid biosynthesis by specifically binding to the *PSY* promoter (Toledo-Ortiz et al., 2010). When the TF analysis was carried out there were not specific records of PIF binding factors but PIF is known to bind G-box motifs and there were a few found. However, in the study mentioned, they found that the gene was still light-responsive even when only possessing a short version of the promoter containing no G-box so this shows there are other elements present in the promoter which can also control the expression of *PSY* in response to light. The ATCTA motif found in the *Arabidopsis PSY* promoter is also present in the chilli pepper promoter. This motif was also found in several other carotenoid and tocopherol biosynthetic genes suggesting a role in the regulation of isoprenoids (Toledo-Ortiz et al., 2010).

3.3.2.2. Phytoene synthase-2

Sequencing of the *PSY2* gene was carried out in chilli pepper because although it is known that there are two phytoene synthase genes in *Capsicum* it has not been previously characterised. The sequencing of this gene was carried out using primers based on the tomato *PSY2* gene. The gene was 1299 bps with 6 exons and 5 introns. The protein sequence was 432 amino acids in length so longer than chilli pepper *PSY1* (419), *PSY2* in maize (402) (AAX13807) and *PSY* in *Arabidopsis* (422) (AT5G17230), but the same length as tomato *PSY2* (438) (NM_001247742). The *PSY2* protein had an insert in the potential chloroplast transit peptide at the N-terminus when comparing to *PSY1*. This was also found in tomato *PSY2* when comparing to the *PSY1* protein. This suggests the differences in transit peptide seen may locate the *PSY2* to a different plastid location to *PSY1* perhaps different plastid membranes which are observed in chloroplasts and chromoplasts (Gallagher, 2004). Or, the difference in sequence differentiates between a chloroplast and a chromoplast transit peptide.

There are two amino acid differences elucidated in the coding region of PSY2 when comparing the two lines analysed. The His²⁵⁷ substitution is close to an active site but when the 3D structures of PSY2 created were compared the structures appeared very similar and there was no noticeable change in shape. These differences, however, do seem to be unique to the R3 PSY2 amino acid sequence as both PSY1 lines analysed and tomato PSY2 seem have this residue conserved. The PSY2 chilli pepper protein had 91.3% and 93.6% identity and similarity, respectively to the tomato PSY2. These sequences were more similar than those found when the PSY1 sequences were compared, with 87% and 91.3% identity and similarity, respectively. Thus showing that the PSY2 enzyme is more conserved between plants when compared to PSY1. This is logical as PSY1 is a paralog of PSY2 derived from a gene duplication event (Giorio et al., 2008). The chilli PSY1 was also more similar to the tomato PSY1 than the chilli PSY2, likewise the chilli PSY2 was more similar to the tomato PSY2 than the chilli PSY1 further supporting the identification of the chilli pepper PSY2.

The *PSY1* and *PSY2* promoters shared little similarity; however, they did share similar regulatory elements. A key putative regulatory element in *PSY2*, which was found to have homology with other plants, was located at the beginning of the 5'UTR (+1- +16). This was a G-box motif and was present in the promoters of flavonoid biosynthesis gene, *CHS*, and phytochrome a and were regulated in response to light (Wade et al., 2001; Li et al., 2010). This motif was also shared with genes which were hormonally regulated by ABA and cytokinin (Buchanan et al., 2004).

Other REs were found in *CAB* promoter and other phenylpropanoid biosynthesis genes. As well as, other binding motifs which were regulated by ABA and auxin were found in genes associated with plant and chloroplast development (Fusada et al., 2005). Finally, the CarG box motif, which was also present in *PSY1*, was identified which binds RIN, a master regulator in the tomato ripening. RIN is thought to be essential in triggering the onset of ripening in tomato fruit. Fruit carrying the mutated gene, *rin*, were affected in processes such as ethylene biosynthesis, cell wall modifications, and induction of *PSY1* expression; thus showing the key role this transcription factor has in the onset of ripening (Fujisawa et al., 2011). The fact that a RIN binding motif is found in both phytoene synthase genes suggests that the RIN transcription factor could have similar fruit ripening regulatory mechanisms as seen in tomato, and the RIN transcription factor may play a role in down-regulating the expression of *PSY2* at the onset of ripening.

Interestingly, when comparing the main regulatory elements in *PSY1* and *PSY2* it is apparent that although both shared homology with light and stress regulated phenylpropanoid related genes, only *PSY2* shares homology with phytohormone regulated genes. This illustrates the differences

in roles which the two phytoene synthases are involved in, the *PSY2* gene has more of a fundamental role in photoprotection in photosynthesis, as well as plant and chloroplast development processes, which are regulated by hormones. In comparison to *PSY1* which is mainly involved in ripening and is regulated by transcription factors involved in the orchestration of the development and ripening of the fruit. This is supported by analysis of gene expression of these paralogs in tomato, whereby *PSY1* is predominantly expressed in the fruit and *PSY2* in the green tissue (Cazzonelli, 2011; Giorio et al., 2008). The differences in the promoter sequence of these genes indicate the different roles these genes have within the plant with only 46% similarity, but the similarities in the REs could suggest perhaps an overlap between roles of these genes. For example, the light regulated *CAB* motif and the phytochrome a motif found in *PSY1*, which are involved in photosynthetic roles, and on the other hand *RIN* transcription factor motif found in *PSY2* related to ripening induced genes. This is not unique to chilli pepper as in maize, the endosperm specific *PSY1* paralog has a role in thermal tolerance in photosynthetic tissue (Li et al., 2008), as well as in tomato when the fruit specific *PSY1* gene is lost in the *r,r* mutant there is a reduction in the carotenoid content in the fruit and the leaf (Fraser et al., 1999).

Both genes contained a CarG box motif which commonly binds MADs box transcription factors involved in flowering time suggesting both paralogs have a role in carotenoid biosynthesis in the flower. This is found to be the case in tomato (Hepworth et al., 2002; Giorio et al., 2008).

3.3.2.3. DXS

Plastids synthesise their own supply of IPP through the MEP pathway using glycolytic intermediates such as pyruvate and glyceraldehyde 3-phosphate. The first step in the MEP pathway is the synthesis of 1-deoxy-D-xylulose 5-phosphate (DXP) from pyruvate and glyceraldehyde 3-phosphate, which is catalysed by the enzyme DXP synthase or DXS. In sweet pepper this enzyme is referred to as *Capsicum* transketolase 2 or CapTKT2; however, in this study it will be referred to as DXS (Bouvier et al., 1998b). This enzyme is a homodimer which works by catalysing a transketolation condensation whereby pyruvate is a C2 donor and the D-glyceraldehyde-3-phosphate is the C2 acceptor. This enzyme also has a requirement for thiamine diphosphate which is a cofactor that assists the reaction by deprotonation of thiazolium ring, the Glu⁴⁴⁹ residue has been identified as being essential for this deprotonation and is present in both lines of the chilli pepper analysed (Bouvier et al., 1998b).

In chilli pepper the gene encoding the DXS protein was found to be 4135 bps in length containing 10 exons and 9 introns. This gave rise to a 719 amino acid sequence which was the same length as the sweet pepper, *Captkt2* (CAA75778) and tomato (NM_001247743), but longer than *Arabidopsis* (714) (CP002688) and maize (716) (EF507248). The first 71 amino acids were not included into the model of the DXS protein suggesting the presence of a putative chloroplast targeting sequence. Transit peptide prediction software did not detect the presence of chloroplast signalling peptide, although presence of one in tomato and pepper has been previously proposed (Lois et al., 2000; Bouvier et al., 1998b). However, further identification of the transit peptide with proteomics using known chloroplast transit peptide sequences would confirm its presence.

The amino acid sequences of the selected lines were compared and it was revealed that there were 5 amino acid substitutions. There were three unique to the R3 line when compared with other higher plants and two unique to R7. In the R7 line, the Val²³² substitution is found in a thiamine diphosphate binding site; however, as both these amino acids are nonpolar the affect it would have on thiamine binding is inconclusive, especially as the Glu⁴⁴⁹ residue which is known to play a crucial role in the interaction with the TPP molecule is present in both lines (Bouvier et al., 1998b).

The transcription factor analysis on the *DXS* promoter region revealed putative regulatory elements which could be involved in the regulation of the *DXS* gene and so the flow of substrate into the carotenoid biosynthesis pathway. There was a key putative RE containing a G-box which shared homology with motifs found in the promoters of genes associated with phenylpropanoid biosynthesis and photosynthesis which were light, stress and phytohormone regulated, similar to ones mentioned previously in *PSY2*. This was expected as being upstream to the carotenoid biosynthesis pathway similar regulatory binding factors which activate the phytoene synthase genes could also bind to *DXS*.

Other REs present in the *DXS* promoter region were also found in genes related to glycolysis, carbon fixation and starch branching (Kim and Guiltinan, 1999; Yanagisawa, 2000). This may be because of the biosynthetic links the MEP pathway has with carbon fixation, as it is known the carbon flows from the starch accumulated during photosynthesis to the carotenoid biosynthesis in chloroplast to chromoplast differentiation.

A major difference between the R3 and R7 promoter regions was the absence of GAPF binding factor motif. This motif was also present in the promoter region of the glyceraldehyde 3-phosphate dehydrogenase (*GapA*) which shares the same substrate as the *DXS* enzyme,

glyceraldehyde 3-phosphate (Conley et al., 1994; Kwon et al., 1994). This finding has resulted in a hypothesis for colour intensity phenotype based on the regulation of the *DXS* gene (Figure 3.19). The mutation in the GAP box binding motif located in the R7 *DXS* promoter region could have a considerable effect on the regulation of the R7 gene. This motif could potentially serve as a switch between the synthesis of carotenoids in secondary metabolism and the breakdown of glucose in primary metabolism. These two genes might be modulated by the same transcription factors because the plant wants to either divert its energy into carotenoid biosynthesis or the plant needs more energy which it obtains through glycolysis.

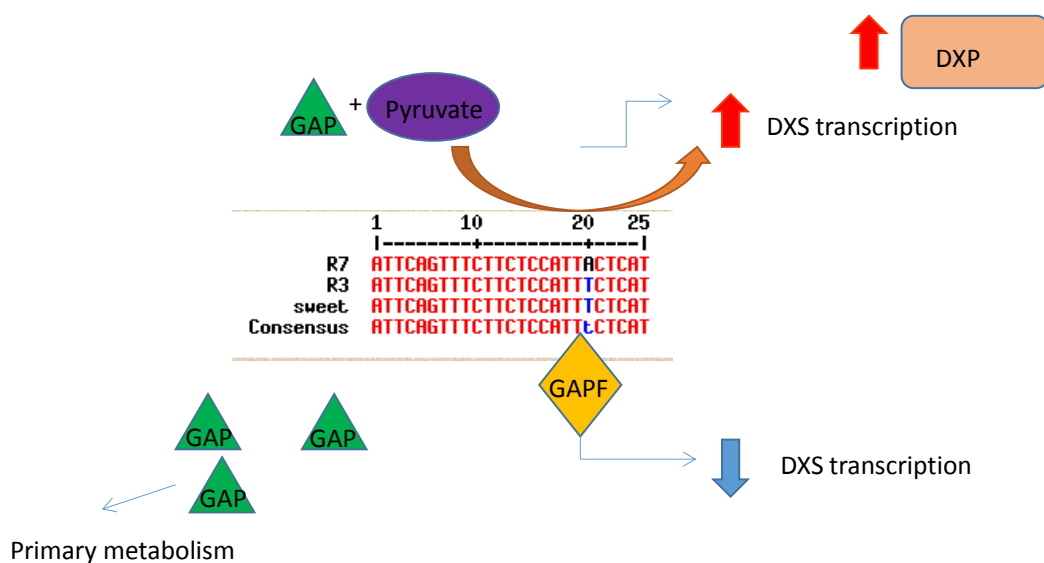


Figure 3.19. Diagram of proposed *DXS* promoter regulation.

This diagram represents the possible differences in regulatory mechanisms between R3 and R7. The R7 *DXS* promoter region has a thymine to adenine substitution present in a G-box motif which binds GAPF binding factor. This motif is also present in the glyceraldehyde 3-phosphate dehydrogenase enzyme. These genes share the substrate so the lack of this binding motif may cause this gene to be regulated differently in R7 when compared to R3.

Therefore, the *DXS* gene may be down-regulated in situations where energy production is needed over carotenoid biosynthesis keeping the carbon flow in primary metabolism as opposed to diverting it into secondary metabolism. Perhaps if the R7 line does not contain this switch it is immune from this signal resulting in a higher flow of carbon into the MEP pathway due to the *DXS* gene not being repressed and therefore a higher production of carotenoids ensues.

In terms of colour intensity in the ripe fruit the results of this study suggest that the differences observed in carotenoid accumulation between the low and the high intensity line are due to the differences in the promoter region or the coding region of the *DXS* gene. This is because when analysing the sequences in *PSY1* there were no differences found between the two lines analysed. This is supported by the fact that in tomato, the *PSY1* deficient *rr* mutant, *DXS* expression levels at the onset of ripening were very similar to the wild type, this indicates that the product of the *PSY1* gene does not initiate expression of the *DXS* gene. However, it was found at the end of ripening the *DXS* transcript levels did not diminish but stays expressed suggesting that the products of the carotenoids biosynthesis pathway are involved in the negative regulation of *DXS* when ripening ceases (Lois et al., 2000). It was also discovered that when tomato fruit were injected with DX the *PSY1* transcript levels were found to be increased suggesting the accumulation of the DX in the plastid affects the regulation of the *PSY1* gene. It is possible that this same regulatory mechanism is present in chilli pepper, whereby, a highly expressed *DXS* gene present in the high intensity phenotype results in the up-regulation of the *PSY1* creating a higher amount of substrate flowing into the pathway.

3.4. Conclusion

In conclusion, when comparing the carotenoid amount and composition it would suggest that when looking at optimally ripe fruit the accumulation of high levels of free capsanthin was found in high intensity phenotype lines; however, when examining the ripening series of the each line this revealed that the high intensity lines accumulated more capsanthin esters than the low and medium intensity lines. This suggests carotenogenic genes are more active in these lines resulting in the accumulation of free capsanthin at the end of the pathway. Due to the high production rates of capsanthin, the plastid cannot keep up during the sequestration and esterification of the compound resulting in its pooling in ripe fruit. Once the ripening processes draw to an end the accumulated free capsanthin is esterified resulting in the high intensity phenotypes having more capsanthin esters at the later stages of ripening when compared to the other lines. This can be seen when analysing the biosynthesis of free capsanthin and capsanthin diesters. However, it is important to bear in mind the red to yellow ratio, as some lines may reach such a high level of capsanthin production that end carotenoid biosynthesis genes become down-regulated and the production of red carotenoids diminishes, but the production of yellow precursors stays the same resulting in a decrease in red to yellow ratio. Therefore concluding

that colour intensity phenotype is related to the accumulation of free and esterified capsanthin throughout ripening. The rate of ripening is also an important factor to consider in the chilli pepper industry, the colour intensity of the chilli, as previously mentioned, directly affects how much the produce can be sold for, concurrently it is also of importance to grow lines which ripen quickly as this results in reduced labour cost and decreased risk of disease (Hornero-Méndez and Mínguez-Mosquera, 2000). Thus, although the R7 line has an extremely high carotenoid content it also has a low red to yellow ratio and it takes much longer to ripen, so the high intensity fast ripening line R1 was to be more desirable from a commercial point of view.

Sequencing of key carotenoid biosynthesis genes revealed that the *PSY1* gene is highly conserved between lines analysed thus indicating that the *DXS* gene may have a key role in the amount of carotenoids accumulated during ripening. The high intensity phenotype of R7 could be caused by the absence of a regulatory motif which would allow regulation from primary metabolism.

Chapter 4. Regulation and
sequestration of carotenoids in red
chilli pepper

4.1. Introduction

In the previous chapter it was found that colour intensity phenotype correlated to free and esterified capsanthin accumulating in the ripe fruit. Sequencing of key carotenoid biosynthetic genes *PSY1*, *PSY2*, and *DXS* revealed possible allelic variations, which may be responsible for altering the expression of carotenoid related genes in the lines analysed. In this chapter, gene expression assays were optimised for key carotenoid related genes in an effort to relate increased carotenogenesis in high intensity phenotype lines to specific carotenoid biosynthetic genes.

In order to ascertain whether the variations in colour intensity phenotype and ripening rate phenotype had a more global effect on the metabolism of the ripening chilli pepper fruit, metabolite profiling was carried out to further characterise selected lines. Thus, giving a broader picture of the metabolome and how it is altered in response to colour intensity and phenotypes associated with ripening rate.

In addition, the subplastid location of the accumulated carotenoids, and therefore the sequestration mechanisms present in the chilli pepper fruit, were investigated. Subchromoplast fractionation was implemented in a high and a medium intensity phenotype line allowing the storage processes for carotenoids and carotenoid esters within lines with perturbed colour intensity phenotype to be determined.

4.2. Results

4.2.1. Expression of carotenoid related genes in in ripe fruit

Gene expression analysis was carried out on carotenoid related genes in an attempt to characterise variations in colour intensity phenotype. First, the quantitative PCR method was optimised for assays specific to chilli pepper, and then experiments were designed to capture the expression profiles of carotenoid related genes within lines and throughout the ripening process.

4.2.1.1. Optimisation of gene expression assays

The transcript profiles of carotenoid related genes were measured using real time PCR (RT-PCR). This method allows the measurement of gene expression in multiple different lines simultaneously. This approach utilises the normalisation of expression to a reference or housekeeping gene. Previous experiments in chilli pepper revealed that actin, which was used in tomato and is a commonly used reference gene, was unstable in chilli pepper. geNorm analysis was carried out on selected chilli lines and the most efficient and stable reference gene was identified. Calculation of the gene stability measure (M) allowed elucidation of the most stable reference gene from a panel of possible genes (Figure 4.1). Gene stability was calculated based on the notion that the expression ratio of two ideal internal control genes is the same in all samples, irrespective of the experimental conditions or cell types. M the standard deviation of the log transformed expression ratios (Vandesompele et al., 2002).

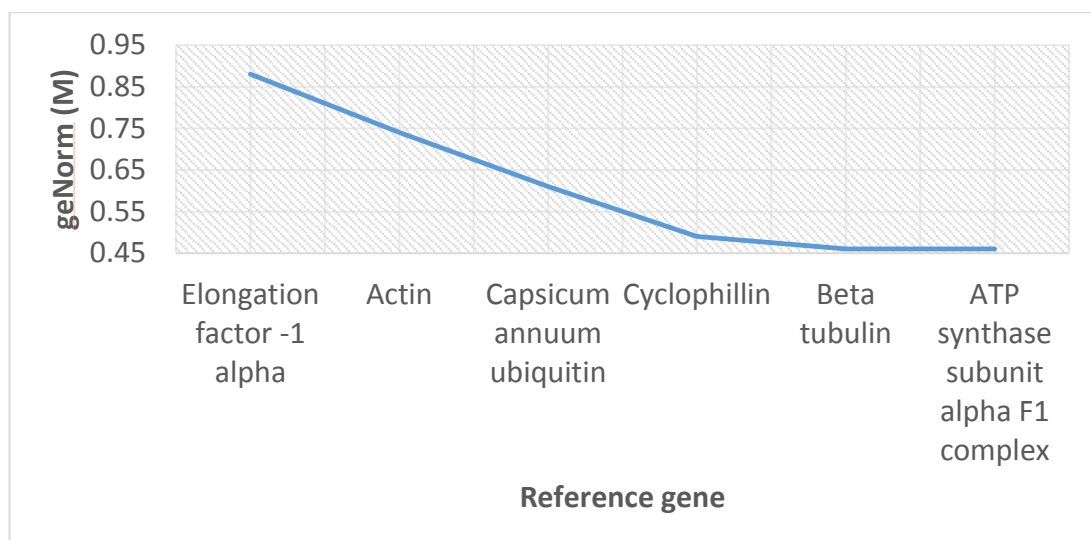


Figure 4.1. Average expression stability of reference targets.

geNorm analysis was carried out on selected lines with a panel of possible reference targets. The geNorm programme calculates the stability of the reference gene to allow selection of the most stable gene. The higher the M value the less stable the reference gene.

Based on the results from the geNorm program the 'ATP synthase subunit alpha F1 complex' gene was selected to use as a reference point for normalisation of all gene expression assays. Although it is recommended to use two reference genes, in this case the difference in variability

of using one reference gene over two was small. Due to this finding, and restricted resources, one reference gene was used and experiments were repeated in triplicate to confirm results.

4.2.1.2. Plastome to genome ratio

A PCR based assay was carried out to detect whether differences observed in the accumulation of carotenoids was due to a higher number of chloroplasts. This is assumed to be equivalent to the number of chromoplasts present within the cell. This assay determined the plastome to genome ratio which was representative of the number of plastids present per cell. The genes utilised for this assay were the large subunit of ribulose-1,5-bisphosphate carboxylase/oxygenase (*rbcl*) located in the plastome and phytoene desaturase (PDS) located in the genome (Enfissi et al., 2010) (Figure 4.2). The calculations of transcript levels were carried out using the $\Delta\Delta C_t$ method, thus giving results in relative amounts.

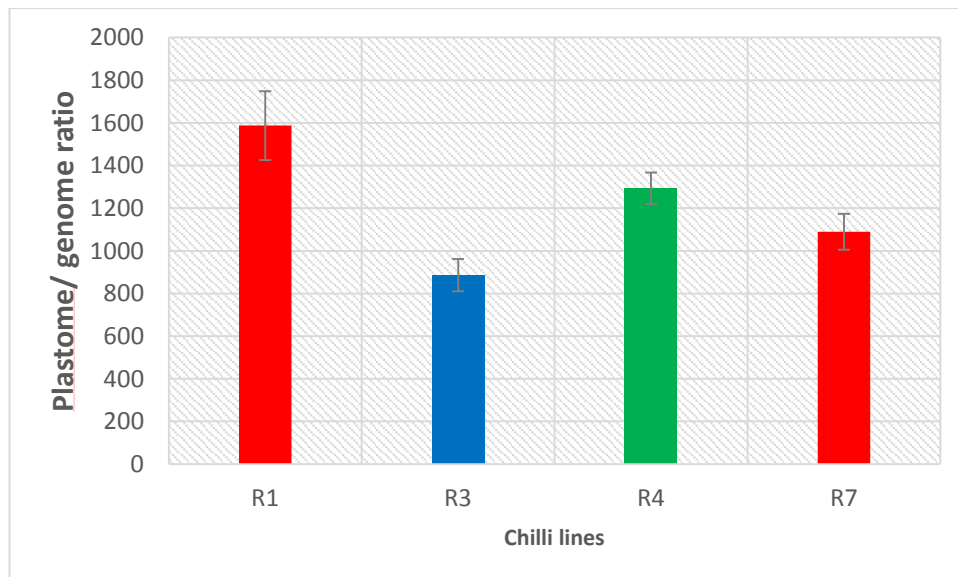


Figure 4.2. Comparison of plastome to genome ratio between selected lines.

The plastome to genome ratio was calculated by measuring the ratio of the large subunit of ribulose-1,5-bisphosphate carboxylase/oxygenase (*rbcl*) gene expression to phytoene desaturase (*PDS*) gene expression which are present in the plastome and genome, respectively.

Key: red, high; intensity lines; green, medium intensity line; and blue, low intensity line. The error bars represent \pm SE (n=3). ANOVA results in supplementary.

The highest plastome to genome ratio was found in the R1 line which suggests it has a higher plastid number when compared to the other lines analysed. There was no significant difference in plastid number between the high intensity line R7 and the low intensity line R3. This showed that plastid number does not correlate with colour intensity phenotype.

4.2.2. Expression of carotenoid related genes in ripe fruit

The carotenoid compositions of 12 varieties of red chilli pepper fruit were analysed. It was found that there was a positive relationship between colour intensity phenotype and the amount of capsanthin accumulated. Whereby, high colour intensity lines accumulated higher levels of free capsanthin when compared to low and medium intensity lines. In order to examine the underlying molecular processes contributing to this high colour intensity phenotype key carotenoid biosynthesis genes were profiled for expression in ripe fruit (Figure 4.3).

4.2.2.1. Phytoene synthase-1 (*PSY1*)

Investigation of the fruit specific phytoene synthase (*PSY1*) expression ascertained that there was a higher level of *PSY1* transcripts present in high intensity lines when compared to low and medium intensity lines (Figure 4.3a). Whereby R1, R2, and R7 were significantly higher than all the other lines analysed. Likewise, there was a strong positive correlation between *PSY1* expression and the amount of free capsanthin accumulated with an R^2 value of 0.76 (Figure 4.3c).

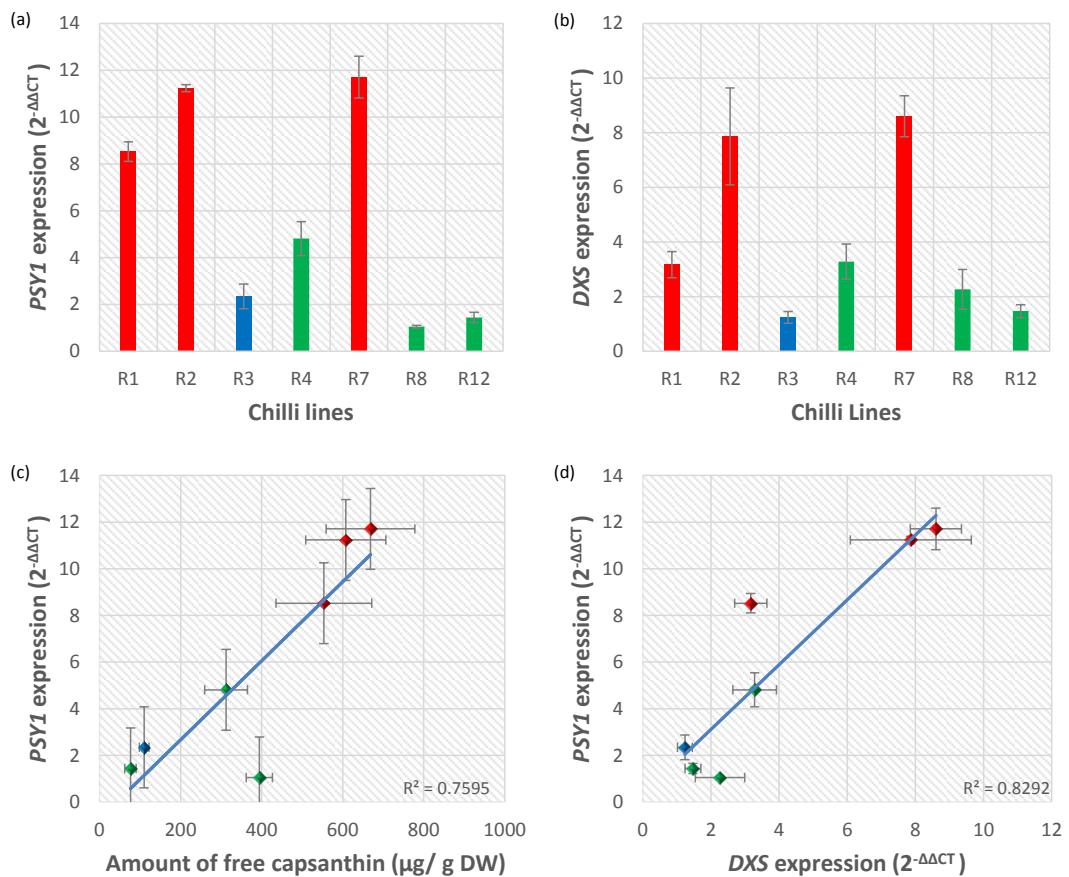


Figure 4.3. Characterisation of phytoene synthase-1 (*PSY1*) and 1-deoxy-D-xylulose 5-phosphate synthase (*DXS*) expression in ripe fruit.

Quantitative PCR was employed on selected lines showing perturbed carotenoid accumulation. Analysis of gene expression in ripe fruit for (a) *PSY1* (b) *DXS*. Linear regression of (c) *PSY1* expression and amount of free capsanthin (d) *PSY1* and *DXS* expression. Key: Red, high intensity lines; green, medium intensity lines; and blue, low intensity lines. Error bars represent ± SE (n=3). AVOVA results in supplementary ($P \leq 0.05$).

4.2.2.2. 1-Deoxy-D-xylulose 5-phosphate synthase (*DXS*)

Similarly, there was a positive relationship between *DXS* gene expression and high colour intensity phenotype (Figure 4.3b). There was found to be a strong positive correlation between *PSY1* and *DXS* gene expression with an R² value of 0.83 (Figure 4.3d).

4.2.2.3. Capsanthin capsorubin synthase (*CCS*)

The gene expression profile for *CCS* in the ripe fruit was analysed in all the chilli lines and there appeared to be no correlation between the colour intensity phenotype and *CCS* expression. There were no significant differences in the transcript levels of *CCS* in the ripe fruit of all lines analysed (Figure 4.4a).

4.2.2.4. β -Carotene hydroxylase-2 (*CHY2*)

There was a positive correlation found with colour intensity and the carotenoid biosynthesis gene β -carotene hydroxylase-2 (*CHY2*) (Figure 4.4b). However, this was not as highly expressed at the *PSY1* or *DXS* gene.

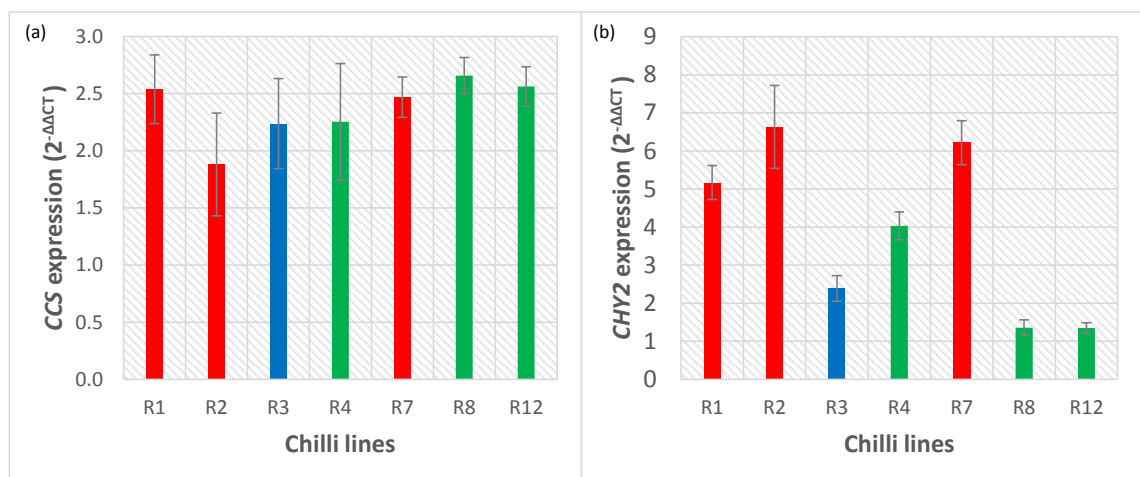


Figure 4.4. Characterisation of the capsanthin capsorubin synthase (*CCS*) and the β -carotene hydroxylase-2 (*CHY2*) gene expression in ripe fruit.

Quantitative PCR was carried on the (a) *CCS* and the (b) *CHY2* genes in the ripe fruit of chilli pepper to see if there was a correlation with colour intensity phenotype. Error bars represent \pm SE (n=3). ANOVA results in supplementary ($P \leq 0.05$).

Other genes in the carotenoid pathway were assayed in ripe fruit, such as *PDS*, *CRTISO*, and *VDE*. However, gene expression levels were either too low at this stage, as for *CRTISO* and *VDE*, or there was no significant difference in transcript levels, which was evident for *PDS*.

4.2.3. Expression of carotenoid related genes throughout ripening

The results in the previous section (4.2.1) revealed that two key carotenoid related genes, *PSY1* and *DXS*, were found to be highly expressed in the high colour intensity phenotype lines. The expression profiles throughout ripening were studied to get a better understanding of the regulatory mechanisms which were operating in chilli pepper. Thus, defining which genes have the most influence over the accumulation of carotenoids in ripe fruit. Carotenoid related genes *PSY1*, *PSY2*, *DXS*, and *CCS* were profiled in selected lines throughout ripening. The stages used to analyse the ripening process were mature green (MG), determined at 55 days post anthesis (dpa), breaker (B), marked by the first sign of red colour, breaker plus three days (B+3), breaker plus 7 days (B+7), breaker plus 10 days (B+10), and breaker plus 14 days (B+14).

To gain insight about the differences in gene expression throughout ripening three lines were chosen to focus on. Two lines with high intensity phenotypes, R1 and R7, were selected due to their differences in ripening rate. The R1 line had a fast ripening rate when compared to the other varieties studied and R7 had a slow ripening rate. R3 was also selected, as this line has a fast ripening but low colour intensity phenotype. There was no line with a slow ripening and low colour intensity phenotype.

4.2.3.1. Phytoene synthase-1 (*PSY1*)

The *PSY1* expression profiles over ripening, in the three lines previously mentioned (R1, R3 and R7), were compared. It was apparent that the rate of ripening was reflected in the expression of the *PSY1* gene (Figure 4.5a-c). Whereby the fast ripening lines, R1 and R3, showed a prominent peak in expression at the B+3 stage and the slow ripening line R7 peaked at the B+14 stage, or possibly continued for longer. Comparison of the shape of the peak in the two fast ripening lines displayed that the fast ripening, high intensity line R1 had a much broader peak of expression of *PSY1* spanning from B to B+7. In comparison, the fast ripening, low intensity line R3 had a

narrower peak. This, therefore, shows that the *PSY1* gene was being expressed for a longer duration in the R1 line when compared to the R3.

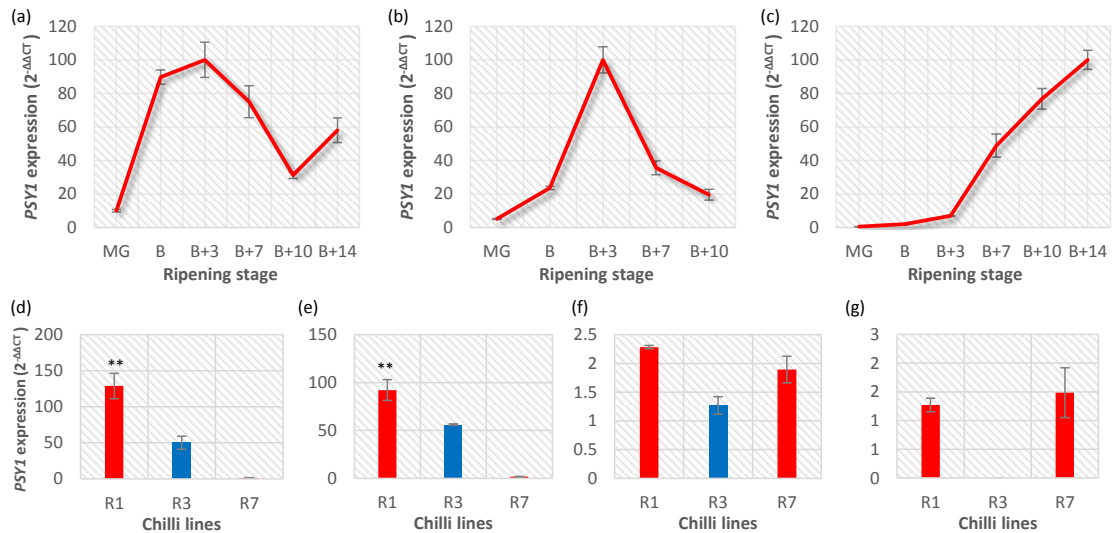


Figure 4.5. *PSY1* expression throughout ripening in high and low intensity lines.

A representation of the trend in *PSY1* expression from mature green (MG) to breaker plus 10/14 days (B+10/14) in (a) R1 a high intensity, fast ripening line. (b) R3 a low intensity, fast ripening line. (c) R7 a high intensity, slow ripening line. A direct comparison of relative *PSY1* expression of the three selected lines R1, R3 and R7 was conducted at (d) breaker (B), (e) breaker plus 3 days (B+3), (f) breaker plus 10 days (B+10) and (g) breaker plus 14 days (B+14). Key for d-g: red, high intensity lines and blue, low intensity line. Error bars represent ± SE (n=3). Statistical analysis was performed using ANOVA ($P \leq 0.05$).

The gene expression analysis carried out was calculated using relative expression thus, the three graphs in the top panel cannot be quantitatively compared but represent qualitative differences throughout ripening (Figure 4.5). The transcript levels were also compared directly between lines at specific stages of ripening. R1 and R3 had higher transcript levels than R7 in the early stages of ripening with R1 showing significantly higher levels (Figure 4.5d). This was consistent with the trends present in the top panel where there was a steep increase in expression witnessed in R1 and R3, but R7 experienced a much slower rise after MG. A similar finding was also present at the B+3 stage of ripening (Figure 4.5e). *PSY1* expression was, again, significantly higher in R1 compared to R3 and R7. When looking at the B+10 stage of ripening the expression levels of *PSY1* become similar, as both R1 and R3 were diminishing in expression and R7 was still increasing (Figure 4.5f). At the B+14 stage there were no data for R3 because the fruit from this

line at this stage was senescing. R1 and R7 had similar levels of *PSY1* expression whereby R7 may still be increasing in expression and R1 was still expressing *PSY1* at a moderate level.

4.2.3.2. 1-Deoxy-D-xyulose 5-phosphate synthase (*DXS*)

The *DXS* gene present in the MEP pathway was investigated throughout ripening. This was to ascertain if there was any relationship between the expression of the *DXS* and *PSY1* genes. Observation of the trend in *DXS* expression throughout ripening showed there was a peak in expression at B+3 for the high intensity, fast ripening line R1, B for the low intensity, fast ripening line R3, and B+10 for the high intensity, slow ripening line R7 (Figure 4.6a-c). This again showed, as seen previously with the *PSY1* gene, that the fast ripening lines were peaking at an earlier stage of ripening when compared to the slow ripening line. Also, the peak in *DXS* expression is occurring at an earlier stage of ripening in R3 and R7, or similar stage of ripening in R1, when compared to *PSY1* expression peaks.

A direct comparison of the relative *DXS* expression in R1, R3, and R7 at specific stages of ripening was made. It was found that at B+3 stage R1 was expressing *DXS* at significantly higher levels when compared to R3 and R7 (Figure 4.6d), at B+7 stage the expression of the *DXS* gene was similar for R1 and R7 but R3 was significantly lower (Figure 4.6e), and at the B+10 stage of ripening R7 had significantly higher expression when compared to R1 and R3 (Figure 4.6f). This showed that for the high intensity lines R1 and R7, although they peak at different stages of ripening due to ripening at different rates, they were consistently expressed at a higher level than the low intensity line R3.

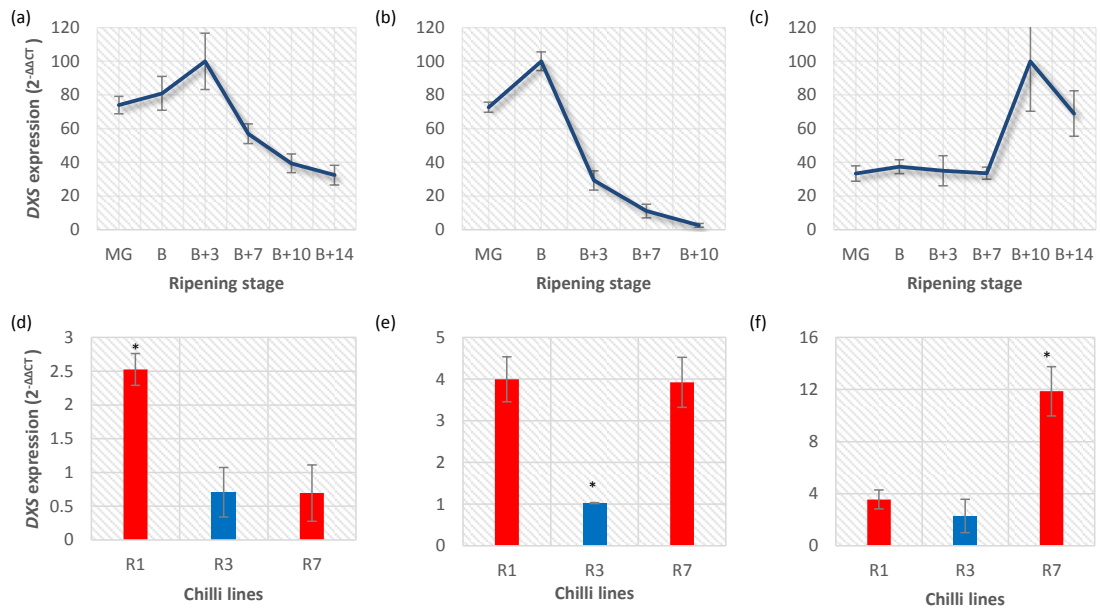


Figure 4.6. *DXS* expression throughout ripening in high and low intensity lines.

A representation of the trend in *DXS* expression from mature green (MG) to breaker plus 10/14 days (B+10/14) in (a) R1 a high intensity, fast ripening line, (b) R3 a low intensity, fast ripening line, and (c) R7 a high intensity, slow ripening line. A direct comparison of relative *DXS* expression in the three selected lines R1, R3 and R7 was conducted at (d) breaker plus three days (B+3), (e) breaker plus 7 days (B+7) and (f) breaker plus 10 days (B+10). Key for d-f: red, high intensity lines and blue, low intensity line. Error bars represent \pm SE ($n=3$). Statistical analysis was performed using ANOVA ($P \leq 0.05$).

4.2.3.3. Capsanthin capsorubin synthase (*CCS*)

The capsanthin capsorubin synthase (*CCS*) gene was also examined throughout ripening to expand understanding of the expression profiles of key carotenoid biosynthesis genes. The two fast ripening lines, R1 and R3, showed a peak in *CCS* expression at the B+3 stage and the slow ripening line was found to peak in expression slightly later at around B+7 (Figure 4.7).

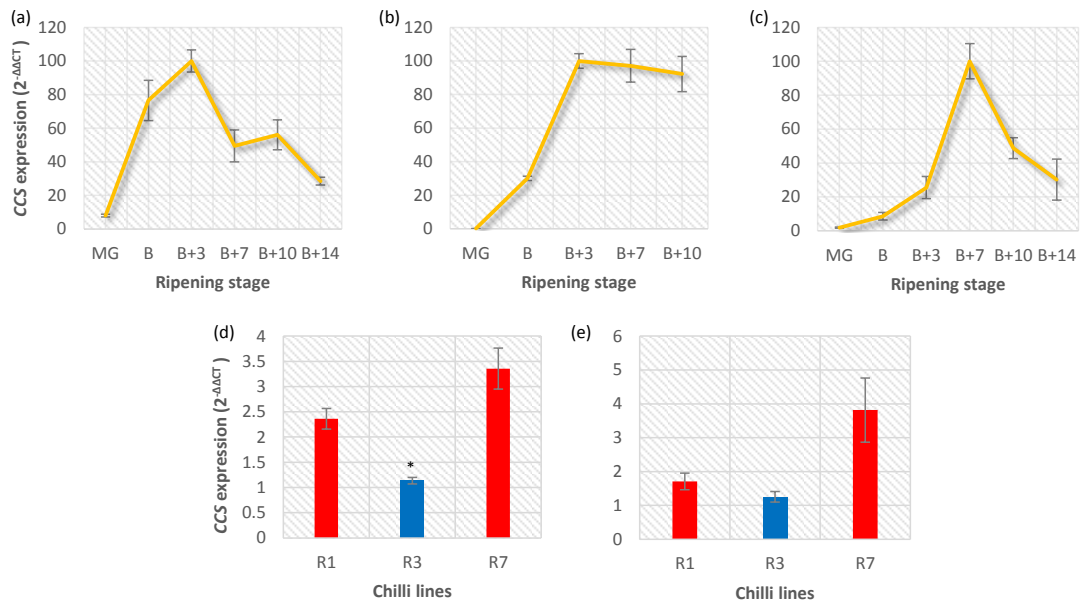


Figure 4.7. CCS expression throughout ripening in high and low intensity lines.

A representation of the trend in CCS expression from mature green (MG) to breaker plus 10/14 days (B+10/14) in (a) R1 a high intensity, fast ripening line, (b) R3 a low intensity, fast ripening line, and (c) R7 a high intensity, slow ripening line. A direct comparison of the relative CCS expression in the three selected lines R1, R3, and R7 was conducted at (d) breaker plus 7 days (B+7) and (e) breaker plus 10 days (B+10). Key for d-e: red, high intensity lines and blue, low intensity line. Error bars represent \pm SE (n=3). Statistical analysis was performed using ANOVA ($P \leq 0.05$).

At the B+7 and B+10 stage of ripening R1 and R7 had similar expression levels, whereas R3 was found to have a lower level of expression of the CCS gene. Comparison of the trends in CCS expression of the three lines studied revealed that the high intensity lines, R1 and R7, decreased at the later stages of ripening (Figure 4.7a and b). However, in the low intensity line, R3, the CCS gene appeared to reach its peak at B+3 and then plateau until B+10 (Figure 4.7c).

4.2.3.4. Phytoene synthase-2 (*PSY2*)

Investigation was carried out to determine whether the fruit specific *PSY1* gene product was solely responsible for the conversion of GGPP into the carotenoid pathway, or whether it was facilitated by the action of the green tissue specific *PSY2*. To ascertain this the expression patterns of *PSY1* and *PSY2* were compared in leaf and throughout ripening (Figure 4.8).

Although the *PSY2* gene was expressed in chilli pepper fruit the levels were very low when compared to the *PSY1*. There was found to be a 2000 fold difference between the *PSY1* and *PSY2* expression in R7 when comparing the *PSY1* peak at B+14 stage with *PSY2* at the same stage (Figure 4.8a). This was double that of the R3 line at the *PSY1* peak at B+3 when comparing with *PSY2* at this stage (Figure 4.8c). However, in both lines there was a similar level of expression of *PSY1* and *PSY2* in the green tissues, such as the leaf and green fruit. Once the onset of ripening commenced *PSY1* expression increased rapidly and *PSY2* decreased but very low levels can still be detected. When just focusing on *PSY2* expression it was apparent that *PSY2* was expressed predominantly in the leaf for both lines analysed (Figure 4.8b and d). The low intensity line, R3, seemed to have a more highly expressed *PSY2* in mature green fruit when compared to the proceeding stages of ripening, whereas the levels of *PSY2* in MG fruit of R7 were similar to the proceeding stages of ripening. When directly comparing the level of *PSY2* transcripts of R3 and R7 in leaf and MG fruit, surprisingly, R3 had significantly higher levels in both leaf and MG when compared to R7 (Figure 4.8e). Of course the caveat with these studies is that an assumption has been made that the transcript levels reflect the protein and enzyme activity trends.

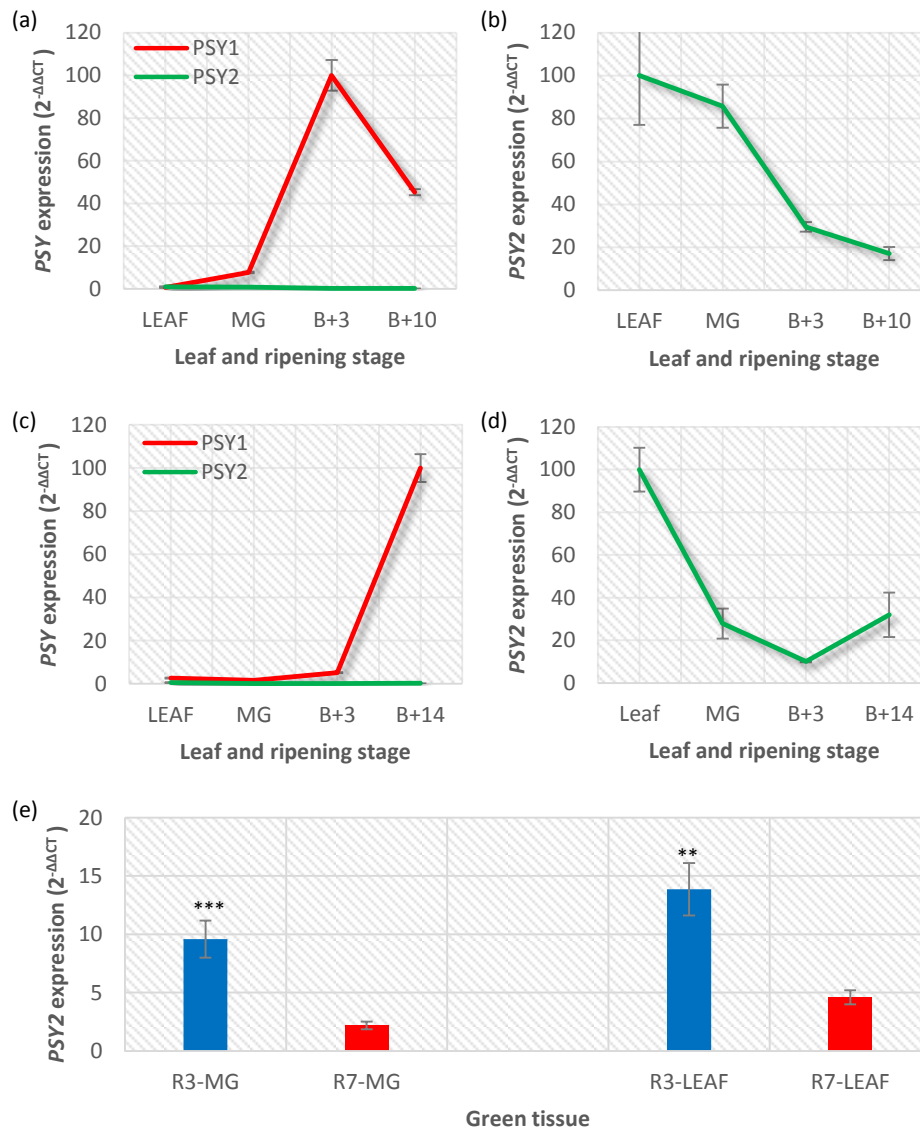


Figure 4.8. Contribution of *PSY2* to the accumulation of carotenoids present in ripe fruit in a high and low intensity line.

The transcript levels of *PSY1* and *PSY2* were compared in leaf tissue and throughout ripening using qPCR to investigate the contribution of *PSY2* in the accumulation of carotenoids. (a) R3 a low intensity, fast ripening line, (b) a refined profile of R3 *PSY2*, (c) R7 a high intensity, slow ripening line, (d) a refined profile of R7 *PSY2*, (e) a comparison of *PSY2* expression levels in both lines in green tissue. Key for e: red, high intensity line and blue, low intensity line. Error bars represent \pm SE (n=3). Statistical analysis was performed using ANOVA ($P \leq 0.05$).

4.2.3.5. Carotenoid acyltransferase

The carotenoids present in the chilli pepper fruit are predominantly found in esterified form. However, little is known about the mechanism of the xanthophyll acyltransferases which are postulated to carry out this esterification. A putative xanthophyll acyltransferase was identified in the tomato pale yellow petal-1 (*pyp1*) mutant, which had a phenotype of reduced xanthophyll levels in the flowers which were not esterified (Ariizumi et al., 2014). This gene (*Solyc01g098110*) was blasted against the chilli pepper genome database and a putative, homologous sequence was identified (Qin et al., 2014). This gene has been denoted ripening specific acyltransferase (*rsAct*). The amplification of a fragment of this gene was achieved from cDNA of ripe fruit, which indicated that this gene was expressed in the fully ripe fruit. The expression profile was analysed throughout ripening to elucidate whether this acyltransferase correlated with ripening related genes (Figure 4.9).

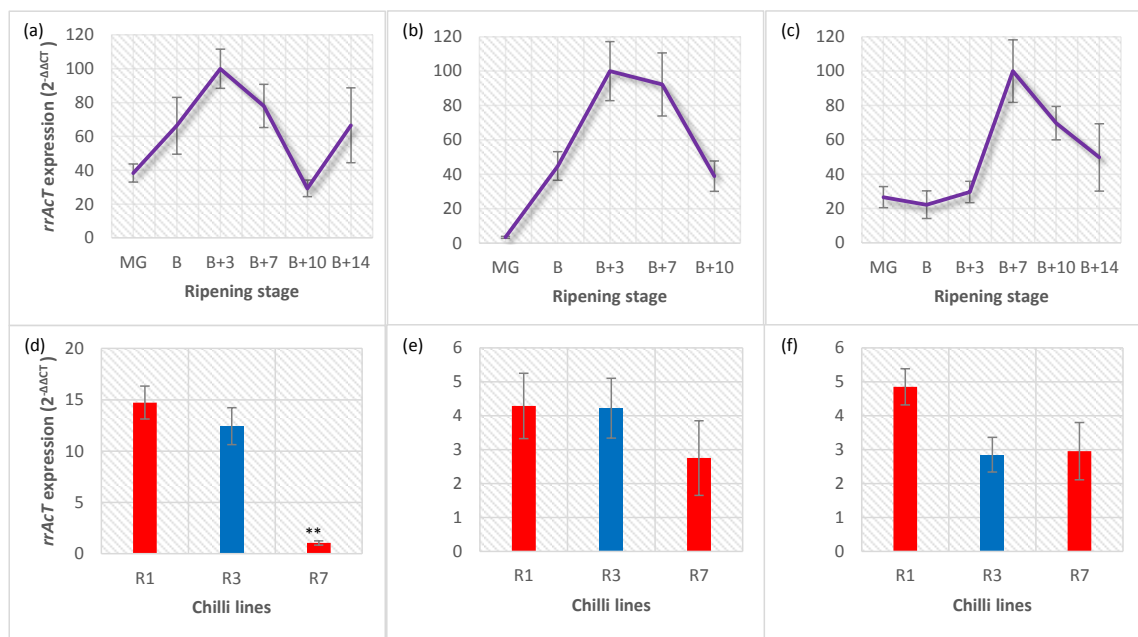


Figure 4.9. Ripening specific acyltransferase (*rsAct*) expression throughout ripening in high and low intensity lines.

A representation of the qualitative trend in *rsAct* expression from mature green (MG) to breker plus 10/14 days (B+10/14) in (a) R1 a high intensity, fast ripening line, (b) R3 a low intensity, fast ripening line and (c) R7 a high intensity, slow ripening line. A direct comparison of the relative *rsAct* expression of three selected lines R1, R3 and R7 was conducted at (d) breker plus 3 days

(B+3), (e) breaker plus 7 days (B+7) and (f) breaker plus 10 (B+10). Key for d-f: red, high intensity lines and blue, low intensity line. Error bars represent \pm SE (n=3). Statistical analysis was performed using ANOVA ($P \leq 0.05$).

Analysis of the expression profile of the *rsAcT* gene showed that it was expressed throughout ripening with a similar pattern to previously analysed carotenoid related genes, such as *PSY1*, *DXS* and *CCS*, whereby the transcripts increased in abundance at the onset of ripening and decreased again when ripening came to a close. The two fast ripening lines, R1 and R3, show as seen in other carotenoid related genes analysed, that there was a peak in expression at around B+3 stage. The slow ripening line, R7, peaked slightly later at B+7 (Figure 4.9a-c). When the levels of transcripts were directly compared between the lines analysed it was revealed that B+3 stage of the high intensity line showed significantly lower levels of *rsAcT* (Figure 4.9d). Whereas, the B+7 and B+10 stages showed no significant differences in the levels of *RsAcT* transcripts accumulated between the lines analysed (Figure 4.9e and f).

4.2.4. Metabolite analysis on lines differing in ripening rates.

Pigment and gene expression analysis revealed that there were variations between lines which possess different colour intensity phenotypes, as well as rate of ripening phenotypes. Observation of these distinct changes led to the evaluation of a more extensive profile of metabolism throughout ripening in the three selected lines R1, R3, and R7, using GC-MS. R1 and R7 share the same colour intensity phenotype (high) but differ in terms of rate of ripening. R1 and R3 differ in colour intensity phenotype but share similar ripening rates (fast), and R3 and R7 differ in both ripening rate and colour intensity phenotype. Three stages of fruit ripening were analysed and over 100 metabolites were identified and quantified relative to the internal standard; thus generating an arbitrary unit (AU). The stages analysed were representative of mature green (MG), turning (B+3 for R1 and R3; B+7 for R7) and ripe (B+10 for R1 and R3; B+14 for R7). This allowed detection of any changes in metabolism which are associated with colour intensity or ripening rate phenotypes during ripening.

4.2.4.1. Overview of metabolites present throughout ripening in chilli pepper fruit

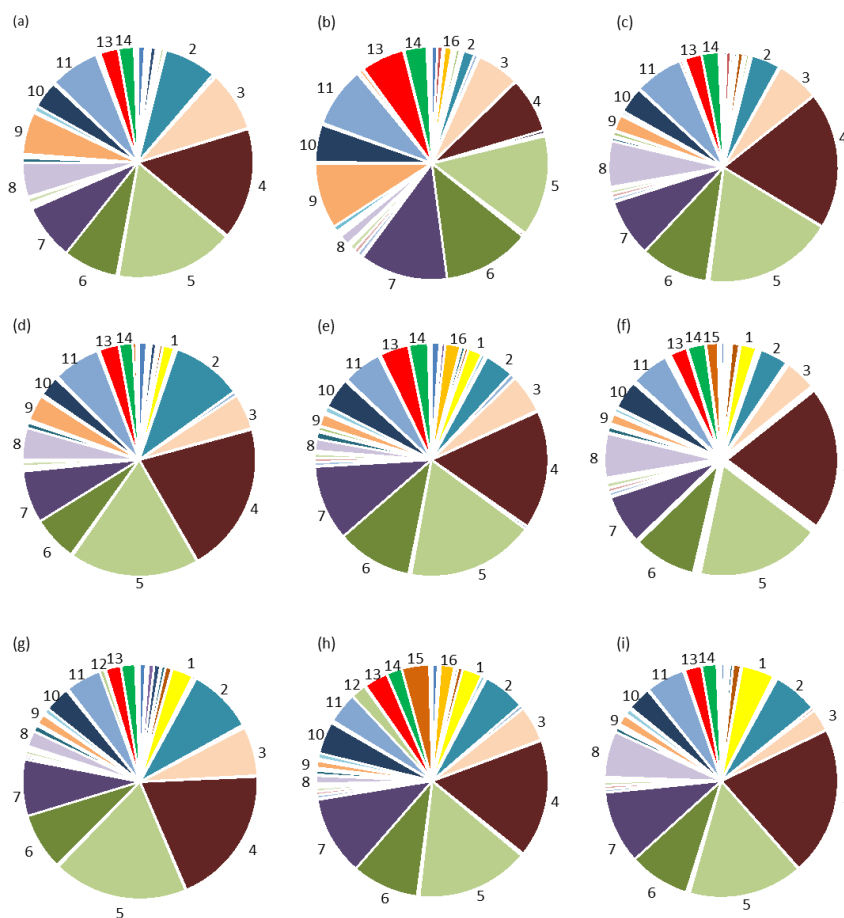


Figure 4.10. Representation of the most abundant metabolites accumulated in the chilli pepper fruit throughout ripening.

The metabolites identified during GC-MS were represented as a percentage of the total metabolites quantified (relative to internal standard) in the selected lines at three stages of ripening. (a, d and g) represent the mature green (MG), turning (B+3) and ripe (B+10) stages of ripening in R1 respectively, (b, e and h) represent the MG, turning (B+3) and ripe (B+10) stages of ripening in R3 respectively and (c, f and i) represent the MG, turning (B+7) and ripe (B+14) stages of ripening in R7 respectively. Key: 1- α -Tocopherol (yellow), 2-Citric acid (blue), 3-Disaccharide (pale pink), 4-Fructose (dark red), 5-Glucose (pale green), 6-Glycero-1-palmitic (dark green), 7-Glycero-1-stearic acid (purple), 8-Inositol (lilac), 9- Malic acid (pale orange), 10- Palmitic acid (dark blue), 11-Phosphate (pale blue), 12-Proline (olive green), 13-Sitosterol (red), 14-Stearic acid (green), 15-Sucrose (dark orange), and 16-Amyrin (orange).

The compounds in all three lines and three stages of ripening were visualised to get an idea of most abundant metabolites accumulated in the chilli pepper fruit (Figure 4.10). The most abundant compounds accumulated were the sugars glucose (13-18%) and fructose (7-20%), and the fatty acids glycerol-1-palmitic acid (7-12%) and glycerol-1-stearic acid (7-12%) at all stages in all lines. Malic acid was abundant at the MG stages of development (2-9%) and citric acid was found at similar levels throughout ripening (2-9%). Palmitic acid and stearic acid were found at around 3-5% and 2-3%, respectively. Sitosterol (2-6%) and amyirin (1-2%) were moderately abundant and they were found to have a high percentage in the R3 line, as was sucrose in ripe fruit of the R3 line (4%) when compared to R1 and R7. There were differences in the percentage of these compounds accumulated between lines which will be explored later (Figure 4.12).

4.2.4.2. Multivariate principle component analysis (PCA)

In order to assess the differences in metabolism over ripening between lines the metabolites identified were subjected to PCA. When the score values were visualised it was apparent that the high intensity, slow ripening phenotype R7 line separated away from the R1 and R3 lines which clustered together (Figure 4.11a). The turning and ripe stages of ripening were very similar in R1 and R3 despite them differing in colour intensity phenotypes. The MG stage of development clustered away from the turning and ripe stages in each line in the top half of the PCA plot. The MG R1 and R3 lines clustered together but they were not as similar as their subsequent turning and ripe stages. The PCA loadings showed that the R7 line was separated based on amino acids, the mature green fruit were separated based on some citric acid cycle metabolites and the two fast ripening lines separated based on fatty acids and alkane hydrocarbons (Figure 4.11b).

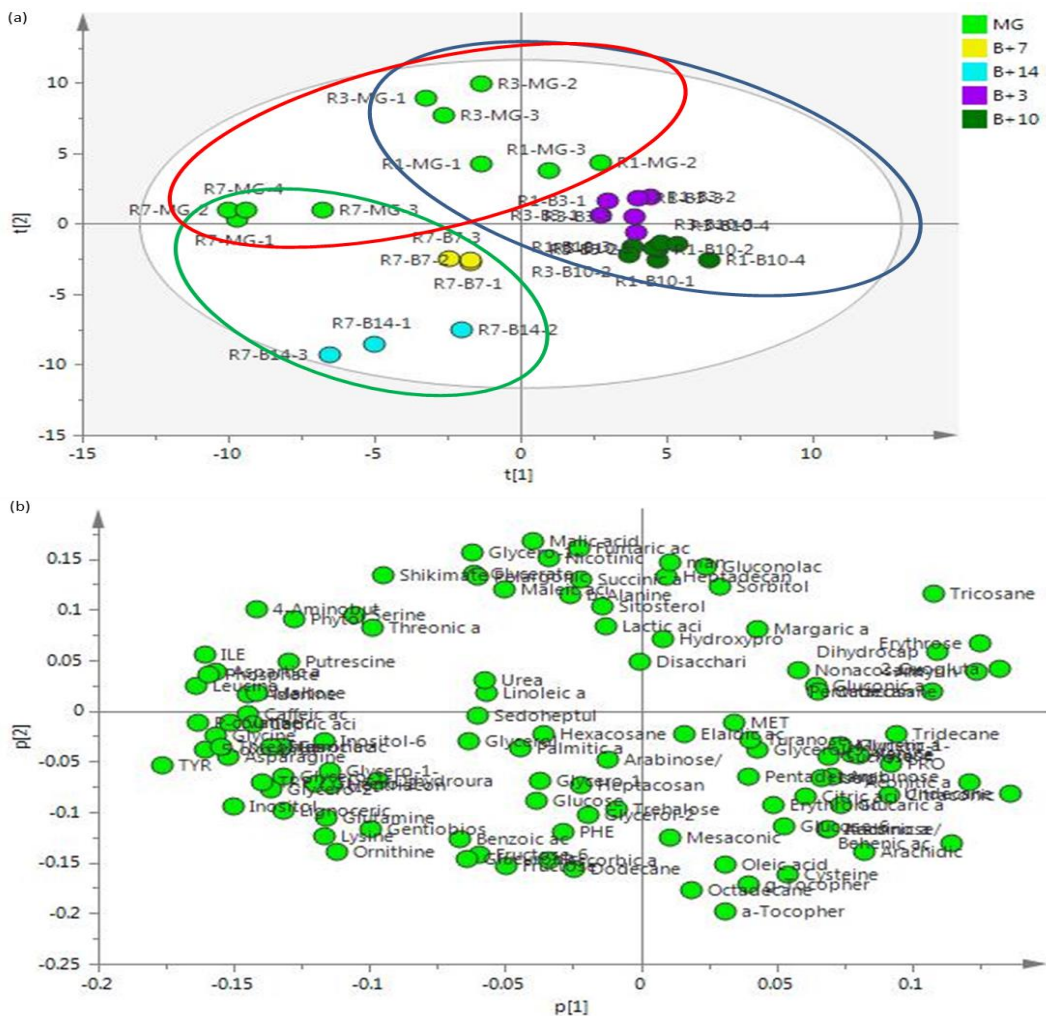


Figure 4.11. PCA analysis of polar and non-polar compounds throughout ripening in selected lines.

The metabolites present in the chilli pepper fruit were profiled throughout ripening using GC-MS. This was carried out on three selected lines with varying colour intensity and ripening rate phenotypes at stages representative of mature green (MG), turning (B+3/7) and ripe (B+10/14). (a) PCA scores and (b) PCA loadings.

To facilitate the visualisation of the data generated by metabolite profiling, heat maps and pathways were constructed displaying the degree of significance of the changes in metabolites observed between lines. The R7 line was used as a control based on the fact that this line was the most ‘different’ from the other lines analysed due to its slow ripening rate phenotype. Therefore, the changes observed for R1 and R3 were with respect to R7. Statistical analysis was performed using one-way ANOVA and BioSynLab software was utilised.

The heat map visualised the overall changes in compounds classes and allowed a global look at the metabolite changes. The significant increases were represented by green boxes, whereas the significant decreases were represented by red boxes (Figure 4.12). The majority of amino acids in both lines were found to be lower when compared to R7. These included lysine, ornithine, and tyrosine for all stages in both lines and 5-oxo-proline and cysteine for R3 in all stages. 5-Oxyproline, asparagine, glutamine, glycine, threonine, and tryptophan were all found to be lower in both lines in ripe fruit as well as aspartic acid, isoleucine, and valine in R3. In MG fruit proline, asparagine, and cysteine were significantly lower in both lines and R1 was found to have lower levels of 4-aminobutyric acid and tryptophan. Overall, there were lower levels of amino acids in the R3 line than the R1 line. There were a few exceptions where the amino acids were found at higher levels in R1 when compared to R7 such as alanine in ripe fruit and β -alanine in turning and ripe fruit. Proline was found to be higher in R3 ripe fruit and methionine was found at higher levels in turning fruit for both lines.

There was no overall trend for the organic acids studied. Caffeic acid was found at lower levels in both lines at MG and turning stages and putrescine was found at lower levels in turning and ripe. 2-Oxoglutamic acid and aconitic acid were found at higher levels at MG and turning stages and dihydrocapsaicin was revealed to be higher in the R3 line in ripe fruit.

Again, there was no strong overall trend for the sugars analysed, but it could be said there were slightly more decreases seen. Inositol was found to be decreased in all stages for both lines. Gentiobiose was decreased in both lines at ripe stage. For both lines, erythronic acid, sedoheptulose, and maltose were decreased at turning stage and maltose and trehalose were down in MG fruit compared to R7. On the other hand, however, increases were seen in mannose and glycerol-2-phosphate in MG fruit and sorbitol and erythrose were increased in turning stage. Mannose, xylose, and glycerol-2-phosphate were found to be significantly higher in the ripe fruit of R1 and sucrose for R3.



Figure 4.12. Heat map of metabolite levels during ripening in selected lines.

Metabolite profiling was carried out in selected lines at mature green (MG), turning (B+3/7) and ripe (B+10/14) stages of ripening in selected lines. R1 has a fast ripening, high intensity phenotype, R3 has a fast ripening, low intensity phenotype and R7 has a slow ripening, high intensity phenotype. R7 was used as a control and the changes in metabolites witnessed are

with respect to R7. Metabolites were grouped by nucleotides, amino acids, organic acids, sugars, sterols, isoprenoids, alkane hydrocarbons and fatty acids. Changes are indicated by white, not present; grey, no change; green, increase; and red, decrease. Abbreviations: ILE, isoleucine; MET, methionine; PHE, phenylalanine; PRO, proline; TRP, tryptophan; TYR, tyrosine; and Isocit, isocitric acid.

In terms of sterols, sitosterol was found to be increased in the MG and turning stages of R3 and amyirin was found at higher levels throughout ripening in both lines when compared to R7, especially in turning and ripe fruit.

The general pattern of change for the carotenoids were that both lines had lower levels when compared to R7 line. This has been previously described as although R1 is a high intensity line too, R7 still had a significantly higher amount of carotenoids. In most cases the degree of significance was lower in the R1 line when compared to R3 illustrating their differences in colour intensity phenotypes. The exceptions were zeaxanthin and its esters, and capsorubin.

The fatty acids were generally found at lower levels, in the fruit, in the fast ripening lines when compared to the slow ripening line, R7, particularly in the R1 line (Figure 4.12). This line was found to have lower levels for cerotic acid, lignoceric acid and stearic acid. Both lines were lower in glycerol- fatty acids particularly at the earlier stages of ripening. Interestingly, the R3 line was found to have higher levels of myristic acid, pelargonic acid, glycerol-1-oleic acid, and glycerol-1-lineolic acid in ripe fruit.

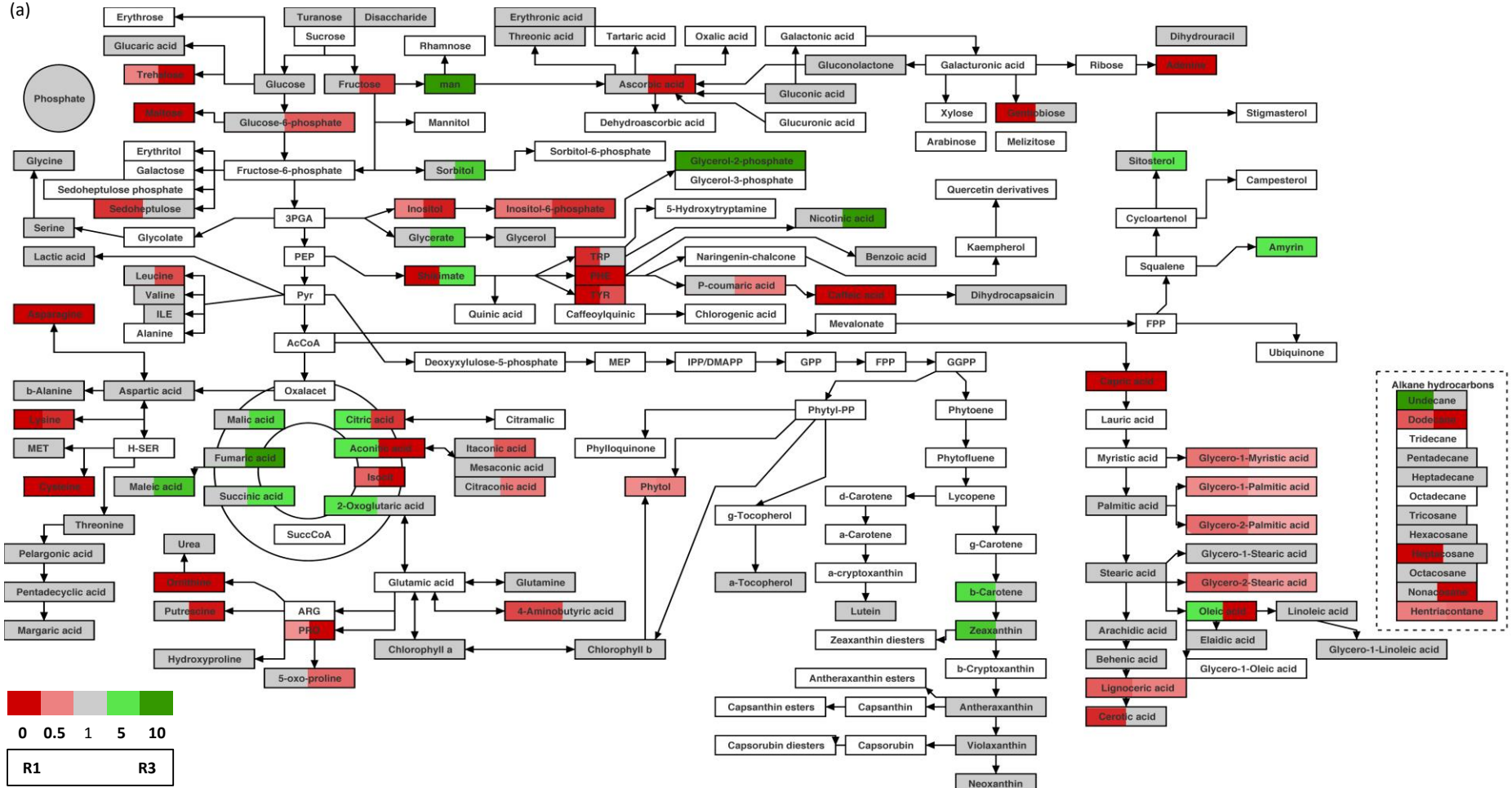
The results described above have been visualised in an alternative manner by constructing a pathway network as a method of linking the metabolite changes to specific areas of metabolism; thus, allowing the upstream and downstream effects of these changes to be taken into consideration. Both R1 and R3 were displayed on pathways constructed for MG, turning, and ripe stages of ripening (Figure 4.13). At mature green stage there were increases seen in the citric acid cycle metabolites for both lines, but the compounds were different. For example, in the R1 line there were increases seen in citric, aconitic, and 2-oxoglutaric acid. Whereas, in the R3 line citric acid and aconitic acid were decreased but there were increases seen in malic, fumaric, and succinic acid. As ripening progressed, increases were seen in these metabolites but there was no trend throughout. Compounds in the shikimic acid pathway were generally decreased in R1 at all stages but in the R3 line there were higher levels of shikimate and dihydrocapsaicin in MG and ripe stages.

The R1 line accumulated higher levels of glycerol-2-phosphate when compared to R7 at the expense of inositol and inositol-6-phosphate throughout ripening. This trend was also seen in the MG fruit of R3 but not at the turning and ripe stages which just showed decreases in the inositol or inositol and inositol-6-phosphate, respectively.

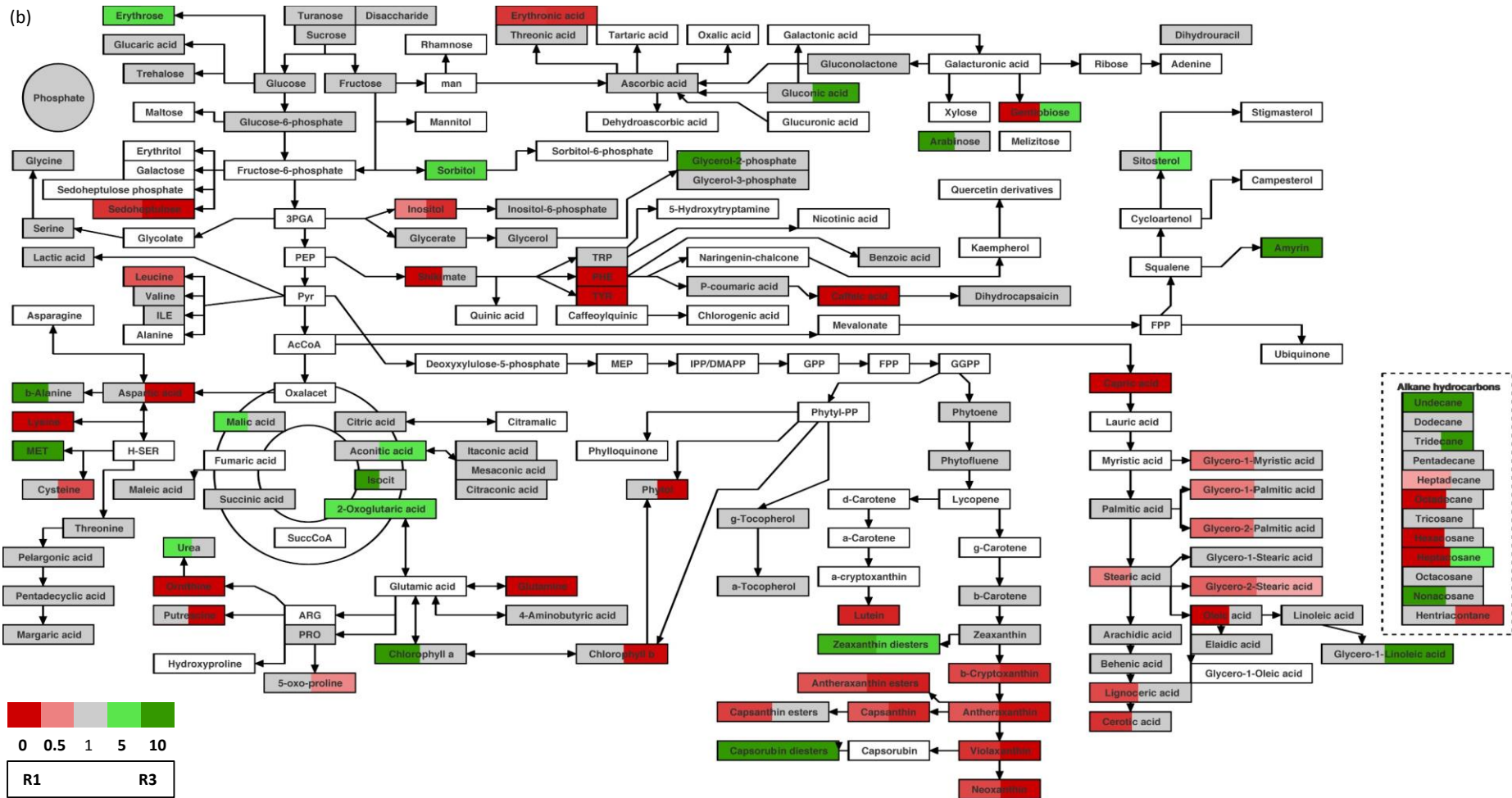
Nitrogen metabolism was down in R3 when compared to R7 with decreases predominantly in ornithine, putrescine, and 5-oxo-proline at all stages and glutamine at turning and ripe stages. Ripe fruit also showed an increase in proline. This was not as strong in MG and ripe stages but was seen in the ripe stage of the R1 line in addition to lower urea levels.

The most striking changes were seen in the fatty acid pathway. In the R1 line there were highly significant decreases observed in the longer chain length fatty acids such as lignoceric acid (C24:0) and cerotic acid (C26:0), and decreased levels of stearic acid (C18:0) throughout ripening as well as capric acid (C10:0) in MG and turning. The glycerol- fatty acids were also reduced in all stages of ripening in this line too. The R3 line experienced similar decreases to R1 in the MG green stage with the exception of cerotic acid and stearic acid; however, the only fatty acids which were lower than those found in the R7 line at turning stage were capric acid and glycerol-2-stearic acid, and there were actually higher amounts of glycerol-1-linoelic. The ripe stage was also very different to the R1 line, although it is similarly lower in stearic acid, lignoceric acid, cerotic acid, glycerol-1-myristic acid, and glycerol-2-stearic acid this line had higher levels of glycerol-1-oleic acid and unsaturated fatty acids, linoleic acid (C18:2) and glycerol-1-linoleic acid.

(a)



(b)



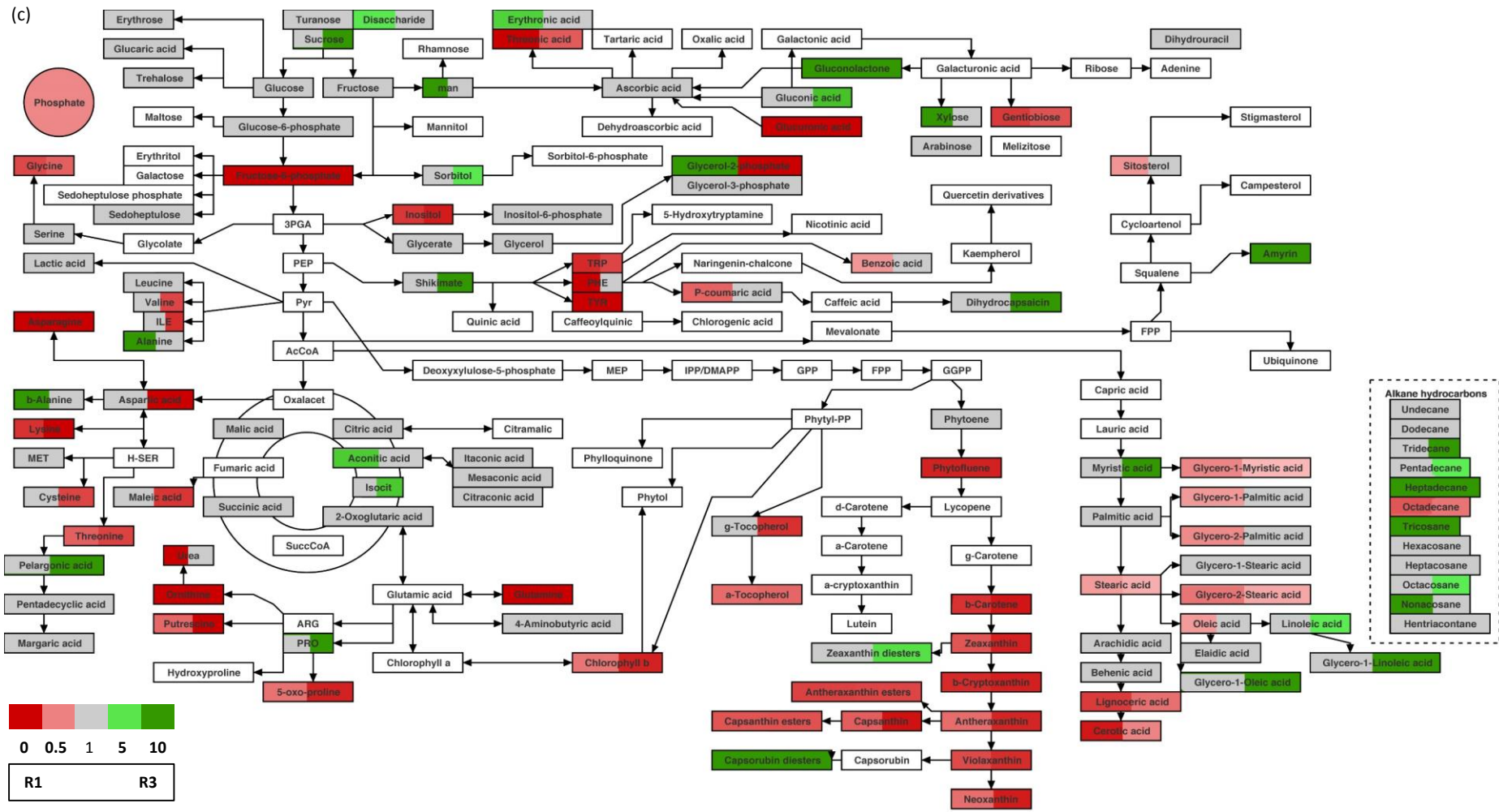


Figure 4.13. Pathway display of metabolite changes over ripening in chili pepper fruit at (a) mature green, (b) turning and (c) ripe stages.

Figure 4.13. Pathway display of metabolite changes over ripening in chilli pepper fruit at (a) mature green, (b) turning and (c) ripe stages.

Metabolite profiling was carried out in selected lines at mature green (MG), turning (B+3/7) and ripe (B+10/14) stages of ripening in selected lines. R1 had a fast ripening, high intensity phenotype, R3 had a fast ripening, low intensity phenotype and R7 had a slow ripening, high intensity phenotype. R7 was used as a control and the changes in metabolites witnessed were with respect to R7. Changes in metabolites were visualised over the pathways for a global look at differences in metabolism. Changes were indicated as increase (green), no change (grey), decrease (red) or not detected (white). R1 represents the change with respect to R7 on the left hand side of the box and R3 represents the change with respect to R7 on the right hand side of the box. Abbreviations: ILE, isoleucine; MET, methionine; PHE, phenylalanine; PRO, proline; TRP, tryptophan; TYR, tyrosine; and Isocit, isocitric acid.

Therefore, the R1 line had significantly less fatty acids compared to the R7 line throughout all stages of ripening but the R3 line actually had higher levels of fatty acids, especially in the ripe stage, when compared to R7. This was also true for the alkane hydrocarbons. The R1 line had predominantly lower levels when compared to the R7 line at the earlier stages of ripening but in ripe fruit there were significantly higher levels of heptadecane, tricosane, and nonacosane. Moreover, the R3 line showed a similar trend in MG fruit but in turning and ripe there were higher levels of hydrocarbons detected to a much higher extent than R1. In ripe fruit there were higher levels of tridecane, pentadecane, heptadecane, tricosane, and octacosane.

4.2.5. Subcellular fractionation

Subchromoplast fractionation was carried out on two chilli pepper lines differing in colour intensity phenotypes. R4 was a medium intensity line and R7 was a high intensity line and the subplastidial components of both lines analysed were isolated. This was in order to identify the location, within the plastid, where the carotenoids and carotenoid esters were sequestered. Characterising differences in sequestration between the medium and high intensity line could determine if this process contributed to intensity.

Fractions (1ml) from the fractionation gradient were collected and following extraction the pigments were analysed using HPLC-PDA. The fractions were collected directly from the top of

the centrifuge tube (fraction 1) to the bottom of the tube (fraction 32). This was to allow quantification of the isoprenoids present.

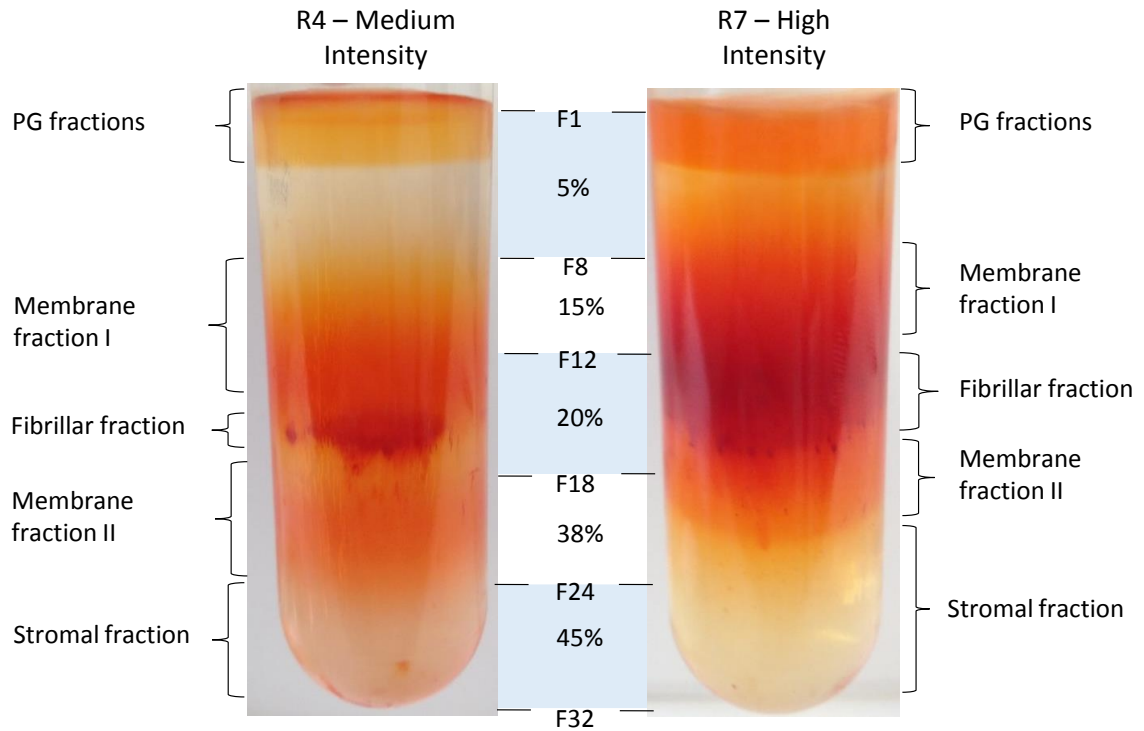


Figure 4.14. Subchromoplast fractionation of red chilli pepper from a medium and a high intensity line.

Chromoplasts were extracted from ripe fruit (30g) and separated on a sucrose gradient. F1-8 had a gradient of 5%, F9-12 15%, F13-18 20%, F21-24 38% and F25-32 45% sucrose w/v as described in the method. Key: PG, plastoglobule.

4.2.5.1. Biochemical characterisation of R4 and R7 subchromoplast fractions

The fractionation exhibited two main areas of carotenoid accumulation (Figure 4.14). The first was at the very top of the tube which is referred to as the plastoglobule (PG) fraction. The second was lower down ranging from fractions 8-24 in R4 and 7-21 in R7. This will be referred to collectively as the membrane fractions which consists of, membrane fraction I, fibrillar fractions, and membrane fraction II. The last portion of the fractionation will be denoted as stromal fractions.

Plastoglobule fractions

The band present in the first 4 fractions located at the very top of the ultracentrifuge tube was believed to be the plastoglobule (PG) fractions (Figure 4.14) as previous work carried out (Nogueira et al., 2013) identified this band as the location of the plastoglobuli. This designation was based on known marker proteins, such as plastoglobule-associated plastoglobulin-1 and chromoplast-specific associated protein C (CHRC), as well as microscopy performed on the isolated fraction (Nogueira et al., 2013).

The first observation to note was that visually the medium intensity line's PG fractions were a different colour when compared to that of the high intensity line. Fractions 2-4 in the medium intensity line, R4, were yellow in colour and the first fraction was orange. The high intensity line, R7, PG fractions were all orange in colour (Figure 4.14).

Membrane fractions

When comparing the most intensely coloured bands in the middle of the tube there were three distinct bands. First, a more uniformly coloured band which appeared orange in R4 and red in R7, which was called membrane fraction I. Then, the next band was red in both lines but the red elements of this band exhibited more threadlike structures that were undergoing aggregation, this band was referred to as the 'fibrillar' fractions. The third band was then much lighter in colour forming a clearly defined orange band just above the 45% gradient buffer in the R7 line but this orange coloured band was more diffuse in the R4 line. This band was designated membrane fraction II. The membrane fractions identified in this study were concurrent with the membrane fractions identified in Nogueira et al., 2013. These membrane fractions in tomato were determined using known protein markers for photosynthetic systems located in the thylakoid membranes, such as ATP synthase subunit β , oxygen-evolving enhancer protein I and II, photosystem I reaction centre subunit II, and photosystem II 22kDa protein (Nogueira et al., 2013). Based on the Nogueira et al 2013 study the fractions after membrane fraction II were stromal derived indicating the presence of the stromal fraction. This was characterised by the presence of the ribulose-1,5-bisphosphate carboxylase/oxygenase protein usually detected in the stroma.

The membrane bands differed greatly in between the two lines. The medium line had a much smaller and lower fibrillar band. In R4 the fibrillar band was located in F15-16 and in R7 F12-15. Membrane fraction I was made up of F8-14 in R4 and F7-11 in R7 and membrane fraction II was found in F17-24 and R7 F16-21. The stromal fractions were described as F25-30 in R4 and F22-30 in R7.

4.2.5.2. Amount of carotenoid in each fraction

Examination of the total amount of each carotenoid in all fractions revealed that there was a significantly higher amount in the high intensity line (R7) when compared to the medium intensity line (R4) (Figure 4.15). This is true for all carotenoids analysed, with the exception of free zeaxanthin.

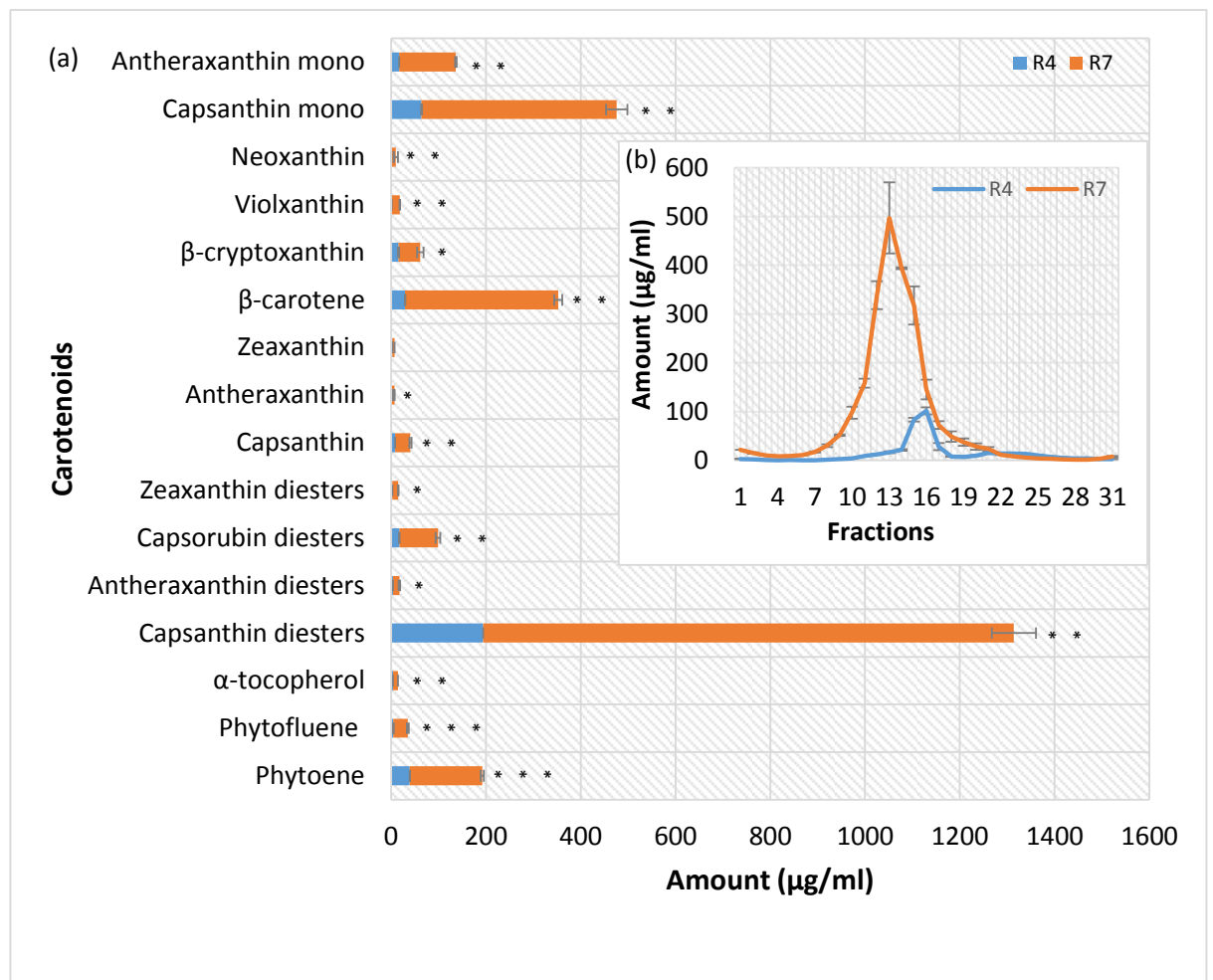


Figure 4.15. Total amount of carotenoids.

(a) Total amount of each carotenoid in R4 and R7, medium and high intensity lines. (b) Total amount of all carotenoids across all fractions. Error bars represent \pm SE (n=2) and statistical analysis was performed with ANOVA ($P \leq 0.05$).

The total pigment content in R4 and R7 were compared. The size and intensity difference observed in the most intense fibrillar band was represented as the main peak in terms of total pigment content where a larger peak in amount which is shifted to the left (or upwards in fractions) in the high line as seen in the fractionation profile. R4, for example, had a peak at F15-16 but in R7 the peak was found in fractions 12-14, with a shoulder at F15. This can be seen when analysing the total pigment of each line, as well as when looking at the pigments individually (Figure 4.15b and Figure 4.16). The difference in the size and intensity of the fibrillar band can be seen in all carotenoid diesters. In terms of actual amount of carotenoid diesters present, the R7 line had approximately 9, 5, 7, and 6 fold more for capsanthin, antheraxanthin, capsorubin, and zeaxanthin diesters, respectively, when compared to R4 (Figure 4.16). This was the same for the free carotenoids there is a higher amount in R7 when compared to R4, for example, free capsanthin, antheraxanthin, zeaxanthin, and β -carotene were 5, 4, 2, and 13 fold higher in the high intensity line (Figure 4.16). In R7 there was a difference in peak shape. The majority of the compounds analysed contained a peak at fraction 13 with a shoulder at fraction 15. However, in phytoene, phytofluene and β -cryptoxanthin the 'shoulder' at fraction 15 was more pronounced giving rise to a double peak shape (Figure 4.16i, n and o).

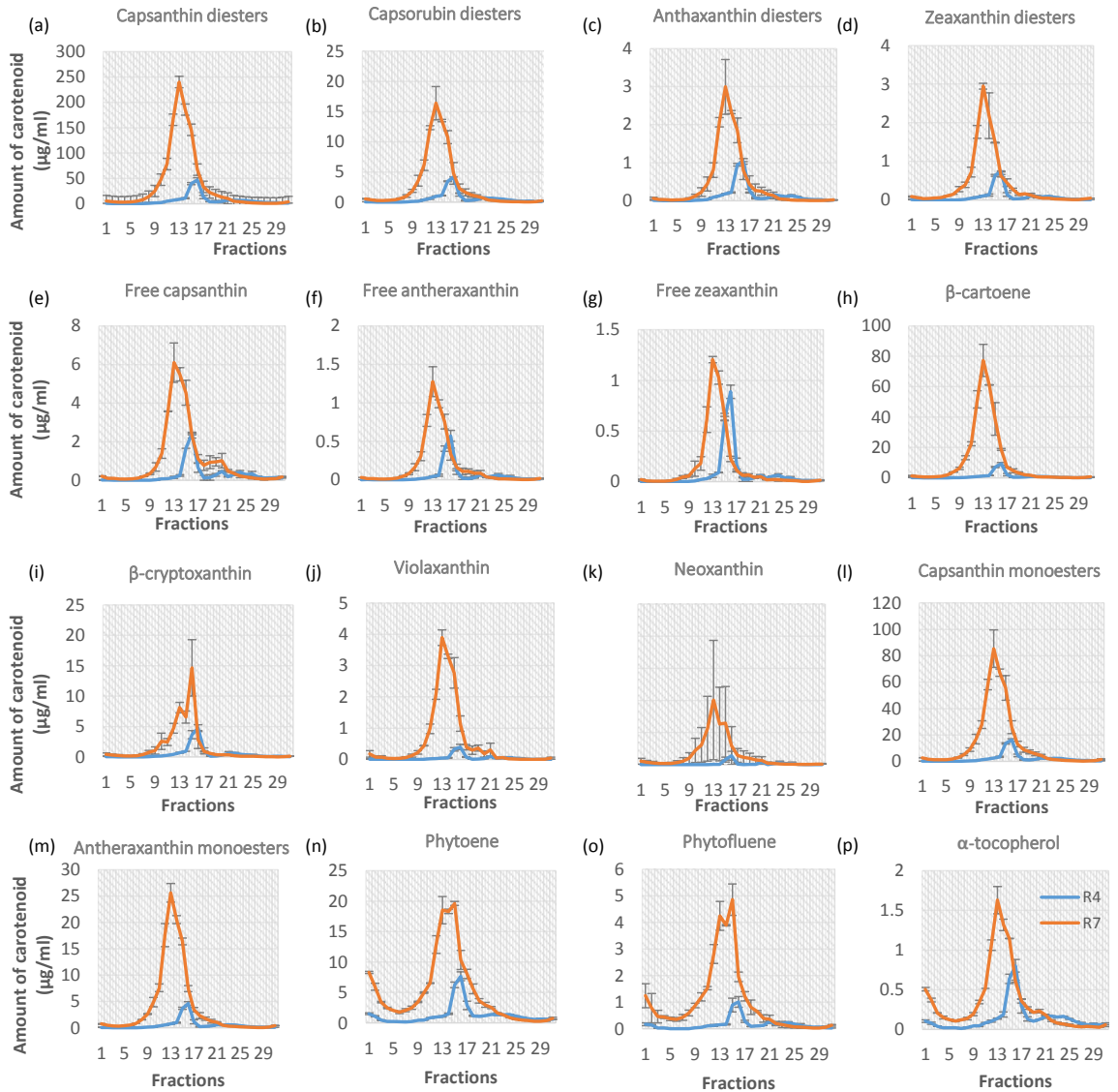


Figure 4.16. A comparison of the amount of each carotenoid analysed in R4 and R7.

Both lines were subjected to subchromoplast fractionation and fractions collected were analysed using HPLC-PDA. A-f displays the quantities of each carotenoid identified. The main peak in each line is representative of the fibrillar fractions. Error bars represent \pm SE ($n=2$).

4.2.5.3. Subplastidial location of carotenoids in R4 and R7

In order to assess the predominant locations of each carotenoid and their corresponding esters, the percentage of total amount of pigment in each fraction was calculated. This was to give insight into the location in which the carotenoids are sequestered.

Plastoglobule fraction

The pigments found to predominantly accumulate in the PG fractions were phytoene, phytofluene and α -tocopherol in both lines (Figure 4.17a-c). In the R4 line, phytoene was responsible for around 45-50% of the total pigments in those fractions and phytofluene contributes 2-6% of the total pigments; however, the percentages observed in phytofluene were more variable than phytoene. The percentage of pigments accumulated in the PG fractions in R7 revealed that phytoene attributed for 27-40%, phytofluene contributed 4-5% and was again far more variable than phytoene. α -Tocopherol was responsible for around 3-4% and 1.7-2.5% of total pigment content in the PG fraction in R4 and R7, respectively (Figure 4.17a-c). Therefore, R4 had a larger percentage of phytoene and α -tocopherol in the PG fractions when compared to R7. The diesters were also found to some extent in the PGs, but not predominantly, whereby capsanthin, capsorubin, antheraxanthin, and zeaxanthin were found at 20-30%, 2-3%, 0.2-0.4% and 0.2-0.4%, respectively when compared to the total amount of pigments per fraction in both lines examined (Figure 4.17a-c). Capsanthin monoesters were found to be responsible for 7-8% and 12-13% of the total pigments in F1-4.

Antheraxanthin monoesters were accountable for 2% and 3-4% in R7 and R4, respectively. The free carotenoids, which become esterified, were found to contribute a very small amount to the total pigments in the PGs, with just under 1% of capsanthin and 0.1% of antheraxanthin and zeaxanthin. However, β -carotene was slightly more abundant with 1-2% and 6-7%, in R4 and R7, respectively. This indicates R7 β -carotene had a more predominant role in the PGs than in R4.

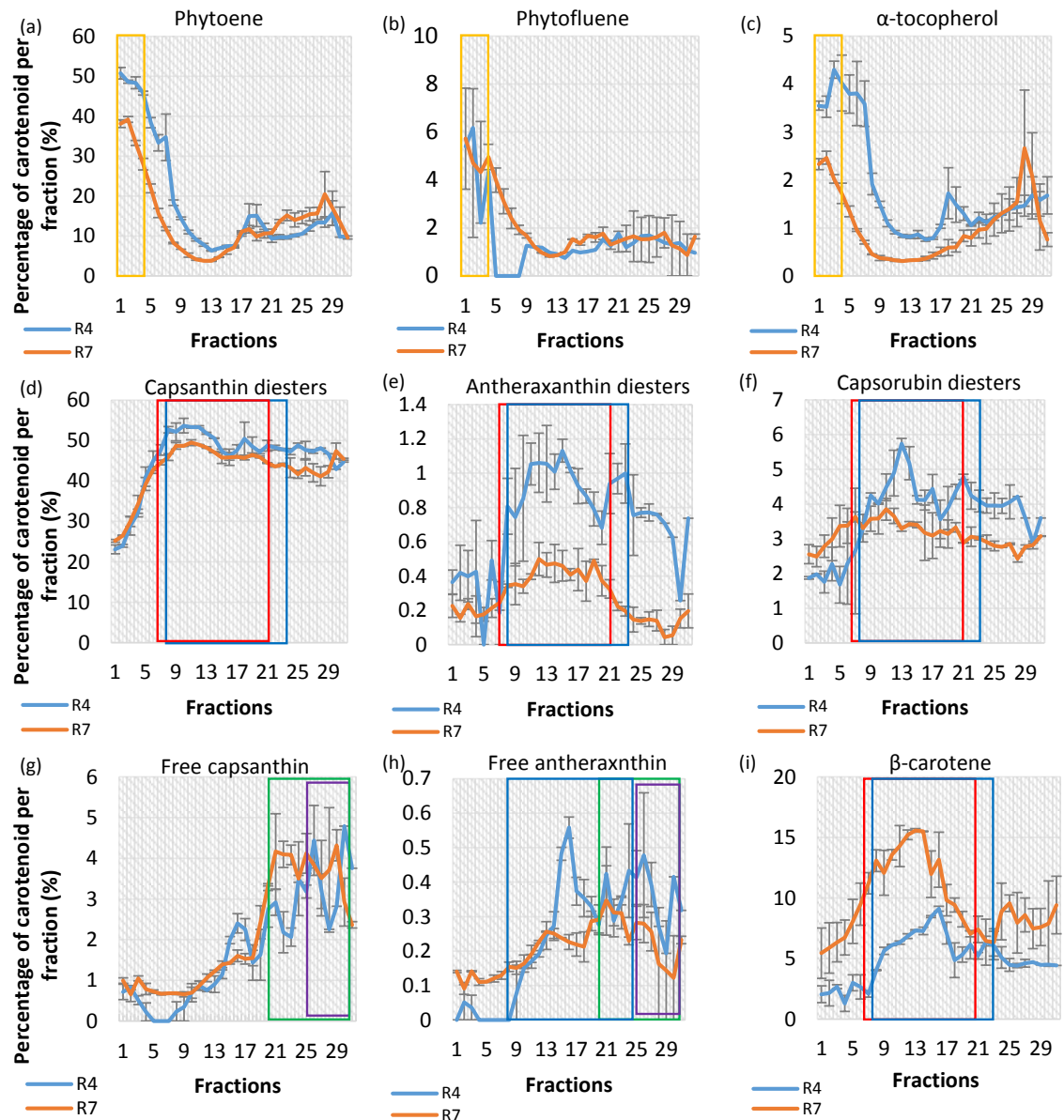


Figure 4.17. Percentage of carotenoids and α -tocopherol per fraction.

The pigments present in each fraction were extracted and subjected to HPLC-PDA. The total pigment content was used to calculate the percentage of carotenoid per fraction. This revealed where the carotenoids were prevalent; (a) phytoene, (b) phytofluene, (c) α -tocopherol, (d) capsanthin diesters, (e) antheraxanthin diesters, (f) capsorubin diesters, (g) free capsanthin, (h) free antheraxanthin and (i) β -carotene. The boxes represent the fractions where each carotenoid is most predominant: the orange box represents the plastoglobule fractions in both lines; the blue box represents R4 membrane fractions; the red box represents R7 membrane fractions; the purple box represents R4 stromal fractions and the green box represents R7 stromal fractions. The errors bars display SE ($n=2$).

Membrane fractions: membrane fraction I, fibrillar fractions and membrane fraction II

Although, as previously mentioned, there were some carotenoid diesters present in the PG band, they were predominantly found in the membrane and fibrillar fractions. In terms of location of diesters this varies slightly between lines (Figure 4.17d-e). Analysis of R4 indicated that capsorubin, antheraxanthin, and zeaxanthin diesters tend to be more prevalent in the membrane fraction I and fibrillar fractions at 4-6, 1, and 0.5%, respectively. However, R7 shows that there were similar percentages of capsorubin and zeaxanthin in all fractions, at around 3 and 0.5%, and antheraxanthin diesters were predominant in both membrane and fibrillar fractions but not to the same extent as R4 with about 0.4-0.5%. The percentage per fraction of capsanthin diesters were very similar in both lines, and besides from contributing only 20% of the total pigment in the PG fractions, in all remaining fractions capsanthin diesters were typically responsible for 45-50% of total pigments for both lines.

The monoesters were also investigated and it was found that capsanthin monoesters were predominantly found in the membrane fractions, in particular membrane fraction II in R7 at around 20% and membrane fraction I and the fibrillar fractions in R4 at around 15-16%. Antheraxanthin monoesters in both lines showed prevalence in membrane I and fibrillar fractions.

The percentages of free carotenoids, such as capsanthin, antheraxanthin, zeaxanthin, and β -carotene were also calculated for each fraction (Figure 4.17g-i). Free capsanthin was located in membrane II and the stromal fractions for both lines, where in R7 it was consistently seen at 4% but R4 varies between 2-4%. Free antheraxanthin was found in the fibrillar and the stromal fractions of both lines at 4%, with a prominent peak at F16. Free zeaxanthin, although very variable in R4, showed a trend towards the fibrillar and stromal fractions in both lines. β -Carotene was found to be located in membrane I and fibrillar fractions in both lines but it represented a higher percentage of the total pigments in R7 than R4 with values of 13-16% and 6-9%, respectively.

The remaining free carotenoids identified β -cryptoxanthin, violaxanthin and neoxanthin were too variable to suggest a location of sequestration. β -Cryptoxanthin and violaxanthin in the R4 line look like they could have some abundance in the fibrillar membranes but the data were too variable to make a robust conclusion. A summary of the predominant locations of carotenoids found throughout the fractionation can be seen in Figure 4.18.

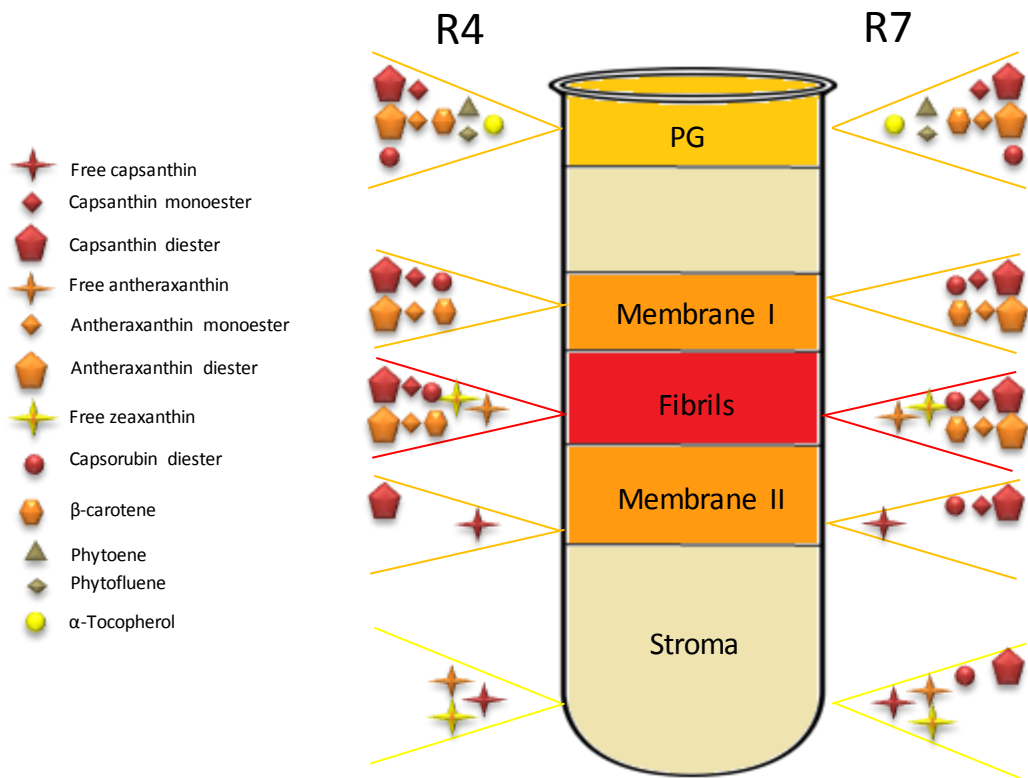


Figure 4.18. Summary of the location of carotenoids; a comparison of R4 and R7.

The percentage of each carotenoid of the total pigment content of each fraction was calculated. This diagram illustrates where the carotenoids were found to reside in each line.

4.2.5.4. Distribution of the total amount of each carotenoid in subplastidial fractions

The percentage of the total pool of each carotenoid across all subplastidial fractions was explored to analyse how the carotenoids were distributed within the subchromoplast fractions and to establish whether this varied between lines (Figure 4.19).

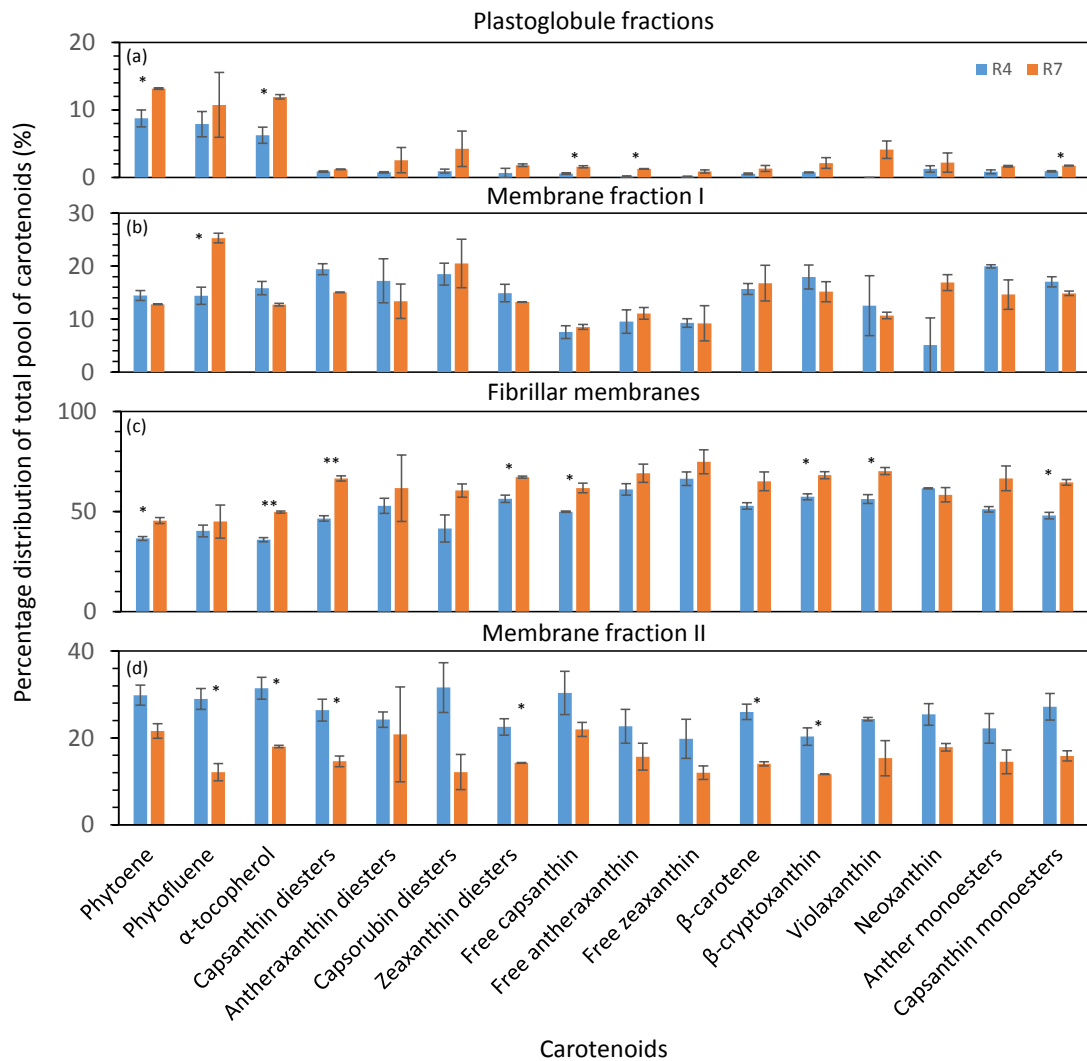


Figure 4.19. The percentage distribution of the total pool of each carotenoid in subplastidial fractions.

The percentages in each of the fractions was taken as a total corresponding to each band characterised. E.g. the plastoglobule fractions consists of 4 fractions so the total percentage of these fractions was calculated. The error bars represent SEM (n=2).

Upon investigating the percentage of phytoene across all fractions, whereby the total phytoene of all fractions was classed as 100%, R4 had around 9% of its phytoene found in the PGs compared to 13% of R7. Phytofluene was found be present in PGs at 8% and 11% for R4 and R7, respectively, although they were not significantly different. α -Tocopherol was found to be present in PGs at 6% and 11% for R4 and R7, respectively (Figure 4.19a). There was a significantly

higher amount of free capsanthin, monoesterified capsanthin, and free antheraxanthin distributed into the PGs in the high line, 1.6%, 1.7% and 1.3% in R7 respectively, when compared to 0.6%, 1% and 0.1% in R4 respectively. Most of the free and monoesters, excluding capsanthin, appeared to have higher percentages distributed into the PG fractions also, but were not significantly different (Figure 4.19a).

All compounds were most abundant in the membrane fractions so when looking at the total pool of each carotenoid the largest percentage was distributed into the membrane fractions. In particular, the largest percentage seen was in the fibrillar fractions. This was F15-16 in R4 and F12-15 in R7. Comparison of the total percentage of each compound in the fibrillar membranes (Figure 4.19c) revealed, in most cases, there was a higher percentage distributed in the fibrillar fractions in R7 when compared to R4. The compounds with a significant difference between R4 and R7 were phytoene, α -tocopherol, and capsanthin (free and esterified). The largest difference was seen in the capsanthin diesters with 1.4 fold more in R7 when compared to R4.

The total percentage distribution of each carotenoid in membrane fraction I revealed that this fraction was very similar in both lines (Figure 4.19b). There were a few exceptions whereby R4 had a higher percentage of isoprenoids, such as phytoene, α -tocopherol, capsanthin mono- and diesters, and antheraxanthin monoesters. Phytofluene was found to have a significantly higher percentage distributed in R7 membrane fraction I. The percentage distribution of carotenoids in membrane fraction II clearly showed that R4 allocates more of its carotenoids into this fraction when compared to R7. Phytofluene showed the largest fold difference between R4 and R7, at 2.4 fold. α -Tocopherol, capsanthin diesters, zeaxanthin diesters, β -carotene, and β -cryptoxanthin all showed 1.5-1.8 fold increases in R4 when compared to R7.

4.2.5.5. Ratio of diesters: free carotenoids

Table 4.1. The ratio of esters: free carotenoids in sub-plastidial fractions (expressed as a percentage).

The percentage of capsanthin, antheraxanthin, and zeaxanthin was calculated in terms of total pigment content per fraction. The total percentage for each subplastidial component was calculated for free and their corresponding esters and then the ratio of esters: free was obtained.

Subplastid location	PG	Membrane I	Fibrillar	Membrane II	Stromal
R4 – Capsanthin	203.4 ±80.2	523.2 ±39.9	58.2 ±4.5	209.9 ±25.2	86.9 ±23.4
R7 – Capsanthin	202.9 ±2.6	456.8 ±21.8	206.5 ±7.5	187.2 ±11.3	151.4 ±20.3
R4 Antheraxanthin	– No free	151 ±10	21.4 ±0.7	107.5 ±1.3	58.5 ±12.5
R7 Antheraxanthin	– 133.2 ±27.1	121.8 ±27	64.6 ±23.8	96.9 ±7.5	137.4 ±10.1
R4 – Zeaxanthin	No free	15.1 ±3.5	4.9 ±3	18.3 ±8.1	5.8 ±1.7
R7 – Zeaxanthin	29.1 ±4.8	26.1 ±6	9.9 ±0.1	24.2 ±3.7	24.9 ±3.5

The ratio of esters to free parent carotenoid were investigated to deduce whether there were different ratios found within the subplastid fractions. When comparing the ratio of esters to free carotenoid in both lines for capsanthin, antheraxanthin, and zeaxanthin, the fibrillar fractions contained the smallest ratio of total esters to free carotenoid. This indicates that there were more free carotenoids present here, when compared to corresponding esters in these fractions, than anywhere else in the plastid. The only exception is capsanthin in R7, whereby there is a similar ratio of esters to free carotenoid in the PGs, fibrillar, membrane I, and stromal fractions (Table 4.1). Antheraxanthin and zeaxanthin had no free carotenoids present in the PGs so the ratio could not be calculated.

For capsanthin the largest ratio of esters to free carotenoid were found in membrane fraction I in both lines. In all other subplastid fractions there were similar ratios in both lines, except fibrillar, where there was a higher ratio of diesters in R7 when compared to R4, as previously mentioned. PGs and membrane fraction II had similar ratios of esters to free carotenoid and the stromal fractions had a lower ratio than the PGs and membrane fractions I and II. Indicating

there were more free carotenoids found here. There was a higher ratio in R7 in the stromal fractions when compared to R4.

In the case of antheraxanthin the PGs and membrane fraction I had the highest ratio of esters to free carotenoid in both lines and in R7 the stromal fractions also had a similar ratio to PGs and membrane I but not in R4. R4 had a much lower ratio here.

Investigation of the ratio of free to esterified zeaxanthin found that although there was more variance in the results obtained when compared to capsanthin and antheraxanthin, there was a similar pattern to antheraxanthin in R7. Whereby PGs, membrane fractions I and II, and stromal fractions were all very similar. In R4 the largest differences were seen in the PGs but the smallest differences were seen in the fibrillar and stromal fractions.

4.3. Discussion

4.3.1. Expression of carotenoid related genes in red chilli pepper

4.3.1.1. Expression of carotenoid related genes in ripe fruit

Understanding the complex expression of carotenoid biosynthesis genes was important to gain insight into regulatory mechanisms which were taking place during ripening. Identification of key genes in the ripening process will allow the vast accumulation of carotenoids to be exploited in the chilli powder industry.

In order to study the changes in gene expression the real time quantitative PCR approach was utilised and optimised. Actin, which is usually employed as a reference gene in such techniques was found to be unstable in chilli pepper and thus, geNorm analysis was performed to identify a stable gene. Out of 6 genes tested the α -subunit of ATPase F1 complex was found to be the most stable and was, therefore, applied to all gene expression assays in this study. One of the first qPCR assays which was carried out was the calculation of the plastome to genome ratio. This was to elucidate whether colour intensity phenotype was a result of increased plastid number. This was investigated because a tomato line with increased carotenoid content caused by the down-regulation of the *DE-ETIOLATED1 (DET1)* gene was revealed to have a high plastome to genome ratio (Enfissi et al., 2010). However, this was not found to the case in chilli pepper, there was no significant difference in plastid copy number when comparing the high intensity line, R7, and the low intensity line, R3. Concurrently, the high intensity line R1 was

found to have a significantly higher plastid number when compared to the other lines analysed. Perhaps this is why, although it has been allocated a high intensity line phenotype and accumulates high levels of carotenoids compared to medium and low intensity lines, when compared with other high intensity lines it has the lowest carotenoid levels of the three high lines analysed (R1, R2, and R7). It is important to consider that this method may not be an accurate measure of the plastid copy number within each cell if the cells are undergoing nuclear endoreduplication (Cookson et al., 2003). Counting of total plastid area per cell and plastid number per cell could perhaps provide insight into the involvement of plastid volume and copy number on colour intensity phenotype (Enfissi et al., 2010).

The transcript levels of *PSY1* and *DXS* were investigated in lines which varied in colour intensity phenotype. The genes were selected based on their strong influence over the carotenoid biosynthesis pathway seen in pepper and tomato (Huh et al., 2001; Fraser et al., 2002; Lois et al., 2000). These genes were found to correlate with colour intensity phenotype whereby the high intensity lines were displaying higher levels of transcripts when compared to the low and medium intensity lines. The highly expressed *PSY1* and *DXS* in the high intensity lines could result in high amounts of substrate being supplied to the carotenoid pathway when compared to the low and medium lines. This was anticipated as it has been shown many times in the previous transgenic studies that the overexpression of *PSY1* and *DXS* have resulted in increased levels of carotenoids accumulated. This has been seen by expressing phytoene synthase in canola, rice, tomato, and potato (Shewmaker et al., 1999; Ye et al., 2000; Fraser et al., 2002; Ducreux et al., 2005). As well as for *DXS* in tomato and potato (Lois et al., 2000; Enfissi et al., 2005; Morris et al., 2006). For example, transgenic tomato lines expressing homozygous *CrtB* experienced a 2 fold increase in lycopene and the *DET1* down-regulated 2A11 variety which displayed increased levels of carotenoids was also found to have 2 fold increases in *DXS* transcript levels (Enfissi et al., 2010; Nogueira et al., 2013). Plus, previous studies of red pepper with differing intensities had elucidated that the darker red lines showed higher *PSY1* expression (Ha et al., 2007). Therefore, this high production of carotenoids produced by the strongly expressed *PSY1* and *DXS* genes could result in the accumulation of free capsanthin at the end of the pathway which was characteristic of the ripe fruit in high intensity lines (3.2.2.2). The later stages of ripening showed that the high intensity lines accumulate high levels of capsanthin diesters as the high levels of accumulated free capsanthin have been esterified and sequestered (3.2.3). The finding that there was no significant difference between the expression levels of the *CCS* gene further suggests that the high capsanthin levels detected in ripe fruit were not due to a

highly expressed *CCS*; thus suggesting that a gene or regulatory processes further upstream in the biosynthesis pathway were responsible.

4.3.1.2. Expression of carotenoid related genes throughout ripening

In order to understand how the previously discussed genes (4.3.1.1) exact control on the carotenoid biosynthesis in chilli pepper, and to identify how they respond to ripening, the expression profiles of these carotenoid biosynthesis genes were determined over ripening. This also provided insight into whether the *DXS* gene upregulated the *PSY1* gene or *vice versa*.

The expression of *PSY1* over ripening in R1 and R3 was consistent with previous studies in the literature whereby transcription is up-regulated at the onset of ripening at breaker stage, peaks at around B+3, and then declines during the later stages of ripening. This has been seen previously in pepper, tomato, and maize (Kim et al., 2010; Huh et al., 2001; Giorio et al., 2008; Giuliano et al., 1993; Li et al., 2008). However, the R7 line showed a different trend in expression where the transcript levels increase throughout ripening. This may be due to slow ripening characteristics of this line where it will continue to ripen for much longer after the 14 days which was usual for other lines; thus, observing the first half of carotenoid biosynthesis. Alternatively, this may be due to the R7 line being unable to receive signals from the end carotenoid biosynthesis products resulting in the expression not becoming 'switched off' as ripening finishes. This was seen with *DXS* in the tomato *rr* mutant which had a defective *PSY1*. In normal circumstances the *DXS* gene becomes down-regulated at the end of ripening but in this mutant there was no accumulation of carotenoids to act as signals for down-regulation of the gene so it continues to be expressed (Lois et al., 2000).

Comparison of the *PSY1* expression profiles of three selected lines differing in colour intensity phenotypes and ripening rates over ripening revealed that the fast ripening lines, R1 and R3, peaked in expression at an earlier stage of ripening when compared to R7, a slow ripening line. This showed that *PSY1* expression may be a good marker for measuring ripening rate and that temporal regulation of the *PSY1* gene may be a factor in colour intensity phenotype for the R7 line, but less so for the R1 line. The R1 line had a highly expressed *PSY1* gene over a short period of time, where it becomes down-regulated at the end of ripening, whereas the R7 line was highly expressed for a much longer time frame showing the highest levels of expression at the later stages of ripening. Comparison of the two fast ripening lines, R1 and R3, showed the differences

in expression of the *PSY1* gene throughout ripening were considerable in high and low intensity phenotypes. Although the trend in expression, which peaks at B+3, was similar, the R1 line had a much broader peak of expression compared to R3 which had a narrow peak in expression. This showed that not only was the R1 line expressing *PSY1* at a significantly higher levels than R3, it was also expressed for a longer duration of time throughout ripening. This would lead to increased levels of substrates into the carotenoid biosynthesis pathway ultimately resulting in the accumulation of free capsanthin in the ripe fruit and capsanthin diesters at later stages of ripening, as previously described in these high intensity phenotype lines. Moreover, these high intensity phenotype lines may also be supplied with high levels of substrate into the carotenoid pathway due to the high intensity lines displaying high levels of *DXS* transcripts. This again supports the hypothesis that the difference in the colour intensity phenotype may be a result of the R7 line carrying mutations in *DXS* which result in the over accumulation of carotenoids, as there were differences in the *DXS* gene in this line but not in the R3 line (3.2.4.3). The highly expressed *PSY1* in the high intensity lines could be a response to a highly expressed *DXS*, as it has been previously shown that the promoter and gene sequences in R3 and R7 are identical (3.2.4.1).

On examination of the transcript levels of the *DXS* gene throughout ripening it was revealed that *DXS* also showed an increase in expression at the onset of ripening which then declined at the end of ripening, similar to that observed with *PSY1*. This was also seen in pepper and tomato (Bouvier et al., 1998; Lois et al., 2000) suggesting that initiation of expression was related to carotenoid biosynthesis and the coordination of genes in the accumulation of carotenoids throughout ripening. The MEP pathway genes are thought to be regulated by retrograde signalling from the chloroplast to the nucleus and so the down-regulation of the *DXS* gene witnessed in this study was a response to the accumulation of carotenoids in the plastid. *DXS* has been known to stay expressed in carotenoid deficient mutants (Lois et al., 2000; Cordoba et al., 2009; Xiao et al., 2012). The expression profile of the *DXS* gene throughout ripening revealed that *DXS* peaks in expression at an earlier or similar time to *PSY1* suggesting that the highly expressed *DXS* gene could be contributing to the up-regulation of the *PSY1* gene in order for the carotenoid biosynthesis pathway to deal with the high substrate levels supplied from *DXS*. In tomato, it was observed that when the mature green fruit were injected with DX this induced carotenoid accumulation, as well as both *PSY1* and *DXS* transcript levels (Lois et al., 2000). Thus, this suggests that similar regulatory mechanisms which were present in tomato could also be present in chilli pepper. A highly expressed *DXS* could result in higher levels of DX accumulating in the plastid, this up-regulates the *PSY1* gene resulting in the high substrate levels supplied into

the carotenoid biosynthesis pathway which go on to cause accumulation of the end product capsanthin. The allelic differences in the promoter region and the amino acid substitutions present in the protein of the high intensity R7 line, previously described (3.2.4.3), may be responsible for the high expression of the *DXS* gene.

Analysis of *CCS* gene throughout ripening was carried out to understand the regulatory mechanisms which may be active in the chilli pepper carotenoid biosynthesis pathway. The expression profiles of the lines studied differed in terms of qualitative trend over ripening. Firstly, the slow ripening rate of the R7 line was also reflected in *CCS* gene expression, as seen previously in the *PSY1* and *DXS* genes in the R7 line, whereby they peaked at a later stage when compared to the fast ripening lines analysed. For the *CCS* gene the peak of expression was B+3 for the fast ripening lines and B+7 for R7. The second observation to note from the determination of *CCS* expression over ripening was the difference in trend for the low intensity R3 line. The high intensity lines showed an increase until *CCS* expression peaked at B+3 and B+7 for R1 and R7, respectively. Followed by a decrease in expression at the end of ripening. Thus, simulating the expression of many other carotenoid genes throughout ripening, whereby gene expression was initiated at the onset of ripening (e.g. breaker stage) and then decreases as ripening terminates (*PSY1* and *DXS*). However, in the low intensity line the expression of the *CCS* gene was initiated as ripening commenced but does not undergo down-regulation when ripening had finished. This indicated the possibility of a negative regulatory feedback loop operating on the *CCS* gene, whereby when the plastid had perceived sufficient accumulation/saturation of capsanthin levels, a signal was initiated to modulate *CCS* gene expression indicating that ripening had terminated, and a high level of expression is no longer needed. Furthermore, if the level of capsanthin does not reach the threshold level, as described previously for the R3 line, then the negative feedback loop would not be activated and the *CCS* expression would not become down-regulated. Resulting in the plateau observed in Figure 4.7b.

Although there have been no previous studies which have identified a negative feedback mechanism acting on the *CCS* gene, in orange fruit varieties there was evidence that showed in some varieties *CCS* gene expression increased throughout ripening, as opposed to becoming down-regulated in the later stages (Rodriguez-Uribe et al., 2012). This was also seen in orange mutants displaying higher levels of *CCS* expression when compared to red fruited varieties (Borovsky et al., 2013). Perhaps this lack of down-regulation was due to the absence of the negative feedback loop acting as orange fruited varieties are known to accumulate lower levels of carotenoids when compared to red (Ha et al., 2007). There have been a number of studies which show regulation of this gene to be complex. Reports for yellow and orange varieties of

pepper with intact forms of the *CCS* gene but no detectable mRNA transcripts present have been observed which suggests the influence of other factors beyond transcriptional regulation (Rodriguez-Urbe et al., 2012).

Evidence supporting this hypothesis can be found when investigating the red to yellow ratio of carotenoids accumulated throughout ripening. As previously mentioned, the red to yellow ratio was surprisingly higher in the low and medium intensity lines than in the high intensity lines (Figure 3.8). Perhaps the reason for this accumulation of 'yellow' carotenoids at the later stages of ripening, visualised by the decrease in the red to yellow ratio found in the high intensity lines, was caused by the down-regulation of the *CCS* gene, resulting from the high accumulation of capsanthin. The down-regulation of the *CCS* gene resulted in the formation of a bottleneck at the end of the pathway. If the high intensity lines were experiencing a higher substrate flow into the pathway and the end of the pathway had been down-regulated then this will inevitably lead to the build-up of yellow precursor carotenoids. The low intensity line does not experience a down-regulation of the *CCS* gene, thus, there was no reduction in the red to yellow ratio of carotenoids as a bottleneck was not formed and the accumulation of yellow precursors did not occur.

A second isoform for the phytoene synthase gene was identified and sequenced in section 3.2.4.2. The presence of a second phytoene synthase has previously been proposed but not yet identified or characterised in pepper (Romer et al, 1993; Rodriguez-Urbe et al., 2012). The expression profile of this gene was analysed in leaf tissue and throughout ripening to confirm its role in green tissue and to assess the contribution of this gene in carotenoid accumulation in fruit. It was found that the *PSY2* gene was predominantly expressed in the leaf and in the mature green fruit. Transcript levels decreased at the onset of ripening but low levels of expression were still detected. This experiment revealed that although *PSY2* is expressed in the fruit the extremely low levels suggest it does not contribute to carotenoid accumulation in ripening. This was also found to be the case in tomato (Fraser et al., 1999). Further evidence for the fact that there is another isoform of *PSY* found in the green tissue was because lines which were deficient in fruit carotenoid accumulation, such as the white fruited variety, display no deficiency in the leaf tissue carotenoid content. The *PSY1* gene was suspected to be mutated in the white variety but the plant still survives due to the *PSY2* genes role in photoprotection (Kim et al., 2010). Additionally, there have been orange fruited varieties with no *PSY1* transcripts detected which implies the *PSY2* gene was acting here (Rodriguez-Urbe et al., 2012). When the expression of *PSY2* was compared in high and a low intensity lines, R7 and R3, respectively it was found that there was significantly higher expression in the low intensity line. This finding was unexpected

as the R3 line had much lighter leaves and mature green fruit when compared to the R7 line. This could be because *PSY2* was being up-regulated in response to inadequate phytoene supplied to the carotenoid pathway as this was seen in orange fruit, and as a response to carotenoid biosynthesis inhibitors in tomato (Kim et al., 2010; Giuliano et al., 1993). Subsequently, this could also be an 'overcompensation' response to the low levels of expression of *PSY1* experienced in the R3 line.

The identification of a xanthophyll acyltransferase enzyme in tomato flowers allowed elucidation of a putative xanthophyll acyltransferase in chilli pepper fruit. Ariizumi et al., 2014 revealed the gene responsible by generation of tomato plants with perturbed flower colour. The *Pale yellow petal -1 (pyp-1)* gene was found to be mutated in two mutants with similar phenotypes of unesterified xanthophylls resulting in a premature stop codon or single amino acid substitution. BLAST search showed that *PYP1* was a member of the acyltransferase family containing α/β hydrolase-hold domain and a lysophospholipid acyltransferase (LPAT) like domain. This domain was found in enzymes which catalyse the incorporation of an acyl group into acceptors (Ariizumi et al., 2014). Analysis of the ripening specific acyltransferase (*rsAcT*) identified in this study in chilli pepper revealed that this gene was related to the ripening process in chilli pepper fruit, showing very similar expression patterns to previously analysed carotenoid related genes such as *PSY1*, *DXS*, and *CCS*. This suggests that perhaps this gene could be responsible for the esterification of carotenoids accumulated in ripe fruit similar to the role of the pale yellow petal-1 gene in tomato flowers (Ariizumi et al., 2014). Consideration of the results previously mentioned, where the key carotenoid biosynthesis related genes *DXS* and *PSY1* were discovered to be highly expressed in the lines possessing a high colour intensity phenotype when compared to low and medium intensity lines, was noteworthy when making the discovery that the *rsAcT* transcript levels of the selected lines were similar at B+7 and B+10 stages of ripening and even significantly lower for the R7 line at B+3. This creates a plausible explanation of the finding that free capsanthin was accumulated at high levels in these same high intensity lines. If *DXS* and *PSY1* were supplying high levels of substrate into the carotenoid pathway in these high intensity phenotype lines and the enzyme responsible for the esterification of the abundant carotenoids accumulated was expressed at a similar level or lower in these high lines then it is reasonable to assume that these high intensity lines accumulate high levels of free capsanthin for this reason. The plastid was inefficient in the esterification step of carotenoid accumulation resulting in a pool of free carotenoids accumulating before they become esterified. These findings led to the investigation of the sequestration mechanisms present in chilli pepper which will be discussed in section 4.3.3.

4.3.2. Metabolic profiling

The compounds identified using GC-MS were visualised based on their statistical variance. It was apparent that the high intensity, slow ripening phenotype line, R7, separated away from R1 and R3, the two fast ripening lines, when compared on a PCA plot. The difference in location of this line compared to R1 and R3 indicated that this line had a chemical composition which was different when compared to other lines analysed, thus indicating that the ripening rate phenotype had a much broader effect on metabolism than colour intensity phenotype. This was suggested as, although the R1 and R3 lines share the same fast ripening rate phenotype, they have different colour intensity phenotypes. The high and the low colour intensity phenotypes of R1 and R3, respectively do not result in perturbed metabolism during ripening as the chemical compositions were similar despite accumulating significantly different pigments levels.

Heat maps and pathway displays were utilised for the visualisation of all polar and non-polar metabolites identified allowing direct comparisons of the changes in metabolites between lines and their degree of significance. This allowed a better understanding of the overall variation occurring in specific compound classes or particular pathways. For example, when investigating the levels of amino acids and organic acids, the increased levels of amino acids seen in the slow ripening line, R7, could be related to the low levels of intermediates in the citric acid cycle when compared to the other lines analysed. The lower level of citric acid cycle intermediates could be caused by the requirement for more amino acids in this slow ripening phenotype line. If this slow ripening line also had a slower metabolism compared to the other lines then perhaps amino acids that accumulate become degraded when not utilised. This could also explain the increased levels of nitrogen metabolism in this line when compared to the others. This would perpetuate the need for synthesising more amino acids.

The most striking difference witnessed when comparing the metabolites of the selected lines was that R1 and R3 accumulated lower levels of fatty acids throughout ripening when compared to R7. This may be because of the high content of fibrillar plastoglobuli present in this line adapting in response to the high levels of capsanthin diesters (4.3.3). Also, the R3 line accumulated more unsaturated fatty acids than R1 and R7 in ripe fruit. In the R1 line, the most significant decreases in fatty acids were seen in lignoceric acid (C24:0) and cerotic acid (C26:0). These fatty acids were not very well characterised in the literature but have been identified in pepper previously (Conforti et al., 2007). These compounds are very long chain fatty acids

(VLCFA) which comprise of fatty acids with acyl chains over 20. They have been characterised as cuticular and epicuticular lipids which associate with triacylglycerides and sphingolipids. The knockout of a key biosynthetic gene in the VLCFA biosynthesis pathway leads to embryo lethality in *Arabidopsis* suggesting these fatty acids play a key role in development (Roudier et al., 2010). It has also been seen that other mutants of VLCFA biosynthesis resulted in defective cell expansion thus leading to the reduced aerial tuber size (Zheng et al., 2005). It could be proposed that the lack of these VLCFA in the R1 and R3 lines when compared to R7 could be causing differences in fruit size. As lignoceric acid and cerotic acid are decreased at all stages of ripening in R1, and they are also decreased in R3 in ripe fruit. The fact that these lines bear small fruit compared to the R7 suggests the reason for this phenotype could be due to the lack of VLCFA available for cell expansion. However, as these VLCFAs were components of cuticular wax it is also very likely that the R7 line has an oilier cuticle than when compared to the others, the other lines could have a waxier cuticle due to having higher levels of alkane hydrocarbons.

The decreased fatty acid levels observed in R1 and R3 was also simultaneous with an increase in amyirin in both lines at all stages compared to R7, as well as sitosterol in MG and turning fruit of R3. This might indicate the decreases seen in the fatty acids were being compensated for by adding more sterols to the membranes. It has also been seen in tomato that decreases in aliphatic components were analogous with increases in triterpenoids (Vogg et al., 2004).

The R1 line experienced much lower levels of stearic acid and glycerol esters of fatty acids, such as glycerol-1-myristic acid, glycerol-1-palmitic acid, glycerol-2-palmitic acid, and glycerol-2-stearic acid. These compounds were likely to have been associated with triacylglycerols which have a role in energy storage in plants. The R1 line had a thick walled phenotype when compared to the other lines. Perhaps this decrease seen in energy storage components, as well as a decrease seen in fatty acids could be because these precursors were being incorporated in the cell membrane/ membranes more efficiently. Therefore, the precursors do not build up as a result.

The R3 line accumulated more unsaturated fatty acids in the ripe fruit, such as linoleic acid (C18:2) and corresponding glycerol monolinoleate, as well as glycerol monooleate (18:1). This could suggest a more fluid membrane present in this line when compared to the other lines as it is known that the abundance of unsaturated fatty acids in the cell membrane functions to keep the membrane at a more fluid state (Marangoni et al., 1996). This finding was of interest as it has been proposed that linoleic acid is particularly prone to oxidation whereby free radicals attack the double bond (Marangoni et al., 1996; Wang and Baker, 1979). Therefore, perhaps this low intensity and retention phenotype was caused by high levels of linoleic acid present in the

membranes resulting in increased lipid peroxidation which creates increased levels of free radicals. The carotenoids will be mobilised for their antioxidant properties resulting in less being stored in the fibrils and plastoglobuli thus, contributing to a low intensity phenotype and perhaps resulting in more colour loss during storage.

The alkane hydrocarbons are waxy components present in the cuticle of the cell wall to prevent water loss and bacterial infection. The R1 and R3 lines start the ripening process with predominantly lower levels when compared to R7. However, levels increase as ripening progresses and at ripe stage there were higher levels of alkane hydrocarbons present in R1 and R3, with R3 having the highest amount in all lines analysed. This was interesting as previous studies have shown that the surface wax of bell pepper was made up of 87% *n*-alkanes (Bauer et al., 2005), thus implying that the surface wax of the R7 line had much less alkanes when compared to the other lines analysed. This could, however, be a consequence of the slow ripening phenotype where the alkanes have not had a chance to accumulate to appropriate levels when compared to the other fast ripening lines. These differences in cuticle fatty acid composition could be linked to the high retention phenotype in R1 as less water loss may be occurring resulting in protection against oxidation. This was suggested as it has been seen previously in pepper that high levels of alkane hydrocarbons, particularly nonacosane and hentriacontane, were negatively correlated to water loss (Parsons et al., 2013). Therefore, the fact that R1 and R3 have higher levels of nonacosane in ripe fruit may enhance their colour retention abilities.

4.3.3. Subchromoplast fractionation

In order to separate chromoplasts present in chilli pepper fruit into their subplastidal components fractionation using a sucrose density gradient was performed. Carotenoid analysis of the fractions obtained enabled the identification of sequestration sites within lines of differing colour intensity phenotypes. Thus, these data could provide insight in to the differences in storage mechanisms associated with the plastidial storage of carotenoids. Also understanding of the sites the carotenoids were sequestered to may provide helpful knowledge for characterising colour retention.

Carotenoids, because of their hydrophobic properties, are found integrated into membranous structures such as lipid -protein complexes facilitated by the hydrophobic domains in the

proteins (Vishnevetsky, 1999). In *Capsicum*, it is known that fibrillar plastoglobuli are predominantly accumulated in chromoplasts. This is the reason that the 'fibrillar' membranes in this study have been denoted as such. Observation of this fibrillar band, when compared to all the others, displayed threadlike structures which aggregated together. This was a typical characteristic of fibrillar plastoglobuli as there is generally a 1:1 ratio of polar (proteins and polar lipids on the surface) and non-polar components (carotenoids and esters in the interior) (Deruère et al., 1994). On the other hand, the plastoglobule (PG) fractions located at the top of the fractionation were 'globular' plastoglobuli. This is known because of their high lipid content compared to the fibrillar plastoglobuli, causing them to migrate to the top of the gradient (Bréhélin et al., 2007; Nogueira et al., 2013).

4.3.3.1. Plastoglobule fractions

In the plastoglobule fractions phytoene, phytofluene, and α -tocopherol were predominantly found in both lines. This has also been seen in tomato; however, the size of the PG fraction was bigger in pepper when compared to tomato. This was probably due to the higher total carotenoid content typically seen in red chilli pepper when compared to tomato (Nogueira et al., 2013). The presence of these early stage precursors of the carotenoid biosynthesis pathway suggests the PGs serve as a sink to deposit excess phytoene and phytofluene, perhaps as a regulatory mechanism through compartmentalisation (Bréhélin et al., 2007). The presence of diesters, monoesters, β -carotene, and other free carotenoids at lower levels show that once these carotenoids start to accumulate in excess they too are moved to the PGs.

The presence of α -tocopherol in the PGs may be due to the presence of biosynthetic cyclases found in the PGs which have been reported in *Arabidopsis* and pepper (Austin et al., 2006; Ytterberg et al., 2006; Vidi et al., 2006). There has also been some evidence in *Capsicum* to suggest the presence of some carotenoid biosynthesis genes: ζ -carotene desaturase, lycopene β -cyclase, and β -carotene hydroxylase (Ytterberg et al., 2006). Thus highlighting potential metabolic roles of the PGs too.

In this study the results indicate that, from the total pool of phytoene and α -tocopherol across all fractions, a higher percentage was distributed into the PGs in the high intensity line. However, when you observe the percentage of phytoene and α -tocopherol in terms of total pigment content it was apparent that there was more in the medium intensity line. This suggests that the

PGs in the medium intensity line were lacking in some of carotenoids accumulated in the high intensity line resulting in phytoene and phytofluene having a more predominant presence.

The amounts and composition of pigments in the PG fractions can be utilised to describe the difference in colour of these fractions witnessed between the high and medium line. Firstly, when looking at the amount of carotenoids accumulated, there was always a much larger amount in the high line when compared to the medium line. Secondly, there was also a higher percentage of the majority of carotenoids analysed distributed in the PGs in the high line compared to the medium. Lastly, due to the medium line accumulating lower amounts of later stage carotenoids, phytoene and phytofluene, which are colourless, were responsible for a larger portion of the PG fractions perhaps resulting in a lighter colour. Thus, giving rise to the yellow colour observed in R4 and the orange colour in R7. The fact that the high line had more carotenoids deposited in these PG fractions further supports the idea that the PGs were used as a sink for excess carotenoid biosynthesis precursors.

4.3.3.2. Membrane fractions

Investigation of the percentage distribution of membrane fraction II (Figure 4.19d) revealed that R4 distributed a higher percentage of isoprenoids in these fractions when compared to R7. In particular, phytofluene, α -tocopherol, capsanthin diesters, zeaxanthin diesters, β -carotene, and β -cryptoxanthin were significantly higher. Some of these carotenoids have been shown previously to be associated with the PGs. The presence of these PG predominant compounds at higher percentages in R4 suggests these fractions could contain membranes comprising carotenoid biosynthesis sites, which due to accumulation of carotenoids, are going to blister to form PGs in the future as a mechanism to store excess precursors. In chloroplasts it has been established that the plastoglobuli remain associated with thylakoid membranes whereby formation arises by blistering of the lipid bilayer. The outer membrane forms the membrane for the PG and the inner thylakoid membrane remains planar. It is thought that the plastoglobulins induce blister formation in response to accumulation of carotenoids and tocopherols (Austin et al., 2006). Although it is known that the thylakoid system becomes degraded in chloroplast to chromoplast transition a lamellae system derived from the envelope is present instead (Camara and Brangeon, 1981). Concurrently, the fact that in R7 these 'PG carotenoids' were found to be distributed at higher percentages into the PGs than R4 suggests that perhaps the extent to which carotenoids accumulate in the synthesis membranes controls when the PG blisters from the

membrane. This would explain why there were more PG associated carotenoids accumulating with the synthesis membranes I and II in R4 as carotenoids accumulated have not reached sufficient levels to cause blistering. Membrane fraction II is also the densest of the fractions suggesting the presence of abundant proteins.

Comparison of the fractionation carried out in the medium and high intensity lines revealed that the band representing the fibrillar fractions was double the size in the high intensity line, R7 (Figure 4.14). The size and shift of the fibril fractions observed in the high line was caused because the amount of carotenoids in these bands were at least twofold or more, when compared to the medium intensity line. In most cases it was much more than twofold, such as 9 and 7 fold more for the red carotenoid esters, capsanthin and capsorubin, and 13 fold more for β -carotene. Such high amounts of these carotenoids identified in this band were responsible for the increased size seen in R7. The fact that the capsanthin diesters were found to be distributed at a higher percentage in the fibrillar fractions in the high intensity line could be a factor contributing to their difference in colour intensity phenotypes; whereby the high levels of capsanthin diesters initiate more fibril formation.

Previous research has indicated that the PGs are thought to be initiation sites for fibril formation and the presence of bicyclic diesters at a critical level has been suggested as essential for initiation of the fibril formation from the PGs (Deruère et al., 1994; Camara et al., 1995; Simpson and Lee, 1976; Simpson et al., 1977). This would explain the finding that when studying the total pool of carotenoids, all carotenoids examined were found to predominantly distribute into these fibrillar fractions. If this is the case and the formation of fibrils is dependent on the composition and amount of carotenoids present in the PGs, a comparison between the medium and high intensity lines could be showing the PGs at different stages of development. As previously shown, there was found to be a higher percentage of carotenoids and carotenoid esters distributed in the PGs in the high line (Figure 4.19). In the R4 line, the PGs were in early stages of development characterised by phytoene and α -tocopherol having a larger percentage of the total pigments (Figure 4.20 stage I). R7, however, was showing much later stages of PG development perhaps before fibril formation was initiated (Figure 4.20 stage II). The presence of other carotenoids and a higher amount and composition of esters seen here may be the trigger for fibril formation (Deruère et al., 1994). Likewise, the expression of carotenoid-associated genes were found to be activated in parallel to carotenoid biosynthesis genes whereby modulation of expression was affected by the composition and amount of carotenoids accumulating in the tissues (Vishnevetsky et al., 1999; Libal-Weksler et al., 1997). Evidence suggests that incubating the carotenoids and lipids with fibrillin caused the formation of fibrils.

Suggesting a major role of fibrillin in the transformation of globular PGs into fibrils (Deruère et al., 1994). This further supports the discovery that the high intensity line, R7, accumulates a larger amount of fibrils, demonstrated with a larger fibrillar band, when compared to R4, as this line had a considerably higher total carotenoid content with particular emphasis on capsanthin diester accumulation. Also, evidence for the fibril remaining attached to the synthesis membranes was that when comparing the ratio of esters to free carotenoids there was a much lower ratio, and so more free carotenoids, found in the fibrils when compared to the PGs; thus, suggesting metabolite exchange after fibril formation (Table 4.1 and Figure 4.20). This was further supported by a study which has shown fibrils forming from PGs. The PGs then get smaller as the fibril develops, and it is proposed that additional carotenoids and lipids are required for fibril development (Simpson and Lee, 1976). Maybe once the fibril is fully developed it detaches itself from the synthesis membranes.

The free carotenoids were predominantly located in the membrane fractions, particularly the fibrillar and the stromal fractions when looking at the percentage of each carotenoid in comparison to the total pigments per fraction (Figure 4.17g-i). With particular emphasis on free capsanthin being located in the stromal fractions. An explanation for this could be that the ZEP and CCS enzymes may be membrane peripheral proteins which become detached easily from the synthesis membranes. In tomato and pepper, reports show that PSY1 was observed mainly in the stroma (Nogueira et al., 2013; Fraser et al., 1994; Dogbo et al., 1988; Shumskaya et al., 2012) and suggest that PSY1 was associated in a membrane complex located near the periphery of the thylakoid membranes; plus red pepper chromoplasts and membrane fractions were found to desaturate phytoene (Camara et al., 1982). In addition, other studies which carried out fractionation of the pepper chromoplast revealed ZDS and CCS to be located in the membrane as opposed to the stroma, and that CCS activity was associated with the membrane fractions with less than 2% associated with the fibrils (Wang et al., 2013; Bouvier et al., 1994). This strongly suggested that this was also true for ZEP and CCS in chilli pepper. Additionally, as previously mentioned, a study of the red pepper PG proteome revealed the presence of carotenoid biosynthetic enzymes in the PG. These were ζ -carotene desaturase (ZDS), lycopene β -cylase (isoform unknown [LCY- β or CYC- β]), and two β -carotene hydroxylases (Ytterberg et al., 2006).

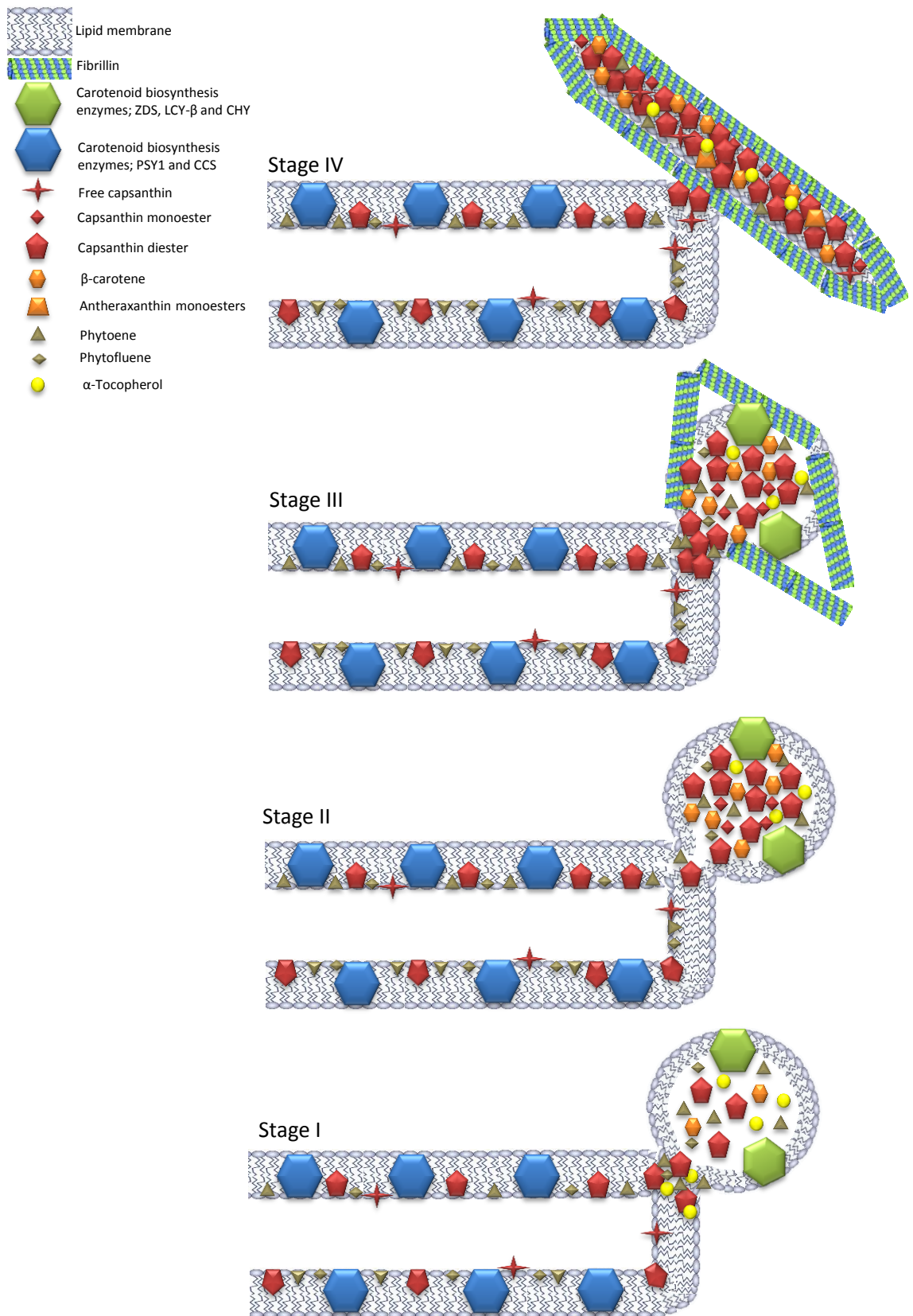


Figure 4.20. Representation of PG and fibril formation in chili pepper.

Stage I represents an early stage PG, similar to PGs in R4, the accumulation of carotenoids within the synthetic membranes initiates blistering of the outer membrane to form a PG to act as a sink for excess carotenoids and perhaps regulate biosynthesis. Stage II represents a later stage PG, similar to PGs in R7, the over accumulation of carotenoids in this high line has resulted in more carotenoids being transported to the PGs. Stage III and IV represents the formation of fibrils from plastoglobuli once the accumulation of bicyclic carotenoids has reached a threshold level. An increase in fibrillin is observed at these stages to have an architectural and protective role in fibril assembly.

This suggested that the early stage biosynthesis enzymes were present in a complex loosely associated with the membranes, then substrates produced were transported to the PGs where biosynthesis steps ζ -carotene to zeaxanthin were carried out, and then they were transported back to the membranes where ZEP and CCS were located possibly for esterification purposes. However, there was conflicting evidence on whether ZDS is located in PGs or the membranes but perhaps this enzyme was found in both locations. Or the PG membrane had incorporated genes from the biosynthesis pathway during blistering. Which poses the question; are the carotenoid biosynthetic enzymes (ZDS, L/CYC- β and CHY) solely found in the PGs or is this a result of the membrane budding off and translocating the enzymes with it? Another important question to answer would be where are the carotenoids esterified? Are the acyl transferases involved as part of a metabolon or are they associated with the membrane or both?

Earlier research in maize has indicated that the expression of the *PSY1* gene could be responsible for the induction of fibril formation, as mutagenesis studies revealed that changing the levels of expression of *PSY1* achieved a fibrillary PG phenotype which was not typical of maize (Shumskaya et al., 2012). With this mind, this could be an explanation for why the R4 line had a medium intensity phenotype. It has been previously characterised as having high total carotenoid content but has only shown a twofold net increase in carotenoids from green to red. This was reflected by the low levels of expression of key carotenoid genes. Consequently, the high total carotenoid content was a result of having abundant photosynthetic carotenoids in green fruit as opposed to synthesising high levels *de novo* at the onset of ripening. Although the total carotenoid content is high, the colour intensity phenotype is medium due to the decreased fibril formation seen in the fractionation studies. Therefore, this suggests that this line has a medium intensity phenotype because it expresses *PSY1* at a low level and does not trigger the expression of carotenoid associated genes, such as fibrillin, and so less fibrils are formed.

4.4. Conclusion

Gene expression studies in this chapter revealed that the high intensity phenotype lines generally had higher levels of key carotenoid related genes which were expressed for longer durations throughout ripening when compared to the low intensity lines. When analysing the expression profiles of *PSY1* and *DXS* it seemed that *DXS* was expressed at an earlier or similar time point to *PSY1* suggesting that the high levels of expression in this gene were causing the up-regulation of the *PSY1*. This was further supported by the allelic variations found in this gene when compared to *PSY1* which was highly conserved between lines. Another feature of carotenoid biosynthesis which was analysed was the possible negative feedback loop which was occurring at the end of the pathway. There was an observed decrease in the *CCS* gene expression once capsanthin levels had reached a sufficient amount, the low intensity line failed to down-regulate the *CCS* gene as capsanthin levels were significantly low compared to other lines. This resulted in a high red to yellow ratio occurring in this line as there was no bottleneck resulting in the accumulation of yellow precursors. Finally, a putative xanthophyll acyltransferase has been identified to have a role in ripening. This gene was found to be expressed at a lower or similar level in high and low intensity lines revealing the reason for the high levels of free capsanthin associated with high intensity phenotype lines. These lines were experiencing increased carotenogenesis when compared to low and medium intensity lines but esterification processes were not sufficient to keep up with the supply of capsanthin therefore resulting in pooling of free capsanthin at ripe stage.

The metabolite profiling revealed that the slow ripening, high intensity line R7 had a significantly different chemical composition to the R1 and R3 lines suggesting the slow ripening phenotype had a more global effect on metabolism than colour intensity phenotypes. The main differences seen in metabolism within these lines were firstly, that R7 had high levels of most of the amino acids identified, this was concurrent with decreases in citric acid cycle intermediates and increases in nitrogen metabolism; therefore indicating that the slow ripening rate phenotype may be having an effect on amino acid biosynthesis and degradation. Secondly, this R7 line had much higher levels of fatty acids and lower levels of alkanes in ripe fruit perhaps signifying different waxy cuticles between lines. The R7 line had a preference for long chain fatty acids and R1 and R3 had a preference for alkanes, or subsequently this finding could just be representing slow ripening rate characteristics whereby the slow ripening line has not yet finished accumulated alkanes when compared to the other lines. A final discovery in these data revealed

that the low intensity, low retention line R3 accumulated significantly higher unsaturated fatty acids when compared to the other lines. This included linoleic acid which has been known to be prone to oxidation thus emphasising a key component of this line which might be a contributing factor to low colour retention phenotype.

Evidence from the subcellular fractionation study suggests that the increased amount of fibrils observed in the high intensity line could be due to vast carotenoid accumulation triggering the initiation of more fibrils from plastoglobuli when compared to the medium intensity line. The higher percentages of carotenoids, particularly capsanthin diesters, in the fibrillar membranes could be a contributing factor to colour intensity phenotype. Similarly, the appearance of higher 'percentage distributed from total pool' and 'amount of carotenoid' analysed in the high intensity line may suggest that PGs role may be a regulatory one. Whereby under 'normal' circumstances the PG was used as a storage vessel as a means of regulation through compartmentalisation. Once a certain level of carotenoid ester accumulation was reached and a higher proportion of the total amount of each carotenoid produced was stored there fibril formation could be initiated, and the role of the fibril type plastoglobule could play more of a storage role as opposed to a regulatory one. This also implied that the change in plastoglobule type is dictated by the contents contained whereby the structure of the plastoglobule adapts to the amount and composition of carotenoids present within, as opposed to a fibrillar structure forming first and then being filled with available carotenoids. This was in agreement with findings in other plants (Fraser et al., 2007; Maass et al., 2009; Nogueira et al., 2013). The abundance of free carotenoids in the stromal fractions, predominantly capsanthin, suggests the presence of the capsanthin capsorubin synthase enzyme being located in the stroma, or perhaps more likely as part of an enzyme complex which becomes detached from the membrane during fractionation.

Chapter 5. Colour retention in red chilli pepper

5.1. Introduction

Red chilli peppers are grown in India for the production of chilli powder or paprika. Once the plant has produced red ripe fruit the chilli peppers are harvested and air dried under natural sunlight. After the chillies are dry they are stored at 10°C in the dark until they are sold. The duration of storage is related to the economic drives leading to the recouping of maximum profit margins. The monsoon season in India is a time when chilli peppers cannot be grown and some varieties of chilli pepper are more susceptible to colour loss during storage. This means that the chilli peppers ability to retain its desirable deep red colour during storage directly determines how much the material can be sold for. Chilli peppers that can retain their deep red colour throughout storage are therefore more profitable than chilli that undergo colour degradation. The reason for the colour degradation during the storage is unknown. Insights into in colour degradation/retention was the focus of chapter 5.

5.2. Results

5.2.1. Colour loss over time under different conditions

To study the colour retention phenotype(s) among the colour diversity panel (described in 3.2.1), lines have to be grown from seed (5 months) and then stored during the monsoon season, which can be up to 8 months. This process is time consuming and the growers miss a season of growth while establishing whether new lines have a high or low retention phenotype. Consequently, in this study chilli pepper fruit were stored under different temperature and light conditions in an effort to speed up the process of colour degradation and thus allowing a faster screening process for growers when new lines are developed.

Chilli peppers were ground to a powder and stored at 15, 20, 30 and 40°C as well as storing the samples under black light and UV light. Image analysis was then used to measure the change in colour over time at weekly time points. The experiment ran for 6 weeks. The image analysis technique allowed quantification of colour by using the RGB values of an image, taken under controlled experimental conditions, and converting them to the CIELAB colour space coordinates L^* , a^* , and b^* , as well as the LCH colour space coordinates lightness, chroma, and hue angle.

5.2.1.1. Lightness (L^* or L)

The lightness (L^*) coordinates represent the lightness of the colour of chillies. Chilli powder with a colour value of 0 represents black and 100 represents diffuse light. Across the duration of the experiment there was a general increase in lightness experienced by the chilli powder samples analysed. There was a stronger increase at the lower temperatures such as 15°C and 20 °C when compared to the higher temperatures, 30°C and 40°C. The UV condition showed the most extreme increase in lightness. There was a sharp decrease in the first week, then a saturation point was reached and the lightness of the powder remained the same. A representation of the trends over ripening at different temperature and light conditions can be seen in Figure 5.1.

The lower temperatures, such as 15°C and 20°C, show that the low intensity, low retention line R3 was significantly the lightest in colour and the medium intensity, high retention line R8 was significantly the darkest in colour, particularly at the last two weeks of the experiment (Figure 5.1a). This trend changes at the higher temperatures, such as, 30°C and 40°C, and under black light whereby the R6 line was significantly the darkest when compared to all the lines analysed (Figure 5.1b). The lightest lines were the same as those determined with previous temperature conditions. The UV condition had the most severe effect on lightness and repeatedly the R6 line was significantly darker than the other lines analysed, while R2, R3, R9, and R8 were the lightest in colour.

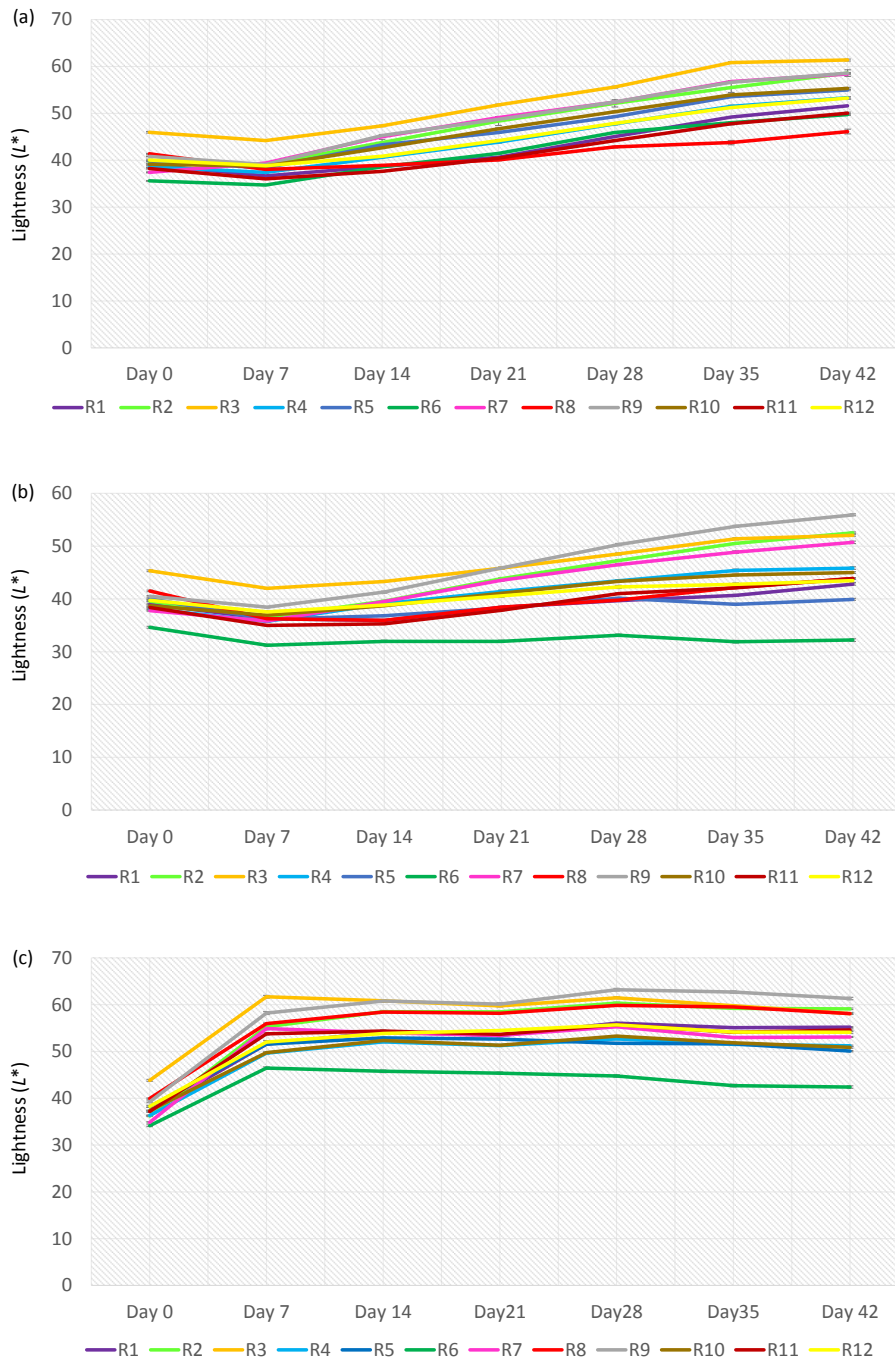


Figure 5.1. Representation of the trend over time for the lightness of chilli powder.

Image analysis was carried out on chilli powder samples under different temperature and light conditions. The lightness (L^*) coordinates over time were displayed at (a) 15°C with 12/12 hr light/ dark cycle, (b) 40°C with a 12/12 hr light dark cycle, and (c) UV (constant) at 30°C, to give a representation of the trends seen in all the conditions analysed. The errors bars displayed represent \pm SE (n=12). Statistical analysis was performed using one-way ANOVA and can be found in supplementary data ($P \leq 0.05$).

5.2.1.2. Red and green (a^*)

The a^* value represented the position in colour between green and red whereby green was represented with negative values and red was represented by positive values. Throughout the experiment the general trend in all conditions was the decrease in red colour. The decline in red colour was inversely proportional to temperature. The higher the temperature, the larger the decrease in red colour over time. The black light condition was similar to 15°C condition, while the UV condition had the most dramatic effect on the red colour of the chilli powder samples. A representation of the trends observed over the course of the experiment were displayed in Figure 5.2.

At temperatures 15, 20 and 30°C the high retention R8 line was consistently and significantly the most red in colour and appears to maintain its red colour over the course of the experiment. This was unique to the R8 line as all other lines experience a decrease. This was also true for the samples stored in the black light condition. As the temperature increases the other two high retention lines, R1 and R11, also become better at retaining their red colour over time with these lines separating away from the other lines analysed (Figure 5.2a). The R7 line, which had a medium colour retention phenotype, undergoes the highest decrease in red colour at 15, 20 and 30°C when compared to all other lines.

At 40°C there was a more dramatic decrease in red colour, especially in the high retention lines (Figure 5.2b). Again, the R7 line, as well as the R6 line, experience significantly the highest decrease in red colour. The most remarkable decrease in red colour was present in the UV condition (Figure 5.2c). Whereby, instead of a steady decrease in red colour as witnessed in all other conditions, the UV condition underwent a steep decrease to saturation point in the first week and then plateaued because its redness could not be reduced further. The R6 line was significantly the most red in colour and the R9 was significantly the least red in colour in the UV condition.

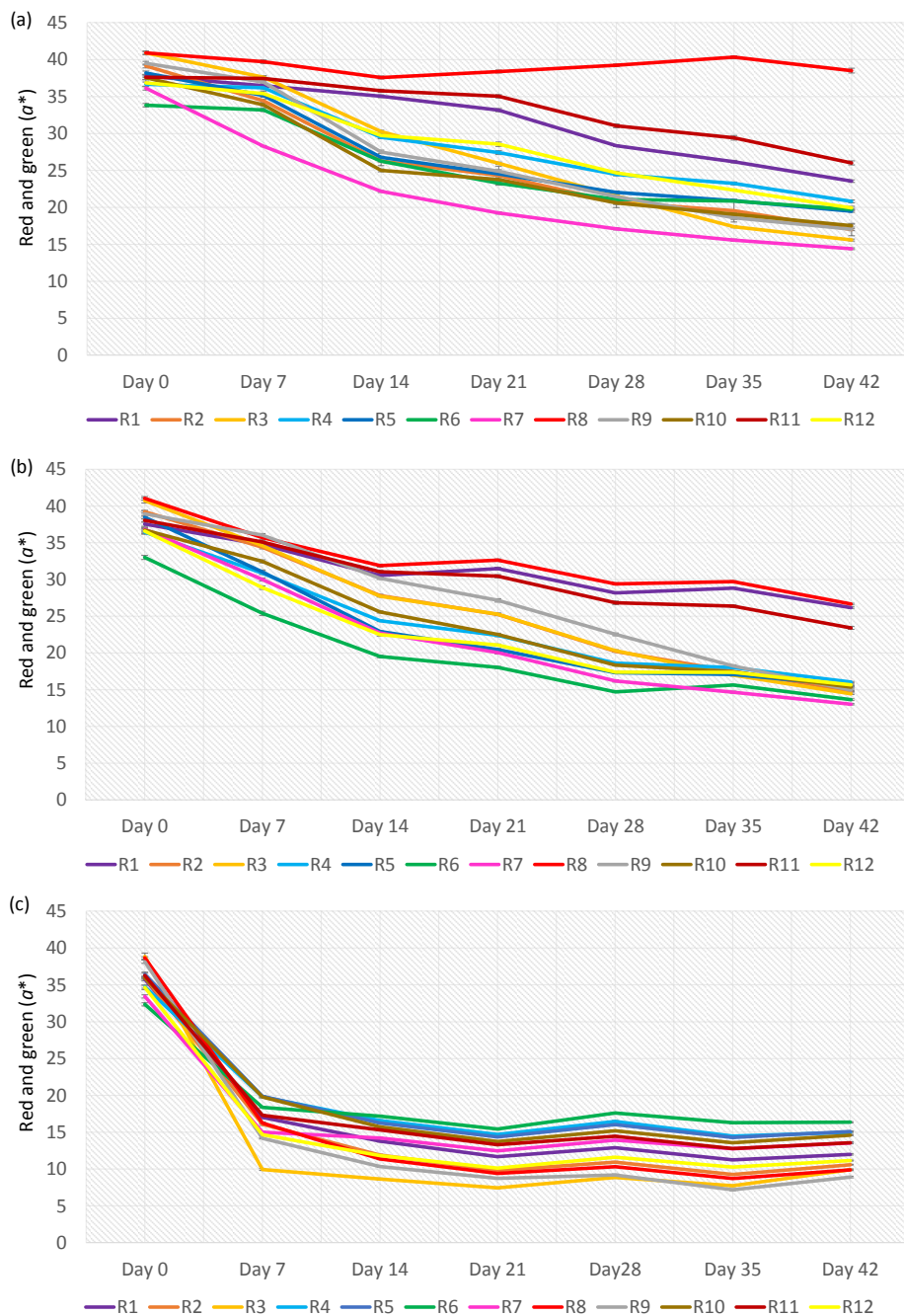


Figure 5.2. Representation of the trend in red colour of chilli powder over time.

Image analysis was carried out on chilli powder samples under different temperature and light conditions. The red colour (a^*) was calculated over time and the trends were displayed at (a) 15°C with a 12/12 hr light dark cycle, (b) 40°C with a 12/12 hr light dark cycle, and (c) UV (constant) at 30°C, to give a representation of the trends seen in all the conditions analysed. The errors bars displayed represent \pm SE (n=12). Statistical analysis was performed using one-way ANOVA and can be found in supplementary ($P \leq 0.05$).

5.2.1.3. Saturation (*chroma*)

The chroma parameter measured the saturation of colour where 0 was completely unsaturated colour, such as grey, white, or black, and 100 was complete colour purity. The general trend of this measurement was initially a decrease in saturation within the first two weeks of the experiment then there was either a plateau or a slight increase in some lines. The black light condition experienced very little variation in saturation over the course of the experiment and the UV condition underwent a decrease in the first week and then plateaued (Figure 5.3).

At the lowest temperature the R8 line had the highest colour saturation when compared to all other lines. This line experienced an initial decrease in colour saturation in the first two weeks and then colour saturation gradually increased for the remaining time eventually finishing at a chroma value similar to day 0 (Figure 5.3a). The R7 line had significantly the lowest colour saturation. There was a similar trend for the 20°C and 30°C conditions. However, at 30°C the other two high intensity lines were showing a similar trend to R8. At the 40°C condition the trend plateaued after an initial decrease, although the high retention lines displayed the most saturated colour. R6 was significantly the most saturated line when compared to all others, excluding R5 (Figure 5.3b). The UV condition displayed a similar trend to the previously described conditions but the lines showed much less variation and the initial decrease occurred in the first week as opposed to the first two weeks (Figure 5.3c). The R6 line was significantly the least saturated when compared to the other lines.

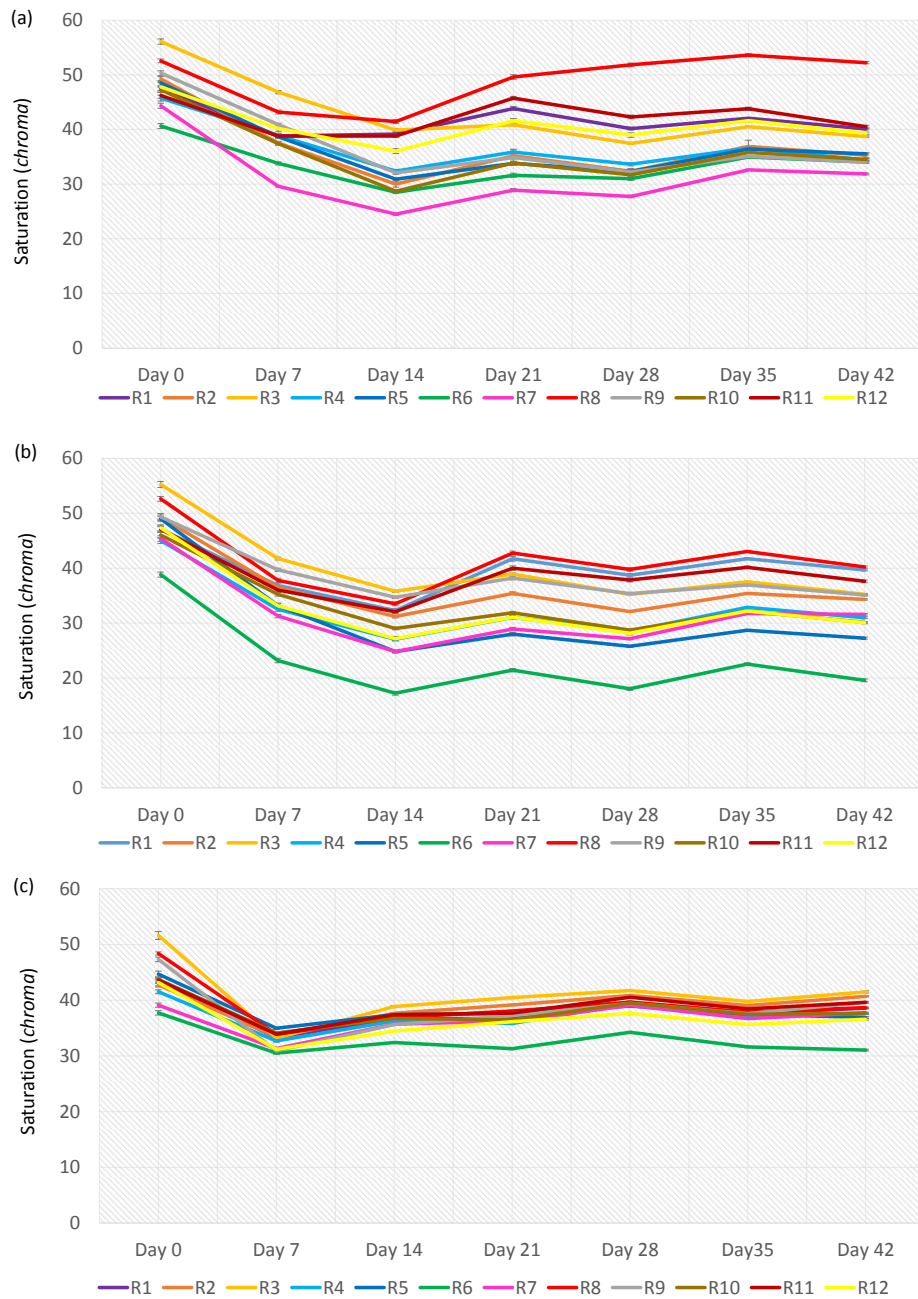


Figure 5.3. Representation of the trend in colour saturation of chilli powder over time.

Image analysis was carried out on chilli powder samples under different temperature and light conditions. The colour saturation (*chroma*) was calculated over time and the trends were displayed at (a) 15°C, (b) 40°C and (c) UV to give a representation of the trends seen in all the conditions analysed. The errors bars displayed represent \pm SE (n=12). Statistical analysis was performed using one-way ANOVA and can be found in supplementary ($P \leq 0.05$).

5.2.1.4. Hue angle (h)

The hue angle represented every possible saturated colour represented on the colour wheel. The values correspond to the 360° of a circle where $0/360^\circ = \text{red}$, $90^\circ = \text{yellow}$, $180^\circ = \text{green}$ and $270^\circ = \text{blue}$. This study focused on the $0\text{-}90^\circ$ portion of the colour wheel between red and yellow. Therefore, the general trend in all conditions experienced was an increase in hue angle throughout the experiment caused by a decrease in red colour. The increase in hue angle was similar in all the temperature conditions and black light but the decrease was more dramatic in the UV condition reaching a hue angle of 80° in some lines.

Samples which were incubated at 15 , 20 , 30 , and 40°C showed similar trends with the three high retention lines displaying the lowest hue values. The R8 line provided the most significant red colouration, when compared to all other lines, except 40°C where it was not found to be significantly redder than R1. R7 had significantly the highest hue angle in all the temperature conditions when compared to all other lines, except R3. The trend was also similar in the black light condition but R3, R7 and R9 were significantly the least red in colour. In the UV condition the line with the lowest hue angle was R6.

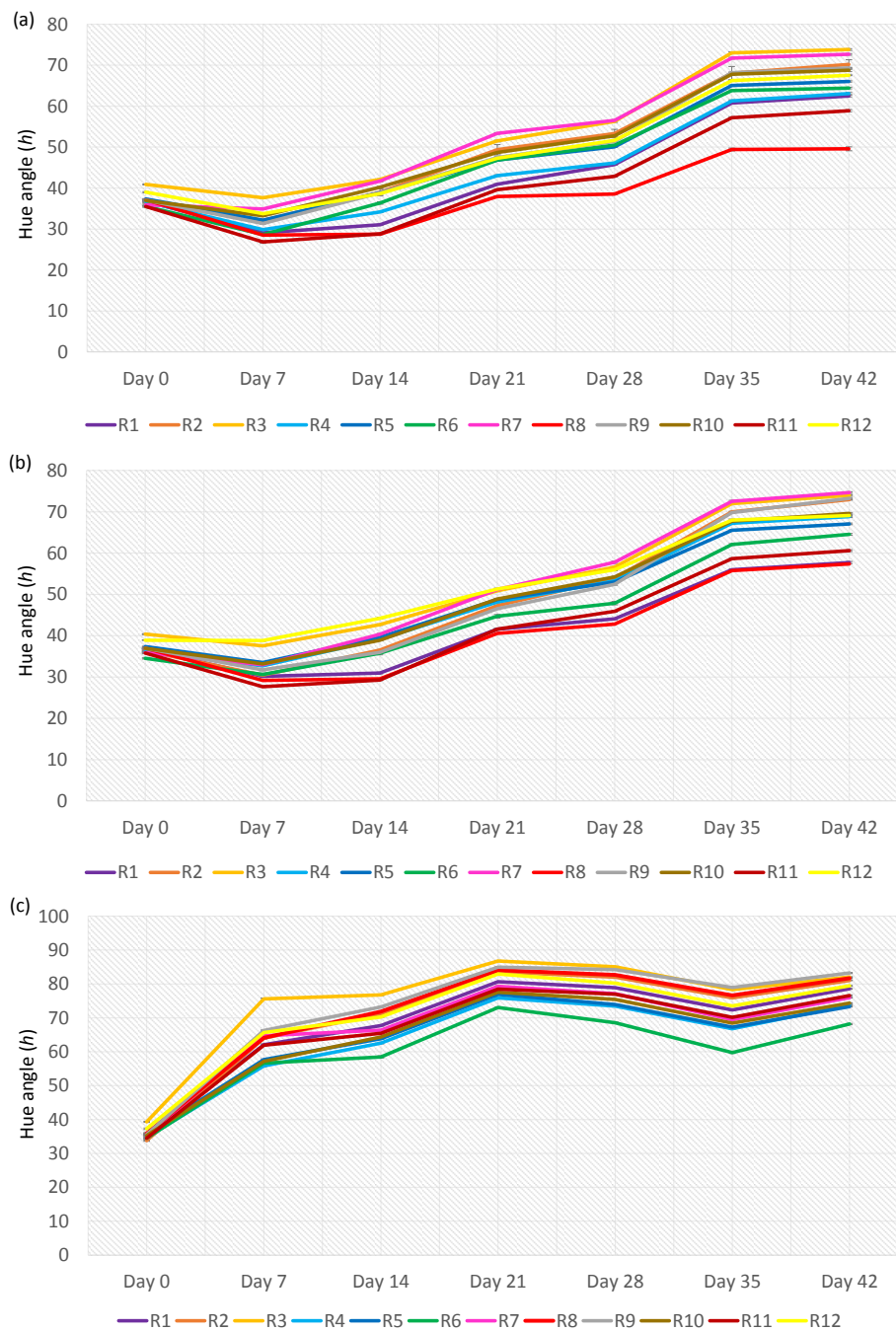


Figure 5.4. Representation of the trend in hue angle of chilli powder over time.

Image analysis was carried out on chilli powder samples under different temperature and light conditions. The hue angle (h) was calculated over time and the trends were displayed at (a) 15°C with a 12/12 hr light dark cycle, (b) 40°C with a 12/12 hr light dark cycle, and (c) UV (constant) at 30°C, to give a representation of the trends seen in all the conditions analysed. The errors bars displayed represent \pm SE (n=12). Statistical analysis was performed using one-way ANOVA and can be found in supplementary ($P \leq 0.05$).

5.2.1.5. Total colour change (ΔE)

The total colour change was calculated based on the CIELAB colour space parameters L^* , a^* , and b^* . The L^* and a^* has been previously discussed and the b^* represents the position in colour between blue and yellow where negative values represent blue and positive values represent yellow. A representation of the total colour changes observed in this study can be found in Figure 5.5.

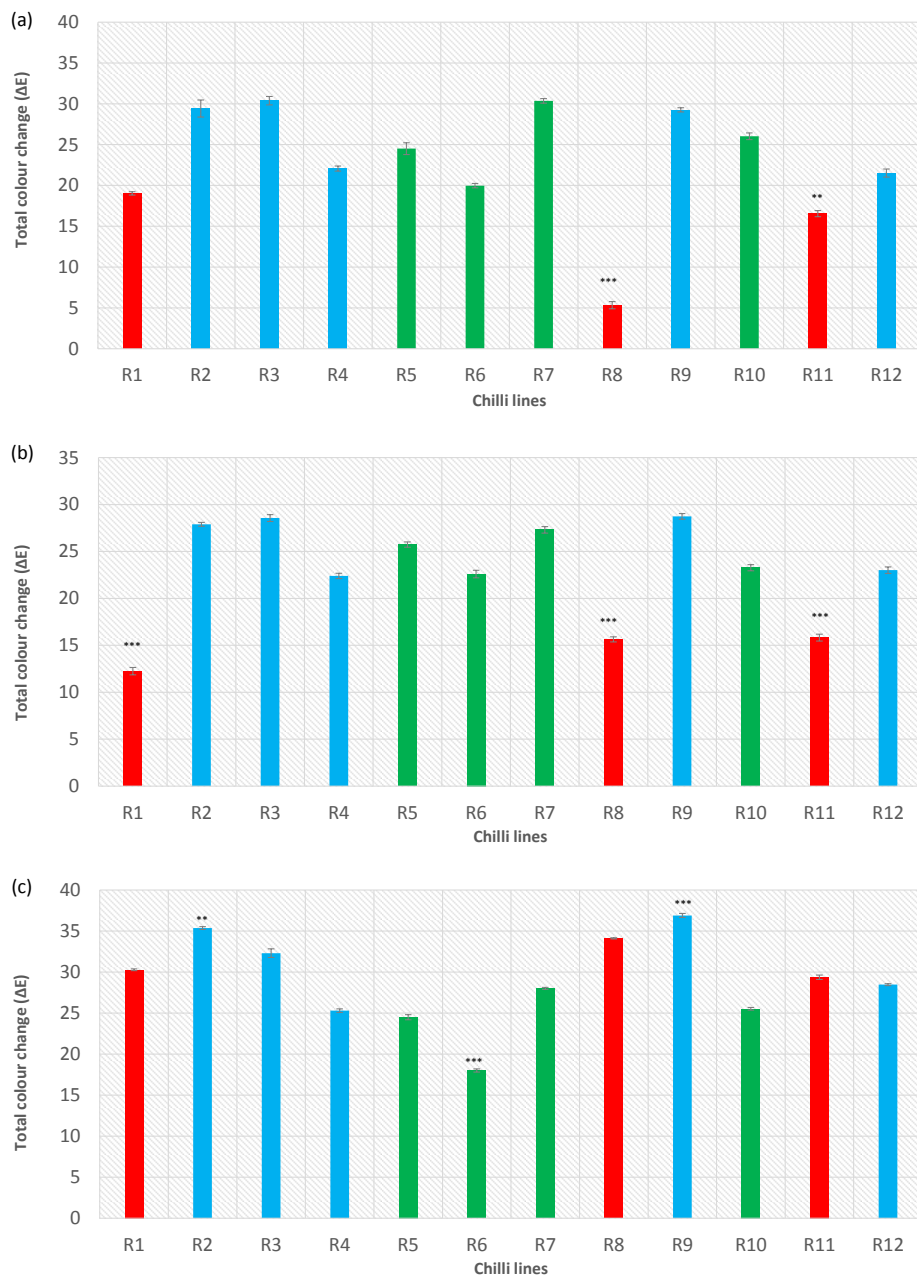


Figure 5.5. A representation of the total colour change in chilli powder over time.

The total colour change (ΔE) was calculated for chilli pepper lines incubated at different temperatures and light conditions. The trends in total colour change at (a) 15°C with a 12/12 hr light dark cycle, (b) 40°C with a 12/12 hr light dark cycle, and (c) UV (constant) at 30°C, conditions were displayed to give a representation for all conditions. Statistical analysis was performed using one-way ANOVA ($P \leq 0.05$). Error bars represent $\pm SE$ ($n=12$). The bar colour represents colour retention phenotype: High (red), medium (green), and low (blue).

The high retention line R8 was found to have significantly the lowest total colour change in conditions of 15, 20, 30, 40°C, and under black light when compared to all other lines analysed. This line was followed by the other high retention phenotype lines, R1 and R11, which also displayed significantly low total colour change, except under black light whereby R6 and R12 displayed the lowest total colour change after R8. In the UV condition R6 was found to have significantly the lowest total colour change.

In terms of high total colour change low retention lines R2, R3 and R9, and medium retention line R7 consistently underwent the largest total colour change compared to the other lines in all temperature conditions and black light, but R7 displayed less total colour change under UV. Interestingly, R8 also displayed high total colour change under UV.

5.2.2. Comparison of colour measurement methods

In an approach to further investigate the colour retention phenotypes of the colour diversity panel, a long storage experiment was set up. This was to study two aspects: firstly, whether the previously allocated colour retention phenotypes were consistent with the results from imaging analysis carried out on whole fruit, and secondly, to test the robustness of the image analysis technique by comparing with the results obtained from pigment analysis and ASTA. This study involved the storage of whole, dry chilli peppers over a 9 month period at 10°C in the dark. These conditions were similar to how they are stored during monsoon season in India.

5.2.2.1. Image analysis on whole chilli pepper fruit

Image analysis was carried out on the material stored in the long storage conditions described above. This was carried out at the beginning of the experiment and then every three months

throughout the experiment. The total colour change in each line over the 9 months was calculated and displayed in Figure 5.6. The results obtained show that statistically the low intensity, low retention phenotype line R3 displayed the highest colour change when compared to all over lines. Therefore, this line experienced the most colour loss when compared to the others. All the remaining lines analysed were not statistically different from each other.

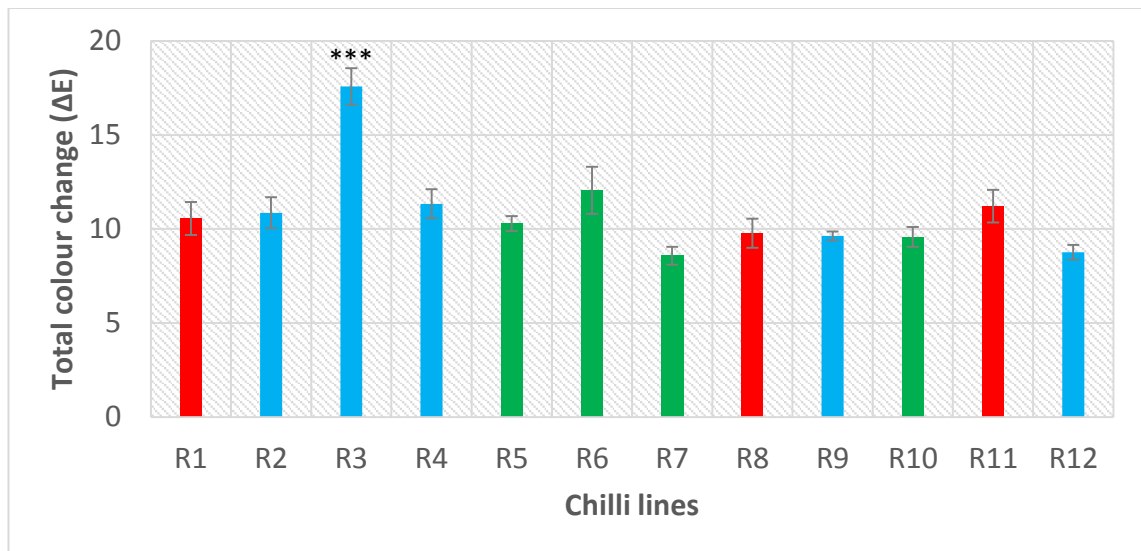


Figure 5.6. Total colour change (ΔE) for chilli pepper lines stored for 9 months.

Image analysis was carried out on a colour diversity panel which was stored for 9 months at 10°C in the dark. The total colour change (ΔE) was calculated to characterise colour retention phenotype. Error bars represent $\pm SE$ ($n=4$). The statistical analysis performed was one-way ANOVA ($P \leq 0.05$). The bar colour represents colour retention phenotype: High (red), medium (green) and low (blue).

5.2.2.2. Pigment analysis on whole chilli pepper fruit

As previously mentioned in the last section (5.2.2.1), dry chilli peppers were stored for 9 months and image analysis was carried out every 3 months. Once image analysis had been carried out at each time point the chillies were frozen and stored to allow pigment analysis to be carried out. The material was subjected to HPLC-PDA.

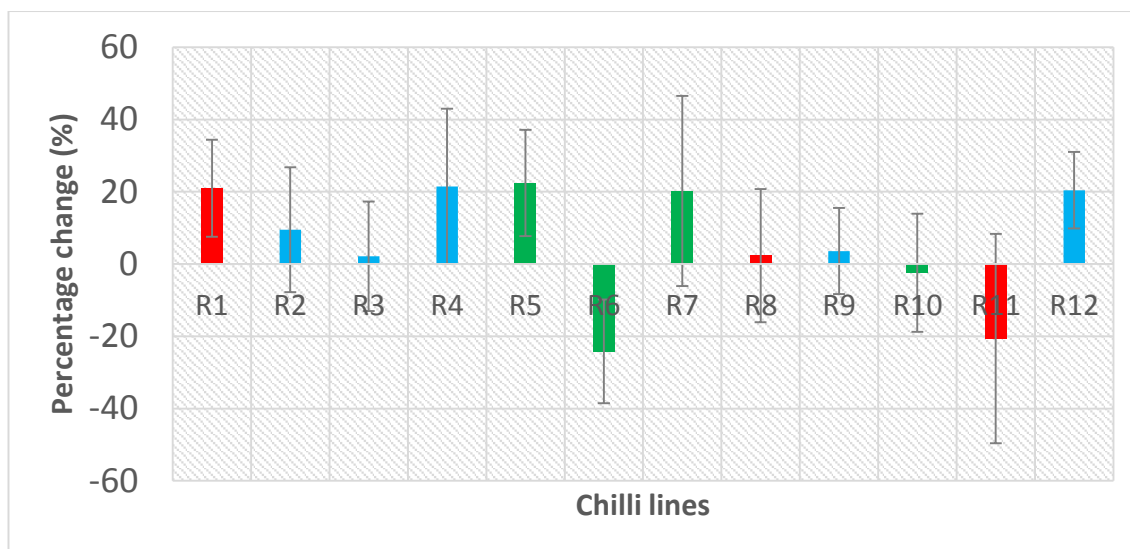


Figure 5.7. Percentage change of total capsanthin over storage.

The colour diversity panel were stored for 9 months in the dark at 10°C to simulate storage conditions in India. Every three months a sample was taken and subjected to HPLC. The error bars represent \pm SE (n=4). The bar colour represents colour retention phenotype: High (red), medium (green) and low (blue).

The total capsanthin in each of the lines was calculated and then the percentage change of total capsanthin was determined for the start to the end of the storage period (Figure 5.7). The results from this experiment were highly variable. They suggest that R1, R4, R5, R7, and R12 experienced the highest loss in capsanthin, while R2, R3, R8, and R9 experienced very low losses of capsanthin. The R6 and R11 lines even increased in capsanthin throughout the experiment. Due to the variability of these samples colour retention phenotypes were unable to be characterised.

5.2.2.3. ASTA colour measurement

In the spice industry a standardised method of evaluating colour measured the extractable colour. The American Spice Trade Association (ASTA) have standardised an extractable method to analyse total pigment content allowing the colour of chilli powder to be compared across countries. This was a spectrophotometer based method. The higher the ASTA value, the more red the chilli powder is. ASTA analysis was carried out on the samples which were imaged at

time points throughout the long storage experiment and from the same pool as the samples described in 5.2.2.2.

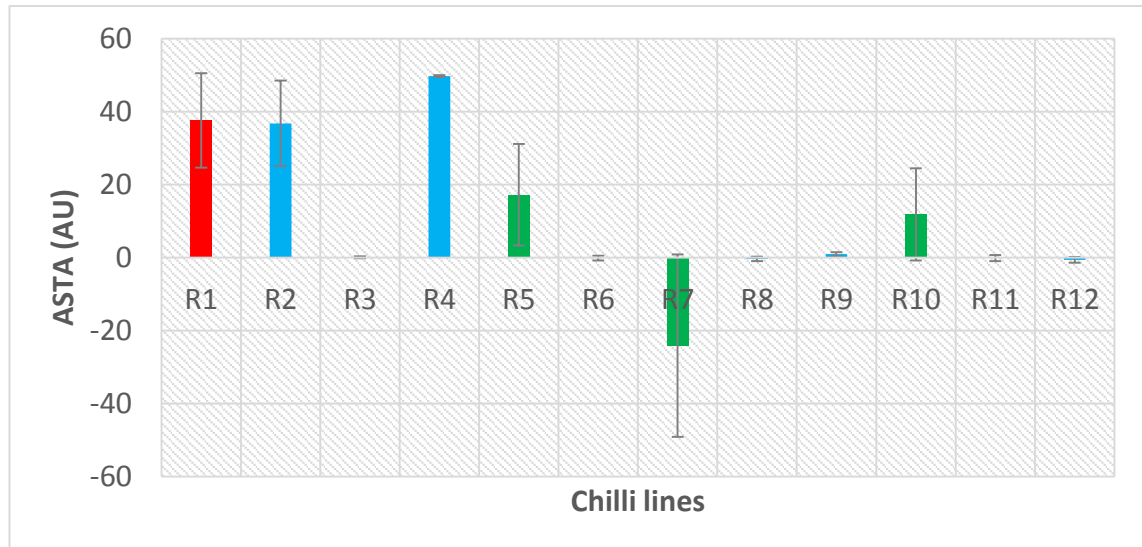


Figure 5.8. Percentage change of ASTA colour during storage.

ASTA measurements were taken at the beginning and end of a 9 month storage experiment and the percentage change was calculated. Error bars represent \pm SE (n=4). The bar colour represents colour retention phenotype: High (red), medium (green) and low (blue).

The results from the ASTA measurements over storage were variable and were not consistent with the previously allocated colour retention phenotypes. The R1 line was showing a high colour loss when compared the other lines analysed regardless of its high retention phenotype. However, the other two high retention lines were showing very low colour loss when compared to the other lines which was analogous to their phenotypes. The two low retention lines, R2 and R4, seem to be displaying the high colour loss when compared to the other lines which was consistent with their colour retention phenotypes; however, other low retention lines (R3, R9 and R12) showed no change. The medium retention line R7 experienced an increase in colour throughout the course of the experiment.

5.2.3. Volatile analysis in fresh and dried chilli pepper fruit

Volatile analysis was carried out on fresh and dry samples of chilli pepper to ascertain information about the degradation processes taking place. The fresh samples were made into a juice and flash frozen. The dry samples were dried for 3 weeks, in conditions simulating air-drying under sunlight in India, then rehydrated and made into a juice and flash frozen. The analysis of volatiles present in the fresh and dry samples gave an insight into the types and levels of degradation taking place within high and low retention lines.

5.2.3.1. Analysis of volatiles produced in fresh and dry chilli pepper

The volatile analysis identified 28 compounds in fresh and dry fruit. The following chemical classes were identified in fresh and dry fruit: alcohols (13%, 14%), aldehydes (32%, 24%), alkane (4% for both), alkene (1% for both), ester (15%, 9%), ketone (20%, 28%), monoterpene (11%, 17%), pyrazine (1%, 2%), and sesquiterpene (2% for both) (Figure 5.9).

In fresh chilli pepper the most predominant compounds found in the ripe fruit were 2-hexenal, β -ionone epoxide, dihydroactinidiolide, guaiacol, hexanal, methyl salicylate, trans-2-nonenal, and trans-2-octenal in most lines. The dry samples contained β -ionone epoxide and dihydroactinidiolide as the most prevalent compounds present.

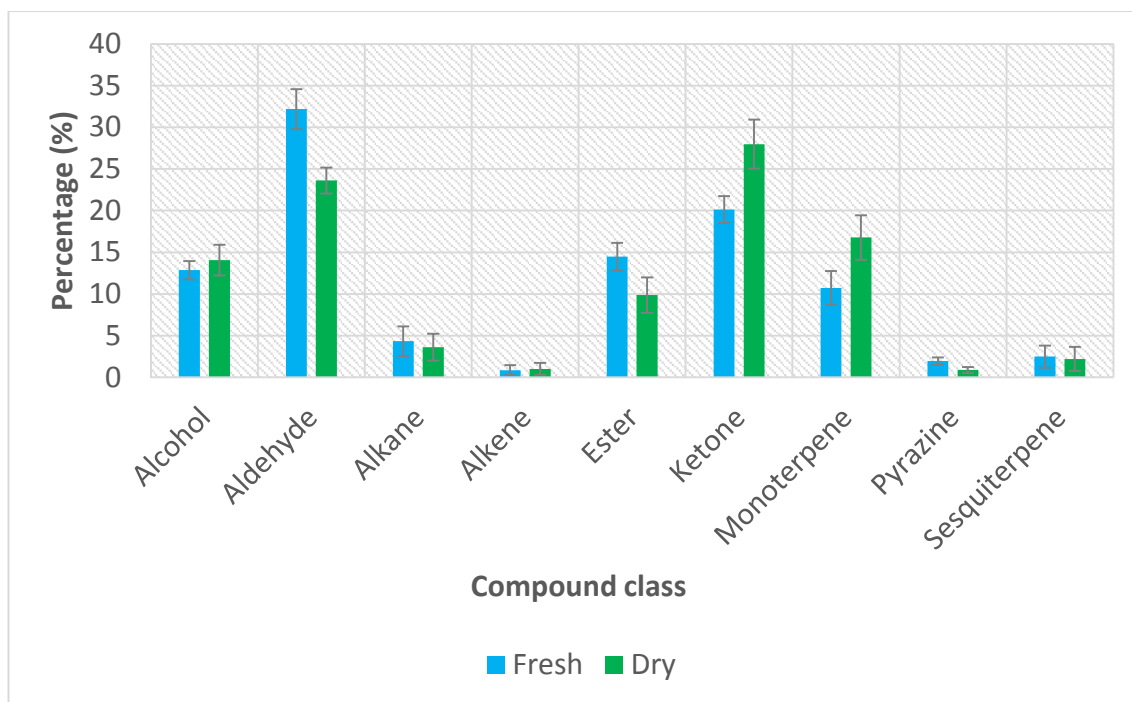


Figure 5.9. Representation of the change in volatile compositions from fresh to dry.

The Percentage of each compound class was calculated for each line compared to the total amount of volatiles. The average percentage for each compound class over all the lines was determined and shown to display the changes in volatile composition in fresh and dry fruit. Error bars represent \pm SE (n=6).

The volatile compounds were compared using a PCA plot. There was a distinct separation between the fresh and the dry samples exhibited on the PCA score plot (Figure 5.10a). The Fresh samples were situated mainly in the top right quadrant compared to the dry samples which were located in the bottom left quadrant. On investigation of the PCA loadings there was a clear association of lipid degradation products driving the fresh separation, such as 2,6-nonadienal, 2-hexenal, hexanal, trans-2-octenal and trans-2-nonenal. Carotenoid degradation products appear to be driving the dry separation including compounds, such as geranyl actone, β -ionone epoxide, 6-methyl-5-hepten-2-one and dihydroactinidiolide, as well as linalool. The dry, high retention lines, R1 and R8, cluster to the centre and the right panel of the PCA plot closer to the fresh samples than to the dry, low retention lines. The R12 line was an outlier in terms of the other lines analysed and there was little difference between the dry and fresh samples in this line. The R12 line separated based on the β -ionone compound (Figure 5.10). This line had dramatically high levels of 2-methylpentyl hexanoate, 2-methyltetradecane, 4-oxononanal,

hexyl 2-methylbutyrate, hexyl 3-methyl butyrate, and isocaryophyllene compared to the other lines analysed. There were similar levels of these compounds found in fresh and dry samples and they displayed considerable variation reducing the validity of this sample.

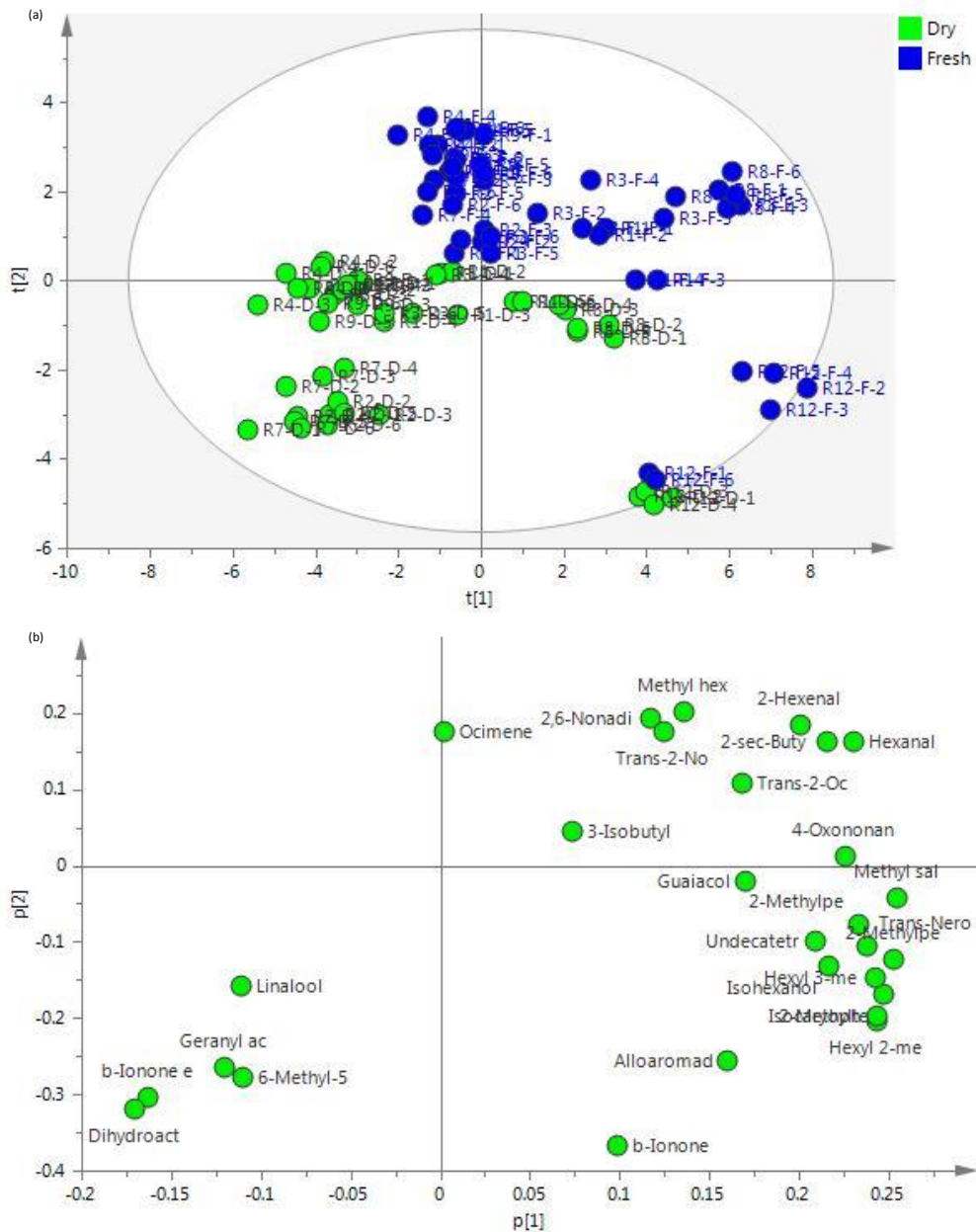


Figure 5.10. PCA of volatile compounds detected in fresh and dry chilli pepper.

Volatile analysis was carried out on fresh and dry chilli peppers which had differing colour intensity and retention phenotypes. (a) PCA scores and the (b) PCA loadings. The values in PCA were log transformed. Key in (a): Fresh fruit, blue and dry fruit, green. Key in (b) Methyl hex, Methyl hexanoate; 2,6-Nonadi, 2,6-Nonadienal; 2-sec-Buty, 2-sec-Butylcyclohexanone; Trans-2-

No, Trans-2-Nonenal; Trans-2-Oc, Trans-2-Octenal; 3-Isobutyl, 3-Isobutyl-2-methoxypyrazine; 4-Oxononan, 4-Oxononanal; Methyl Sal, Methyl salicylate; 2-Methylpe, 2-Methylpentadecane and 2-Methylpentyl hexanoate; Trans-Nero, Trans-Nerolidol; Undecatetr, Undecatetraene; Isocaryoph, Isocaryophyllene; Hexyl 2-me, Hexyl 2-methylbutyrate; Hexyl 3-me, Hexyl 3-methylbutyrate; Alloaromad, Alloaromadendrene; Geranyl ac, Geranyl acetone; b-Ionone e, b-Ionone epoxide; 6-Methyl-5, 6-Methyl-5-hepten-2-one; Dihydroact, Dihydroactinidiolide.

The volatile compounds identified were visualised using a heat map display in order to compare the changes in metabolites between fresh and dry samples (Figure 5.11).

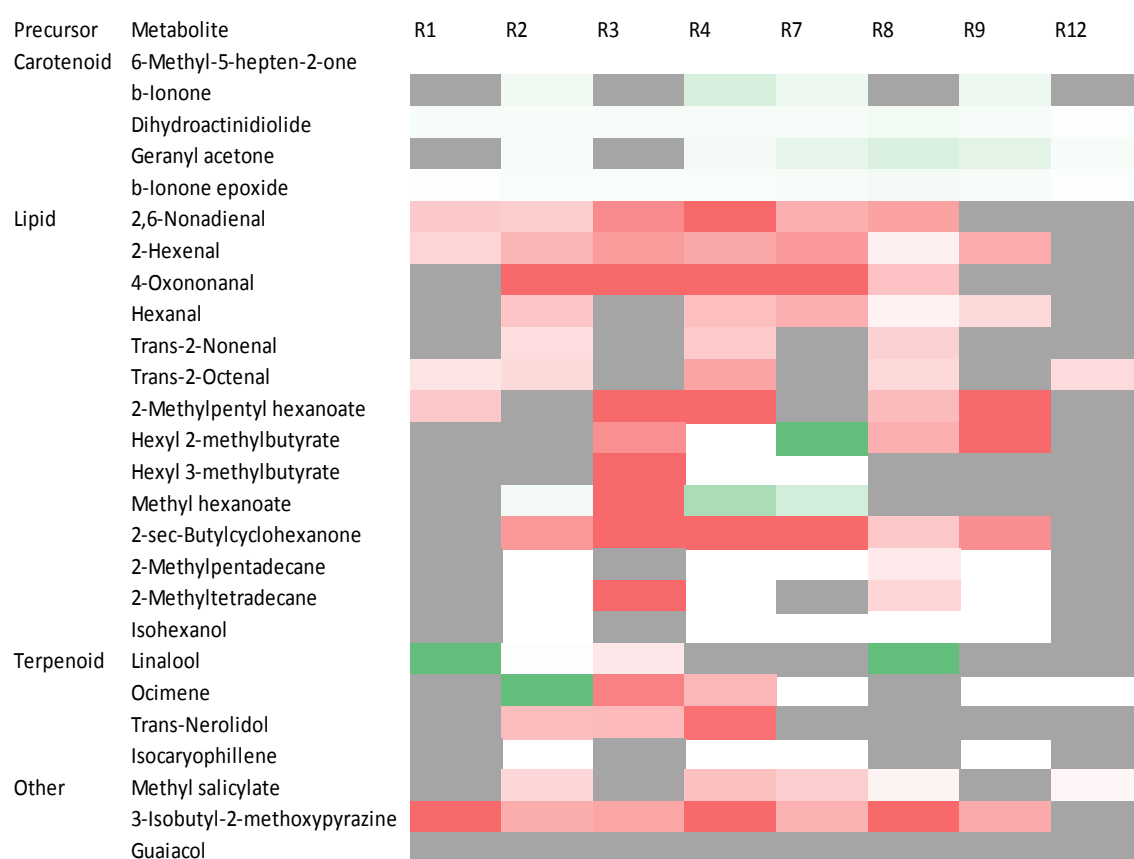


Figure 5.11 Heat map displaying the change in volatile compounds in dry fruit when compared to fresh fruit.

Volatile analysis was carried out on a colour diversity panel to examine the differences in volatile composition between fresh and dry fruit. The changes in compounds displayed were compared to fresh fruit. The volatiles compounds identified were grouped based the chemical class the volatile was derived from: carotenoid, lipid, terpenoid or other. Results were the means for 6

biological replicates and significant differences were calculated using one-way ANOVA ($P \leq 0.05$). Increases in metabolites in dry fruit are represented by green, decreases by red, no change by grey and not present by white.

The heat map reflected the findings from the PCA plot. The carotenoid associated degradation products were found to be increased as the fruit transitions from fresh to dry. Subsequently, the lipid derived volatile compounds were found to be decreased in the majority of lines analysed. 2,6-nonadienal and 2-hexenal were decreased in the majority of the lines analysed, except R9 and R12, and R12, respectively. The high retention lines, R1 and R8, showed a less dramatic decrease in lipid derived volatiles when compared to the other lines analysed (excluding R12). Linalool was found to be increased in the two high retention lines, R1 and R8, but decreased in R3 the low retention line.

5.2.3.2. Analysis of volatile compounds present in fresh fruit

The volatile compounds were examined in each condition separately in an effort to determine if there were any specific volatile compounds exclusively associated with colour intensity and retention phenotype.

The PCA plots displaying the variance in volatile compounds for colour intensity and colour retention phenotypes in fresh fruit were compared (Figure 5.12a-b). The high intensity lines (excluding R1) showed separation to the top left quadrant based on the colour intensity phenotypes. This separation was caused by carotenoid derived volatiles. The medium intensity lines were clustered into two separate locations on the bottom left and right hand side indicating significant differences in volatile compositions within the medium retention lines (Figure 5.12a). The colour retention phenotypes show much clearer separation between high and low retention lines. The low retention lines were located mainly on the left hand side of the plot (excluding R12) and the high retention lines were found in the bottom left quadrant (Figure 5.12b). The high colour retention phenotypes separated based on lipid derived degradation products, such as undecatetraene, 2-methylpentadecane, 2-methylpentyl hexanoate, 2-methyltetradecane, hexyl 2-methylbutyrate and hexyl 3-methylbutyrate. Mainly derived from fatty acid esters and hydrocarbons.

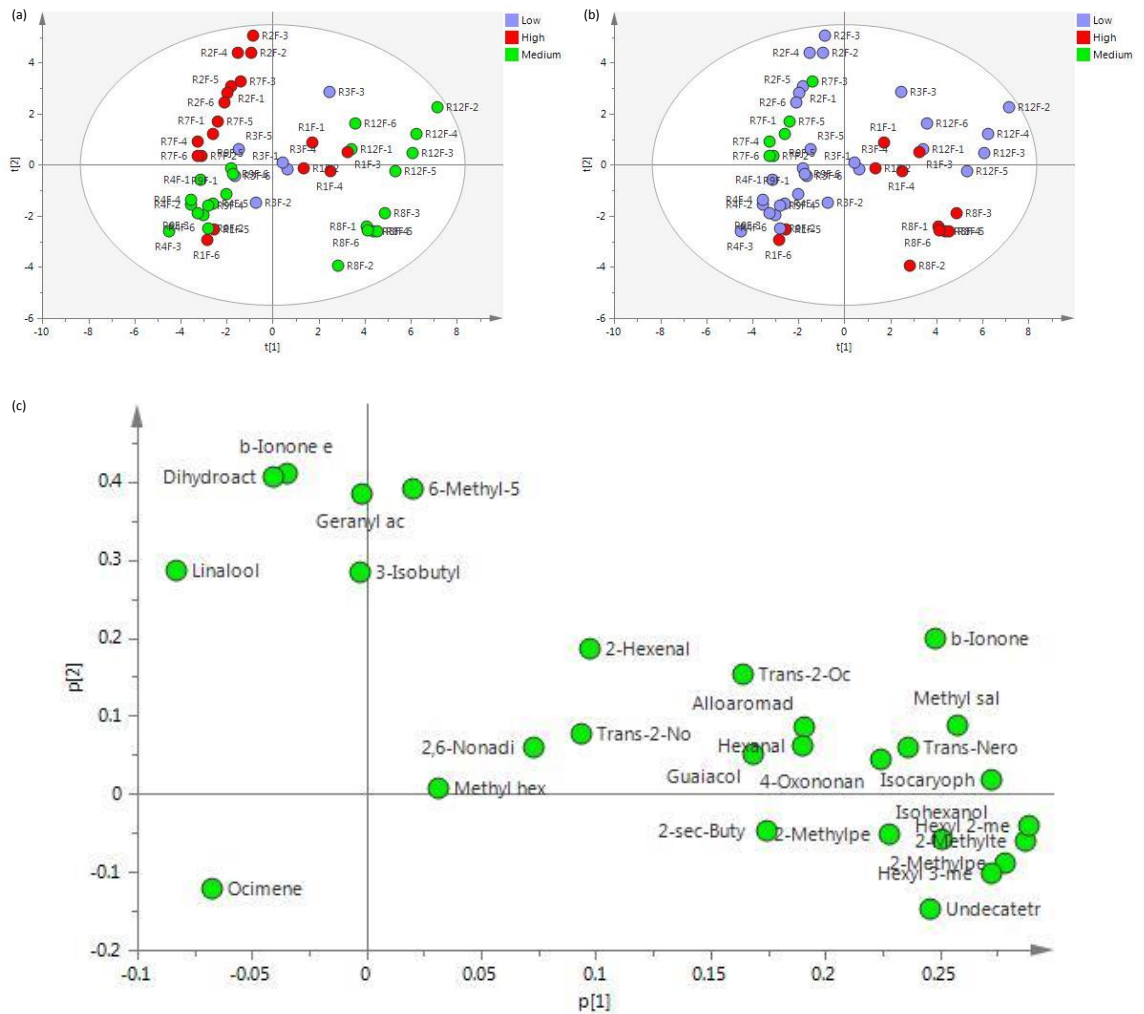


Figure 5.12. PCA of volatile compounds identified in fresh ripe fruit.

Volatile analysis was carried out on fresh samples from a colour diversity panel. The top panel displays PCA scores colour coded for (a) colour intensity and (b) colour retention. (c) Displays the PCA loadings. Key in (a) and (b) low (blue), medium (green), and high (red). Key in (c) Methyl hex, Methyl hexanoate; 2,6-Nonadi, 2,6-Nonadienal; 2-sec-Buty, 2-sec-Butylcyclohexanone; Trans-2-No, Trans-2-Nonenal; Trans-2-Oc, Trans-2-Octenal; 3-Isobutyl, 3-Isobutyl-2-methoxypyrazine; 4-Oxononan, 4-Oxononanal; Methyl Sal, Methyl salicylate; 2-Methylpe, 2-Methylpentadecane and 2-Methylpentyl hexanoate; Trans-Nero, Trans-Nerolidol; Undecatetr, Undecatetraene; Isocaryoph, Isocaryophillene; Hexyl 2-me, Hexyl 2-methylbutyrate; Hexyl 3-me, Hexyl 3-methylbutyrate; Alloaromad, Alloaromadendrene; Geranyl ac, Geranyl acetone; b-Ionone e, b-Ionone epoxide; 6-Methyl-5, 6-Methyl-5-hepten-2-one; Dihydroact, Dihydroactinidiolide.

Colour retention

Orthogonal projections of latent structures with discriminant analysis (OPLS-DA) was carried out as this type of prediction modelling filters out variation that was not directly related to the response. This increased the interpretability of the model. This method also contained improved detection limits for outliers (Sadeghi-Bazargani et al., 2010). Thus, the method considers the outlier R12 and only compares variation based on colour retention phenotypes as opposed to other factors which were not directly related. The medium retention line R7 was also removed from the data set due to the discrepancy over the true retention phenotype it had. This was based on previous image analysis findings on chilli powder in section 5.2.1. Therefore just the high and low phenotypes were analysed.

The OPLS-DA plot revealed that the volatile compositions of volatiles identified in high and low retention lines were significantly different. Figure 5.13a shows the low retention lines clustering on the left hand side of the ellipse and the high retention lines clustering on the right hand side. The loadings showed, again, that the key volatiles driving the low retention lines were linalool, β -ionone epoxide, dihydroactinidiolide and 6-methyl-5-hepten-2-one. The compounds separating the high retention lines were undecatetraene, 2-methylpentadecane, 2-methylpentyl hexanoate, 2-methyltetradecane, hexyl 2-methylbutyrate and hexyl 3-methylbutyrate, as mentioned in the PCA plots as well as, 2,6-nonadienal and trans-2-nonenal.

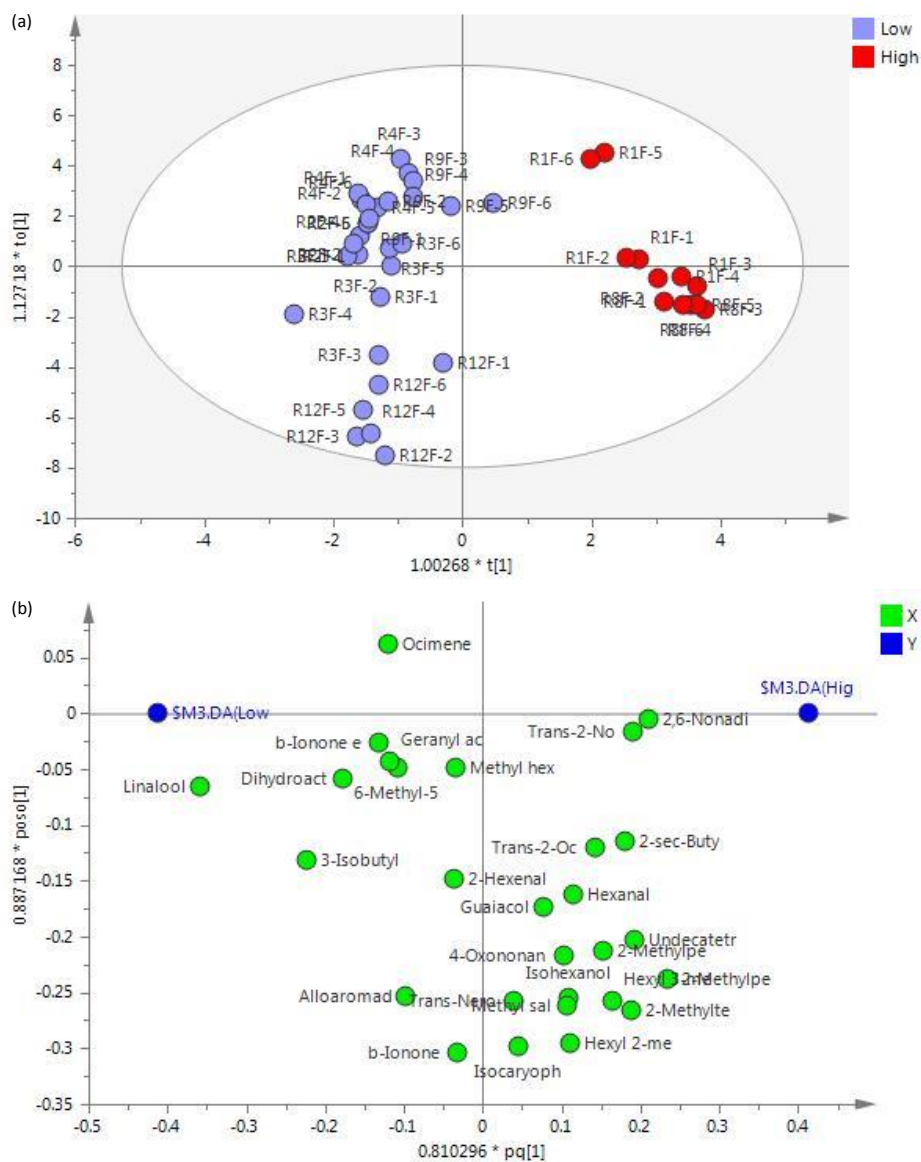


Figure 5.13. OPLS-DA of volatile compounds identified in fresh chilli pepper in high and low retention lines.

OPLS-DA was performed in order to create a clearer picture of the relationship between volatile compounds and colour retention phenotype. (a) scores and (b) loading. Key in (a) low (blue) and high (red). Key in (b) Methyl hex, Methyl hexanoate; 2,6-Nonadi, 2,6-Nonadienal; 2-sec-Buty, 2-sec-Butylcyclohexanone; Trans-2-No, Trans-2-Nonenal; Trans-2-Oc, Trans-2-Octenal; 3-Isobutyl, 3-Isobutyl-2-methoxypyrazine; 4-Oxononan, 4-Oxononanal; Methyl Sal, Methyl salicylate; 2-Methylpe, 2-Methylpentadecane and 2-Methylpentyl hexanoate; Trans-Nero, Trans-Nerolidol; Undecatetr, Undecatetraene; Isocaryoph, Isocaryophyllene; Hexyl 2-me, Hexyl 2-methylbutyrate; Hexyl 3-me, Hexyl 3-methylbutyrate; Alloaromad, Alloaromadendrene; Geranyl

ac, Geranyl acetone; b-Ionone e, b-Ionone epoxide; 6-Methyl-5, 6-Methyl-5-hepten-2-one; Dihydroact, Dihydroactinidiolide.

In order to understand how these differences in metabolites were effecting colour retention phenotypes in fresh fruit a heat map was used to visualise the differences when compared to R8, the highest retention line (Figure 5.14).

The heat map showed that there were lower amounts of lipid derived volatiles in the majority of other lines when compared to R8. The R1 line, also high retention, displayed that compared to R8 it still had lower levels but compared to the other lines the decreases were not as dramatic. Therefore, the high retention lines displayed higher amounts of 2-methylpentyl hexanoate, hexyl 2-methylbutyrate, hexyl 3-methylbutyrate, 2-methylpentadecane, 2-methyltetradecane, and isohexanol when compared to the low and medium retention lines. They also showed lower amounts of linalool compared to the other lines and R8 displayed lower levels of β -ionone epoxide and dihydroactinidiolide but this was not a characteristic of R1.

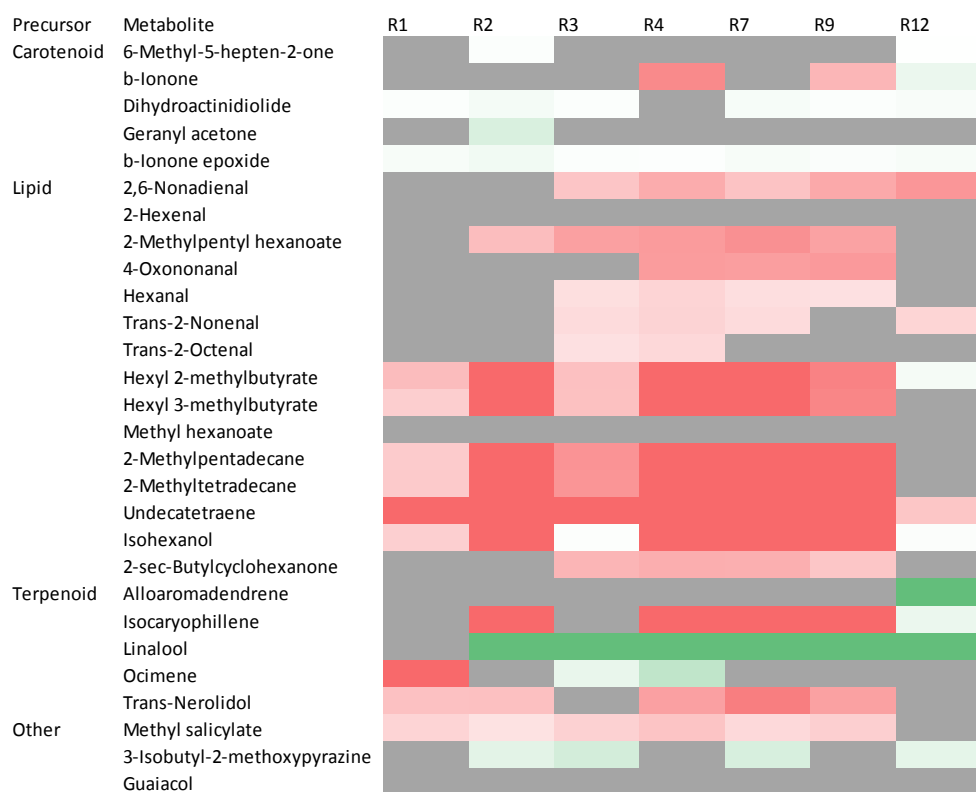


Figure 5.14. Heat map visualising the differences in volatile compounds between high and low retention lines in fresh fruit.

The heat map shows the significant differences in volatile compounds between, R8 the high retention line, and all other lines. Statistical analysis was performed using one-way ANOVA ($P \leq 0.05$). Differences were indicated by increase (green), decrease (red) and no change (grey).

Colour intensity

OPLS-DA was carried out for fresh samples to examine what metabolites were related to the colour intensity phenotype. The high and the low intensity lines were examined so the metabolites which were indicative of high or low colour intensity phenotype could be identified.

The OPLS-DA plot visualised an excellent separation of metabolites between high and low intensity lines. The high intensity lines, R2 and R7, separated based on carotenoid derived volatiles, such as β -ionone epoxide, dihydroactinidiolide, 6-methyl-5-hepten-2-one, geranyl acetone, as well as, 2-hexenal. The R1 line separated based on methyl salicylate, tran-2-octenal, trans-2-nonenal, hexanal, 2,6-nonadienal, 2-sec-butylcyclohexanone, and 2-methylpentyl hexanoate. The low intensity line separated based on methyl hexanoate, ocimene, trans-nerolidol, 3-isobutyl-2-methoxypyrazine, and hexyl 2-methylbutyrate.

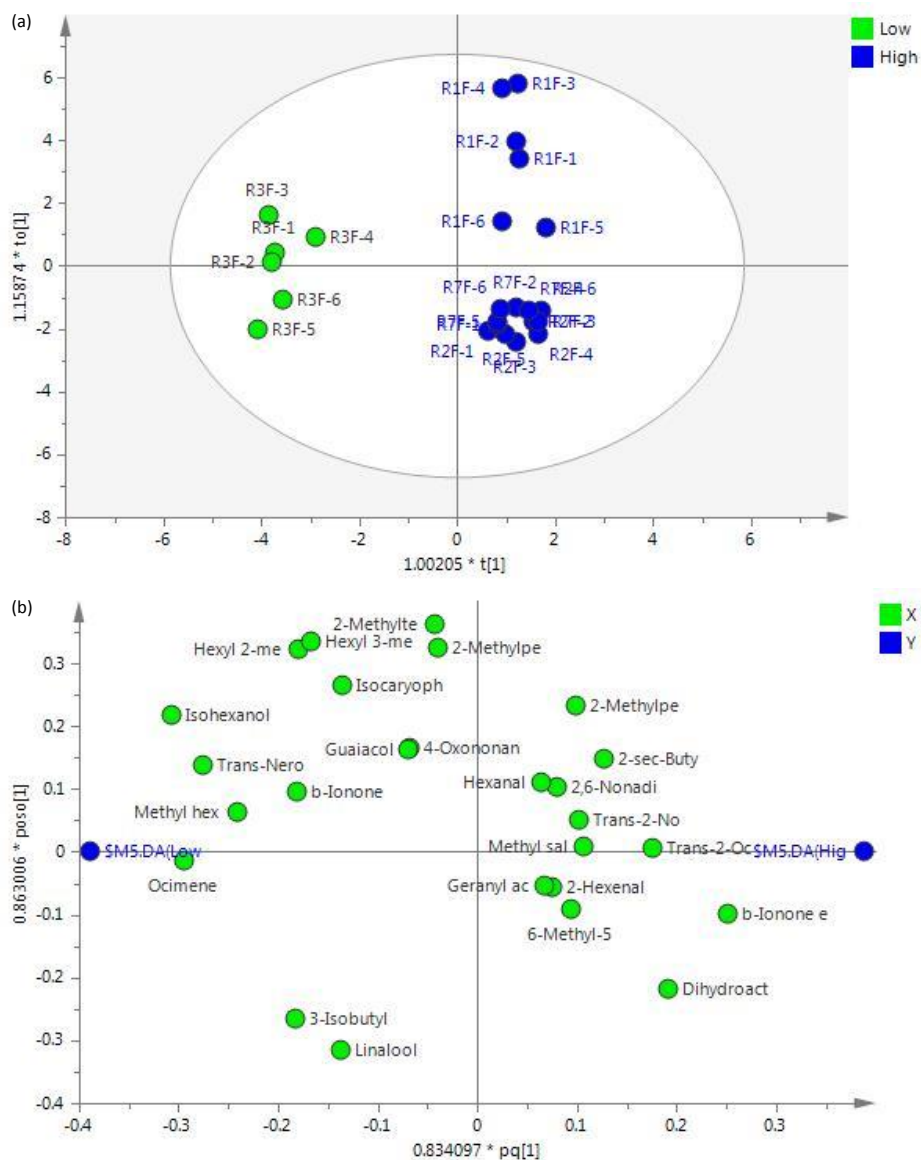


Figure 5.15. OPLS-DA on volatile compounds identified in the fresh fruit of high and low intensity lines.

OPLS-DA was performed to create a clearer picture of the volatile compounds related to colour intensity phenotype in ripe fruit. (a) scores and (b) loadings. Key in (a) low (green) and high (red). Key in (b) Methyl hex, Methyl hexanoate; 2,6-Nonadi, 2,6-Nonadienal; 2-sec-Buty, 2-sec-Butylcyclohexanone; Trans-2-No, Trans-2-Nonenal; Trans-2-Oc, Trans-2-Octenal; 3-Isobutyl, 3-Isobutyl-2-methoxypyrazine; 4-Oxononan, 4-Oxononanal; Methyl Sal, Methyl salicylate; 2-Methylpe, 2-Methylpentadecane and 2-Methylpentyl hexanoate; Trans-Nero, Trans-Nerolidol; Undecatetr, Undecatetraene; Isocaryoph, Isocaryophillene; Hexyl 2-me, Hexyl 2-methylbutyrate; Hexyl 3-me, Hexyl 3-methylbutyrate; Alloaromad, Alloaromadendrene; Geranyl

ac, Geranyl acetone; b-Ionone e, b-Ionone epoxide; 6-Methyl-5, 6-Methyl-5-hepten-2-one; Dihydroact, Dihydroactinidiolide.

5.2.3.3. Analysis of volatile compounds in dry fruit

The volatile compounds identified in dry fruit were analysed to examine any variations between lines differing in colour intensity or retention phenotype.

The colour intensity phenotypes of the lines analysed were displayed on the PCA plot of dry volatile compounds (Figure 5.16). The separation was similar to fresh fruit where two of the high intensity lines, R2 and R7, clustered in the top left quadrant but the other high intensity line R1 clustered on the right hand side. The top right quadrant separation was driven by carotenoid derived volatiles. The medium intensity lines were also separated in two groups, with R4 and R9 on the left and R8 and R12 on the right. The separation of volatile compounds correlated more strongly with colour retention phenotype where the low and medium retention phenotypes lines clustered over the left hand side of the plot (excluding R12), and the high retention lines clustered in the bottom right quadrant. The volatile compounds driving the separation of the high retention lines were undecatetraene and isohexanol, which was also seen in fresh fruit, and in contrast methyl hexanoate, which was not seen in the fresh fruit. Although, it was difficult to determine which compounds were exerting the most influence on colour retention because of the R12 outlier.

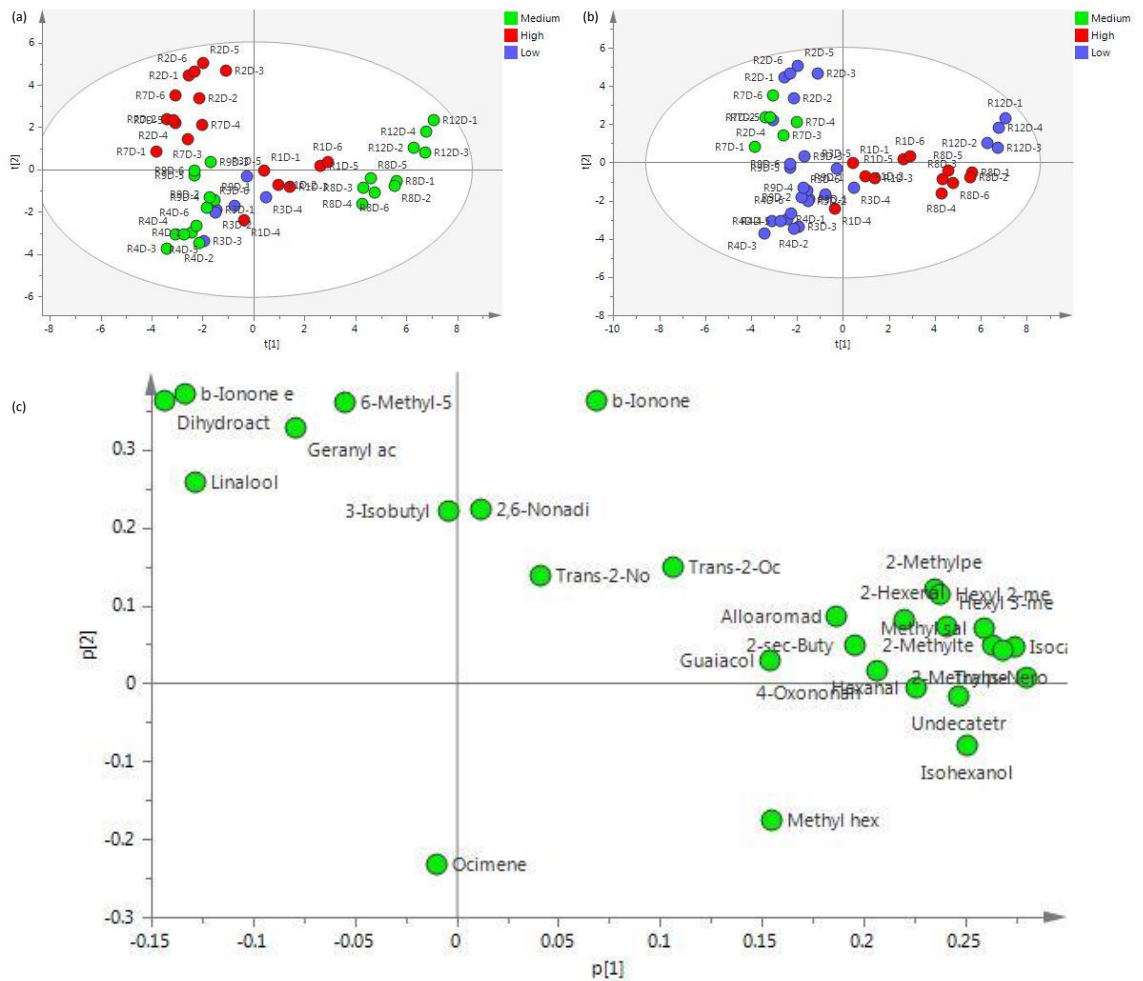


Figure 5.16. PCA of volatile compounds identified in dry fruit.

Volatile analysis was carried out on dry samples from a colour diversity panel. The top panel displays PCA scores colour coded for (a) colour intensity and (b) colour retention. (c) Displays the PCA loadings. Key in (a) and (b) low (blue), medium (green) and high (red). Key in (c) Methyl hex, Methyl hexanoate; 2,6-Nonadi, 2,6-Nonadienal; 2-sec-Buty, 2-sec-Butylcyclohexanone; Trans-2-No, Trans-2-Nonenal; Trans-2-Oc, Trans-2-Octenal; 3-Isobutyl, 3-Isobutyl-2-methoxypyrazine; 4-Oxononan, 4-Oxononanal; Methyl Sal, Methyl salicylate; 2-Methylpe, 2-Methylpentadecane and 2-Methylpentyl hexanoate; Trans-Nero, Trans-Nerolidol; Undecatetr, Undecatetraene; Isocaryoph, Isocaryophyllene; Hexyl 2-me, Hexyl 2-methylbutyrate; Hexyl 3-me, Hexyl 3-methylbutyrate; Alloaromad, Alloaromadendrene; Geranyl ac, Geranyl acetone; b-Ionone e, b-Ionone epoxide; 6-Methyl-5, 6-Methyl-5-hepten-2-one; Dihydroact, Dihydroactinidiolide.

Colour retention

OPLS-DA was also carried out on the dry samples to create a better visualisation of the volatile compounds by eliminating variation that was not directly affected by colour retention phenotype, as well as having improved detection limits for outliers. Thus, allowing the high retention lines to be separated from the R12 outlier. The OPLS-DA plots displayed that the volatile composition of high and low retention lines were significantly different. The high retention phenotype lines cluster to the left hand side of the ellipse and the low retention lines cluster on the right hand side (Figure 5.17). The loadings showed that the low retention lines were separated based on similar compounds as seen in dry conditions, such as linalool, β -ionone epoxide, and dihydroactinidiolide, in addition to ocimene and geranyl acetone. The high retention lines were separated based on similar compounds to fresh fruit, such as undecatetraene, 2-methylpentadecane, 2-methylpentyl hexanoate, 2-methyltetradecane, and 2,6-nonenal, in addition to hexanal and 2-hexenal.

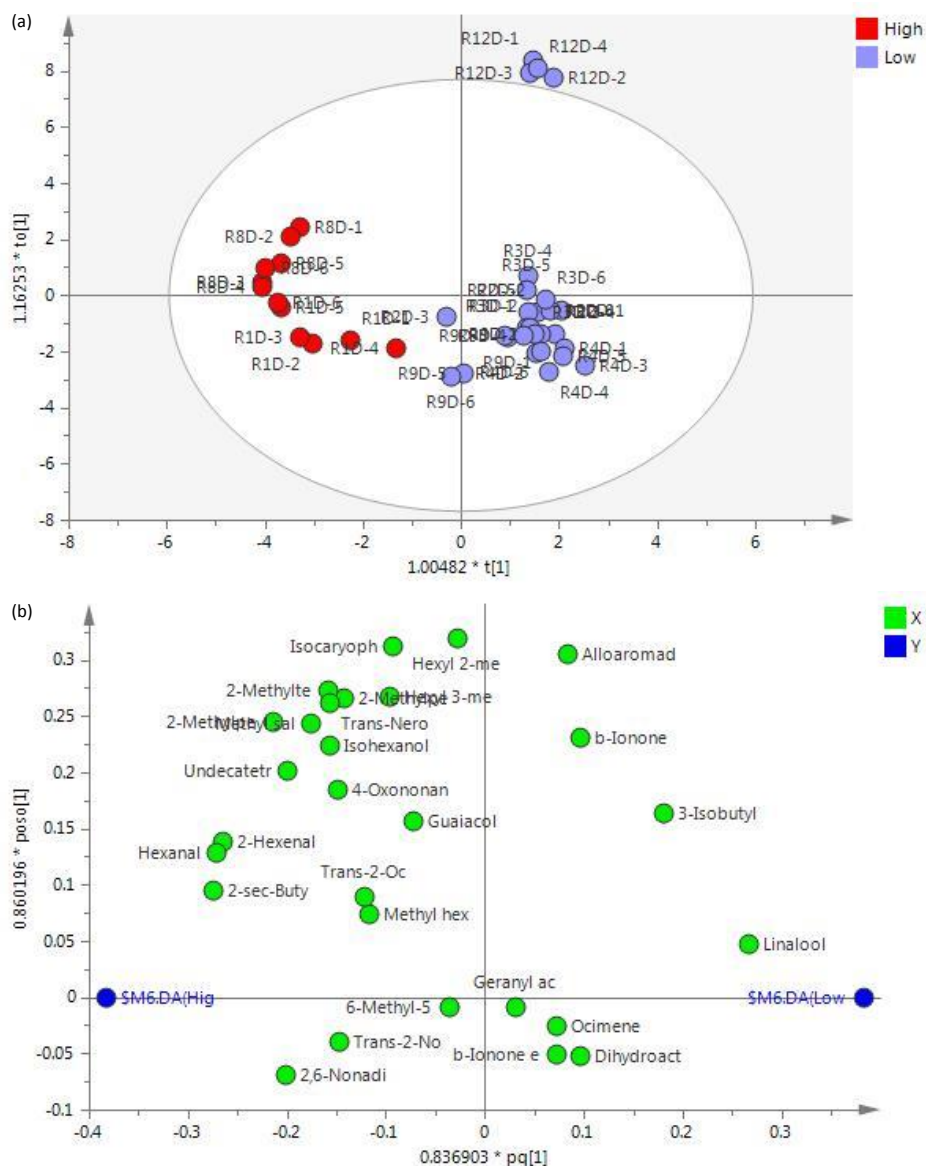


Figure 5.17. OPLS-DA of volatile compounds identified in dry chilli pepper in high and low retention lines.

OPLS-DA was performed in order to create a clearer picture as to the relationship between volatile compounds and colour retention phenotype. (a) Scores and (b) loadings. Key in (a) low (blue) and high (red). Key in (b) Methyl hex, Methyl hexanoate; 2,6-Nonadi, 2,6-Nonadienal; 2-sec-Buty, 2-sec-Butylcyclohexanone; Trans-2-No, Trans-2-Nonenal; Trans-2-Oc, Trans-2-Octenal; 3-Isobutyl, 3-Isobutyl-2-methoxypyrazine; 4-Oxononan, 4-Oxononanal; Methyl Sal, Methyl salicylate; 2-Methylpe, 2-Methylpentadecane and 2-Methylpentyl hexanoate; Trans-Nero, Trans-Nerolidol; Undecatetr, Undecatetraene; Isocaryoph, Isocaryophillene; Hexyl 2-me, Hexyl 2-methylbutyrate; Hexyl 3-me, Hexyl 3-methylbutyrate; Alloaromad, Alloaromadendrene;

Geranyl ac, Geranyl acetone; b-Ionone e, b-Ionone epoxide; 6-Methyl-5, 6-Methyl-5-hepten-2-one; Dihydroact, Dihydroactinidiolide.

In order to observe how these volatile compounds differed when comparing high and low retention lines a heat map was constructed to visualise the significant differences (Figure 5.18).

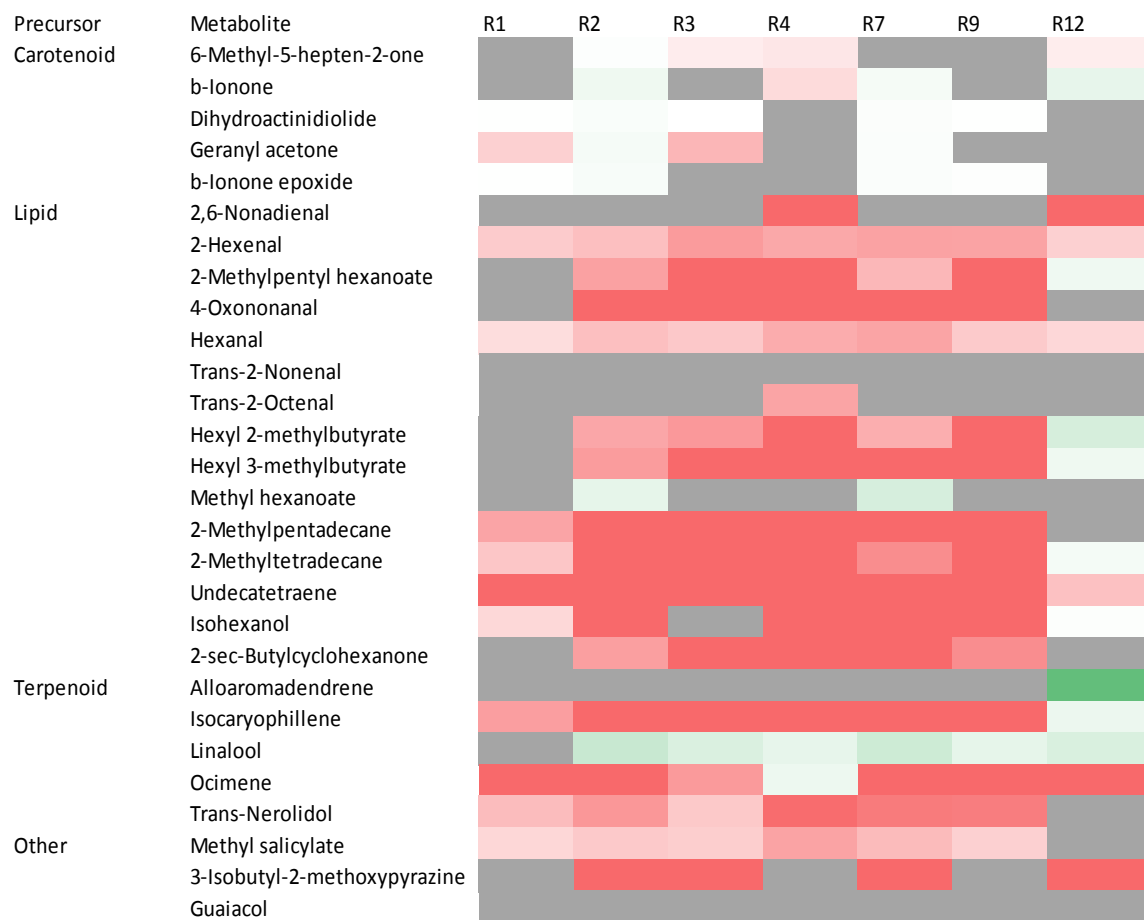


Figure 5.18. Heat map displaying the changes in volatile compounds in between high and low retention lines in dry fruit.

The heat map shows the significant changes in volatile compounds between, R8 the high retention line, and all the other lines. Statistical analysis was performed using one-way ANOVA ($P \leq 0.05$). Changes are indicated by increase (green), decrease (red) and no change (grey).

The heat map showed that the β -ionone was increased in the R2 and R7 lines which have high colour intensity phenotypes, and R12. However, when comparing with R3, R4 and R12 these lines showed decreases compared to R8. The other high retention line R1 had similar amounts

of carotenoid derived volatiles when compared to R8, excluding a decrease in geranyl acetone. Similarly to the findings in fresh fruit, the lipid derived volatiles were mainly decreased in the majority of lines when compared to R8. Although the decreases experienced in the R1 high retention line were not as dramatic as the other low and medium retention lines. The R1 line showed no change in 2-methylpentyl hexanoate, 4-oxononanal, hexyl 2-methyl butyrate, hexyl 3-methylbutyrate, and 2-sec-butylcyclohexanone when compared to R8, but the remaining lines (excluding R12) all show decreased levels. The volatiles 2-methylpentadecane, 2-methyltetradecane, and isohexanol all show decreased amounts in the R1 line compared to the R8 but these decreases were not as large as the decreases seen in all other lines (except R12). Again, there was an increase in the levels of linalool in all lines when compared to the high retention lines R1 and R8. All lines showed significant decreases in 2-hexenal, hexanal, and undecatriene. The two of the high intensity lines R2 and R7 showed increases in methyl hexanoate compared to R8 when all other lines showed no change.

Colour intensity

OPLS-DA was carried out on volatiles identified in dry fruit with respect to colour intensity phenotype. This was to allow any metabolites which influence colour intensity phenotype in dry fruit to be determined.

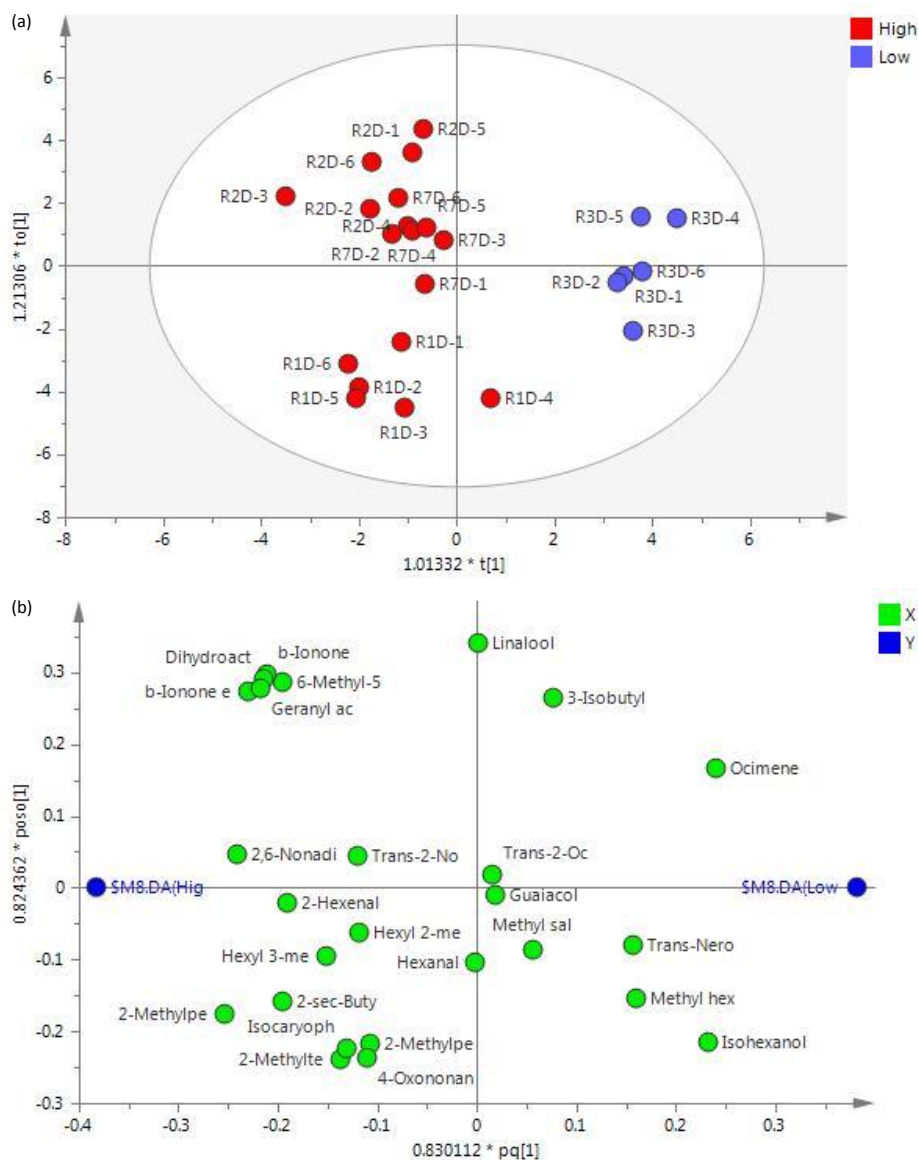


Figure 5.19. OPLS-DA of volatile compounds identified in dry chilli pepper in high and low intensity lines.

OPLS-DA was performed in order to create a clearer picture as to the relationship between volatile compounds and colour intensity phenotype. (a) Scores and (b) loadings. Key in (a) low (blue) and high (red). Key in (b) Methyl hex, Methyl hexanoate; 2,6-Nonadi, 2,6-Nonadienal; 2-sec-Buty, 2-sec-Butylcyclohexanone; Trans-2-No, Trans-2-Nonenal; Trans-2-Oc, Trans-2-Octenal; 3-Isobutyl, 3-Isobutyl-2-methoxypyrazine; 4-Oxononan, 4-Oxononanal; Methyl Sal, Methyl salicylate; 2-Methylpe, 2-Methylpentadecane and 2-Methylpentyl hexanoate; Trans-Nero, Trans-Nerolidol; Undecatetr, Undecatetraene; Isocaryoph, Isocaryophyllene; Hexyl 2-me, Hexyl 2-methylbutyrate; Hexyl 3-me, Hexyl 3-methylbutyrate; Alloaromad, Alloaromadendrene;

Geranyl ac, Geranyl acetone; β -ionone e, β -ionone epoxide; 6-Methyl-5, 6-Methyl-5-hepten-2-one; Dihydroact, Dihydroactinidiolide.

The high intensity lines separated away from the low intensity line in Figure 5.19. The R2 and R7 also cluster away from R1. The R2 and R7 lines separated based on the carotenoid derived volatiles dihydroactinidiolide, β -ionone, β -ionone epoxide, geranyl actone, and 6-methyl-5-hepten-2-one. The R1 line separated based on lipid derived volatiles 2-methylpentadecane, 2-methyltetradecane, isocaryophyllene, 2-sec-butylcyclohexanone, hexyl 2-methylbutyrate, hexyl 3-methylbutyrate, hexanal, and 2-hexenal. The R3 low intensity line separated from the high intensity lines based on the trans-nerolidol, ocimene, methyl hexanoate, and isohexanol.

5.2.4. Analysis of superoxide dismutase (SOD) activity in fresh and dry pepper

The previous sections of this chapter have similar themes throughout in relation to lipid peroxidation and the production of ROS. This therefore led to the last section of this chapter whereby a preliminary look into the superoxide dismutase (SOD) activity was conducted and the role it plays in colour retention phenotype.

The SOD activity was investigated using native protein gels stained with nitroblue tetrazolium (NBT). Extracts of chilli pepper powder were run on the gels and the SOD activity was visualised as clear areas by negative staining where the NBT had not become oxidised and turned blue. The assay was carried out on fresh material which had been freeze dried and stored at 10°C for 90 days (Figure 5.20), as well as dry material which had been incubated for 6 weeks at 20°C under a light/ dark cycle to induce colour loss (Figure 5.21).



Figure 5.20. Superoxide dismutase (SOD) activity in fresh and dry chilli pepper.

A SOD assay was carried out to qualitatively analyse the activity of the SOD enzyme in fresh and dry chilli pepper. The two lanes for each condition represent 20 µl and 10µl of protein extract added to the gel.

The SOD assay on fresh and dry chilli powder showed that there were four isoforms of the SOD isoenzymes present in fresh and dry fruit (Figure 5.20). These four isoforms have been previously identified and characterised by other studies (Gupta et al., 1993; León et al., 2002; Xu et al., 2013) and based on their results were thought to comprise the cofactors manganese, iron and copper zinc, which is typical of SOD. There was even evidence of activity 90 days after storage in the dark at 10°C, especially the isoform with the copper zinc cofactor. The two lanes for each condition represent the 20 µl and 10µl of protein extract added to the gel in each condition. This showed that there was slightly more intense activity when loading 20µl as opposed to 10µl. The 10µl lane gives a clearer banding pattern in the fresh condition but the bands are more predominant in the 20µl lanes for the fruit that had been dried for three weeks and incubated for 90 days.

SOD activity was then investigated in three high and three low retention lines to determine whether there were any differences in activity or particular isoforms that could contribute to colour retention phenotype (Figure 5.21).

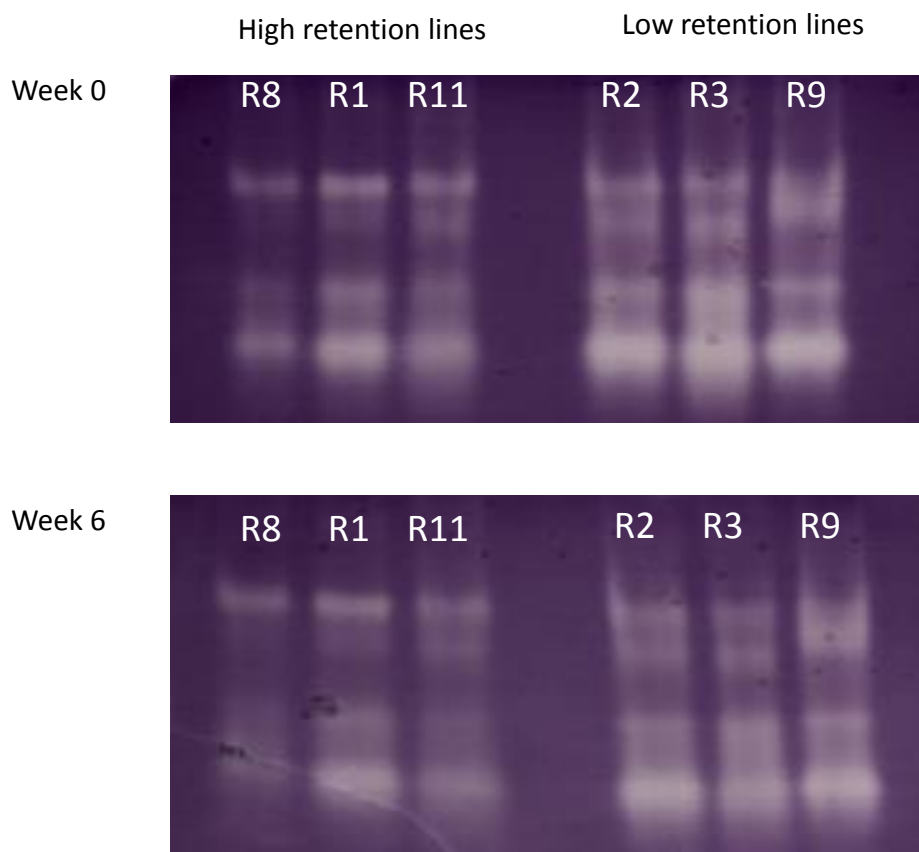


Figure 5.21. Superoxide dismutase (SOD) activity in dried chilli pepper.

The SOD activity was visualised in dried chilli pepper samples which had been incubated for 6 weeks at 20°C to initiate colour loss. This was conducted in three high retention lines and three low retention lines.

The SOD activity was investigated at the start and the end of the 6 weeks incubation time and it was revealed that the SOD activity was more intense in the low retention lines, R2, R3 and R9. This was true for both time points analysed. All four isoforms were visible in all lines at the start and the end of the experiment, with the last band showing the most predominant activity. This band was thought to be an isoform which has a copper zinc cofactor, as previously mentioned. SOD activity was particularly low in the high retention R8 line. It could be said that there was slightly less activity at the end of the experiment in the high retention lines when comparing to the start of the experiment suggesting the decrease in activity over the course of the experiment. This could also be said for the low retention lines, but decrease in activity is far less pronounced.

5.3. Discussion

The classification of colour can be difficult to describe consistently because the perception of colour by the naked eye can be very variable between individuals, therefore classifying colour is subjective as well as hard to control. For example, the light, size, texture and shape of the object can be contributing factors resulting in the colour being perceived differently. Based on this knowledge there has been an effort to quantify colour using digital images eradicating variation in perception of colour between individuals by implementing a standardised and objective method. In this study image analysis was employed to quantify the colour of chilli peppers based on an image taken in standardised conditions.

Establishing reliable methods to measure colour is important when understanding and quantifying colour loss. Colour retention is a desirable trait in the chilli pepper industry and it is paramount to measure this correctly to enable the further investigation of lines with high or low colour retention properties. Characterisation of the retention phenotypes allowed further study of colour retention to be carried out. Thus, the volatile profiles of the colour diversity panel were analysed to investigate the degradation processes taking place that lead to colour loss, as well as, taking a preliminary look at some other defensive mechanisms present in the cell which may also affect colour loss.

5.3.1. Colour loss in chilli powder over time

Image analysis was carried out on a colour diversity panel of chilli powder. These lines differed in their colour retention phenotypes and the imaging technique was utilised to quantify colour. Due to the deep red colour and the length of time the fruit can retain this colour throughout storage being directly related to the value of the material, it is important for growers to have lines with high colour intensity and retention. Some chilli pepper lines were more susceptible to colour loss during the storage period than others but the reason for this is unknown therefore a method to speed up colour loss when screening new lines for colour retention was investigated.

5.3.1.1. Lightness of colour

The general consensus for all the chilli lines analysed in this experiment was that lightness increases over time rendering the different chilli pepper lines lighter in colour when incubated in any of the conditions they were exposed to. In the conditions 15, 20, 30, 40°C and black light there was a steady and gradual increase in lightness. However, in the UV condition there was a steep increase in lightness taking place in the first week then the chilli lines reached a saturation point of lightness for the remaining time. This plateau of saturation can also be seen after 5 weeks of incubation at 15°C. On comparison of the inclines in lightness in different conditions it becomes apparent that there was less of an increase in lightness as temperature increased. Therefore, the higher the temperature, the darker in colour the lines remain when compared to lower temperatures. This was also noticeable visually as the samples appeared to be getting browner at higher temperatures. This could be a result of the chilli powders experiencing non-enzymatic browning through the Maillard reaction resulting from a chemical reaction between amino acids and reducing sugars, and autoxidation reactions involving phenolic compounds. Also, the Maillard reaction can take place in foods with non-sugar molecules containing carbonyl groups, such as ascorbic acid, phenols and lipid oxidation products which are prevalent in chilli pepper fruit (Lee et al., 1991; Manzocco et al., 2001). The rate of the Maillard reaction was increased at higher temperatures and this reaction leads to the production of volatile compounds, such as strecker aldehydes, and melanoidins (Cremer and Eichner, 2000b). Therefore, the increase in the rate of the Maillard reaction and so the formation of the brown compounds, such as melanoidins, contribute to making the colour of the chilli powder darker at higher temperatures. This was also supported by the fact that the chilli powder exhibited decreases in red colour when looking at a^* and hue angle coordinates which become more pronounced as temperature increased (Figure 5.2 and Figure 5.4). Previous studies support these findings as bell peppers and paprika have been found to contain strecker aldehydes which increased with temperature when carrying out volatile analysis; this indicated that the Maillard reaction was taking place and the reaction rate was increased at higher temperatures. This was concurrent with a decrease in colour measured by ASTA (Cremer and Eichner, 2000b, 2000a; Van Ruth et al., 1995). Another study also found the L^* , a^* and b^* values coordinated with non-enzymatic browning (Lee et al., 1991). The possibility that enzymatic browning, through polyphenol oxidases, contributed to the brown colour cannot be ruled out, but due to the lack of water in the samples non-enzymatic browning is more likely to be the predominant cause (Martinez and Whitaker, 1995).

In addition to the temperature conditions affecting the overall change in the lightness of the samples it was also observed that the performances of specific lines throughout the 6 weeks changed in response to higher temperatures too. At 15°C and 20°C the most prominent line which underwent significantly the smallest increase in lightness was R8 which had a high retention phenotype. However, as the incubation temperature increased to 30°C and 40°C and under black light, the R8 line was no longer the darkest in colour but clustered in a group with the darkest lines. Under these conditions it was now the R6 line which experienced the lowest decrease in lightness. This line was significantly darker than all the other lines analysed and proceeded to become darker at the end of the experiment when compared to the beginning. Based on this observation it could be proposed that the R6 line had a higher amount of carbonyl molecules, such as phenolics, available to participate in Maillard reactions than compared to other lines analysed thus causing it become browner at higher temperatures.

Under the UV condition the chilli lines all behaved in a similar way, the UV light had a more powerful effect on the colour of the samples analysed resulting in a more uniform decrease in lightness. This was because UV light contains UV-A and UV-B wavelengths; the short UV-B wavelengths are more damaging than the longer UV-A wavelengths. This condition results in the chilli powder becoming exposed to ionising radiation which results in photo-oxidative stress caused by the production of reactive oxygen species (ROS). The ROS produced reacts with the pigments, as well as the lipids, proteins and nucleic acids (Edge et al., 1997). This led to the increase in lightness observed, caused by the loss of carotenoids through photo-protective quenching of reactive compounds in order to protect the photosynthetic machinery, particularly when exposed to high energy, short wavelengths of UV-B (Mahdavian et al., 2008). It had been previously reported that pepper plants grown under UV-A, UV-B and UV-C wavelengths showed decreased chlorophyll and carotenoid contents, as well as increased flavonoid and lipid peroxidation. The oxidative stress caused UV-B and UV-C was far greater than the UV-A (Mahdavian et al., 2008). This explains why the increase in lightness observed in the UV condition was more severe than that in the black light condition, as black light contains UV-A wavelengths which causes less oxidative damage.

5.3.1.2. Red and green colour

The CIELAB colour space used the a^* parameter to quantify the position in colour between red and green whereby positive values represent red and negative values represent green. The red

colour of the chilli powder samples studied declined over the course of the experiment in all conditions analysed. This was because the carotenoids were easily oxidised due to being electron rich molecules making them very susceptible to nucleophilic attack. This therefore leads to the degradation of the molecule when exposed to oxygen and light (Britton, 1995a). The subsequent degradation of the carotenoid molecule renders it colourless as the chromophore is broken thus resulting in a decrease in carotenoid content and therefore a decrease in red colour (a^*). At levels of low oxygen concentration the carotenoids can break the chain associated with free radical production but at high concentrations the carotenoid could act as a pro-oxidant (Halliwell and Gutteridge, 1999). The carotenoids are highly hydrophobic and so are located in hydrophobic areas of the cell such as the inner core of the membranes or in fibrillary and plastoglobuli storage structures (Britton, 1995a; Deruère et al., 1994). This suggested that the decrease in red colour, and so the concurrent degradation of carotenoids, observed in this experiment may be caused by the quenching of free radicals formed from the products of lipid peroxidation, as previous studies have shown that lipid peroxidation increases in response and exposure to UV light (Mahdavian et al., 2008). The more dramatic decreases in red colour witnessed at higher temperatures may be caused by increased rates of autoxidative reactions, as well as lipoxygenase (LOX) catalysed oxidation processes taking place (Cremer and Eichner, 2000a).

The lines were compared within the different treatment conditions and the high retention line R8 was the most efficient at retaining the red colour of the chilli powder when compared to all other lines. This line was previously mentioned for undergoing the lowest decrease in lightness. The R8 line did not experience any red colour loss at 15°C, 20°C, and 30°C and was significantly the reddest line when compared to the other lines analysed. Only in the 40°C and black light conditions did this line show a decrease in red colour causing it to cluster with the other high retention lines, R1 and R11. This larger loss of red colour, resulting for the high temperature and black light conditions, may be directly related to the rate of lipid peroxidation occurring. In previous studies where paprika was heated there was an increase in volatiles which are known products of carotenoid degradation and lipid peroxidation (Cremer and Eichner, 2000a). These conditions must overcome the defence mechanisms of the cell, which were being utilised to protect the molecular components susceptible to oxidative damage, resulting in the degradation of carotenoids. Therefore, subsequently in these conditions the oxidative damage outweighs the protective mechanisms.

Under UV light all the lines experience a sharp decrease in red colour in the first week and from that time point onwards a saturation point was reached. All the lines respond in a similar way to

UV light with no significant differences between them. The photo-oxidation of carotenoids initiated by the UV light had a much stronger impact on the degradation rate and composition of carotenoids when compared to oxygen (Morais et al., 2001). It was also found that *C. annuum* leaves had lower levels of carotenoids when transferred to higher light because the rate of oxidation exceeded the rate of carotenoid synthesis (Simkin et al., 2003). This therefore describes why there was such a dramatic decrease occurring in the UV condition. This was also supported by the results from the black light condition as this condition only contained the longer UV-A wavelength. The loss of red colour in this condition was not as detrimental as the colour loss experienced in the UV condition. In the UV condition, the concentration of carotenoids or other antioxidant compounds was greatly outweighed by the degree of photo-oxidation produced from the UV light. This resulted in rapid degradation of carotenoids and therefore red colour.

The two other high retention lines studied, R1 and R11, also showed low decreases in red colour compared to the other lines analysed in most of the conditions. However, when observing the loss of red colour in the R1 line at different temperatures it was evident that this line became better at retaining its red colour at higher temperatures. This may be related to the composition of saturated and unsaturated fatty acids in this line as previously described (4.2.2) this line was found to have low levels of unsaturated fatty acids, compared to the low retention line R3. Unsaturated fatty acids are more prone to oxidation due the double bonds present. It has also been found that plants with a higher percentage of unsaturated fatty acids have a higher survival at low temperatures. This suggested perhaps plants with higher levels of saturated fatty acids would be more efficient at maintaining the membrane integrity at higher temperatures due to the saturated fatty acids being packed together more tightly than unsaturated fatty acids resulting in a higher melting point and viscosity. Therefore, the R1 line may experience less colour loss at higher temperatures as the membrane integrity was being efficiently maintained and the rate of lipid peroxidation was lower. In the 40°C condition, however, this temperature exceeds the capacity of all the lines ability to retain red colour, including the high colour retention lines. This was the same for the black light and UV conditions.

The R7 line which has a high intensity, medium retention phenotype experienced the highest loss of red colour throughout the experiment in all conditions, except UV. When the metabolite profile of this line was analysed and compared with the R1 and R3 lines in the previous chapter (4.2.2) this line had significantly high fatty acid levels. This again suggested that perhaps these high levels of fatty acids resulted in higher rates of lipid peroxidation generating higher amounts of ROS, which the carotenoids scavenged to protect to cell. Thus, resulting in more degradation

of the carotenoids and therefore decreasing the red colour of the chilli powder. The R7 has been previously characterised as having the highest total carotenoid content with particular emphasis on the red carotenoid capsanthin. It could be feasible to suggest that this line has developed an over accumulation of carotenoids in response to protect the high levels of fatty acids present.

5.3.1.3. Red colour

The red colour was also analysed using an alternative colour space model to CIELAB, which was the LCH colour wheel. This was to see if the two colour models were consistent in describing which lines were the most efficient at retaining their red colour over the course of the experiment. The hue angle (h) parameter corresponded to a colour wheel whereby the 0/360° position of the wheel was red, 90° was yellow, 180° was green and 270° was blue. Over the course of the experiment there was an increase in hue angle which was equivalent to a decrease in red colour, and an increase in yellow colour in all conditions analysed. There was a linear increase in hue angle seen at all temperatures and black light conditions. However, in the UV condition the increase in hue angle was far steeper and occurs in the first week, then a saturation point was reached for the remaining duration of the experiment. This was concurrent with the results described in 5.3.1.2, and as previously mentioned, the decrease in red colour was caused by the degradation of the carotenoid compounds during the scavenging of ROS production from lipid peroxidation.

The observations from the hue angle parameters confirmed the trends seen in the a^* measurements whereby the R8 line was the most red in colour when compared to all other lines analysed, closely followed by the other two high retention lines, R1 and R11. This was true for all conditions except the UV treatment where the R6 line was the most red. This was also true for the a^* measurements. It has been proposed due to the R6 line showing high rates of non-enzymatic browning that there were high levels of phenolics present thus rendering it more protection from UV-B wavelengths when compared to the other lines (Mahdavian et al., 2008). Other findings from the a^* measurements have been confirmed such as the R1 line becoming more efficient at retaining its red colour, and the R7 line predominantly being the least efficient in most conditions. Therefore, the agreement of results from both colour space measurements increase the validity of the findings. Previous studies on investigating the correlation between hue angle and visual scores found that there was strong correlation between the two measurements suggesting this method was a good alternative to people grading the colour,

which as previously mentioned is subjective (Hernández et al., 2004). It also surprisingly found no correlation between visual scores and a^* , which was contrasting to the results of this experiment as hue angle and a^* show similar trends in all conditions.

5.3.1.4. Saturation of colour

The saturation of colour of the chilli powder was observed over time in different conditions where 0 represented white, grey or black, and 100 represented total colour purity. The results showed an initial decrease for the first two weeks in colour saturation then an increase, followed by a plateau. This could be explained by the chilli powders initially becoming less saturated by the loss of red colour but subsequently becoming more saturated later on in the experiments as the brown compounds associated with non-enzymatic browning started to accumulate.

The R8 line displayed the highest levels of saturation at 15°C and black light and was joined by the other two high retention lines, R1 and R11, at higher temperatures reflecting the high retention of red colour (a^* and hue angle) experienced in these lines. The R7 line was the least saturated line and the R6 line was the most saturated line under UV, again, mirroring the previously described findings when analysing red colour and lightness, respectively.

5.3.1.5. Total colour change

The investigation of the trends in different colour space parameters in the previous sections has shown how the different aspects of colour can change over time in response to different conditions. It has also revealed that they were all associated with each other too. For example, when just describing 'lightness of colour' it may seem at first glance that the chilli powders were getting darker red at higher temperatures but when taken with other parameters it was revealed that they were in fact becoming brown. Since the total colour change of the powder is a response from all these aspects it was important to analyse them in a holistic manner. The total colour change equation takes into consideration all parameters of the CIELAB colour space to give a measurement for all aspects of colour change and was a good way to summarise the findings from all the parameters studied.

The R8 line showed significantly the lowest total colour change and so the highest colour retention abilities in 15, 20, 30°C, and black light conditions, as well as being one of the highest

in the other conditions. The R1 line became more efficient at retaining its red colour at higher temperatures and the R6 line performed well under UV. Again, this confirmed the results previously described contributing to the robustness of the findings. Some of the findings from this study do not reflect the colour retention phenotypes previously allocated to the colour diversity panel. For example, R7 has been previously designated as having a medium retention but when looking at the results in the total colour change this line was consistently in the low colour retention group and should perhaps be reassigned as a low retention line. Other lines which do not correlate with the allocated phenotypes were R10, which should move from a high to medium colour retention group, and R4 and R12, which should move from low to medium.

5.3.2. Comparison of colour measurement methods

The image analysis technique is fairly new in the field of describing the colour of chilli pepper so the method was compared with other known methods of analysing colour. The traditional way to analyse colour in the field was to carry out ASTA analysis which is a standardised technique used in the spice trade industry, and so the results from the image analysis were compared to ASTA values from the same chillies that were imaged. Another method, which has been previously described in chapter 3 was the analysis of the carotenoid content using HPLC-PDA. This allowed the amount of red pigments to be determined which has been seen previously to correlate with colour intensity.

During the long storage experiment, whereby the whole fruits of chilli were stored for 9 months in the dark at 10°C, the image analysis data revealed that the R3 line experienced significantly the highest colour loss when compared to all other lines. All the other lines analysed showed similar values of colour change and were not significantly different. This suggested that the image analysis method may not be sensitive enough to detect the colour changes taking place when analysing whole peppers, as opposed to chilli powder. This could be due to there being less contact between substrates involved in the production of ROS during lipid peroxidation in the whole fruit as they compartmentalised within the cell (Lee et al., 1991). Therefore the lower levels of ROS production result in slower rates of carotenoid degradation during scavenging producing a less dramatic change in colour. This emphasises the success in enhancing colour loss in the previous section (5.2.1). It can be seen that there was a much faster rate of colour loss in the chilli powder incubated at 15°C on a day/ night light schedule when compared to whole

chillies incubated at 10°C in the dark. The light the samples were exposed to was also another influencing factor in increasing the rate of colour loss.

Pigment analysis was carried out to quantify the levels of red carotenoids present in these lines during storage. This was because it has been previously shown there was a strong positive correlation between colour intensity phenotype and red carotenoid content. However, the percentage change displayed throughout storage was highly variable rendering the changes between lines not significant. This was likely to be due to the sampling material used. Four chillies from each time point were used and due to this small sample size the variation between lines cannot not be distinguished from the natural variation within lines. This experiment would preferably be repeated using a much larger sample set from each line at each time point analysed. The results from this experiment were of low validity due to R8, a high retention line, and R3, a low retention line, showing similar percent changes. This was an unlikely result due to their different colour retention phenotypes and they have already been characterised using the chilli powder image analysis technique. Although the R8 line displays lower loss of red carotenoids when compared to most other lines, which is concurrent with previous results obtained from 5.2.1, the variation was too large rendering the result not significantly different to the other lines. Another unlikely result in this experiment was that the lines, R6 and R11, appear to experience an increase in red carotenoids by 20%. It was improbable that these lines underwent carotenogenesis after being dried in the sun and then stored in the dark. Although carotenogenesis has been known to occur off the plant once harvested this does not usually occur in dry fruit. The variation in these lines was considerable and so it was more likely that these differences were due to natural variation within lines; the chillies picked for the start of the experiment were naturally less red than the ones picked for the end of the experiment. Thus this was not a feature of the colour retention phenotype but individual variation.

The results from the ASTA measurement showed different overall changes in colour when compared to pigment and image analysis. The high retention line R1 displayed high colour loss when compared to all the other lines analysed which was also comparable to the pigment analysis experiment, but not in terms of the powder image analysis. The low retention line R3 showed very low colour loss in the both the pigment and ASTA experiment but was revealed to undergo significantly the highest colour loss in the image analysis experiment. In comparison of the medium retention R6 line between different colour measurement methods this line was seen to show a decrease, no change, and an increase in the image analysis, pigment analysis, and ASTA analysis methods, respectively. This was also true for the R7 line where it experienced a decrease in pigments but an increase in ASTA. R8 high retention line was found to show no

change during the pigment and ASTA analysis which was consistent with the allocated colour retention phenotype but the image analysis suggested the colour loss in this line was similar to all other lines, excluding R3. Therefore, it can be said that the findings from these data were inconsistent, variable and lack validity. This may not be a testament of the reliability of the methods used but a consequence of using a sample size which was too small or the fact that colour loss can occur in a non-uniform manner across in the surface of the fruit. The ASTA values for the start of experiment were compared with total carotenoid content on the same lines, but harvested fresh and freeze-dried, and there were similar trends seen between the two techniques (data not shown). Other studies have also found extractable colour analysis methods such as pigment analysis and ASTA to be more sensitive and reliable than just measuring colour surface colour (Vracar et al., 2007). This perhaps indicates that these methods were more desirable when investigating colour change between lines on a more detailed level but image analysis would be more efficient to use when carrying out colour retention phenotype screens on a much larger population. Previous studies also displayed only a 20% colour loss when measuring the ASTA values of chilli powder which had been incubated at ambient temperature in the light (Tepić and Vujičić, 2004). Since the results in this ASTA experiment show up to 50% colour loss in whole fruit exposed to less oxidising conditions this further suggests the results from the long storage experiment were unreliable and a consequence of small sample size. However, in contrast to this a paper measuring colour intensity of fruit dried on or off the plant found that L^* , a^* and b^* measurements did not always mirror changes in ASTA (Krajayklang et al., 2000).

5.3.3. Volatile analysis in fresh and dry chilli pepper fruit

Analysis of the volatile compounds produced in fresh and dry fruit were examined in a colour diversity panel. This was to gain a better understanding of the oxidation and degradation processes occurring during storage. The volatiles detected were analysed to identify these degradation products.

There were 28 compounds identified in fresh and dry fruit. The chemical composition of fresh and dry fruit differed. The dry fruit experienced a decrease in the percentage of aldehydes and esters released and an increase in ketones and monoterpenes. The percentages of alcohols, alkanes, alkenes, pyrazines, and sesquiterpenes were very similar in fresh and dry fruit. The chilli lines in this study showed a predominance of volatile aldehydes (approx. 30% and 20% in fresh

and dry fruit, respectively) and ketones (approx. 20% and 30% in fresh and dry fruit, respectively); however, these compositions can vary considerably depending on the variety of chilli pepper analysed (Bogusz Junior et al., 2012).

The volatile compounds identified in this study have all been detected in pepper or tomato previously (Buttery et al., 1988; Luning et al., 1994; Pino et al., 2006, 2011; Bogusz Junior et al., 2012). The volatile monoterpene, δ -3-carene, was not identified in this study but has been reported as a component in bell pepper odour in many other studies (Luning et al., 1994; Mazida et al., 2005; Bogusz Junior et al., 2012). It was also not identified in the study by Pino et al., 2006. The most abundant volatile compounds found in fresh fruit were a mixture of fatty acid and carotenoid degradation products, as well as amino acid degradation products and organic aroma compounds, such as 2-hexenal, hexanal, trans-2-nonenal, trans-2-octenal, β -ionone epoxide, dihydroactinidiolide, methyl salicylate and guaiacol. However, when the dry fruit were analysed the most abundant compounds were carotenoid degradation products, predominantly β -ionone epoxide and dihydroactinidiolide. This was reflected in the PCA loading plot whereby fresh and dry samples separated based on fatty acid and carotenoid degradation products, respectively. The volatile compounds driving the fresh separation were mainly unsaturated aldehydes 2,6-nonadienal, 2-hexenal, hexanal, trans-2-nonenal and trans-2-octenal. The first three volatile compounds listed were derived from the unsaturated C18:3 fatty acid called linolenic acid. The formation of these lipid derived volatiles are initiated when the chilli pepper fruit undergoes disruption of intact cells. This results in lipid degrading enzymes, such as lipoxygenases, coming into contact with membrane lipid and storage lipids (Galliard et al., 1977). Linolenic acid is particularly prone to oxidation due to the presence of double bonds. The volatile aldehydes formed from linolenic acid were produced by first cleaving linolenic acid from the lipid membranes by lipolytic enzymes. This enables the free linolenic acid to be available to lipoxygenase (LOX) and hydroperoxide cleavage enzymes which were responsible for the lipid peroxidation processes leading to C₆ aldehydes identified in this study. The polyunsaturated fatty acids, linoleic acid and linolenic acid, constitute 66% of the total lipid content in tomato (Galliard et al., 1977).

The compounds causing separation of the dry samples were carotenoid derived volatiles: geranyl acetone, β -ionone epoxide, β -ionone, 6-methyl-5-hepten-2-one, dihydroactinidiolide, and linalool (terpenoid derived). These compounds were formed via the oxidative cleavage of the carotenoids by various carotenoid cleavage dioxygenase (CCDs) which cleave the carotenoids at various double bond locations (Simkin et al., 2004). Geranyl acetone is thought to be derived from phytoene, β -ionone and β -ionone epoxide from β -carotene, and 6-methyl-5-hepten-2-one from lycopene (Goff and Klee, 2006). Other mechanisms for cleavage of

carotenoids generating carotenoid volatiles was through free radical mediated cleavage (Simkin et al., 2004). The heat map displays that from the transition from fresh to dry fruit there was an increase in the amount of carotenoid derived volatiles and simultaneously a decrease in lipid derived volatiles. The dry, high retention lines R1 and R8 appear to cluster closer to the fresh samples compared to the dry, low retention lines. This suggested that these lines were showing more similar volatile compositions to the fresh samples due to containing higher levels of lipid derived volatiles. This was reflected when analysing the heat map showing change in compounds from fresh to dry. In comparison to all other lines analysed these two high retention lines showed less dramatic decreases in lipid derived volatiles, particularly linolenic acid derived 2,6-nonadienal and 2-hexenal. Interestingly, this fatty acid was found to be the most abundant in the chloroplast membrane (Matsui et al., 1997). Thus suggesting these high retention lines were experiencing a slower rate of degradation of chloroplast or chromoplast membranes. This therefore results in less carotenoid degradation as the integrity of the chloroplast or chromoplast was more efficiently maintained. Another characteristic of the high retention lines was that linalool increased from fresh to dry in these lines but stayed the same or decreased in all other lines analysed.

The R12 line was an outlier when compared to all the other lines analysed. It had significantly high levels of fatty acids and fatty acid esters. There have been previous reports showing that the majority of bell pepper volatiles decreased and some even disappeared throughout ripening (Luning et al., 1994). Perhaps this line was harvested at a stage which was not fully mature suggesting why there were such high levels of these specific volatiles compared to the other lines.

5.3.3.1. Colour retention

The colour retention phenotypes show much better separation when compared to the colour intensity phenotypes. This suggested that the volatile compounds released play a larger role in colour retention as opposed to colour intensity. This further supports that the expression of the carotenoid biosynthesis genes throughout ripening is directly responsible for the intensity of the red fruit and the oxidation/ degradation processes are responsible for the decrease in colour once the fruit has been harvested. The fresh fruit of the high retention line R8 were showing lower levels of carotenoid derived volatiles, such as β -ionone epoxide and dihydroactinidiolide, indicating that there was less carotenoid degradation taking place resulting in maintenance of

the red colour. It was thought that carotenoid cleavage plays a minor role in carotenoid turnover in pepper and so it was likely that the decrease in carotenoid derived volatiles in the high retention line was caused by less free radical mediated cleavage (Simkin et al., 2003). Although, the fact that these lines could be exhibiting lower expression or activity levels of CCDs cannot be ruled out. The high retention lines were also showing increased levels of fatty acid derived volatiles compared to the other lines. These included fatty acid esters: 2-methylpentyl hexanoate, hexyl 2-methylbutyrate, and hexyl 3-methylbutyrate. Alkanes: 2-methyltetradecane and 2-methylpentadecane, and fatty acid alcohol, isohexanol. The abundance of aliphatic esters has been previously described for the mature fruit of chilli pepper (Pino et al., 2006; Forero et al., 2009). Perhaps the higher levels of fatty acid derived volatiles and lower levels of carotenoid derived volatiles witnessed here was a reflection of the more efficient fibrillar plastoglobuli present within these high intensity lines. These lines could contain plastoglobuli with thicker more protective outer lipid layers resulting in less carotenoid degradation.

The volatiles identified in the dry fruit of chilli pepper told a similar story to the volatiles identified in fresh fruit. The carotenoid derived volatiles were found to be increased in R2 and R7 but in contrast to fresh fruit lines R3, R4, and R12 showed decreases when compared to R8. The dry fruit of the low and medium retention lines once again showed decreases in lipid derived volatiles compared to the high intensity lines. These included fatty acid esters, such as 2-methylpentyl hexanoate, hexyl 2-methylbutyrate, and hexyl 3-methylbutyrate, and hydrocarbons 2-methyltetradecane and 2-methylpentadecane, and isohexanol. However, in contrast to fresh fruit the high retention lines were also found to be higher in 4-oxononanal and 2-sec-butylcyclohexanone. Interestingly, the high retention lines also showed decreased levels of linalool, as previously seen in fresh fruit. Despite that finding that linalool was also found to increase in the transition from fresh to dry only in the high intensity lines.

The fact that these high retention lines were showing higher levels of ester and alkane volatiles derived from lipids in both fresh and dry fruit, and that the dry fruit resembles the fresh fruit volatile composition more than when compared to the other dry, low retention lines, suggests perhaps that these lines may be undergoing slower rates of lipid peroxidation. This was because the dry fruit were still experiencing oxidation even after three weeks of drying whereas the low retention lines have a much faster rate which rapidly oxidises available lipids at an earlier time point. Thus, resulting in the low colour retention phenotype as the carotenoids scavenge the free radicals produced in these processes more quickly. The slower rate of lipid peroxidation could be a result of more efficiently packed membranes comprising more saturated fatty acids as opposed to unsaturated. It has been mentioned previously that the fresh, high retention lines

exhibit lower decreases of unsaturated fatty acid derived volatiles from the fresh to dry transition. As well as, in the previous chapter the high retention line R1 was shown to have lower levels of unsaturated fatty acids. This was therefore important when considering that the unsaturated fatty acids comprise 66% of the fatty acid content in tomato, and chloroplasts are a major site for fatty acid derived volatile production (Galliard et al., 1977). Therefore, lower levels of unsaturated fatty acids present result in slower rates of lipid oxidation. This leads to lower levels of ROS formation resulting in the chloroplasts being more efficient at maintaining their integrity throughout storage, which ultimately results in less carotenoid degradation, culminating in the manifestation of high colour intensity.

Another factor to consider was the composition of the waxy cuticle of the chilli pepper. These high retention lines could have high levels of hydrocarbons which prevent them losing as much water as the low lines in the drying process. When GC-MS was carried out on the R1, R3, and R7 lines in the previous chapter (4.2.2) the R1 and R3 lines were found to have high levels of hydrocarbons in the ripe fruit which are components of the cuticle. The R3 line also had high levels of unsaturated fatty acids. This suggests although it had a waxy cuticle it was prone to increased levels of oxidation due to the high levels of unsaturated fatty acids. The R1 line, however, had high levels of hydrocarbons, as well as low levels of unsaturated fatty acids, which would be contributing factors to less carotenoid degradation. A previous study found that there were negative correlations between water loss and the levels of nonacosane (C29) and hentriacontane (C31). Therefore, less water loss was experienced in chilli varieties with high levels of the previously mentioned alkane hydrocarbons (Parsons et al., 2013). This was particularly noteworthy as the R1 high retention line was found to have significantly higher levels of nonacosane in ripe fruit when compared to the low and medium retention lines analysed R3 and R7, respectively (Figure 4.13c). Thus, suggesting that this line experienced less water loss. Therefore, the high retention lines were undergoing less unsaturated fatty acid oxidation, caused by slower rates of lipid oxidation, resulting in less oxidative cleavage of carotenoids therefore maintaining the intense red colour for longer. The increased fatty acid esters, alkanes and alcohols observed in the high retention lines were caused by a combination of high levels of alkane hydrocarbons in the cuticle and slow oxidation rates due to lower levels of unsaturated fatty acids. The lipid layer of the plastoglobuli present in the high retention lines could also be a factor for the higher levels of fatty acid derived volatiles whereby the carotenoids were more protected from degradative compounds and processes by a thicker lipid layer.

5.3.3.2. Colour intensity

The colour intensity phenotypes were investigated to visualise volatile compounds associated with colour intensity. The colour intensity phenotypes did not separate as well as the colour retention phenotypes. Although two of the highest intensity lines, R2 and R7, previously shown to accumulate high levels of total carotenoids and capsanthin separated based on carotenoid derived volatiles. This was understandable as these lines contain high levels of pigment but have been allocated low and medium retention phenotypes. There has been reports of there being a direct correlation between precursor content and volatile emissions, which was case the carotenoids (Goff and Klee, 2006). Although the R7 line had been previously labelled as a medium retention line, in the previous image analysis section on chilli powder, the R7 line displayed characteristics of a low retention phenotype. Therefore, these lines were both high pigment but low retention indicating high levels of carotenoid degradation taking place in these lines. The other high intensity line R1 separated away from the carotenoid derived volatiles due to also having high retention phenotype.

The low intensity lines separated based on methyl hexanoate, ocimene, trans-nerolidol, 3-isobutyl-2-methoxypyrazine, and hexyl 2-methylbutyrate. The volatile compounds ocimene and 3-isobutyl-2-methoxypyrazine have been previously described as being 'green' aroma characteristics which decrease as ripening increases (Luning et al., 1994). This suggests that the chemical composition of the low intensity lines was showing similarities to unripe fruit in comparison to high intensity lines.

5.3.4. Analysis of superoxide dismutase (SOD) activity in fresh and dry pepper

In the previous sections of this chapter there has been strong indications of the role lipid peroxidation in the rate of colour loss taking place within the chilli during storage. The main cause of this could be the production of ROS which the carotenoids quench in order to prevent further damage occurring to the molecular components, such as protein, DNA and lipids within the cell (Apel and Hirt, 2004). However, the carotenoids are not the only line of defence against ROS. There are many other enzymatic and non-enzymatic protection mechanisms. Other non-enzymatic antioxidant compounds include: ascorbate, glutathione, tocopherols, alkaloids, and flavonoids. Enzymatic defences include: ascorbate peroxidase, glutathione peroxidase, catalase, and superoxide dismutase (SOD). SOD acts as the first line of defence against the production of

ROS by converting superoxide into hydrogen peroxide (Beauchamp and Fridovich, 1971). Thus this enzyme was selected to study to assess the role it may play in the prevention of degradation processes taking place in chilli pepper resulting in differences in colour retention phenotypes identified.

The SOD activity was qualitatively analysed by using a native protein gel based assay. This was carried out in fresh and dry fruit. The results from the fresh tissue revealed that there were four types of SOD isoenzymes present in chilli pepper. These isoforms have been previously identified in tobacco, pepper and cassava and show the same typical banding pattern in this study (Gupta et al., 1993; León et al., 2002; Xu et al., 2013). These were MnSOD, FeSOD and two CuZnSOD. The CuZnSOD has been identified as being located in the chloroplast (Apel and Hirt, 2004) and interestingly the second CuZnSOD band identified in this study displayed the most intense activity, even after the chilli fruit had been dried for 3 weeks and stored for 90 days. This was because it was thought that most ROS originates from the chloroplasts (and peroxisomes) therefore creating a higher demand for enzymatic antioxidants (Xu et al., 2013).

Next the SOD activity was compared between lines differing in colour retention phenotype. This showed surprising results as the low retention lines exhibited the most intense SOD activity when compared to the high retention lines. However, it could be likely that high levels of ROS produced by these low intensity lines signal for the increased expression/ activation of SOD to defend the chloroplasts/ chromoplasts from oxidative damage (Apel and Hirt, 2004). Therefore, resulting in the low retention lines displaying higher levels of SOD. It is also important to consider the activity of catalase at this stage as this enzyme works with SOD to neutralise the hydrogen peroxide compounds it produces. This could result in the accumulation of hydrogen peroxide if sufficient levels of catalase were not active/ available to neutralise it thus perpetuating the production of ROS and intensifying the need for carotenoids to protect the cell through quenching. This would lead to faster rates of colour loss seen in the low retention phenotype lines.

5.4. Conclusions

5.4.1. Colour change in chilli powder

The first thing to conclude about the results from this study was that there were some lines which may not possess the colour retention phenotype previously allocated. Therefore, further

characterisation of colour retention phenotype is crucial. This will allow the robustness of the image analysis technique to be evaluated. Secondly, it was difficult to identify the optimum method for the speeding up of the colour loss process due the fact some lines behave differently depending on the condition. It was clear that the UV condition was too severe and the rate of colour loss resulted in complete colour loss from all samples in one week and so would not be good for selecting high colour retention lines. Alternatively, when investigating the higher temperature conditions (30°C and 40°C) some lines became better colour retainers at higher temperatures but this was not helpful when the normal storage conditions were 10°C. This was because although these lines were showing high retention phenotypes at higher temperatures when they are stored for the monsoon season they will not be stored at these conditions and so their high retention phenotypes at high temperatures will be irrelevant, and thus these lines will not respond in the same way in the normal storage conditions. On the other hand, if high temperature conditions were used to speed up colour loss and select the best lines then lines which perform well at lower temperatures will go unnoticed. Therefore, the optimum conditions to speed up colour loss in chilli powder would be at temperatures between 15-20°C. The colour loss in these conditions will be the most representative of the colour occurring during storage.

This study was beneficial in identifying strong candidate lines for future work. The R8 line will be further investigated due to its high colour retention observed in many different conditions when compared to the other lines analysed. The R1 line will continue to be studied based on its ability to retain red colour at higher temperatures. The R6 line will be investigated based on its high retention performance under UV. The low retention lines R2, R3 and R9 will also be further investigated based on their low retention phenotypes.

5.4.2. Characterisation of colour retention phenotype

The data from the long storage experiment gave inconsistent and variable findings when comparing the change in colour over time between different methods. Due to the sample size of this experiment the techniques employed were unable to distinguish actual colour loss experienced between lines from natural variation within lines. This therefore concludes that the best method for characterising colour retention phenotype was by incubating the powder at 15-20°C in a day/ night cycle for 6 weeks. This method was the most efficient at characterising the colour loss occurring between lines of differing colour retention phenotype. It could be proposed that the pigment and ASTA analysis were more suitable methods for investigating

colour in detail between lines but the image analysis technique would be more appropriate when carrying out large scale colour screen of populations of samples.

5.4.3. Volatile analysis

The volatile compounds of fresh and dry chilli pepper were analysed to gain insight into the types of compounds which were undergoing degradation in the drying process to see if there was any notable variation between high and low retention lines. A schematic of the mechanisms present responding to ROS in relation to colour retention phenotype is described in Figure 5.22. The fresh fruit of the high retention phenotype lines displayed lower levels of carotenoid derived volatiles when compared to the low and medium retention lines suggesting that there was less carotenoid degradation taking place. The dry fruit of high retention lines analysed in this study showed a more similar volatile composition to the fresh fruit analysed than the dry, low and medium retention lines. This was characterised by high levels of fatty acid derived volatiles suggesting that the rate of lipid peroxidation taking place in these high retention lines was much slower than when compared to the other lines. In the low and medium retention lines lipid peroxidation occurs rapidly resulting concurrently in the larger loss of colour characterised by the low retention phenotypes. The rate of lipid peroxidation within lines could be an important factor in determining the colour retention phenotype as it has been previously seen that in conditions which speed up the rate of lipid peroxidation the colour loss experienced was more uniform and dramatic; thus, resulting in the oxidative processes outweighing the protective mechanisms. However, in more ambient conditions like the long storage experiment the lines with slower rates of lipid peroxidation will inevitably experience slower colour degradation as seen with the high retention lines.

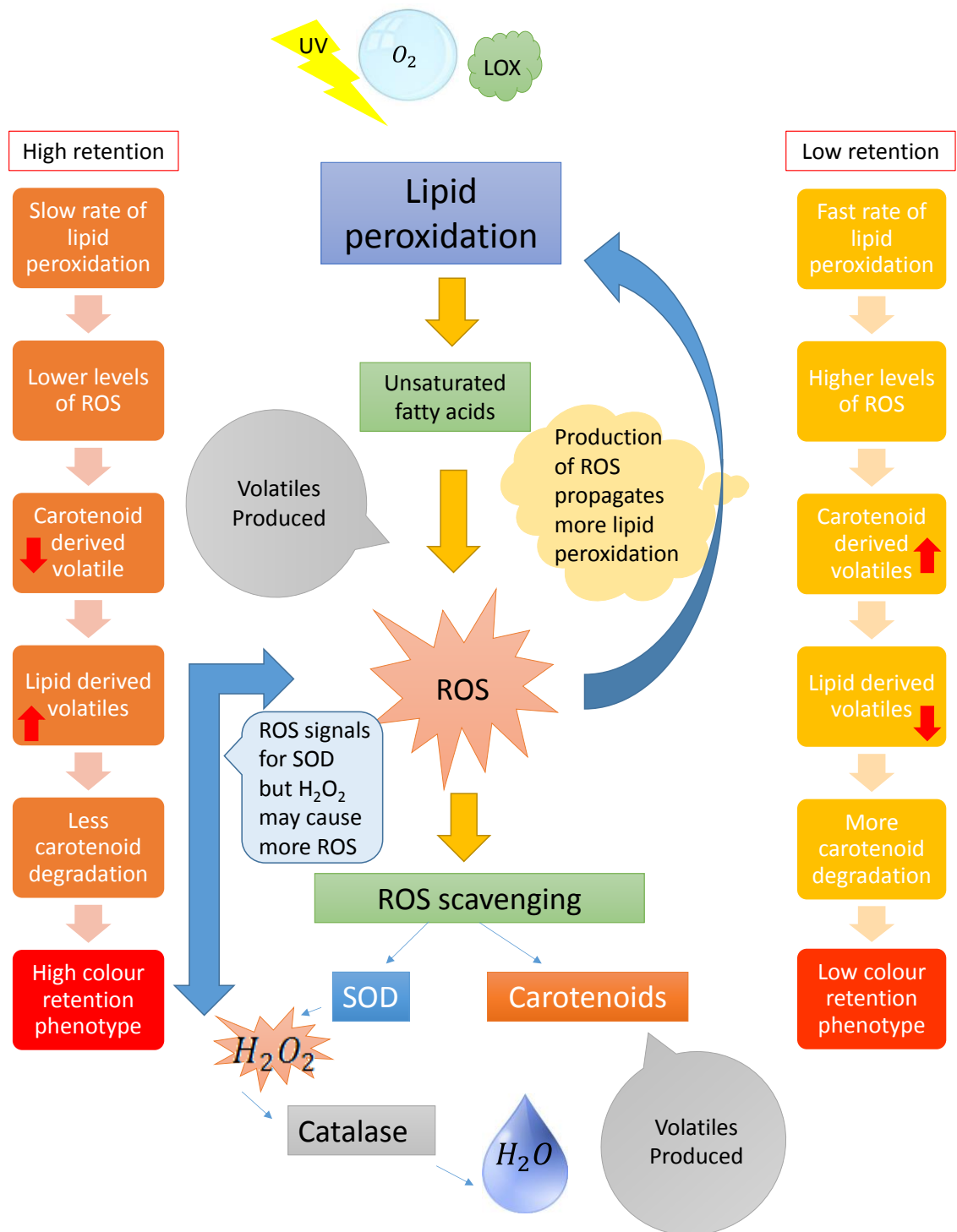


Figure 5.22. Schematic illustration of the hypothesis of the relationship of lipid peroxidation and carotenoid degradation present in high and low retention lines.

Exposure to light, oxygen, and lipoxygenases (LOX) can lead to lipid peroxidation in plants. Substrates of lipid peroxidation are usually unsaturated fatty acids which give rise to lipid volatiles and reactive oxygen species (ROS). In high retention lines there could be slower rates of lipid peroxidation resulting in the formation of less ROS than low retention lines. The fast

rates of lipid peroxidation and so the high production of ROS in low retention lines could result in the degradation of carotenoids resulting in low colour phenotype. The superoxide dismutase (SOD) enzyme also defends the cell against ROS and is thought to be signalled in response to high ROS production but its product hydrogen peroxide could also form more ROS. The differences between the high and low retention lines are described in flow diagrams on the left and right hand side of the diagram, respectively.

The slower rates of lipid oxidation could be because the antioxidant systems in place do not allow autoxidation processes to spiral out of control, but keep lipid peroxidation at a rate which allows the lipid oxidation products to be managed at a low level.

These differences in lipid and carotenoid derived volatiles could also be reflecting the efficiency in which the carotenoids are packaged within the storage lipids. High lipid degradation and low carotenoid degradation could be representing fibrils with larger lipid layers protecting the carotenoids from degradation. Higher levels of alkane volatiles as well as high levels of alkane hydrocarbons, previously characterised in the high retention line R1, suggest that cuticle thickness and composition may also contribute to colour retention phenotype.

The presence of more intense SOD activity in the low retention lines further supports the higher rates of lipid peroxidation and subsequent ROS production occurring within these lines. The SOD enzyme was more active here perhaps due to high levels of ROS signalling the up-regulation of its expression or activity. However, the level of catalase activity is also essential to consider as these enzymes work together in the cell and low levels of catalase could result in accumulation of hydrogen peroxide perpetuating the production of ROS.

The findings from this chapter have highlighted that there were a number of factors which could be contributing the colour retention abilities of chilli pepper effecting the degradation of the carotenoids during storage. Differences in levels of enzymes such as lipoxygenases and carotenoid cleavage enzymes, as well as variations in levels of non-enzymatic compounds such as carotenoids, flavonoids, anthocyanins or enzymatic antioxidants are all important to consider. The variations in lipid compositions affecting the rate of lipid peroxidation occurring, the mechanisms increasing chromoplast integrity, and the efficiency of carotenoid storage techniques are also essential to consider. It was evident that different lines may have different strengths and weaknesses in these areas and it is a sum of oxidative rates versus protective mechanisms which ultimately defines the colour retention phenotype.

Chapter 6. General discussion

6.1. Summary and general discussion

6.1.1. Aims and objectives

The aims of this project were to elucidate the underlying molecular and biochemical mechanisms associated with colour intensity and colour retention in fresh and dried chilli pepper (*Capsicum annuum*).

The first objective was to characterise colour intensity within a colour diversity panel. This was carried out by analysing the pigment profiles of 12 chilli pepper lines at ripe stage and throughout ripening, to gain understanding of the carotenoid biosynthesis and accumulation taking place within these lines. Thus, resulting in the discovery that carotenoid quantity and composition are directly related to colour intensity phenotype (Chapter III).

The second objective was to identify components responsible for the colour intensity phenotypes. This was achieved when lines were selected with perturbed pigment profiles and analysed at a gene, transcript, and metabolite level (Chapter IV). This revealed the influence of the *PSY1* and *DXS* gene products on the accumulation of carotenoids and regulatory mechanisms associated with this process. These key carotenoid biosynthetic genes that were found to influence the accumulation of carotenoids in high and low colour intensity lines were sequenced and subjected to transcription factor analysis to further examine carotenoid regulation at a transcriptional level (Chapter III). Additionally, the subchromoplast location of the carotenoids within the plastids were analysed using a subplastid fractionation technique. This emphasised differences in sequestration mechanisms which were a contributing factor to colour intensity phenotype (Chapter IV).

The third objective was focused on characterising colour retention in a colour diversity panel. This was first addressed by designing a protocol to speed up colour loss in chilli pepper to allow colour retention to be analysed more rapidly. This was achieved using an image analysis technique and subjecting the ground powder to heat and light (Chapter V).

The fourth objective was to identify mechanisms responsible for colour retention. The focus for this objective was to identify antioxidant or degradative mechanisms involved in protecting or degrading the carotenoids present in the colour diversity panel. Volatile analysis uncovered possible lipid peroxidation processes taking place characteristic of high and low retention lines, and analysis of superoxide dismutase activity highlighted potential ROS signalling pathways possibly acting in the plastid.

The findings from this project revealed that the factors involved in influencing the accumulation of carotenoids in ripe fruit and the degradation of carotenoids in dry fruit were complex, involving multiple levels of regulatory control. It has been shown in this study that expression of key carotenoid biosynthetic genes influenced colour intensity phenotype. The plastids' ability to adapt sequestration and storage mechanisms in response to the increased accumulation of carotenoids, found in high intensity lines, is fundamental to colour intensity phenotype. This was because the increased precursor metabolite levels can lead to negative feedback loops. Thus, resulting in the down-regulation of biosynthetic steps at the transcriptional, translational and enzyme levels. It was also shown that lipid peroxidation and carotenoid degradation products characterise colour retention phenotypes. However, the processes that lead to the formation of these products remain unknown in the lines studied. Differences in enzymatic antioxidant activities and/ or locations could be involved. The focus of the following sections is to: (i) summarise the processes identified relating to colour intensity and colour retention phenotypes, (ii) discuss the relevance of the information obtained, and (iii) consider how it can be applied to the chilli pepper industry and utilised in plant engineering.

6.1.2. Summary and general conclusions

The determination of colour intensity and colour retention started with the characterisation of the components responsible for the red colour. It was important to understand and define the colour of the ripe fruit, primarily in order to allow characterisation of colour retention.

6.1.3. Colour intensity

During ripening chilli peppers undergo profound morphological and metabolic transformations associated with chloroplast differentiation, biosynthesis and accumulation of carotenoids, and the degradation and breakdown of the photosynthetic machinery. High levels of lutein and chlorophylls were characteristic of green fruit which diminish as ripening progresses and high levels of xanthophylls and their corresponding esters were prevalent in red fruit (Figure 3.18). High levels of free capsanthin were identified in the ripe fruit of the high intensity lines when compared to other lines in the colour diversity panel (Figure 3.3). This corresponded with high levels of capsanthin diesters identified in those lines at later stages of ripening. These findings

were observed when comparing the transition from biosynthesis of capsanthin to the accumulation of capsanthin diesters in selected lines. This showed there was a linear increase in the amount of capsanthin diesters produced throughout ripening in the high intensity lines when compared to the low intensity line which experienced a plateau at the end of ripening despite still expressing the *CCS* gene (Figure 3.6).

The vast accumulation of capsanthin and capsanthin esters present in the high intensity lines resulted in changes in the sequestration mechanisms and storage sites of the carotenoids as an adaptation response. The accumulation of carotenoids at membrane biosynthesis sites results in the formation of PGs once the levels have reached a sufficient amount. Thus displaying the PGs role as a regulatory mechanism to store excess substrates. However, once the amount of carotenoid and carotenoid esters have reached a critical level in the PGs, the initiation of fibril formation was induced. Therefore, the higher the concentration of capsanthin diesters produced within the plastid, the more fibrils were formed in order to store them efficiently (Figure 6.1b). This was elucidated because there were higher percentages of carotenoids distributed in the membrane fractions of the medium intensity line, and alternatively there were higher percentages of carotenoids distributed in the PGs and fibrils of the high intensity line. A putative carotenoid acyl transferase (*rsAcT*) indicated that the accumulation of free capsanthin characteristic of ripe fruit was caused by this gene being expressed at low levels.

The high levels of capsanthin diesters that were achieved may be due to the high levels of carotenogenesis occurring in these lines as a result of highly expressed key carotenoid genes, such as *PSY1* and *DXS* (Figure 4.3 and Figure 6.1a). However, it was important to stress that transcript levels should not be extrapolated to enzyme activity. Enhanced carotenogenesis in these lines led to the accumulation of free carotenoids, particularly capsanthin, as a result of inefficient esterification mechanisms (*rsAcT*). Analysis of the *DXS* and *PSY1* transcript levels during fruit development and ripening uncovered regulatory mechanisms whereby the *DXS* gene peaked in expression at a time point just before or similar to that of *PSY1* in selected lines (Figure 4.5 and Figure 4.6). This implied that the *PSY1* gene was responding to the increase in substrate corresponding to the highly expressed *DXS*, which was also the case for tomato (Lois et al., 2000). It seemed likely that *DXS* expression or products of expression were affecting *PSY1* expression, and not *vice versa*. Sequencing of these genes in a high (R7) and a low (R3) intensity line provided further evidence of the underlying role *DXS* plays in the high intensity phenotype. In the high and low intensity lines, the *PSY1* gene and promoter region were highly conserved between both lines. However, the *DXS* gene was found to have 5 amino acid substitutions whereby one of them was located in the thiamine binding site in the R7 line. Additionally, the *DXS* gene showed

a mutation in the GAPF binding motif in the R7 line when compared to R3. This motif was also present in the promoter region of glyceraldehyde 3-phosphate dehydrogenase (*GapA*). The fact that these two genes share the same substrate (G3P) suggests that a transcription factor which modulates substrate flow into primary or secondary metabolism could be acting as a switch. The flow of carbon is either needed for the plant to produce more energy through glycolysis (primary metabolism) or the plant wants to divert the carbon into the carotenoid pathway (secondary). The R7 line, however, was missing this switch which could result in the flow of carbon being diverted into the carotenoid biosynthesis resulting in the over accumulation of carotenoids experienced in this line. This, therefore, results in the up-regulation of the *PSY1* gene to deal with the increased substrate flow, which could result in the slow ripening phenotype witnessed in the R7 line, whereby there is less energy available from glycolysis resulting in a slower ripening rate. The R1 line had a high intensity phenotype, but was not as intense as the R7 line. This line only possessed a highly expressed *PSY1* and did not have a highly expressed *DXS* but had a fast ripening phenotype (Figure 3.19).

The *PSY2* gene was identified and sequenced for the first time in *Capsicum*. Analysis of the expression profile during ripening showed that although this gene was expressed in ripe fruit the levels were very low when compared to *PSY1*, and therefore do not contribute to carotenoid biosynthesis in ripe fruit. This was concurrent with tomato (Fraser et al., 1999). There were other factors which could also modulate the expression of carotenoid biosynthesis genes. Key REs in *PSY1* which could be light and stress regulated were identified in the promoter region. A master regulator CarG box motif was found to have involvement in embryonic development, flowering, and cell wall modification during ripening. Transcription factor analysis also found that the *PSY2* promoter region contained an RE controlled by light, stress, and hormones. Presence of a W-box RE in the R7 line was located but was not present in the R3 line. The differences in the REs identified in *PSY1* and *PSY2* illustrated the more fundamental roles played by *PSY2*. This gene was regulated by light and stress but also by phytohormones with roles in plant and chloroplast development, as well as photo-protection. In comparison, the *PSY1* gene was regulated by light and stress and, therefore, was more related to fruit ripening (Figure 6.1). Furthermore, the *DXS* gene displayed REs related to light, stress, and hormones similar to *PSY2*, in addition to REs related to sugar metabolism; thus, highlighting the role of *DXS* in channelling the flow of carbon from sugar metabolism into the isoprenoid pathway during the chloroplast to chromoplast transition.

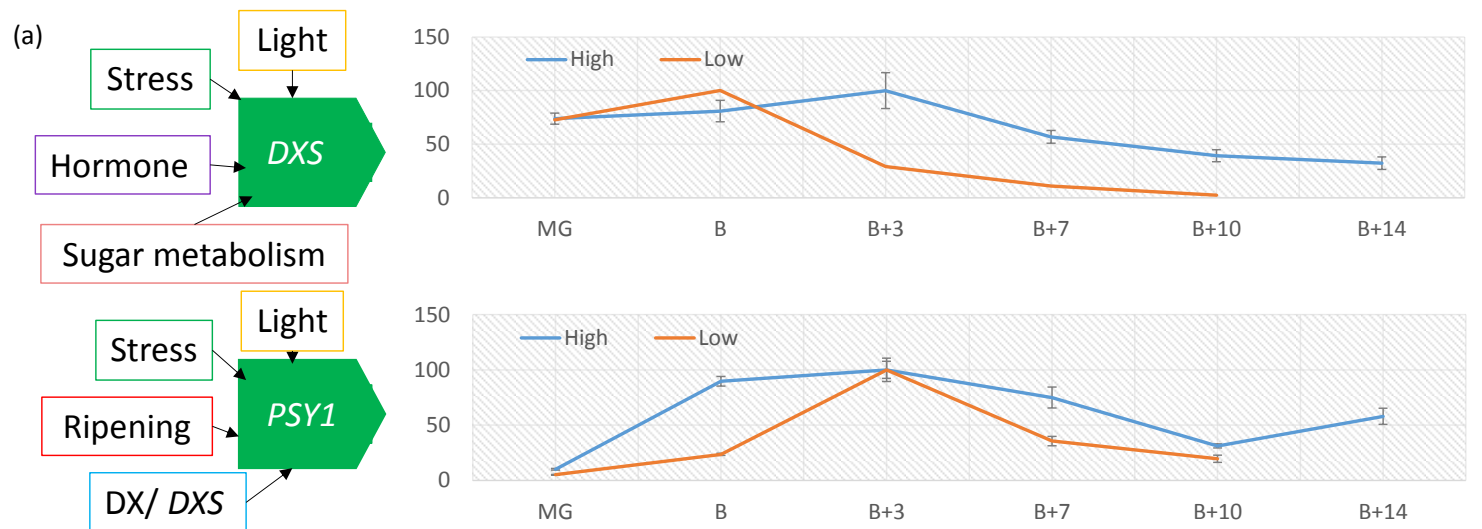
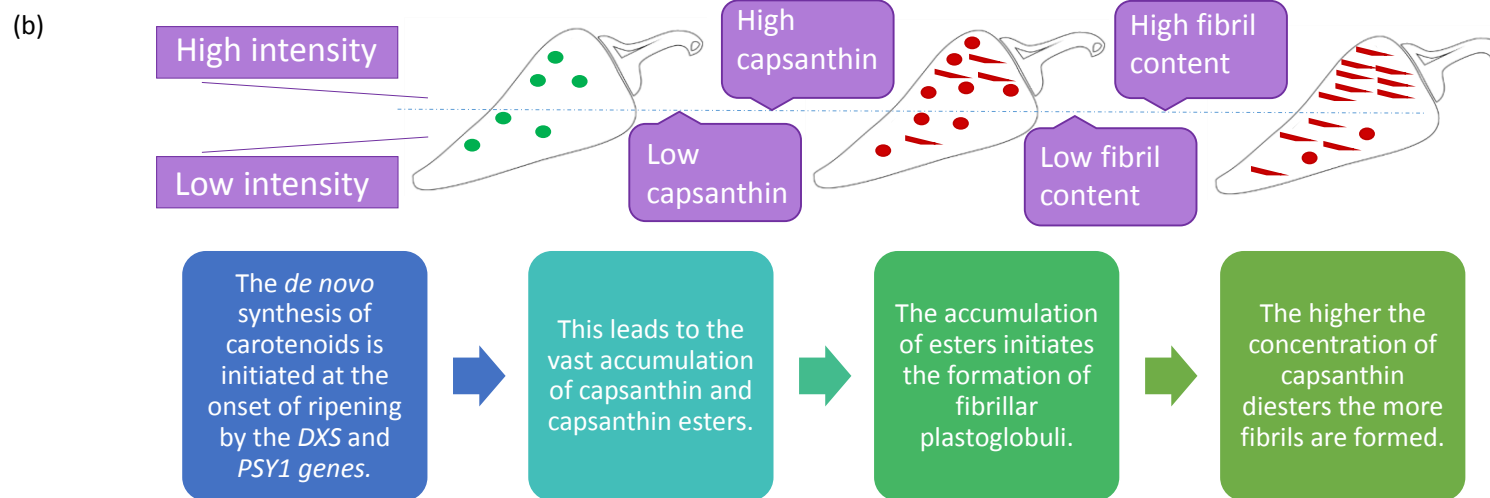


Figure 6.1. Colour intensity in red chilli pepper.

A schematic of the underlying mechanisms responsible for colour intensity at a metabolite and transcript level. (a) Represents the factors which affect expression of phytoene synthase -1 (*PSY1*) and deoxyxulose 5-phosphate (*DXS*) in chilli pepper and how high levels of expression for longer periods of time can lead to high levels of capsanthin accumulated. (b) Represents the accumulation of capsanthin and capsanthin esters associated with high and low colour intensity phenotype, and the relationship between concentration of esterified carotenoids and the formation of fibrillar plastoglobuli. Key: Fibrillar plastoglobuli (—) and globular plastoglobuli (●).



The differences in REs identified illustrated the presence of complex signalling pathways which synchronise fruit development and ripening with the accumulation of carotenoids at the onset of ripening, as well as in response to stress. The REs also demonstrated the different roles between these genes whereby *DXS* and *PSY2* have more links to primary metabolism and plant development when compared to *PSY1* which is a fruit specific gene expressed at the onset of ripening (Figure 6.1).

High intensity lines had a surprisingly low red to yellow carotenoid ratio when compared to the other lines in the colour diversity panel. These data were compared with the gene expression of key carotenoid biosynthetic genes analysed, such as *PSY1*, *DXS*, and *CCS*, as well as with the amount of free capsanthin accumulated. This exposed the presence of a negative regulatory feedback loop acting at the end of the carotenoid pathway in chilli pepper. Once the accumulated free capsanthin reached a certain threshold level, signalling to the plastid that free capsanthin was being created more rapidly than it could be esterified and stored, the *CCS* gene was down-regulated to stop further accumulation. However, this created a bottleneck in the high intensity lines analysed due to a large amount of substrate being supplied into the pathway. Therefore, these high intensity lines experienced an accumulation of yellow precursor carotenoids which was demonstrated by the decline in red to yellow ratio at the end of ripening. The low intensity line did not reach the threshold level to trigger the down-regulation of the *CCS* gene resulting in the *CCS* staying up-regulated throughout ripening; therefore, accumulation of yellow precursors did not occur and the red to yellow ratio did not decline (Figure 6.2).

The ripening rates of the colour diversity panel were also characterised as it was clear that some lines were ripening more slowly than others. Metabolic profiling revealed that the differences in ripening rate had a broader effect on metabolism than colour intensity phenotype. The slow ripening phenotype displayed higher levels of amino acids and higher levels of metabolites involved in nitrogen metabolism. Thus, the slow ripening rate of this line could lead to amino acids which have accumulated to be degraded when not utilised. The most striking difference in metabolites in the slow ripening line was the high levels of fatty acids which were accumulated when compared to the fast ripening lines. Very long chain fatty acids (VLCFA) associated with cell expansion in the cuticle were particularly prevalent possibly explaining the large fruit phenotype of the R7 line. The slow ripening line appeared to have a more oily cuticle than the fast ripening lines characterised by higher levels of VLCFAs and lower levels of alkane hydrocarbons.

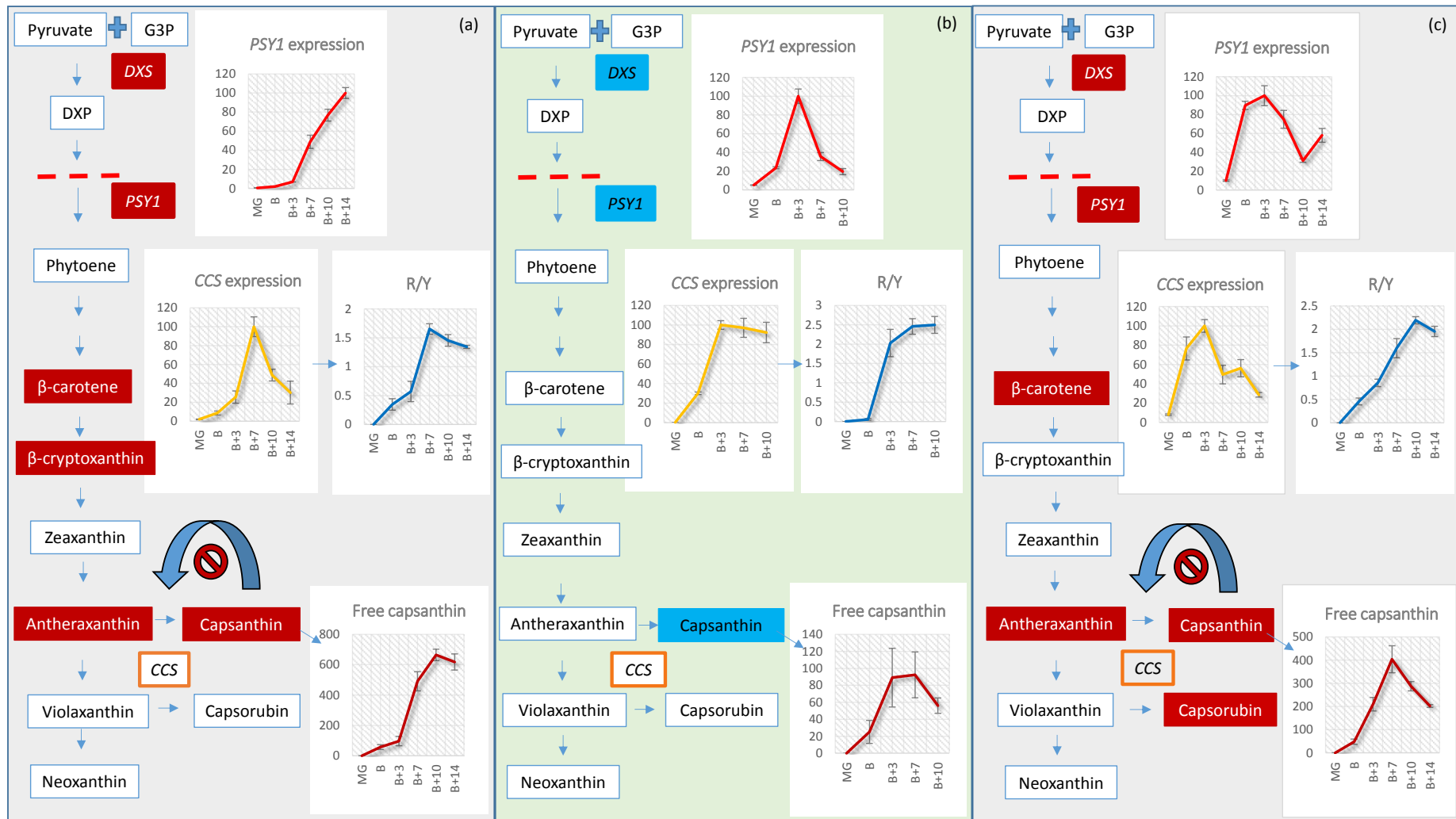


Figure 6.2. Regulatory mechanisms associated with the expression of the capsanthin capsorubin synthase (*CCS*) gene in red chilli pepper.

Figure 6.2. Regulatory mechanisms associated with the expression of the capsanthin capsorubin synthase (CCS) gene in red chilli pepper.

The expression profile of key carotenoid biosynthesis genes and carotenoid content were determined in red chilli pepper throughout ripening in selected lines. (a) R7 was a high intensity line which highly expressed *DXS* and *PSY1* providing a large substrate pool into the pathway. This resulted in the accumulation of high levels of free capsanthin. The amount of free capsanthin reached a threshold level which resulted in the down-regulation of the *CCS* gene caused a bottleneck at the end of the biosynthesis pathway. As the *PSY1* gene was still highly expressed at the end of ripening this led to the accumulation of yellow precursor carotenoids which causes a decrease in the red to yellow ratio at the end of ripening in this line. (b) R3 was a low intensity line which expressed *DXS* and *PSY1* at a low level resulting in the accumulation of low levels of free capsanthin. This did not reach the threshold level and so the *CCS* gene remains expressed until the end of ripening. Therefore, a bottleneck did not form at the end of the pathway, accumulation of yellow precursors did not occur and the red to yellow ratio did not decrease. (c) R1 is also a high intensity line with a highly expressed *PSY1*. However, when the free capsanthin levels reached a threshold and down-regulated the *CCS* gene, the *PSY1* expression was also down-regulated resulting in a smaller decrease in red to yellow ratio than when compared to the R7 line. Key: Red box represents an increase in gene or metabolite and blue represents a decrease, red dashed line represents the transition from the MEP pathway to the carotenoid pathway and the no entry symbol represents the down-regulation of the *CCS* gene. Abbreviations: *DXS*, 1-deoxy-D-xyulose 5-phosphate synthase; *G3P*, glyceraldehyde 3-phospahte; *DXP*, 1-deoxy-D-xyulose 5-phosphate; *PSY1*, phytoene synthase-1; *CCS*, capsanthin capsorubin synthase; and R/Y, ratio of red to yellow carotenoids.

This project has seen the complex levels of regulation present in the carotenoid biosynthesis pathway with developmental, environmental, and hormonal cues which may alter gene expression. In addition to genetic variation which can affect the expression of key biosynthesis genes. It has also been established that the metabolites themselves produced in the pathway can modulate how the genes are expressed, as well as influencing storage structures to adapt to increased production.

6.1.4. Colour retention

The image analysis technique used in this project allowed development of a protocol to aid colour loss in the colour diversity panel. This was achieved by grinding the chillies harvested and incubating at around 15-20°C in a light/ dark cycle for 6 weeks. However, attempts to evaluate the robustness of the image analysis technique using whole fruit stored over 9 months were unsuccessful. The chilli powder experiment identified the high retention R8 line as the most efficient line for retaining its colour throughout storage, followed by the other high retention lines, R1 and R11. It also characterised the R1 line as becoming better at retaining colour at high temperatures and the R6 line as the most efficient at retaining its red colour under UV light. The R2, R3, and R9 lines were classified as having low colour retention phenotypes.

Analysis of the volatile compounds present in fresh and dry fruit of the colour diversity panel allowed identification of characteristic compositions related to high and low colour intensity phenotypes. A notable discovery in this study was that the dry fruit of high retention lines reflected the chemical composition of the fresh fruit more than that of the dry, low retention lines. This was characterised by high levels of lipid derived volatiles present suggesting slower rates of lipid peroxidation in these lines. The low retention lines oxidise available lipids at a much faster rate when compared to the high intensity lines resulting in less lipid derived volatiles after three weeks of drying. The fresh fruit of the high retention lines also showed lower levels of carotenoid derived volatiles further reflecting the low levels of lipid peroxidation occurring in these lines. Mechanisms in place in these high retention lines were more efficient at maintaining the rate of lipid peroxidation at a manageable level whereby the antioxidant systems present can dissipate the formation of ROS effectively. This could be achieved by containing lower levels of unsaturated fatty acids in fibrillar plastoglobuli and chromoplast membranes, as well as, higher levels of hydrocarbons present in the cuticle preventing water loss. However, the low retention lines undergo lipid peroxidation at a level which cannot be maintained by the cells antioxidant defences, resulting in autooxidative processes rapidly degrading the lipids and carotenoids present. Another factor which implied the high rates of ROS production in these low retention phenotypes lines was the activity of the SOD enzyme. SOD activity was found to be more prevalent in the low intensity lines and it was thought that high levels of ROS production can directly recruit more SOD expression or activity. This could be true for the low retention lines. Alternatively, high levels of SOD activity which was not complemented by high levels of catalase activity could lead to the accumulation of hydrogen peroxide perpetuating ROS production in these low retention lines. Therefore, it was evident that colour retention

phenotype can be defined as a sum of oxidation rates versus antioxidant systems present. Variations in these factors led to the manifestation of the various colour retention phenotypes investigated in this study (5.22.).

The findings from this project have also confirmed there is no link between colour intensity and colour retention.

6.2. Relevance to current literature and applications

6.2.1. Colour intensity

In the chilli pepper industry the three most important traits are colour, size, and pungency. A colour which is deep red is most desirable to consumers as it is subconsciously related to the quality and nutritional content of the product. In this study it was found that the deep red colour was directly related to amount of capsanthin and capsanthin diesters present in the fruit. Capsanthin is a potent antioxidant and has many beneficial health properties due to quenching free radicals produced which can lead to diseased states. Therefore, producing chilli lines with high colour intensity phenotypes are not only profitable for the growers but better for the health of the consumers too. The in depth study of the colour diversity panel has allowed the selection of candidates which could be used in a breeding programme aimed at producing chilli pepper lines with high intensity phenotypes by enhancing capsanthin diester production but keeping undesirable traits to a minimum. The R7 line had the highest colour intensity phenotype but has some undesirable characteristics, such as slow ripening rate, low expression of *rsAcT*, and low red to yellow ratio in ripe fruit. Therefore, it could be crossed with the R1 line, as although this line was not as intensely red as R7, it did still carry a high intensity phenotype, fast ripening rate phenotype and a higher red to yellow ratio.

The information collected from this project can be used to select traits which would be beneficial to introduce into the domesticated chilli pepper gene pool. For example, discovery of a putative, ripening specific, xanthophyll acyl transferase can lead to development of a molecular marker which can be utilised to screen populations for high expressers of this gene. This would, therefore, benefit the chilli pepper industry as highly expressing carotenoid acyl transferases could be used as a tool for reducing the accumulation of end products which result in the down-regulation of the *CCS* gene. This would ultimately lead to higher red to yellow ratios which would stimulate red carotenoid production in the later stages of ripening and so boost colour intensity.

Identification of this enzyme could also lead to the discovery of the relationship between gene expression, carotenoid ester concentration, and fibril formation. The discovery that the fibril formation present in the chromoplasts was related to capsanthin content and highly expressed key biosynthetic genes in this study was concurrent with the present literature in describing that the concentration of specific esterified carotenoids may be essential for fibril formation (Deruère et al., 1994). As well as, the expression of the carotenoid biosynthesis genes. It has been suggested that a highly expressed *PSY1* may cause fibril formation in maize (Shumskaya et al., 2012). This, therefore, supports the notion that carotenoid biosynthesis genes trigger the expression of carotenoid sequestration related genes, such as fibrillin. It would be interesting to address the question, 'Do the fibrils form when this xanthophyll esterifying enzyme is knocked out in pepper or is it solely the expression of the carotenoid biosynthetic genes which trigger fibrillin expression?' It is, therefore, paramount that the esterification and sequestration processes are characterised more rigorously.

The regulatory mechanisms uncovered here in chilli pepper provide a more holistic picture of a very complex regulatory / homeostasis modulation. This study further supports the phenomenon of the negative feedback loop previously identified in tomato (Corona et al., 1996; Lois et al., 2000). This highlights the prominence of the role of the metabolites produced in the carotenoid pathway in terms of regulating gene expression. In particular, this is noteworthy in terms of transgenic plants altered to contain enhanced nutritional value. Improvement of sequestration mechanisms could lead to an overall increased carotenoid content by preventing the metabolites from accumulating to levels which result in the down-regulation of biosynthetic genes. This occurrence further highlights the presence of retrograde signalling from the chloroplast to the nuclear encoded genes, as seen previously in *Arabidopsis* (Xiao et al., 2012).

The relevance of the finding that the high intensity lines were expressing *PSY1* and *DXS* at a high level is of particular importance for genetic engineering approaches to produce crops with enhanced nutritional and industrial carotenoid contents. There has been a vast wealth of studies which have focused on using fruit specific promoters and bacterial genes to increase the amount of carotenoids in many crop plants including canola, rice, tomato, and potato. Particular interest in the field of enhancing the nutrient content in tomato has proved difficult as constitutively expressing *PSY1* led to deleterious effects on the plants vigour, as well as other problems whereby the endogenous genes were down-regulated in response to increased substrate production (Fray et al., 1995). Perhaps the use of a highly expressed *DXS* promoter from the chilli pepper in this study would lead to the strong expression of transgenes in a fruit specific manner. This strongly expressed *DXS* promoter, which appears to be deregulated from primary

metabolism, may also prove useful in molecular farming studies which use fruits as a vessel for recombinant protein or vaccine production. The highly expressed *DXS* promoter discovered may also prove useful in bacterial systems to enhance production of food colorants and dyes.

In terms of the putative regulatory elements identified in the promoter regions of the *PSY1*, *DXS*, and *PSY2*, these could help identify transcription factors which may be acting on the MEP and carotenoid biosynthesis pathway simultaneously. This could further strategies for altering carotenoid biosynthesis in crop plants as the absence of any known transcription factors which have a global effect on the MEP and carotenoid biosynthesis genes have yet to be discovered. The REs identified have similarities in both the phytoene synthases and *DXS* which implies there could be *trans*-acting factors which affect all three genes, particularly in response to light and stress.

Photosynthesis-related genes, isoprenoid biosynthesis genes, and responses to environmental, developmental, and metabolic cues are all known regulatory influences on the expression of *PSY*. Consequently REs identified in this study were analogous to known regulatory factors previously identified. The differences in REs determined in these genes accentuate the tissue specific qualities of these genes. The *PSY1* gene showed similar regulatory elements to other genes involved in ripening, whereas the *PSY2* showed REs which respond to hormonal signals related to plant development. The presence of W-box RE in the R7 could result in increased tolerance to drought stress. The RE was also found in the *Boea hygrometrica* and was found to be activated in drought stress in response to ABA. It would, therefore, be interesting to investigate the R7 line's tolerance to drought stress and possibly use this SNP to screen populations to breed plants more tolerant to drought.

The discovery of the difference in ripening rate impacts the chilli pepper industry in two aspects. On one hand, faster ripening lines are more desirable as growers can have reduced labour costs and decreased risks of disease. This means the chilli peppers can be harvested and dried more quickly in the preparation for producing chilli powder (Hornero-Méndez and Mínguez-Mosquera, 2000). Contrastingly, it is also important to consider that slow ripening rates may be beneficial in the fresh pepper industry for shelf life extension.

6.2.2. Colour retention

Identification of volatiles released in the high retention lines has enabled progress towards the identification of mechanisms relating to colour loss to be advanced. Selecting lines with high colour retention phenotypes can now be achieved at a faster rate thus advancing breeding programmes. This can be achieved by subjecting new populations to volatile analysis in dry fruit and selecting for lines with high levels of lipid derived volatiles. By implementing a much more accurate method of identifying high intensity lines, which can be analysed in sun dried fruit, the growers do not have to wait 9 months while storage experiments take place. This could also be conducted in conjunction with flavour/ taste studies to assess other important traits at the same time. Alternatively, if the volatile analysis of the chilli pepper fruit is too expensive or labour intensive then an image analysis approach can be applied. Incubating dry, ground material at 15-20°C in a light/ dark cycle can speed up the characterisation of retention phenotype from 9 month of storage to just 6 weeks.

This study also resulted in the elucidation of high retention lines which would be ideal candidates for breeding programmes in the optimisation of colour retention. The R8 line in particular performed significantly better than all other lines analysed and it is strongly recommended that future colour retention populations should involve this line. A cross with the high intensity, high retention line R1 would be interesting as it could lead to populations with higher colour retention and intensity. Or alternatively, a cross with the R7 and R8 lines may yield high pigment, high retention lines taking on more desirable traits from the parents, i.e. high capsanthin and fibril formation in R7 and the slow lipid peroxidation rates of R8. The SNPs identified to be characteristic in these high and low intensity lines, as well as possible genes which may be found to be related to colour retention phenotype, in the future can be used as molecular markers to allow marker assisted breeding to be carried out for the development of high intensity, high retention populations.

Other mechanisms which may act to protect against lipid peroxidation:

Discovery that the SOD enzyme was more active in the low colour retention lines suggested that the ROS produced in lipid peroxidation can provide signalling pathways to activate antioxidant processes. The activity of the SOD enzyme could perhaps be used as a marker for distinguishing between high and low retention lines. In addition, perhaps in the future, identification of the molecular component responsible for lower levels of unsaturated fatty acids found in the high retention line R1, can be applied to other crops which undergo post-harvest deterioration.

6.3. Future prospects and directions

Although findings from the studies described previously have illuminated many regulatory mechanisms involved in carotenoid biosynthesis in chilli pepper, there are still many levels of regulation which need to be addressed, such as post-translational regulation, carotenoid degradation processes, subchromoplast compartmentalisation, and enzyme activities. Additionally, there are many aspects of colour retention which have yet to be explored too. These involve a more in depth look at lipid composition, quantification of enzymatic antioxidant systems, and measurement of the rates of lipid peroxidation.

6.3.1. Genetic engineering

Analysis of the expression profiles of the *DXS* gene showed that the promoter region was highly expressed and fruit specific. Expression cassettes using this promoter region could be used to enhance production of ketocarotenoids in tomato fruit. Perhaps the R7 promoter region and *DXS*, in addition to bacterial β -carotene hydroxylase (*CrtZ*), and ketolase (*CrtW*), and the putative xanthophyll acyl transferase would prove an interesting construct. Maybe the optimisation of the esterification processes of the ketocarotenoids produced by maintaining the pool of parent carotenoid at a low level, will result in the carotenoid biosynthesis genes being expressed for longer, as well as more intensely. This is therefore an example of the how the *DXS* gene and promoter region could be exploited.

6.3.2. Regulatory mechanisms

This project has provided valuable information on the regulatory mechanisms present in chilli pepper at a transcriptional level. However, there are still many questions which remain to be answered. Based on the data provided by the transcription factor analysis, expression studies using the highly expressed R7 promoter of *DXS* would be useful. The promoter region of the R7 *DXS* gene could be fragmented and transiently expressed with a reporter gene to allow elucidation of the key regulatory elements contributing to colour intensity phenotype, perhaps relating a particular motif to the high levels of expression observed. Potentially the SNP found

in R7 could be used as a molecular marker in marker assisted breeding to identify lines which carry the mutated GAPF box, thus, enabling lines with highly expressed *DXS* genes to be identified more rapidly. The transcription factor GAPF binding factor, which binds the GAPF box, would need further investigation to understand the link between the sugar metabolism and isoprenoid biosynthesis.

Further characterisation of the sequence and expression pattern of this gene in response to ripening may prove to be valuable in understanding how carotenoid biosynthesis is synchronised with primary metabolism.

Electrophoretic mobility-shift assay (EMSA) or DNase I footprinting could be utilised to identify possible transcription factors, at identified key REs, controlling regulation of the carotenoid related genes. This would be useful for understanding the regulatory mechanisms involved in the expression of these key isoprenoid biosynthesis genes allowing identification of *trans*-acting factors operating in the isoprenoid and carotenoid pathways. Advances in tomato, in the creation of gene regulatory networks from global correlation analysis, provide good candidates for investigating ripening related transcription factors. The REs containing *RIN* transcription factor binding motifs offer an interesting area of study; or at a higher level, the *APRR2*-like transcription factor could be of relevance as this gene has already been shown to be related to pigmentation in pepper (Fujisawa et al., 2011; Pan et al., 2013).

Discovery of the affect that the accumulation of end-product metabolites has on the regulation of the biosynthetic genes poses the question of how these end-products initiate regulation of the nuclear genes. How does the plastid signal to the nucleus to modulate gene expression? Therefore, it would also be imperative to investigate how the metabolites of the carotenoid pathway go on to modulate gene expression by retrograde signalling.

There are a number of key areas where future work is required to advance our knowledge of carotenoid formation and accumulation in chilli peppers. For example, it would prove interesting to study the enzyme activity of *PSY1* and *DXS*. This would allow confirmation that the accumulation of the gene transcripts analysed is comparable to the enzyme activity and highlight possible post-translational regulatory mechanisms in play. In the future, the purity and protein composition of the membrane fractions, and other fractions will be carried out by western blotting using antibodies for enzymes/proteins that are known to be specific to subplastid compartments. Investigation of the protein profile and lipid profile associated with designated fractions/structures would also prove useful.

Another important experiment would be to carry out further enzyme activity studies to try and find the location of more carotenoid biosynthesis enzymes, particularly CCS, as well as the acyltransferase/s responsible for the esterification of carotenoids.

In terms of the esterification mechanisms present in chilli pepper the sequencing of the *rsAcT* and further characterisation on a transcript and protein level, would be interesting to carry out. Does this enzyme esterify carotenoids *in vitro*? Would expression of this gene in tomato fruit lead to the formation of carotenoid esters? And would repression of this gene in pepper lead to low levels of fibril formation? Although the last question may be more challenging to answer, due to the difficulties in transforming chilli pepper, hopefully advances in transformation techniques will lead to the discovery of suitable approaches in the not too distant future. For example, the recently described CRISPR-cas system of genome targeted editing may facilitate progression in this area (Shan et al., 2013). Moreover, if the knockout of this gene was successful in chilli pepper, or another fibril forming plant, then it would be interesting to compare the fibrillar fractions of a subchromoplast fractionation between a wild type and knockout line.

6.3.3. Lipidomics

The preliminary discoveries into the differences observed in the fatty acid composition of ripening fruit, as well as the differences observed in lipid derived volatiles present in the colour diversity panel have opened up new possible avenues to explore further. More detailed analysis of lipid compositions in chilli pepper fruit is essential for understanding the differences occurring between lines differing in colour retention phenotype. The analysis of lipid composition on fractions of a subchromoplast fractionation would be worthwhile to identify possible lipid profiles unique to the fibrillar and globular plastoglobuli, and profiles unique to high and low retention lines. It would also prove advantageous to investigate the lipid profiles of the carotenoid biosynthesis membranes. This may also prove useful when considering the differences in volatile composition in high and low retention lines. Perhaps the fatty acid composition of specific membranes are responsible for the slow rate of lipid peroxidation.

It would also be valuable to investigate the components of the cuticular wax. Analysis of the colour diversity panel revealed variations in composition of alkane hydrocarbons which could lead to prevention of water loss when air drying the chillies. The differences in cuticular wax were also noticeable when handling the chillies too. Therefore, a quantitative metabolomics approach would be useful here, carried out on the peel cuticle of the chilli pepper fruit.

In parallel with analysing the lipid composition it would be advantageous to measure the rate of lipid peroxidation taking place in high and low retention lines. This can be achieved by using thiobarbituric acid reactive substance (TBAR) assays. This assay measures the accumulation of fatty acid degradation products produced by lipid peroxidation, such as malondialdehyde. This will be helpful in understanding the differences seen in volatile composition present in the high and low retention lines.

6.3.4. Antioxidants and degradation

Comparison of the image analysis method with other known methods of colour quantification, such as pigment analysis and ASTA, would be beneficial to evaluate the robustness of the method. However, it is recommended that a large sample size is utilised in order to distinguish the differences between lines from the natural differences in colour within lines.

It would also be helpful to quantitatively measure the activities of enzymatic antioxidants present in the cell such as SOD, catalase, and peroxidases. These data would validate the model proposed in Figure 5.22 and help decipher whether the high levels of SOD observed in the low intensity lines are cause or effect.

Although the transcriptional regulation of carotenoid biosynthesis in response to different stimuli, plant development and end products, as well as genetic variation have been described in this project there are many avenues which have not been explored. The degradation of carotenoids by the NCED and CCD families requires addressing as they play a major role in the turnover of carotenoids. It would be interesting to see how these genes and enzyme activities could affect colour intensity and colour retention phenotypes in ripe fruit. Furthermore, although transcription factor analysis has provided information about the types of transcription factors and regulation that may be occurring it would be necessary to also consider epigenetic regulation.

In conclusion, the colour diversity panel supplied by Syngenta has resulted in the characterisation and identification of regulatory mechanisms on multiple levels in the carotenoid biosynthesis pathway. Thus, highlighting that the colour of chilli pepper is not the consequence of one single factor but the summation of complex, synchronised systems which have the ability to adapt and modulate at various levels of regulation, in response to environmental cues as well as genetic variations. This study has opened up many potential new

avenues of research in the colour intensity of the chilli pepper and other fruits, plus has expanded and supported already established ideas in carotenoid biosynthesis. Therefore highlighting the importance of the effects of the carotenoid pathway metabolites on esterification and sequestration mechanisms. As well as focusing on the regulation of the biosynthetic genes.

This project has also progressed the knowledge of what determines colour retention phenotype in chilli pepper. Although, as with colour intensity, there are multiple, complex systems operating simultaneously which result in the degradation of colour. Thus, emphasising that colour retention is a manifestation of antioxidant systems in combat against the production of destructive free radicals. However, it does appear that the high retention lines studied in this project have more efficient mechanisms for slowing lipid peroxidation rates, which provides an optimistic path towards to the identification of the major components acting in colour retention in chilli pepper.

A table displaying the key outcomes and future directions can be found in the appendix (Table A3.1).

Appendices

Appendix 1:

	1	10	20	30	40	50	60	70	80	90	100	110	120	130
PSY1_R3_gDNA PSY1_R7_gDNA Consensus	GTTGGCTACTGGGCGGAGCTAGAGTATCAGTTACGGATTAGTTGARTTAGTAGCTAGCTTAAACCCGTARACATAGTACTTAAARATTTGTAARATTTAGACATCAAACTTCAAAATTTGA TGTGGCTACTGGGCGGAGCTAGAGTATCAGTTACGGATTAGTTGARTTAGTAGCTAGCTTAAACCCGTARACATAGTACTTAAARATTTGTAARATTTAGACATCAAACTTCAAAATTTGA GTTGGCTACTGGGCGGAGCTAGAGTATCAGTTACGGATTAGTTGARTTAGTAGCTAGCTTAAACCCGTARACATAGTACTTAAARATTTGTAARATTTAGACATCAAACTTCAAAATTTGA													
PSY1_R3_gDNA PSY1_R7_gDNA Consensus	CTCAATACATTTCTGATATCAAAAGTGCARTCTTGACATCTGTGTGGCTTTTATGCTATGGTTGCGCCTGTTGCTATACATGGGCGGATCAGAGTGTAGTACGGGTTAGTGTGARTTCA CTCAATACATTTCTGATATCAAAAGTGCARTCTTGACATCTGTGTGGCTTTTATGCTATGGTTGCGCCTGTTGCTATACATGGGCGGATCAGAGTGTAGTACGGGTTAGTGTGARTTCA CTCAATACATTTCTGATATCAAAAGTGCARTCTTGACATCTGTGTGGCTTTTATGCTATGGTTGCGCCTGTTGCTATACATGGGCGGATCAGAGTGTAGTACGGGTTAGTGTGARTTCA													
PSY1_R3_gDNA PSY1_R7_gDNA Consensus	GTARCTTAGTTCARACCCCGTATGTTTACTTAGAARATTAGAATTTAGAACCTAARATTTCAAAATTTGGTTCGTACATTTCTGATATTAARATTTGCARTCTTGACATCTCTGTGGCTC GTARCTTAGTTCARACCCCGTATGTTTACTTAGAARATTAGAATTTAGAACCTAARATTTCAAAATTTGGTTCGTACATTTCTGATATTAARATTTGCARTCTTGACATCTCTGTGGCTC GTARCTTAGTTCARACCCCGTATGTTTACTTAGAARATTAGAATTTAGAACCTAARATTTCAAAATTTGGTTCGTACATTTCTGATATTAARATTTGCARTCTTGACATCTCTGTGGCTC													
PSY1_R3_gDNA PSY1_R7_gDNA Consensus	TTTATGCTATGGTAGTGTGCTTGTGCTATACAGGGGAGGAGCTAGAGTGCARTTAGGTTGGTGTGARTTAGTAGTACTTATGCTCAACCCCATACAGTGTAAACCTAGAARATTAGAATTTA TTTATGCTATGGTAGTGTGCTTGTGCTATACAGGGGAGGAGCTAGAGTGCARTTAGGTTGGTGTGARTTAGTAGTACTTATGCTCAACCCCATACAGTGTAAACCTAGAARATTAGAATTTA TTTATGCTATGGTAGTGTGCTTGTGCTATACAGGGGAGGAGCTAGAGTGCARTTAGGTTGGTGTGARTTAGTAGTACTTATGCTCAACCCCATACAGTGTAAACCTAGAARATTAGAATTTA													
PSY1_R3_gDNA PSY1_R7_gDNA Consensus	GAACCTAARACTTCAAAATTTGACTCGTTACATTTCTGATATCAAGAGTGCARTCTTGACATCTGTGTGACATTTCTATGCTATGTAAGTGTGTTGTTGCTATACAGGGGAGGAGCTAGAGT GAACCTAARACTTCAAAATTTGACTCGTTACATTTCTGATATCAAGAGTGCARTCTTGACATCTGTGTGACATTTCTATGCTATGTAAGTGTGTTGTTGCTATACAGGGGAGGAGCTAGAGT GAACCTAARACTTCAAAATTTGACTCGTTACATTTCTGATATCAAGAGTGCARTCTTGACATCTGTGTGACATTTCTATGCTATGTAAGTGTGTTGTTGCTATACAGGGGAGGAGCTAGAGT													
PSY1_R3_gDNA PSY1_R7_gDNA Consensus	GTGAGTATGATGATTCAGTGTGARTTCAGTAGCTTGGTTCARACCCCATACATAGTACTTAAARATTTGTAARATTTAGAACCTAARACTTCAAAATTTGGTTCGTACATTTCTGATATCAAAAGT GTGAGTATGATGATTCAGTGTGARTTCAGTAGCTTGGTTCARACCCCATACATAGTACTTAAARATTTGTAARATTTAGAACCTAARACTTCAAAATTTGGTTCGTACATTTCTGATATCAAAAGT GTGAGTATGATGATTCAGTGTGARTTCAGTAGCTTGGTTCARACCCCATACATAGTACTTAAARATTTGTAARATTTAGAACCTAARACTTCAAAATTTGGTTCGTACATTTCTGATATCAAAAGT													
PSY1_R3_gDNA PSY1_R7_gDNA Consensus	TGCARTCTTGACATCTCTGGGCTTTTATGCTATGGTTGCTGCTGTTGCTATACATGGGCGGAGCTAGAGTGTAGTACGGGTTAGTGTGARTTAGTAGGTTAGTGTGACAGCCCGTAAATTT TGCARTCTTGACATCTCTGGGCTTTTATGCTATGGTTGCTGCTGTTGCTATACATGGGCGGAGCTAGAGTGTAGTACGGGTTAGTGTGARTTAGTAGGTTAGTGTGACAGCCCGTAAATTT TGCARTCTTGACATCTCTGGGCTTTTATGCTATGGTTGCTGCTGTTGCTATACATGGGCGGAGCTAGAGTGTAGTACGGGTTAGTGTGARTTAGTAGGTTAGTGTGACAGCCCGTAAATTT													
PSY1_R3_gDNA PSY1_R7_gDNA Consensus	GTARCTTAAARACTTAGAATTTGACCCATCAAGTTCARATTTGACTCGGTCGACTCTAGATGATTAARATTTCAAAATTTGGTTCGTACATTTCTGATATCAAAAGT GTARCTTAAARACTTAGAATTTGACCCATCAAGTTCARATTTGACTCGGTCGACTCTAGATGATTAARATTTCAAAATTTGGTTCGTACATTTCTGATATCAAAAGT GTARCTTAAARACTTAGAATTTGACCCATCAAGTTCARATTTGACTCGGTCGACTCTAGATGATTAARATTTCAAAATTTGGTTCGTACATTTCTGATATCAAAAGT													
PSY1_R3_gDNA PSY1_R7_gDNA Consensus	GCTATACAGGGGCGGAGCTAGAGTGTAGTGCARTTCAGTAGCTTGGTTCARACCCCATACATAGTACTTAAARATTTGTAARATTTAGAACCCCATACAACTTCAAAATTTAGCTCCGACTATACAA GCTATACAGGGGCGGAGCTAGAGTGTAGTGCARTTCAGTAGCTTGGTTCARACCCCATACATAGTACTTAAARATTTGTAARATTTAGAACCCCATACAACTTCAAAATTTAGCTCCGACTATACAA GCTATACAGGGGCGGAGCTAGAGTGTAGTGCARTTCAGTAGCTTGGTTCARACCCCATACATAGTACTTAAARATTTGTAARATTTAGAACCCCATACAACTTCAAAATTTAGCTCCGACTATACAA													
PSY1_R3_gDNA PSY1_R7_gDNA Consensus	GATATGARTTTGAGAGTGGCTTAAARATTTAGTGTCCATGTTAGTGGGAGGACCAATATCAGAGGTTGTTCCCTTCACCTCTGATATACAGTGTGCAATGCTTACCTGCTGACTTCTATTC GATATGARTTTGAGAGTGGCTTAAARATTTAGTGTCCATGTTAGTGGGAGGACCAATATCAGAGGTTGTTCCCTTCACCTCTGATATACAGTGTGCAATGCTTACCTGCTGACTTCTATTC GATATGARTTTGAGAGTGGCTTAAARATTTAGTGTCCATGTTAGTGGGAGGACCAATATCAGAGGTTGTTCCCTTCACCTCTGATATACAGTGTGCAATGCTTACCTGCTGACTTCTATTC													
PSY1_R3_gDNA PSY1_R7_gDNA Consensus	CACTGCTAGTGTGCTTGTGCTATACAGGGGAGGAGCTAGAGTGTAGTACGGGTTGGTGCARTTAGTAGGGGAGCCGGTCACTACAGCTCCCGCTATGCGCAGGGTGGCGGAGGGGCGGACCA CACTGCTAGTGTGCTTGTGCTATACAGGGGAGGAGCTAGAGTGTAGTACGGGTTGGTGCARTTAGTAGGGGAGCCGGTCACTACAGCTCCCGCTATGCGCAGGGTGGCGGAGGGGCGGACCA CACTGCTAGTGTGCTTGTGCTATACAGGGGAGGAGCTAGAGTGTAGTACGGGTTGGTGCARTTAGTAGGGGAGCCGGTCACTACAGCTCCCGCTATGCGCAGGGTGGCGGAGGGGCGGACCA													
PSY1_R3_gDNA PSY1_R7_gDNA Consensus	CARGACTCTTTACATTTTTCARAGGACTGTTCCACGCTTGARCCGGGAGCTCCGACTAGTACTAGARTTCAGTAGCTTAGTTCAGARTCCACAACTTCAAAATTTAGCTCCGCTACTAGTAGCT CARGACTCTTTACATTTTTCARAGGACTGTTCCACGCTTGARCCGGGAGCTCCGACTAGTACTAGARTTCAGTAGCTTAGTTCAGARTCCACAACTTCAAAATTTAGCTCCGCTACTAGTAGCT CARGACTCTTTACATTTTTCARAGGACTGTTCCACGCTTGARCCGGGAGCTCCGACTAGTACTAGARTTCAGTAGCTTAGTTCAGARTCCACAACTTCAAAATTTAGCTCCGCTACTAGTAGCT													
PSY1_R3_gDNA PSY1_R7_gDNA Consensus	ATAAATATAGAAATGAGCACTTGCCTTAGAATAGCTTCAGCTGACCAAAATTAGAAGTGGGAGGCTTATATARTACTAGTGTACTAAATATAGAAAGTCCCAATCTCCAGAGGTTG ATAAATATAGAAATGAGCACTTGCCTTAGAATAGCTTCAGCTGACCAAAATTAGAAGTGGGAGGCTTATATARTACTAGTGTACTAAATATAGAAAGTCCCAATCTCCAGAGGTTG ATAAATATAGAAATGAGCACTTGCCTTAGAATAGCTTCAGCTGACCAAAATTAGAAGTGGGAGGCTTATATARTACTAGTGTACTAAATATAGAAAGTCCCAATCTCCAGAGGTTG													
PSY1_R3_gDNA PSY1_R7_gDNA Consensus	ATCCACTTGTGCTTCAATAGTGTAAATAGTTTCTCAAACTCCTCTTGTGCGCATTGGTAGGTAGAGTGTGCTTTGCTGCTGTTTGGAGATGTTTTTAAAGTAAATTTGTTATACCTAG ATCCACTTGTGCTTCAATAGTGTAAATAGTTTCTCAAACTCCTCTTGTGCGCATTGGTAGGTAGAGTGTGCTTTGCTGCTGTTTGGAGATGTTTTTAAAGTAAATTTGTTATACCTAG ATCCACTTGTGCTTCAATAGTGTAAATAGTTTCTCAAACTCCTCTTGTGCGCATTGGTAGGTAGAGTGTGCTTTGCTGCTGTTTGGAGATGTTTTTAAAGTAAATTTGTTATACCTAG													
PSY1_R3_gDNA PSY1_R7_gDNA Consensus	GARGCTATATGCTGGTACGAGTTCATGTGAACCTAGTAGTTTCGCTAGCAATCCACTATATCTAARATTTGACCGTGAACCTCCGCTGATCATTTCAATACCTTAGGCTCCTATAGGAG GARGCTATATGCTGGTACGAGTTCATGTGAACCTAGTAGTTTCGCTAGCAATCCACTATATCTAARATTTGACCGTGAACCTCCGCTGATCATTTCAATACCTTAGGCTCCTATAGGAG GARGCTATATGCTGGTACGAGTTCATGTGAACCTAGTAGTTTCGCTAGCAATCCACTATATCTAARATTTGACCGTGAACCTCCGCTGATCATTTCAATACCTTAGGCTCCTATAGGAG													
PSY1_R3_gDNA PSY1_R7_gDNA Consensus	CCGAARCTCCCACTTCTGARTCAGTTTTGTTATACCTAGTATGATTTGGTTATCTCATATTCGAGAGCCAGAAATAGGTTATTTCTTGTGATAGTGGAGATATCTAGTGGGAA CCGAARCTCCCACTTCTGARTCAGTTTTGTTATACCTAGTATGATTTGGTTATCTCATATTCGAGAGCCAGAAATAGGTTATTTCTTGTGATAGTGGAGATATCTAGTGGGAA CCGAARCTCCCACTTCTGARTCAGTTTTGTTATACCTAGTATGATTTGGTTATCTCATATTCGAGAGCCAGAAATAGGTTATTTCTTGTGATAGTGGAGATATCTAGTGGGAA													
PSY1_R3_gDNA PSY1_R7_gDNA Consensus	TCTACTAGGAGTACTATTTCTATARAAGAGCAAAACCTGGAGTTGCTTAGACACCAAGGTTTTCTGCTCAGARTGCTGTGCTCTGTTATGGGTTGTTCTCTTGTGAGCTCCTCAAAAC TCTACTAGGAGTACTATTTCTATARAAGAGCAAAACCTGGAGTTGCTTAGACACCAAGGTTTTCTGCTCAGARTGCTGTGCTCTGTTATGGGTTGTTCTCTTGTGAGCTCCTCAAAAC TCTACTAGGAGTACTATTTCTATARAAGAGCAAAACCTGGAGTTGCTTAGACACCAAGGTTTTCTGCTCAGARTGCTGTGCTCTGTTATGGGTTGTTCTCTTGTGAGCTCCTCAAAAC													
PSY1_R3_gDNA PSY1_R7_gDNA Consensus	GGGACGAGTCTTGGTATCCGTCGAGGGGAAACCGAATTTTGTTCGTCGGGGCTAGGAAATTTGGCGTGCARTGAGAGAACTAGAGAGAGGGTGGAAACCAAGGTTGGAGTTTGGTCTTACT GGGACGAGTCTTGGTATCCGTCGAGGGGAAACCGAATTTTGTTCGTCGGGGCTAGGAAATTTGGCGTGCARTGAGAGAACTAGAGAGAGGGTGGAAACCAAGGTTGGAGTTTGGTCTTACT GGGACGAGTCTTGGTATCCGTCGAGGGGAAACCGAATTTTGTTCGTCGGGGCTAGGAAATTTGGCGTGCARTGAGAGAACTAGAGAGAGGGTGGAAACCAAGGTTGGAGTTTGGTCTTACT													
PSY1_R3_gDNA PSY1_R7_gDNA Consensus	TGGAGGAGCAAACTGAGAGTGGACGAAATTTCTGTACTGCTGCTATCGTCCGCTAGGAAATTTGGCGTGCARTGAGAGAACTAGAGAGAGGGTGGAAACCAAGGTTGGAGTTTGGTCTTACT TGGAGGAGCAAACTGAGAGTGGACGAAATTTCTGTACTGCTGCTATCGTCCGCTAGGAAATTTGGCGTGCARTGAGAGAACTAGAGAGAGGGTGGAAACCAAGGTTGGAGTTTGGTCTTACT TGGAGGAGCAAACTGAGAGTGGACGAAATTTCTGTACTGCTGCTATCGTCCGCTAGGAAATTTGGCGTGCARTGAGAGAACTAGAGAGAGGGTGGAAACCAAGGTTGGAGTTTGGTCTTACT													
PSY1_R3_gDNA PSY1_R7_gDNA Consensus	GGTGARGAGACGCTGAGATCGCCAGTGGTATGATGTGARGAGGATATACCTATTCGCGGAGCTTGGGCTGTTGAGTGAAGCATATGATAGGCTGATGARGATGTGCGAGATCCCAAGAGCG GGTGARGAGACGCTGAGATCGCCAGTGGTATGATGTGARGAGGATATACCTATTCGCGGAGCTTGGGCTGTTGAGTGAAGCATATGATAGGCTGATGARGATGTGCGAGATCCCAAGAGCG GGTGARGAGACGCTGAGATCGCCAGTGGTATGATGTGARGAGGATATACCTATTCGCGGAGCTTGGGCTGTTGAGTGAAGCATATGATAGGCTGATGARGATGTGCGAGATCCCAAGAGCG													

2601	2610	2620	2630	2640	2650	2660	2670	2680	2690	2700	2710	2720	2730
PSY1_R3_gDNA	TTTACTTAGGTAGCTCTTATCTATCCGTCGTTACCAATCTATATATGCTTGTATGATCTGATGAGACAAATTTGATCTTGGTTGGTTATTCAGGACATGCTATGACTCCGAGAA												
PSY1_R7_gDNA	TTTACTTAGGTAGCTCTTATCTATCCGTCGTTACCAATCTATATATGCTTGTATGATCTGATGAGACAAATTTGATCTTGGTTGGTTATTCAGGACATGCTATGACTCCGAGAA												
Consensus	TTTACTTAGGTAGCTCTTATCTATCCGTCGTTACCAATCTATATATGCTTGTATGATCTGATGAGACAAATTTGATCTTGGTTGGTTATTCAGGACATGCTATGACTCCGAGAA												
2731	2740	2750	2760	2770	2780	2790	2800	2810	2820	2830	2840	2850	2860
PSY1_R3_gDNA	GAGGAAAGGCTATCGGGCAATATACGGTAGGATTTAGCCATGTTGTATCAGATACACACTAACACATATGATTAATCGGACGAGAAAGAAAGACTAGATTTGAGTTGAGGGTCACCACTGA												
PSY1_R7_gDNA	GAGGAAAGGCTATCGGGCAATATACGGTAGGATTTAGCCATGTTGTATCAGATACACACTAACACATATGATTAATCGGACGAGAAAGAAAGACTAGATTTGAGTTGAGGGTCACCACTGA												
Consensus	GAGGAAAGGCTATCGGGCAATATACGGTAGGATTTAGCCATGTTGTATCAGATACACACTAACACATATGATTAATCGGACGAGAAAGAAAGACTAGATTTGAGTTGAGGGTCACCACTGA												
2861	2870	2880	2890	2900	2910	2920	2930	2940	2950	2960	2970	2980	2990
PSY1_R3_gDNA	TACGTAARATCTGAGTTTCCACTAGCTTGAAGGATCGTAGAGGTTTATGTCATATCAGCTTATCTTACATGATTCGAGAGGTTCCGGTATTCATATATACACAACTTCGTGAGTGGAT												
PSY1_R7_gDNA	TACGTAARATCTGAGTTTCCACTAGCTTGAAGGATCGTAGAGGTTTATGTCATATCAGCTTATCTTACATGATTCGAGAGGTTCCGGTATTCATATATACACAACTTCGTGAGTGGAT												
Consensus	TACGTAARATCTGAGTTTCCACTAGCTTGAAGGATCGTAGAGGTTTATGTCATATCAGCTTATCTTACATGATTCGAGAGGTTCCGGTATTCATATATACACAACTTCGTGAGTGGAT												
2991	3000	3010	3020	3030	3040	3050	3060	3070	3080	3090	3100	3110	3120
PSY1_R3_gDNA	AGTTTCTCATATCTGCTGTTTAAACAGTATGGTCGAGGACACAGCAACTTGTGATGGTCCGATGCATCACACTTACCCGGCCCTAGATAGTGGGAGACAGGCTAGAGATGTTTTCAC												
PSY1_R7_gDNA	AGTTTCTCATATCTGCTGTTTAAACAGTATGGTCGAGGACACAGCAACTTGTGATGGTCCGATGCATCACACTTACCCGGCCCTAGATAGTGGGAGACAGGCTAGAGATGTTTTCAC												
Consensus	AGTTTCTCATATCTGCTGTTTAAACAGTATGGTCGAGGACACAGCAACTTGTGATGGTCCGATGCATCACACTTACCCGGCCCTAGATAGTGGGAGACAGGCTAGAGATGTTTTCAC												
3121	3130	3140	3150	3160	3170	3180	3190	3200	3210	3220	3230	3240	3250
PSY1_R3_gDNA	GTGAGCGCCATTTGACATGCTCATGCTGCTTTGTCGACACAGTTCCAAATTTCCAGTTGATATCAGGTTAGTCTCCATCTATGATCTTTATCTTTGTTGATTCAGAGTCTACGTCGCTT												
PSY1_R7_gDNA	GTGAGCGCCATTTGACATGCTCATGCTGCTTTGTCGACACAGTTCCAAATTTCCAGTTGATATCAGGTTAGTCTCCATCTATGATCTTTATCTTTGTTGATTCAGAGTCTACGTCGCTT												
Consensus	GTGAGCGCCATTTGACATGCTCATGCTGCTTTGTCGACACAGTTCCAAATTTCCAGTTGATATCAGGTTAGTCTCCATCTATGATCTTTATCTTTGTTGATTCAGAGTCTACGTCGCTT												
3251	3260	3270	3280	3290	3300	3310	3320	3330	3340	3350	3360	3370	3380
PSY1_R3_gDNA	AGCTGAACTGTTCCGATGGATCTCGTATCTTTCATCTCCACAGAAATGCTTTAGTGGATCAGTCCCTCGCTCAGATTACGCTGATCTCGGTTTCTGTTTACAGTCTTCCGAACTCT												
PSY1_R7_gDNA	AGCTGAACTGTTCCGATGGATCTCGTATCTTTCATCTCCACAGAAATGCTTTAGTGGATCAGTCCCTCGCTCAGATTACGCTGATCTCGGTTTCTGTTTACAGTCTTCCGAACTCT												
Consensus	AGCTGAACTGTTCCGATGGATCTCGTATCTTTCATCTCCACAGAAATGCTTTAGTGGATCAGTCCCTCGCTCAGATTACGCTGATCTCGGTTTCTGTTTACAGTCTTCCGAACTCT												
3381	3390	3400	3410	3420	3430	3440	3450	3460	3470	3480	3490	3500	3510
PSY1_R3_gDNA	TGTTTTTCACCTTTGGTGTGCTTCCACTACACTTTTGGCTCGTTCCTGGACAGATACATTTTCATTCACATATTTGATTTGCTTCTTCACACAGTAAATTTTATCTTATCTTCGATAT												
PSY1_R7_gDNA	TGTTTTTCACCTTTGGTGTGCTTCCACTACACTTTTGGCTCGTTCCTGGACAGATACATTTTCATTCACATATTTGATTTGCTTCTTCACACAGTAAATTTTATCTTATCTTCGATAT												
Consensus	TGTTTTTCACCTTTGGTGTGCTTCCACTACACTTTTGGCTCGTTCCTGGACAGATACATTTTCATTCACATATTTGATTTGCTTCTTCACACAGTAAATTTTATCTTATCTTCGATAT												
3511	3520	3530	3540	3550	3560	3570	3580	3590	3600	3610	3620	3630	3640
PSY1_R3_gDNA	ATGTTGACGCCATTCAGAGATATGATGAGGATGCGTATGGCTTGGAGAGTCAGATACAGAACTTGGACAACTATACCTATATGTTATTCGTTGCTGGTCCGTTGGTGGTGGTGGTGGT												
PSY1_R7_gDNA	ATGTTGACGCCATTCAGAGATATGATGAGGATGCGTATGGCTTGGAGAGTCAGATACAGAACTTGGACAACTATACCTATATGTTATTCGTTGCTGGTCCGTTGGTGGTGGTGGTGGT												
Consensus	ATGTTGACGCCATTCAGAGATATGATGAGGATGCGTATGGCTTGGAGAGTCAGATACAGAACTTGGACAACTATACCTATATGTTATTCGTTGCTGGTCCGTTGGTGGTGGTGGTGGT												
3641	3650	3660	3670	3680	3690	3700	3710	3720	3730	3740	3750	3760	3770
PSY1_R3_gDNA	CAATTTGGGATCGCACTGATCAAGGACACAGCGAGAGCGTATATATGCTGCTTGGCTTGGGATCGCAACTGACCACTATACAGATGTTGGAGAGAGTAGTACACAGATA												
PSY1_R7_gDNA	CAATTTGGGATCGCACTGATCAAGGACACAGCGAGAGCGTATATATGCTGCTTGGCTTGGGATCGCAACTGACCACTATACAGATGTTGGAGAGAGTAGTACACAGATA												
Consensus	CAATTTGGGATCGCACTGATCAAGGACACAGCGAGAGCGTATATATGCTGCTTGGCTTGGGATCGCAACTGACCACTATACAGATGTTGGAGAGAGTAGTACACAGATA												
3771	3780	3790	3800	3810	3820	3830	3840	3850	3860	3870	3880	3890	3900
PSY1_R3_gDNA	CATTTTATGCACATCAAAAGATTGCTACACCTGCTCCTCGACGCTTATCACTTAAAGAGATTCGATTTAGTTATCTTCAGGCCCAAAATTTTCATGCTGGGATCTTCCGCCCTGCACATATA												
PSY1_R7_gDNA	CATTTTATGCACATCAAAAGATTGCTACACCTGCTCCTCGACGCTTATCACTTAAAGAGATTCGATTTAGTTATCTTCAGGCCCAAAATTTTCATGCTGGGATCTTCCGCCCTGCACATATA												
Consensus	CATTTTATGCACATCAAAAGATTGCTACACCTGCTCCTCGACGCTTATCACTTAAAGAGATTCGATTTAGTTATCTTCAGGCCCAAAATTTTCATGCTGGGATCTTCCGCCCTGCACATATA												
3901	3910	3920	3930	3940	3950	3960	3970	3980	3990	4000	4010	4020	4030
PSY1_R3_gDNA	GACTTGCACAGGACAGCTTCAATCGCTTTCCCTTTCCTTTCATGAGTACATATTTGCTCTTARGGCTTCCCTTTCATATATGCTTCCGTCGAGTCCAGAGAGAGAGGCTATTTTG												
PSY1_R7_gDNA	GACTTGCACAGGACAGCTTCAATCGCTTTCCCTTTCCTTTCATGAGTACATATTTGCTCTTARGGCTTCCCTTTCATATATGCTTCCGTCGAGTCCAGAGAGAGAGGCTATTTTG												
Consensus	GACTTGCACAGGACAGCTTCAATCGCTTTCCCTTTCCTTTCATGAGTACATATTTGCTCTTARGGCTTCCCTTTCATATATGCTTCCGTCGAGTCCAGAGAGAGAGGCTATTTTG												
4031	4040	4050	4060	4070	4080	4090	4100	4110	4120	4130	4140	4150	4160
PSY1_R3_gDNA	CTCAGATGATTTAGCAGCGGAGCTTATCCGACAGACATATTTGCTGAGAGATGACCGATTAATGAGAACTTCATGAGAAACAAATTCAGAGGACAGAACTTTCGACAGGACAGAA												
PSY1_R7_gDNA	CTCAGATGATTTAGCAGCGGAGCTTATCCGACAGACATATTTGCTGAGAGATGACCGATTAATGAGAACTTCATGAGAAACAAATTCAGAGGACAGAACTTTCGACAGGACAGAA												
Consensus	CTCAGATGATTTAGCAGCGGAGCTTATCCGACAGACATATTTGCTGAGAGATGACCGATTAATGAGAACTTCATGAGAAACAAATTCAGAGGACAGAACTTTCGACAGGACAGAA												
4161	4170	4180	4190	4200	4210	4220	4230	4240	4250	4260	4270	4280	4290
PSY1_R3_gDNA	AAGAGTGCACGATTTAGGCGAGCTAGTAGTGGCTGTAGGATTCATTAACACTCTAGTTTATGATATGATTCCTTCCCTTCCGCTTTCGAGTACAGTGTCCGAGGAGGCTTGGCTTGTGGCTA												
PSY1_R7_gDNA	AAGAGTGCACGATTTAGGCGAGCTAGTAGTGGCTGTAGGATTCATTAACACTCTAGTTTATGATATGATTCCTTCCCTTCCGCTTTCGAGTACAGTGTCCGAGGAGGCTTGGCTTGTGGCTA												
Consensus	AAGAGTGCACGATTTAGGCGAGCTAGTAGTGGCTGTAGGATTCATTAACACTCTAGTTTATGATATGATTCCTTCCCTTCCGCTTTCGAGTACAGTGTCCGAGGAGGCTTGGCTTGTGGCTA												
4291	4300	4310	4320	4330	4340	4350	4360	4370	4380	4390	4400	4410	4420
PSY1_R3_gDNA	GACATACATAGCGCTGCGGACACTGCCATACCGGCTCACCTCCAGGATGCTGGGACAGAGGAGGATGGTGGTGGCTGATACCACTGTTAGCTATAGGTTGGAGAGCCGAGGCTATTAATA												
PSY1_R7_gDNA	GACATACATAGCGCTGCGGACACTGCCATACCGGCTCACCTCCAGGATGCTGGGACAGAGGAGGATGGTGGTGGCTGATACCACTGTTAGCTATAGGTTGGAGAGCCGAGGCTATTAATA												
Consensus	GACATACATAGCGCTGCGGACACTGCCATACCGGCTCACCTCCAGGATGCTGGGACAGAGGAGGATGGTGGTGGCTGATACCACTGTTAGCTATAGGTTGGAGAGCCGAGGCTATTAATA												
4421	4430	4440	4450	4460	4470	4480	4490	4500	4510	4520	4530	4540	4550
PSY1_R3_gDNA	ACCCCGCCATACCTTTGATGACCAATGTGAGACTTTTGCACGCGATCATACATATTTCTGGTGCATGAGTTGAGACAGAGGGTTTGAAGTTTACACATGTTTACTGGGTCGCTATTTGC												
PSY1_R7_gDNA	ACCCCGCCATACCTTTGATGACCAATGTGAGACTTTTGCACGCGATCATACATATTTCTGGTGCATGAGTTGAGACAGAGGGTTTGAAGTTTACACATGTTTACTGGGTCGCTATTTGC												
Consensus	ACCCCGCCATACCTTTGATGACCAATGTGAGACTTTTGCACGCGATCATACATATTTCTGGTGCATGAGTTGAGACAGAGGGTTTGAAGTTTACACATGTTTACTGGGTCGCTATTTGC												
4551	4560	4570	4580	4590	4600	4610	4620	4630	4640	4650	4660	4670	4680
PSY1_R3_gDNA	TACCCATCCGAGGCTAGGAAATGGTCATGTTACTGACGAGACTAGAAATTCACCTTATATCAGGACTACAGACGATGTTTACCTTGCATTTCCGAAATTTTGCCTTACATGACATTTGTTGG												
PSY1_R7_gDNA	TACCCATCCGAGGCTAGGAAATGGTCATGTTACTGACGAGACTAGAAATTCACCTTATATCAGGACTACAGACGATGTTTACCTTGCATTTCCGAAATTTTGCCTTACATGACATTTGTTGG												
Consensus	TACCCATCCGAGGCTAGGAAATGGTCATGTTACTGACGAGACTAGAAATTCACCTTATATCAGGACTACAGACGATGTTTACCTTGCATTTCCGAAATTTTGCCTTACATGACATTTGTTGG												
4681	4690	4700	4710	4720	4730	4740	4750	4760	4770	4780	4790	4800	4810
PSY1_R3_gDNA	ATCTGAAATGCTTGGATGGATCAACAAACAAATTCATCTACACATACATATGATGATGATGATATTCATAGCTGCATCTTATATCTCTTATTTACTTGTATCAGGATTTT												
PSY1_R7_gDNA	ATCTGAAATGCTTGGATGGATCAACAAACAAATTCATCTACACATACATATGATGATGATGATATTCATAGCTGCATCTTATATCTCTTATTTACTTGTATCAGGATTTT												
Consensus	ATCTGAAATGCTTGGATGGATCAACAAACAAATTCATCTACACATACATATGATGATGATGATATTCATAGCTGCATCTTATATCTCTTATTTACTTGTATCAGGATTTT												
4811	4820	4830	4840	4850	4860	4870	4880	4890	4900	4910	4920	4930	4940
PSY1_R3_gDNA	GGAGATACCTCACCGGCTCGGATTTTTCAGGTGGTGGCTCTGCTGTTGACCGAGGATTCGGACGAGTTCAGGCGCATGACTACACAACTTCACAAAGAGAGCTTATGTGAGCAAA												
PSY1_R7_gDNA	GGAGATACCTCACCGGCTCGGATTTTTCAGGTGGTGGCTCTGCTGTTGACCGAGGATTCGGACGAGTTCAGGCGCATGACTACACAACTTCACAAAGAGAGCTTATGTGAGCAAA												
Consensus	GGAGATACCTCACCGGCTCGGATTTTTCAGGTGGTGGCTCTGCTGTTGACCGAGGATTCGGACGAGTTCAGGCGCATGACTACACAACTTCACAAAGAGAGCTTATGTGAGCAAA												
4941	4950	4960	4970	4980	4990	5000	5010	5020	5030	5040	5050	5060	5070
PSY1_R3_gDNA	CCAAAGAGTGGATGATACCTATTCATATGCAATCTCTTGGCTTCCACAGGACATGAAATCAGGATTTATATTAATCAGGCGCAATGAGGCGAATATACATTTAGAGAAARAAACAG												
PSY1_R7_gDNA	CCAAAGAGTGGATGATACCTATTCATATGCAATCTCTTGGCTTCCACAGGACATGAAATCAGGATTTATATTAATCAGGCGCAATGAGGCGAATATACATTTAGAGAAARAAACAG												
Consensus	CCAAAGAGTGGATGATACCTATTCATATGCAATCTCTTGGCTTCCACAGGACATGAAATCAGGATTTATATTAATCAGGCGCAATGAGGCGAATATACATTTAGAGAAARAAACAG												
5071	5080	5090	5100	5110	5120	5130	5140	5150	5160	5170	5180	5190	5200
PSY1_R3_gDNA	TGTTTTAAAGTAGAATTTAGAGGAGAGGCTTGGAGTACCTGATAGGTTGTTGCTGATGACTGGAGAGTACCGGTTTCCAGCTTGGAAACAGCTCTGGCAGAAATCAGGATAGGTTGCTGTC												
PSY1_R7_gDNA	TGTTTTAAAGTAGAATTTAGAGGAGAGGCTTGGAGTACCTGATAGGTTGTTGCTGATGACTGGAGAGTACCGGTTTCCAGCTTGGAAACAGCTCTGGCAGAAATCAGGATAGGTTGCTGTC												
Consensus	TGTTTTAAAGTAGAATTTAGAGGAGAGGCTTGGAGTACCTGATAGGTTGTTGCTGATGACTGGAGAGTACCGGTTTCCAGCTTGGAAACAGCTCTGGCAGAAATCAGGATAGGTTGCTGTC												

Appendix 2:

Table A2. 1. ANOVA for plastome genome ratio.

Tukey's multiple comparisons test	Mean Diff.	Significant? P < 0.05	Summary	95% CI of diff.
R1 vs. R3	701.1	Yes	**	223.8 to 1178
R1 vs. R4	294.6	No	ns	-182.7 to 771.9
R1 vs. R7	497.4	Yes	*	20.14 to 974.7
R3 vs. R4	-406.5	No	ns	-883.8 to 70.77
R3 vs. R7	-203.7	No	ns	-681.0 to 273.6
R4 vs. R7	202.8	No	ns	-274.5 to 680.1

Table A2. 2. ANOVA for *PSY1* gene expression in ripe fruit.

Tukey's Multiple Comparison Test	Mean Diff.	Significant P < 0.05	Summary	95% CI of diff
R1 vs R2	-2.710	No	ns	-5.590 to 0.1702
R1 vs R3	6.180	Yes	***	3.300 to 9.060
R1 vs R4	3.715	Yes	*	0.8348 to 6.595
R1 vs R7	-3.185	Yes	*	-6.065 to -0.3048
R1 vs R8	7.475	Yes	***	4.595 to 10.36
R1 vs R12	7.085	Yes	***	4.205 to 9.965
R2 vs R3	8.890	Yes	***	6.010 to 11.77
R2 vs R4	6.425	Yes	***	3.545 to 9.305
R2 vs R7	-0.4750	No	ns	-3.355 to 2.405
R2 vs R8	10.19	Yes	***	7.305 to 13.07
R2 vs R12	9.795	Yes	***	6.915 to 12.68
R3 vs R4	-2.465	No	ns	-5.345 to 0.4152
R3 vs R7	-9.365	Yes	***	-12.25 to -6.485
R3 vs R8	1.295	No	ns	-1.585 to 4.175
R3 vs R12	0.9050	No	ns	-1.975 to 3.785
R4 vs R7	-6.900	Yes	***	-9.780 to -4.020
R4 vs R8	3.760	Yes	*	0.8798 to 6.640
R4 vs R12	3.370	Yes	*	0.4898 to 6.250
R7 vs R8	10.66	Yes	***	7.780 to 13.54
R7 vs R12	10.27	Yes	***	7.390 to 13.15
R8 vs R12	-0.3900	No	ns	-3.270 to 2.490

Table A2. 3. ANOVA for *DXS* gene expression for ripe fruit.

Tukey's Multiple Comparison Test	Mean Diff.	Significant P < 0.05	Summary	95% CI of diff
R1 vs R2	-4.693	Yes	*	-8.954 to -0.4323
R1 vs R3	1.933	No	ns	-2.328 to 6.194
R1 vs R4	-0.1167	No	ns	-4.378 to 4.144
R1 vs R7	-5.433	Yes	**	-9.694 to -1.172
R1 vs R8	0.9033	No	ns	-3.358 to 5.164

R1 vs R12	1.700	No	ns	-3.064 to 6.464
R2 vs R3	6.627	Yes	**	2.366 to 10.89
R2 vs R4	4.577	Yes	*	0.3156 to 8.838
R2 vs R7	- 0.7400	No	ns	-5.001 to 3.521
R2 vs R8	5.597	Yes	**	1.336 to 9.858
R2 vs R12	6.393	Yes	**	1.629 to 11.16
R3 vs R4	-2.050	No	ns	-6.311 to 2.211
R3 vs R7	-7.367	Yes	***	-11.63 to -3.106
R3 vs R8	-1.030	No	ns	-5.291 to 3.231
R3 vs R12	- 0.2333	No	ns	-4.997 to 4.531
R4 vs R7	-5.317	Yes	*	-9.578 to -1.056
R4 vs R8	1.020	No	ns	-3.241 to 5.281
R4 vs R12	1.817	No	ns	-2.947 to 6.581
R7 vs R8	6.337	Yes	**	2.076 to 10.60
R7 vs R12	7.133	Yes	**	2.369 to 11.90
R8 vs R12	0.7967	No	ns	-3.967 to 5.561

Table A2. 4. ANOVA for *CCS* gene expression in ripe fruit.

Tukey's multiple comparisons test	Mean Diff.	Significant P < 0.05	Summary	95% CI of diff.
R1 vs. R2	0.6567	No	ns	-0.9722 to 2.286
R1 vs. R3	0.3000	No	ns	-1.329 to 1.929
R1 vs. R4	0.2833	No	ns	-1.346 to 1.912
R1 vs. R7	0.06667	No	ns	-1.562 to 1.696
R1 vs. R8	-0.1167	No	ns	-1.746 to 1.512
R1 vs. R12	- 0.02333	No	ns	-1.652 to 1.606
R2 vs. R3	-0.3567	No	ns	-1.986 to 1.272
R2 vs. R4	-0.3733	No	ns	-2.002 to 1.256
R2 vs. R7	-0.5900	No	ns	-2.219 to 1.039
R2 vs. R8	-0.7733	No	ns	-2.402 to 0.8555
R2 vs. R12	-0.6800	No	ns	-2.309 to 0.9489
R3 vs. R4	- 0.01667	No	ns	-1.646 to 1.612
R3 vs. R7	-0.2333	No	ns	-1.862 to 1.396
R3 vs. R8	-0.4167	No	ns	-2.046 to 1.212
R3 vs. R12	-0.3233	No	ns	-1.952 to 1.306
R4 vs. R7	-0.2167	No	ns	-1.846 to 1.412
R4 vs. R8	-0.4000	No	ns	-2.029 to 1.229
R4 vs. R12	-0.3067	No	ns	-1.936 to 1.322
R7 vs. R8	-0.1833	No	ns	-1.812 to 1.446
R7 vs. R12	-0.0900	No	ns	-1.719 to 1.539
R8 vs. R12	0.09333	No	ns	-1.536 to 1.722

Table A2. 5. ANOVA for *CHY2* gene expression throughout ripening.

Tukey's multiple comparisons test	Mean Diff.	Significant P < 0.05	Summary	95% CI of diff.
R1 vs. R2	-1.463	No	ns	-4.070 to 1.143
R1 vs. R3	2.783	Yes	*	0.1771 to 5.390
R1 vs. R4	1.137	No	ns	-1.470 to 3.743

R1 vs. R7	-1.047	No	ns	-3.653 to 1.560
R1 vs. R8	3.813	Yes	**	1.207 to 6.420
R1 vs. R12	3.820	Yes	**	1.214 to 6.426
R2 vs. R3	4.247	Yes	**	1.640 to 6.853
R2 vs. R4	2.600	No	ns	-0.006265 to 5.206
R2 vs. R7	0.4167	No	ns	-2.190 to 3.023
R2 vs. R8	5.277	Yes	***	2.670 to 7.883
R2 vs. R12	5.283	Yes	***	2.677 to 7.890
R3 vs. R4	-1.647	No	ns	-4.253 to 0.9596
R3 vs. R7	-3.830	Yes	**	-6.436 to -1.224
R3 vs. R8	1.030	No	ns	-1.576 to 3.636
R3 vs. R12	1.037	No	ns	-1.570 to 3.643
R4 vs. R7	-2.183	No	ns	-4.790 to 0.4229
R4 vs. R8	2.677	Yes	*	0.07040 to 5.283
R4 vs. R12	2.683	Yes	*	0.07707 to 5.290
R7 vs. R8	4.860	Yes	***	2.254 to 7.466
R7 vs. R12	4.867	Yes	***	2.260 to 7.473
R8 vs. R12	0.006667	No	ns	-2.600 to 2.613

Appendix 3

Table A3. 1. Corrections: Table displaying key outcomes and future directions.

Key outcomes	Key future area of research	Comment
High intensity phenotypes have highly expressed carotenoid biosynthetic genes (<i>PSY1</i> and <i>DXS</i>).	Fragmentation of the <i>DXS</i> promoter region transiently expressed with a reporter gene to allow elucidation of putative regulatory elements to be characterised. Alongside EMSA to identify potential transcription factors involved in fruit ripening and carotenoid accumulation. Enzyme activities should also be measured to confirm the gene expression results.	Possible future project.
High intensity phenotypes contain higher concentrations of capsanthin diesters and fibrils.	Breeding of lines with high levels of capsanthin diesters and so fibril content will create elite lines with high colour intensity.	Information will be used by Syngenta.
Potential acyl transferase responsible for fruit carotenoid esterification.	Characterisation of the gene on a transcript and protein level. VIGS to knockout the gene.	Will be addressed in post doc.
Pooling of free capsanthin may cause the down-regulation of the <i>CCS</i> gene.	Use carotenoid cleavage inhibitors to elucidate whether apocarotenoids are	Will be addressed by the new PhD CASE study student.

	responsible for the down-regulation of the <i>CCS</i> gene.	
High retention lines released more lipid-derived volatiles in dry fruit when compared to low and medium retention lines.	Analysis of lipid profile in subchromoplast fractions of chilli pepper. TBARs to characterise rates of lipid peroxidation.	Will be addressed by the new PhD CASE study student.
Low retention lines had higher levels of unsaturated fatty acids. Whereas high retention lines had higher levels of hydrocarbon alkanes associated with the cuticle.	Detailed analysis of lipid profiles of chilli pepper fruit flesh and surface wax.	Will be addressed by the new PhD CASE study student.
Low retention lines had more intense SOD activity when compared to high retention lines.	Quantitative SOD, CAT and PER assays.	Will be addressed by the new PhD CASE study student.

References

- Ahmed, F.** (1999). Vitamin A deficiency in Bangladesh: a review and recommendations for improvement. *Public Health Nutr.* **2**: 1–14.
- Albrecht, M., Klein, a, Hugueney, P., Sandmann, G., and Kuntz, M.** (1995). Molecular cloning and functional expression in *E. coli* of a novel plant enzyme mediating zeta-carotene desaturation. *FEBS Lett.* **372**: 199–202.
- Ament, K., Van Schie, C.C., Bouwmeester, H.J., Haring, M. a., and Schuurink, R.C.** (2006). Induction of a leaf specific geranylgeranyl pyrophosphate synthase and emission of (E,E)-4,8,12-trimethyltrideca-1,3,7,11-tetraene in tomato are dependent on both jasmonic acid and salicylic acid signaling pathways. *Planta* **224**: 1197–1208.
- Ames, B.N., Shigenaga, M.K., and Hagen, T.M.** (1993). Oxidants, antioxidants, and the degenerative diseases of aging. *Proc. Natl. Acad. Sci. U. S. A.* **90**: 7915–7922.
- Apel, K. and Hirt, H.** (2004). Reactive oxygen species: metabolism, oxidative stress, and signal transduction. *Annu. Rev. Plant Biol.* **55**: 373–399.
- Ariizumi, T. et al.** (2014). Identification of the carotenoid modifying gene *PALE YELLOW PETAL 1* as an essential factor in xanthophyll esterification and yellow flower pigmentation in tomato (*Solanum lycopersicum*). *Plant J.* **79**: 453–465.
- Arimboor, R., Natarajan, R.B., Menon, K.R., Chandrasekhar, L.P., and Moorkoth, V.** (2014). Red pepper (*Capsicum annuum*) carotenoids as a source of natural food colors: analysis and stability-a review. *J. Food Sci. Technol.* **52**: 1–14.
- Asilbekova, D.T.** (2003). Lipids of *Capsicum annuum* fruit pulp. *Chem. Nat. Compd.* **39**: 442–445.

- Austin, J.R., Frost, E., Vidi, P.-A., Kessler, F., and Staehelin, L.A.** (2006). Plastoglobules are lipoprotein subcompartments of the chloroplast that are permanently coupled to thylakoid membranes and contain biosynthetic enzymes. *Plant Cell* **18**: 1693–1703.
- Baker, N.R.** (2008). Chlorophyll fluorescence: a probe of photosynthesis in vivo. *Annu. Rev. Plant Biol.* **59**: 89–113.
- Baron, M., Davies, S., Alexander, L., Snellgrove, D., and Sloman, K. a.** (2008). The effect of dietary pigments on the coloration and behaviour of flame-red dwarf gourami, *Colisa lalia*. *Anim. Behav.* **75**: 1041–1051.
- Bartley, G.E., Scolnik, P.A., and Beyer, P.** (1999). Two *Arabidopsis thaliana* carotene desaturases, phytoene desaturase and ζ -carotene desaturase, expressed in *Escherichia coli*, catalyze a poly-cis pathway to yield pro-lycopen. *Eur. J. Biochem.* **259**: 396–403.
- Bartley, G.E., Viitanen, P. V, Bacot, K.O., and Scolnik, P.A.** (1992). A tomato gene expressed during fruit ripening encodes an enzyme of the carotenoid biosynthesis pathway. *J. Biol. Chem.* **267**: 5036–9.
- Bauer, S., Schulte, E., and Thier, H.P.** (2005). Composition of the surface waxes from bell pepper and eggplant. *Eur. Food Res. Technol.* **220**: 5–10.
- Beauchamp, C. and Fridovich, I.** (1971). Superoxide dismutase: Improved assays and an assay applicable to acrylamide gels. *Anal. Biochem.* **44**: 276–287.
- Bekker, N. and Asilbekova, D.T.** (2003). Lipids of *Capsicum annuum* fruit pulp. *Chem. Nat. Compd.* **39**: 442–445.
- Bell-Lelong, D. a, Cusumano, J.C., Meyer, K., and Chapple, C.** (1997). Cinnamate-4-hydroxylase expression in *Arabidopsis*. Regulation in response to development and the environment. *Plant Physiol.* **113**: 729–738.
- Beyer, P., Kroncke, U., and Niewelstein, V.** (1991). On the Mechanism of the Lycopene Isomerase Cyclase Reaction in *Narcissus-Pseudonarcissus* L Chromoplasts. *J. Biol. Chem.* **266**: 17072–17078.
- Biasini, M., Bienert, S., Waterhouse, A., Arnold, K., Studer, G., Schmidt, T., Kiefer, F., Cassarino, T.G., Bertoni, M., Bordoli, L., and Schwede, T.** (2014). SWISS-MODEL: Modelling protein tertiary and quaternary structure using evolutionary information. *Nucleic Acids Res.* **42**: 252–258.
- Blokhina, O., Virolainen, E., and Fagerstedt, K. V.** (2003). Antioxidants, oxidative damage and oxygen deprivation stress: A review. *Ann. Bot.* **91**: 179–194.
- Blum, E., Mazourek, M., O’Connell, M., Curry, J., Thorup, T., Liu, K., Jahn, M., and Paran, I.** (2003). Molecular mapping of capsaicinoid biosynthesis genes and quantitative trait loci analysis for capsaicinoid content in *Capsicum*. *Theor. Appl. Genet.* **108**: 79–86.
- Bogusz Junior, S., Tavares, A.M., Filho, J.T., Zini, C.A., and Godoy, H.T.** (2012). Analysis of the volatile compounds of Brazilian chilli peppers (*Capsicum* spp.) at two stages of maturity by solid phase micro-extraction and gas chromatography-mass spectrometry. *Food Res. Int.* **48**: 98–107.
- Bohs, L. and Olmstead, R.G.** (1997). Phylogenetic relationships in *Solanum* (Solanaceae) based on *ndhF* sequences. *Syst. Bot.* **22**: 5–17.
- Borovsky, Y., Tadmor, Y., Bar, E., Meir, A., Lewinsohn, E., and Paran, I.** (2013). Induced mutation in β -CAROTENE HYDROXYLASE results in accumulation of β -carotene and conversion of red to orange color in pepper fruit. *Theor. Appl. Genet.* **126**: 557–65.
- Bosland, P.W.** (1996). Progress in new crops. In *Capsicums: Innovative uses of the ancient crop*. J. Janick, ed (ASHS press: Arlington, VA).

- Bosland, P.W. and Baral, J.B.** (2007). "Bhut Jolokia" - The world's hottest known chile pepper is a putative naturally occurring interspecific hybrid. *HortScience* **42**: 222–224.
- Boter, M., Ruíz-Rivero, O., Abdeen, a, and Prat, S.** (2004). Conserved MYC transcription factors\nplay a key role in jasmonate signaling\nboth in tomato and Arabidopsis. *Genes Dev.* **18**: 1577–1591.
- Bouvier, F., Backhaus, R. a., and Camara, B.** (1998a). Induction and control of chromoplast-specific carotenoid genes by oxidative stress. *J. Biol. Chem.* **273**: 30651–30659.
- Bouvier, F., d'Harlingue, a, Suire, C., Backhaus, R. a, and Camara, B.** (1998b). Dedicated roles of plastid transketolases during the early onset of isoprenoid biogenesis in pepper fruits1. *Plant Physiol.* **117**: 1423–1431.
- Bouvier, F., D'Harlingue, A., Backhaus, R. a., Kumagai, M.H., and Camara, B.** (2000). Identification of neoxanthin synthase as a carotenoid cyclase paralog. *Eur. J. Biochem.* **267**: 6346–6352.
- Bouvier, F., Hugueney, P., Harlingue, A., I, M.K., and Camara, B.** (1994). Xanthophyll biosynthesis in chromoplasts: Isolation and Molecular Cloning of an Enzyme Catalyzing the conversion of 5,6-epoxycarotenoid into ketocarotenoid. *Plant J.* **6**: 45–54.
- Bouvier, F., Keller, Y., D'Harlingue, A., and Camara, B.** (1998c). Xanthophyll biosynthesis: molecular and functional characterization of carotenoid hydroxylases from pepper fruits (*Capsicum annuum* L.). *Biochim Biophys Acta* **1391**: 320–8.
- Bréhélin, C. and Kessler, F.** (2008). The plastoglobule: A bag full of lipid biochemistry tricks. *Photochem. Photobiol.* **84**: 1388–1394.
- Bréhélin, C., Kessler, F., and van Wijk, K.J.** (2007). Plastoglobules: versatile lipoprotein particles in plastids. *Trends Plant Sci.* **12**: 260–266.
- Breithaupt, D.E. and Schwack, W.** (2000). Determination of free and bound carotenoids in paprika (*Capsicum annuum* L.) by LC/MS. *Eur. Food Res. Technol.* **211**: 52–55.
- Britton, G.** (1995a). Structure and properties of carotenoids in relation to function. *FASEB J.* **9**: 1551–8.
- Britton, G.** (1995b). Structure and properties of carotenoids in relation to function. *FASEB J.* **9**: 1551–1558.
- Britton, G., Liaaen-Jensen, S., and Pfander, H.** (2004). *Carotenoids Handbook* 1st editio. G. Britton, S. Liaaen-Jensen, and H. Pfander, eds (Birkhauser Verlag: Basel).
- Buchanan, C.D., Kein, P.E., and Mullet, J.E.** (2004). Phylogenetic analysis of 5-noncoding regions from the ABA-responsive rab16/17 gene family of sorghum, maize and rice provides insight into the composition, organization and function of cis-regulatory modules. *Genetics* **168**: 1639–1654.
- Burkhardt, P.K., Beyer, P., Wunn, J., Kloti, A., Armstrong, G.A., Schledz, M., Lintig, J., and Potrykus, I.** (1997). Transgenic rice (*Oryza sativa*) endosperm expressing daffodil (*Narcissus pseudonarcissus*) phytoene synthase accumulates phytoene, a key intermediate of provitamin A biosynthesis. *Plant J.* **11**: 1071–1078.
- Buttery, R.G., Teranishi, R., Ling, L.C., Flath, R. a, and Stern, D.J.** (1988). Quantitative studies on origins of fresh tomato aroma volatiles. *J. Agric. Food Chem.* **36**: 1247–1250.
- Camara, B., Bardat, F., and Monéger, R.** (1982). Sites of biosynthesis of carotenoids in *Capsicum* chromoplasts. *Eur. J. Biochem.* **127**: 255–258.
- Camara, B. and Brangeon, J.** (1981). Carotenoid metabolism during chloroplast to chromoplast transformation in *Capsicum annuum* fruit. *Planta* **4**: 359–364.
- Camara, B., Hugueney, P., Bouvier, F., Kuntz, M., and Monéger, R.** (1995). Biochemistry and

- Molecular Biology of Chromoplast Development. *Int. Rev. Cytol.* **163**: 175–247.
- Campbell, R., Ducreux, L.J.M., Morris, W.L., Morris, J. a, Suttle, J.C., Ramsay, G., Bryan, G.J., Hedley, P.E., and Taylor, M. a** (2010). The metabolic and developmental roles of carotenoid cleavage dioxygenase4 from potato. *Plant Physiol.* **154**: 656–664.
- Cánovas, F.M., Avila, C., Cantón, F.R., Cañas, R. a., and De La Torre, F.** (2007). Ammonium assimilation and amino acid metabolism in conifers. *J. Exp. Bot.* **58**: 2307–2318.
- Cazzonelli, C.I.** (2011). Goldacre Review: Carotenoids in nature: insights from plants and beyond. *Funct. Plant Biol.* **38**: 833–847.
- Cazzonelli, C.I., Roberts, A.C., Carmody, M.E., and Pogson, B.J.** (2010). Transcriptional control of SET DOMAIN GROUP 8 and CAROTENOID ISOMERASE during Arabidopsis development. *Mol. Plant* **3**: 174–91.
- Chen, A., Gu, M., Sun, S., Zhu, L., Hong, S., and Xu, G.** (2011). Identification of two conserved cis-acting elements, MYCS and P1BS, involved in the regulation of mycorrhiza-activated phosphate transporters in eudicot species. *New Phytol.* **189**: 1157–1169.
- Collard, B.C.Y., Jahufer, M.Z.Z., Brouwer, J.B., and Pang, E.C.K.** (2005). An introduction to markers, quantitative trait loci (QTL) mapping and marker-assisted selection for crop improvement: The basic concepts. *Euphytica* **142**: 169–196.
- Conforti, F., Statti, G. a., and Menichini, F.** (2007). Chemical and biological variability of hot pepper fruits (*Capsicum annum* var. *acuminatum* L.) in relation to maturity stage. *Food Chem.* **102**: 1096–1104.
- Congdon, N. and West, K.P.J.** (1999). Nutrition and the eye. *Curr. Opin. Ophthalmol.* **10**: 464–73.
- Conley, T.R., Park, S.C., Kwon, H.B., Peng, H.P., and Shih, M.C.** (1994). Characterization of cis-acting elements in light regulation of the nuclear gene encoding the A subunit of chloroplast isozymes of glyceraldehyde-3-phosphate dehydrogenase from *Arabidopsis thaliana*. *Mol. Cell. Biol.* **14**: 2525–2533.
- Cook, D., Grierson, D., Jones, C., Wallace, A., West, G., and Tucker, G.** (2002). Modification of fatty acid composition in tomato (*Lycopersicon esculentum*) by expression of a borage delta6-desaturase. *Mol. Biotechnol.* **21**: 123–128.
- Cookson, P.J., Kiano, J.W., Shipton, C. a., Fraser, P.D., Romer, S., Schuch, W., Bramley, P.M., and Pyke, K. a.** (2003). Increases in cell elongation, plastid compartment size and phytoene synthase activity underlie the phenotype of the high pigment-1 mutant of tomato. *Planta* **217**: 896–903.
- Cordoba, E., Salmi, M., and León, P.** (2009). Unravelling the regulatory mechanisms that modulate the MEP pathway in higher plants. *J. Exp. Bot.* **60**: 2933–2943.
- Corona, V., Aracri, B., Kosturkova, G., Bartley, G.E., Pitto, L., Giorgetti, L., Scolnik, P.A., and Giuliano, G.** (1996). Regulation of a carotenoid biosynthesis gene promoter during plant development. *plant J.* **9**: 505–512.
- Cremer, D.R. and Eichner, K.** (2000a). Formation of volatile compounds during heating of spice paprika (*Capsicum annum*) powder. *J. Agric. Food Chem.* **48**: 2454–60.
- Cremer, D.R. and Eichner, K.** (2000b). The influence of the pH value on the formation of Strecker aldehydes in low moisture model systems and in plant powders. *Eur. Food Res. Technol.* **211**: 247–251.
- Deli, J., Molnár, P., Matus, Z., and Tóth, G.** (2001). Carotenoid Composition in the Fruits of Red Paprika (*Capsicum annum* var. *lycopersiciforme rubrum*) during Ripening; Biosynthesis of Carotenoids in Red Paprika. *J. Agric. Food Chem.* **49**: 1517–1523.

- Dellapenna, D. and Pogson, B.J.** (2006). Vitamin Synthesis in Plants : Tocopherols and Carotenoids. *Annu. Rev. Plant Biol.* **57**: 711–38.
- Deruère, J., Römer, S., d’Harlingue, a, Backhaus, R. a, Kuntz, M., and Camara, B.** (1994). Fibril assembly and carotenoid overaccumulation in chromoplasts: a model for supramolecular lipoprotein structures. *Plant Cell* **6**: 119–133.
- Dogbo, O. and Camara, B.** (1987). Metabolism of plastid terpenoids. II. Regulation of phytoene synthesis in plastid stroma isolated from higher plants. *Plant Sci.* **49**: 103–109.
- Dogbo, O., Laferrière, a, D’Harlingue, a, and Camara, B.** (1988). Carotenoid biosynthesis: Isolation and characterization of a bifunctional enzyme catalyzing the synthesis of phytoene. *Proc. Natl. Acad. Sci. U. S. A.* **85**: 7054–7058.
- Ducieux, L.J.M., Morris, W.L., Hedley, P.E., Shepherd, T., Davies, H. V., Millam, S., and Taylor, M. a.** (2005). Metabolic engineering of high carotenoid potato tubers containing enhanced levels of ??-carotene and lutein. *J. Exp. Bot.* **56**: 81–89.
- Edge, R., McGarvey, D.J., and Truscott, T.G.** (1997). The carotenoids as anti-oxidants--a review. *J. Photochem. Photobiol. B.* **41**: 189–200.
- Egea, I., Barsan, C., Bian, W., Purgatto, E., Latché, A., Chervin, C., Bouzayen, M., and Pech, J.C.** (2010). Chromoplast differentiation: Current status and perspectives. *Plant Cell Physiol.* **51**: 1601–1611.
- Enfissi, E.M. a, Barneche, F., Ahmed, I., Lichtlé, C., Gerrish, C., McQuinn, R.P., Giovannoni, J.J., Lopez-Juez, E., Bowler, C., Bramley, P.M., and Fraser, P.D.** (2010). Integrative transcript and metabolite analysis of nutritionally enhanced DE-ETIOLATED1 downregulated tomato fruit. *Plant Cell* **22**: 1190–215.
- Enfissi, E.M. a, Fraser, P.D., Lois, L.M., Boronat, A., Schuch, W., and Bramley, P.M.** (2005). Metabolic engineering of the mevalonate and non-mevalonate isopentenyl diphosphate-forming pathways for the production of health-promoting isoprenoids in tomato. *Plant Biotechnol. J.* **3**: 17–27.
- Erdman, J.W., Ford, N. a., and Lindshield, B.L.** (2009). Are the health attributes of lycopene related to its antioxidant function? *Arch. Biochem. Biophys.* **483**: 229–235.
- Estévez, J.M., Cantero, a, Romero, C., Kawaide, H., Jiménez, L.F., Kuzuyama, T., Seto, H., Kamiya, Y., and León, P.** (2000). Analysis of the expression of CLA1, a gene that encodes the 1-deoxyxylulose 5-phosphate synthase of the 2-C-methyl-D-erythritol-4-phosphate pathway in Arabidopsis. *Plant Physiol.* **124**: 95–104.
- Forero, M.D., Quijano, C.E., and Pino, J. a.** (2009). Volatile compounds of chile pepper (*Capsicum annum* L. var. *glabriusculum*) at two ripening stages. *Flavour Fragr. J.* **24**: 25–30.
- Frank, H.A. and Cogdell, R..** (1993). Carotenoids in Photosynthesis A.J. Young and G. Britton, eds (Springer Netherlands: Dordrecht).
- Fraser, P.D. and Bramley, P.M.** (2004). The biosynthesis and nutritional uses of carotenoids. *Prog. Lipid Res.* **43**: 228–65.
- Fraser, P.D., Enfissi, E.M. a, and Bramley, P.M.** (2009). Genetic engineering of carotenoid formation in tomato fruit and the potential application of systems and synthetic biology approaches. *Arch. Biochem. Biophys.* **483**: 196–204.
- Fraser, P.D., Enfissi, E.M. a, Halket, J.M., Truesdale, M.R., Yu, D., Gerrish, C., and Bramley, P.M.** (2007). Manipulation of phytoene levels in tomato fruit: effects on isoprenoids, plastids, and intermediary metabolism. *Plant Cell* **19**: 3194–211.
- Fraser, P.D., Kiano, J.W., Truesdale, M.R., Schuch, W., and Bramley, P.M.** (1999). Phytoene synthase-2 enzyme activity in tomato does not contribute to carotenoid synthesis in ripening

- fruit. *Plant Mol. Biol.* **40**: 687–698.
- Fraser, P.D., Romer, S., Shipton, C. a, Mills, P.B., Kiano, J.W., Misawa, N., Drake, R.G., Schuch, W., and Bramley, P.M.** (2002). Evaluation of transgenic tomato plants expressing an additional phytoene synthase in a fruit-specific manner. *Proc. Natl. Acad. Sci. U. S. A.* **99**: 1092–7.
- Fraser, P.D., Schuch, W., and Bramley, P.M.** (2000). Phytoene synthase from tomato (*Lycopersicon esculentum*) chloroplasts--partial purification and biochemical properties. *Planta* **211**: 361–369.
- Fraser, P.D., Truesdale, M.R., Bird, C.R., Schuch, W., and Bramley, P.M.** (1994). Carotenoid Biosynthesis during Tomato Fruit Development (Evidence for Tissue-Specific Gene Expression). *Plant Physiol.* **105**: 405–413.
- Fray, R.G. and Grierson, D.** (1993). Identification and genetic analysis of normal and mutant phytoene synthase genes of tomato by sequencing, complementation and co-suppression. *Plant Mol. Biol.* **22**: 589–602.
- Fray, R.G., Wallace, A., Fraser, P.D., Valero, D., Hedden, P., Bramley, P.M., and Grierson, D.** (1995). Constitutive expression of a fruit phytoene synthase gene in transgenic tomatoes causes dwarfism by redirecting metabolites from the gibberellin pathway. *Plant J.* **8**: 693–701.
- Frey-Wyssling, A. and Kreutzer, E.** (1958). The submicroscopic development of chromoplasts in the fruit of *Capsicum annuum* L. *J. Ultrastruct. Res.* **1**: 397–411.
- Fridman, E., Carrari, F., Liu, Y.-S., Fernie, A.R., and Zamir, D.** (2004). Zooming in on a quantitative trait for tomato yield using interspecific introgressions. *Science* **305**: 1786–1789.
- Fujisawa, M., Nakano, T., and Ito, Y.** (2011). Identification of potential target genes for the tomato fruit-ripening regulator RIN by chromatin immunoprecipitation. *BMC Plant Biol.* **11**: 26.
- Fusada, N., Masuda, T., Kuroda, H., Shimada, H., Ohta, H., and Takamiya, K.I.** (2005). Identification of a novel cis-element exhibiting cytokinin-dependent protein binding in vitro in the 5'-region of NADPH-protochlorophyllide oxidoreductase gene in cucumber. *Plant Mol. Biol.* **59**: 631–645.
- Gady, A.L.F., Vriezen, W.H., Van de Wal, M.H.B.J., Huang, P., Bovy, A.G., Visser, R.G.F., and Bachem, C.W.B.** (2012). Induced point mutations in the phytoene synthase 1 gene cause differences in carotenoid content during tomato fruit ripening. *Mol. Breed.* **29**: 801–812.
- Gallagher, C.E.** (2004). Gene Duplication in the Carotenoid Biosynthetic Pathway Preceded Evolution of the Grasses. *PLANT Physiol.* **135**: 1776–1783.
- Galliard, T., Matthew, J.A., Wright, A.J., and Fishwick, M.J.** (1977). The enzymatic breakdown of lipids to volatile and non-volatile carbonyl fragments in disrupted tomato fruits. *J. Sci. Food Agric.* **28**: 863–868.
- Galpaz, N., Wang, Q., Menda, N., Zamir, D., and Hirschberg, J.** (2008). Abscisic acid deficiency in the tomato mutant high-pigment 3 leading to increased plastid number and higher fruit lycopene content. *Plant J.* **53**: 717–30.
- Giorio, G., Stigliani, A.L., and D'Ambrosio, C.** (2008). Phytoene synthase genes in tomato (*Solanumlycopersicum* L.) - New data on the structures, the deduced amino acid sequences and the expression patterns. *FEBS J.* **275**: 527–535.
- Giovannucci, E., Ascherio, A., Rimm, E.B., Stampfer, M.J., Colditz, G.A., and Willett, W.C.** (1995). Intake of Carotenoids and Retino in Relation to Risk of Prostate Cancer. *JNCI J. Natl. Cancer Inst.* **87**: 1767–1776.
- Giuffrida, D., Dugo, P., Torre, G., Bignardi, C., Cavazza, A., Corradini, C., and Dugo, G.** (2013). Characterization of 12 *Capsicum* varieties by evaluation of their carotenoid profile and pungency determination. *Food Chem.* **140**: 794–802.
- Giuliano, G., Bartley, G.E., and Scolnik, P. a** (1993a). Regulation of carotenoid biosynthesis during

- tomato development. *Plant Cell* **5**: 379–387.
- Giuliano, G., Bartley, G.E., and Scolnik, P. a** (1993b). Regulation of carotenoid biosynthesis during tomato development. *Plant Cell* **5**: 379–387.
- Gnayfeed, M., Daood, H., Biacs, P., and Alcaraz, C.** (2001). Content of bioactive compounds in pungent spice red pepper (paprika) as affected by ripening and genotype. *J. Sci. Food Agric.* **81**: 1580–1585.
- Goff, S. a and Klee, H.J.** (2006). Plant volatile compounds: sensory cues for health and nutritional value? *Science* **311**: 815–819.
- Gómez-García, M.D.R. and Ochoa-Alejo, N.** (2013). Biochemistry and molecular Biology of carotenoid biosynthesis in chili peppers (*Capsicum* spp.). *Int. J. Mol. Sci.* **14**: 19025–19053.
- Gregory, G.K., Chen, T.-S., and Phillip, T.** (1987). Quantitative Analysis of Carotenoids and Carotenoid Esters in Fruits by HPLC: Red Bell Peppers. *J. Food Sci.* **52**: 1071–1073.
- Grimmig, B. and Matern, U.** (1997). Structure of the parsley caffeoyl-CoA O-methyltransferase gene, harbouring a novel elicitor responsive cis-acting element. *Plant Mol. Biol.* **33**: 323–341.
- Gu, P., Ishii, Y., Spencer, T.A., and Shechter, I.** (1998). Function-Structure Studies and Identification of Three Enzyme Domains Involved in the Catalytic Activity in Rat Hepatic Squalene Synthase. *J. Biol. Chem.* **273**: 12515–12525.
- Guevara-garci, A., Roman, C.S., Corte, E., Guevara-garci, A., and Leo, P.** (2005). Characterization of the Arabidopsis *clb6* Mutant Illustrates the Importance of Posttranscriptional Regulation of the Methyl- D -Erythritol 4-Phosphate Pathway. *Plant Cell* **17**: 628–643.
- Gupta, a S., Heinen, J.L., Holaday, a S., Burke, J.J., and Allen, R.D.** (1993). Increased resistance to oxidative stress in transgenic plants that overexpress chloroplastic Cu/Zn superoxide dismutase. *Proc. Natl. Acad. Sci. U. S. A.* **90**: 1629–1633.
- Gururaj, H.B., Padma, M.N., Giridhar, P., and Ravishankar, G. a.** (2012). Functional validation of *Capsicum frutescens* aminotransferase gene involved in vanillylamine biosynthesis using *Agrobacterium* mediated genetic transformation studies in *Nicotiana tabacum* and *Capsicum frutescens* calli cultures. *Plant Sci.* **195**: 96–105.
- Guzman, I., Hamby, S., Romero, J., Bosland, P.W., and O'Connell, M. a** (2010). Variability of Carotenoid Biosynthesis in Orange Colored *Capsicum* spp. *Plant Sci.* **179**: 49–59.
- Ha, S.H., Kim, J.B., Park, J.S., Lee, S.W., and Cho, K.J.** (2007a). A comparison of the carotenoid accumulation in *Capsicum* varieties that show different ripening colours: Deletion of the capsanthin-capsorubin synthase gene is not a prerequisite for the formation of a yellow pepper. *J. Exp. Bot.* **58**: 3135–3144.
- Ha, S.-H., Kim, J.-B., Park, J.-S., Lee, S.-W., and Cho, K.-J.** (2007b). A comparison of the carotenoid accumulation in *Capsicum* varieties that show different ripening colours: deletion of the capsanthin-capsorubin synthase gene is not a prerequisite for the formation of a yellow pepper. *J. Exp. Bot.* **58**: 3135–44.
- Halliwell, B. and Gutteridge, J.M.C.** (1999). *Free radicals in biology and medicine.* (Oxford university press: New York).
- Harrison, P.J. and Bugg, T.D.H.** (2014). Enzymology of the carotenoid cleavage dioxygenases: Reaction mechanisms, inhibition and biochemical roles. *Arch. Biochem. Biophys.* **544**: 105–111.
- Hartmann, U., Sagasser, M., Mehrtens, F., Stracke, R., and Weisshaar, B.** (2005). Differential combinatorial interactions of cis-acting elements recognized by R2R3-MYB, BZIP, and BHLH factors control light-responsive and tissue-specific activation of phenylpropanoid biosynthesis genes. *Plant Mol. Biol.* **57**: 155–171.

- Hepworth, S.R., Valverde, F., Ravenscroft, D., Mouradov, A., and Coupland, G.** (2002). Antagonistic regulation of flowering-time gene *SOC1* by *CONSTANS* and *FLC* via separate promoter motifs. *EMBO J.* **21**: 4327–4337.
- Hernández, B., Sáenz Gamasa, C., Alberdi, C., Alfonso, S., Berroguí, M., and Dineiro, J.M.** (2004). Design and performance of a color chart based in digitally processed images for sensory evaluation of piquillo peppers (*Capsicum annuum*). *Color Res. Appl.* **29**: 305–311.
- Hornero-Méndez, D., Gómez-Ladrón de Guevara, R., and Mínguez-Mosquera, M.I.** (2000). Carotenoid Biosynthesis Changes in Five Red Pepper (*Capsicum annuum* L.) Cultivars during Ripening. *Cultivar Selection for Breeding. J. Agric. Food Chem.* **48**: 3857–3864.
- Hornero-Méndez, D. and Mínguez-Mosquera, M.I.** (2000). Xanthophyll Esterification Accompanying Carotenoid Overaccumulation in Chromoplast of *Capsicum annuum* Ripening Fruits Is a Constitutive Process and Useful for Ripeness Index. *J. Agric. Food Chem.* **48**: 1617–1622.
- Hugueney, P., Badillo, A., Chen, H.C., Klein, A., Hirschberg, J., Camara, B., and Kuntz, M.** (1995). Metabolism of cyclic carotenoids: a model for the alteration of this biosynthetic pathway in *Capsicum annuum* chromoplasts. *Plant J.* **8**: 417–24.
- Hugueney, P., Bouvier, F., Badillo, a, Quennemet, J., d’Harlingue, a, and Camara, B.** (1996). Developmental and stress regulation of gene expression for plastid and cytosolic isoprenoid pathways in pepper fruits. *Plant Physiol.* **111**: 619–626.
- Huh, J.H., Kang, B.C., Nahm, S.H., Kim, S., Ha, K.S., Lee, M.H., and Kim, B.D.** (2001). A candidate gene approach identified phytoene synthase as the locus for mature fruit color in red pepper (*Capsicum* spp.). *Theor. Appl. Genet.* **102**: 524–530.
- Humphrey, J.H., West, K.P., and Sommer, A.** (1992). Vitamin A deficiency and attributable mortality among under-5-year-olds. *Bull. World Health Organ.* **70**: 225–32.
- Hunter, W.N.** (2007). The non-mevalonate pathway of isoprenoid precursor biosynthesis. *J. Biol. Chem.* **282**: 21573–21577.
- Hurtado-Hernandez, H. and Smith, P.G.** (1985). Inheritance of mature fruit color in *Capsicum annuum* L. *J. Hered.* **76**: 211–213.
- Isaacson, T., Ronen, G., Zamir, D., and Hirschberg, J.** (2002). Cloning of tangerine from tomato reveals a carotenoid isomerase essential for the production of beta carotene and xanthophylls in plants. *Plant Cell* **14**: 333–342.
- Ito, M., Ichinose, Y., Kato, H., Shiraishi, T., and Yamada, T.** (1997). Molecular evolution and functional relevance of the chalcone synthase genes of pea. *Mol. Gen. Genet.* **255**: 28–37.
- Ittah, Y., Kanner, J., and Granit, R.** (1993). Hydrolysis study of carotenoid pigments of paprika (*Capsicum annuum* L. variety Lehava) by HPLC/photodiode array detection. *J. Agric. Food Chem.* **41**: 899–901.
- Jeknić, Z., Morré, J.T., Jeknić, S., Jevremović, S., Subotić, A., and Chen, T.H.H.** (2012). Cloning and functional characterization of a gene for capsanthin-capsorubin synthase from tiger lily (*Lilium lancifolium* thunb. “splendens”). *Plant Cell Physiol.* **53**: 1899–1912.
- Jeong, M.J. and Shih, M.C.** (2003). Interaction of a GATA factor with cis-acting elements involved in light regulation of nuclear genes encoding chloroplast glyceraldehyde-3-phosphate dehydrogenase in *Arabidopsis*. *Biochem. Biophys. Res. Commun.* **300**: 555–562.
- Josse, E.M., Simkin, a J., Gaffé, J., Labouré, a M., Kuntz, M., and Carol, P.** (2000). A plastid terminal oxidase associated with carotenoid desaturation during chromoplast differentiation. *Plant Physiol.* **123**: 1427–1436.
- Kato, H., Wada, M., Muraya, K., Malik, K., Shiraishi, T., Ichinose, Y., and Yamada, T.** (1995). Characterization of nuclear factors for elicitor-mediated activation of the promoter of the pea

- phenylalanine ammonia-lyase gene 1. *Plant Physiol.* **108**: 129–139.
- Kim, K.N. and Guiltinan, M.J.** (1999). Identification of cis-acting elements important for expression of the starch-branching enzyme I gene in maize endosperm. *Plant Physiol.* **121**: 225–236.
- Kim, O.R., Cho, M.C., Kim, B.D., and Huh, J.H.** (2010). A splicing mutation in the gene encoding phytoene synthase causes orange coloration in Habanero pepper fruits. *Mol. Cells* **30**: 569–574.
- Knapp, S., Bohs, L., Nee, M., and Spooner, D.M.** (2004). Solanaceae - A model for linking genomics with biodiversity. *Comp. Funct. Genomics* **5**: 285–291.
- Kothari, S.L., Joshi, A., Kachhwaha, S., and Ochoa-Alejo, N.** Chilli peppers--a review on tissue culture and transgenesis. *Biotechnol. Adv.* **28**: 35–48.
- Kovanen, P.T., Nikkilä, E. a, and Miettinen, T. a** (1975). Regulation of cholesterol synthesis and storage in fat cells. *J. Lipid Res.* **16**: 211–223.
- Kraft, K.H., Brown, C.H., Nabhan, G.P., Luedeling, E., Luna Ruiz, J.D.J., Coppens d'Eeckenbrugge, G., Hijmans, R.J., and Gepts, P.** (2014). Multiple lines of evidence for the origin of domesticated chili pepper, *Capsicum annum*, in Mexico. *Proc. Natl. Acad. Sci.* **111**: 1–6.
- Krajayklang, M., Klieber, A., and Dry, P.R.** (2000). Colour at harvest and post-harvest behaviour influence paprika and chilli spice quality. *Postharvest Biol. Technol.* **20**: 269–278.
- Krinsky, N.I. and Johnson, E.J.** (2005). Carotenoid actions and their relation to health and disease. *Mol. Aspects Med.* **26**: 459–516.
- Krinsky, N.I. and Yeum, K.J.** (2003). Carotenoid-radical interactions. *Biochem. Biophys. Res. Commun.* **305**: 754–760.
- Kwon, H.B., Park, S.C., Peng, H.P., Goodman, H.M., Dewdney, J., and Shih, M.C.** (1994). Identification of a light-responsive region of the nuclear gene encoding the B subunit of chloroplast glyceraldehyde 3-phosphate dehydrogenase from *Arabidopsis thaliana*. *Plant Physiol.* **105**: 357–367.
- Lagrange, T., Gauvin, S., Yeo, H.J., and Mache, R.** (1997). S2F , a Leaf-Specific trans-Acting Factor , Binds to a Nove1 cis-Acting Element and Differentially Activates the RPL21 gene. *Plant Cell* **9**: 1469–1479.
- Lang, Y.-Q., Yanagawa, S., Sasanuma, T., and Sasakuma, T.** (2004). Orange Fruit Color in *Capsicum* due to Deletion of Capsanthin-capsorubin Synthesis Gene. *Breed. Sci.* **54**: 33–39.
- Lee, D.S., Chung, S.K., Kim, H.K., and Yam, K.L.** (1991). NONENZYMATIC BROWNING IN DRIED RED PEPPER PRODUCTS. *J. Food Qual.* **14**: 153–163.
- Lefebvre, V., Kuntz, M., Camara, B., and Palloix, A.** (1998). The capsanthin-capsorubin synthase gene: a candidate gene for the γ locus controlling the red fruit colour in pepper. *Plant Mol. Biol.* **36**: 785–9.
- León, A.M., Palma, J.M., Corpas, F.J., Gómez, M., Romero-Puertas, M.C., Chatterjee, D., Mateos, R.M., Del Río, L. a., and Sandalio, L.M.** (2002). Antioxidative enzymes in cultivars of pepper plants with different sensitivity to cadmium. *Plant Physiol. Biochem.* **40**: 813–820.
- Lewinsohn, E., Sitrit, Y., Bar, E., Azulay, Y., Ibdah, M., Meir, A., Yosef, E., Zamir, D., and Tadmor, Y.** (2005). Not just colors - Carotenoid degradation as a link between pigmentation and aroma in tomato and watermelon fruit. *Trends Food Sci. Technol.* **16**: 407–415.
- Li, F., Vallabhaneni, R., Yu, J., Rocheford, T., and Wurtzel, E.T.** (2008). The maize phytoene synthase gene family: overlapping roles for carotenogenesis in endosperm, photomorphogenesis, and thermal stress tolerance. *Plant Physiol.* **147**: 1334–1346.
- Li, J., Li, G., Gao, S., Martinez, C., He, G., Zhou, Z., Huang, X., Lee, J.-H., Zhang, H., Shen, Y., Wang, H., and Deng, X.W.** (2010). *Arabidopsis* transcription factor ELONGATED HYPOCOTYL5 plays a

- role in the feedback regulation of phytochrome A signaling. *Plant Cell* **22**: 3634–3649.
- Li, W., Ma, M., Feng, Y., Li, H., Wang, Y., Ma, Y., Li, M., An, F., and Guo, H.** (2015). EIN2-Directed Translational Regulation of Ethylene Signaling in Arabidopsis. *Cell* **163**: 670–83.
- Li, Z., Ahn, T.K., Avenson, T.J., Ballottari, M., Cruz, J. a, Kramer, D.M., Bassi, R., Fleming, G.R., Keasling, J.D., and Niyogi, K.K.** (2009). Lutein accumulation in the absence of zeaxanthin restores nonphotochemical quenching in the Arabidopsis thaliana npq1 mutant. *Plant Cell* **21**: 1798–1812.
- Liang, X.W., Dron, M., Cramer, C.L., Dixon, R. a, and Lamb, C.J.** (1989). Differential regulation of phenylalanine ammonia-lyase genes during plant development and by environmental cues. *J. Biol. Chem.* **264**: 14486–14492.
- Libal-Weksler, Y., Vishnevetsky, M., Ovadis, M., and Vainstein, a** (1997). Isolation and regulation of accumulation of a minor chromoplast-specific protein from cucumber corollas. *Plant Physiol.* **113**: 59–63.
- Lichtenthaler, H.K., Rohmer, M., and Schwender, J.** (1997). Two independent biochemical pathways for isopentenyl diphosphate and isoprenoid biosynthesis in higher plants. *Plant Physiol.* **101**: 643–652.
- Lieberman, M., Segev, O., Gilboa, N., Lalazar, A., and Levin, I.** (2004). The tomato homolog of the gene encoding UV-damaged DNA binding protein 1 (DDB1) underlined as the gene that causes the high pigment-1 mutant phenotype. *Theor. Appl. Genet.* **108**: 1574–81.
- Lindgren, L.O., Stålberg, K.G., and Höglund, A.-S.** (2003). Seed-specific overexpression of an endogenous Arabidopsis phytoene synthase gene results in delayed germination and increased levels of carotenoids, chlorophyll, and abscisic acid. *Plant Physiol.* **132**: 779–85.
- Liu, W., Parrott, W.A., Hildebrand, D.F., Collins, G.B., and Williams, E.G.** (1990). Agrobacterium induced gall formation in bell pepper (*Capsicum annuum* L.) and formation of shoot-like structures expressing introduced genes. *Plant Cell Rep.* **9**: 360–4.
- Liu, Y., Wang, M.M., Ai, L.F., Zhang, C.K., Li, X., and Wang, X.S.** (2014). Determination of Sudan dyes in chili pepper powder by online solid-phase extraction with a butyl methacrylate monolithic column coupled to liquid chromatography with tandem mass spectrometry. *J. Sep. Sci.* **37**: 1648–1655.
- Logemann, E., Parniske, M., and Hahlbrock, K.** (1995). Modes of expression and common structural features of the complete phenylalanine ammonia-lyase gene family in parsley. *Proc. Natl. Acad. Sci. U. S. A.* **92**: 5905–5909.
- Lois, L.M., Rodríguez-Concepción, M., Gallego, F., Campos, N., and Boronat, A.** (2000). Carotenoid biosynthesis during tomato fruit development: Regulatory role of 1-deoxy-D-xylulose 5-phosphate synthase. *Plant J.* **22**: 503–513.
- Lu, S. et al.** (2006). The cauliflower Or gene encodes a DnaJ cysteine-rich domain-containing protein that mediates high levels of beta-carotene accumulation. *Plant Cell* **18**: 3594–3605.
- Luan, S. and Bogorad, L.** (1992). A rice cab gene promoter contains separate cis-acting elements that regulate expression in dicot and monocot plants. *Plant Cell* **4**: 971–981.
- Luning, P.A., de Rijk, T., Wichers, H.J., and Roozen, J.P.** (1994). Gas chromatography, Mass spectrometry, and sniffing port analyses of volatile compounds of fresh bell peppers (*Capsicum annuum*) at different ripening stages. *J. Agric. Food Chem.:* 977–983.
- Maass, D., Arango, J., Wüst, F., Beyer, P., and Welsch, R.** (2009a). Carotenoid crystal formation in Arabidopsis and carrot roots caused by increased phytoene synthase protein levels. *PLoS One* **4**.
- Maass, D., Arango, J., Wüst, F., Beyer, P., and Welsch, R.** (2009b). Carotenoid crystal formation in

- Arabidopsis and carrot roots caused by increased phytoene synthase protein levels. *PLoS One* **4**: e6373.
- Maeda, K., Kimura, S., Demura, T., Takeda, J., and Ozeki, Y.** (2005). DcMYB1 acts as a transcriptional activator of the carrot phenylalanine ammonia-lyase gene (DcPAL1) in response to elicitor treatment, UV-B irradiation and the dilution effect. *Plant Mol. Biol.* **59**: 739–752.
- Mahdavian, K., Ghorbanli, M., and Kalantari, K.M.** (2008). The effects of ultraviolet radiation on the contents of chlorophyll, flavonoid, anthocyanin and proline in *Capsicum annum* L. *Turk. J. Botany* **32**: 25–33.
- Mali, P., Esvelt, K.M., and Church, G.M.** (2013). Cas9 as a versatile tool for engineering biology. *Nat. Methods* **10**: 957–63.
- Manning, K., Tör, M., Poole, M., Hong, Y., Thompson, A.J., King, G.J., Giovannoni, J.J., and Seymour, G.B.** (2006). A naturally occurring epigenetic mutation in a gene encoding an SBP-box transcription factor inhibits tomato fruit ripening. *Nat. Genet.* **38**: 948–52.
- Manzara, T., Carrasco, P., and Gruissem, W.** (1991). Developmental and organ-specific changes in promoter DNA-protein interactions in the tomato *rbcS* gene family. *Plant Cell* **3**: 1305–1316.
- Manzocco, L., Mastrocola, D., Nicoli, M.C., and Marangoni, V.** (2001). Review of non- enzymatic browning and antioxidant capacity in processed foods. *Trends Food Sci. Technol.* **11**: 340–346.
- Marangoni, a. G., Palma, T., and Stanley, D.W.** (1996). Membrane effects in postharvest physiology. *Postharvest Biol. Technol.* **7**: 193–217.
- Marechal, E., Block, M. a, Dorne, a J., Douce, R., and Joyard, J.** (1997). Lipid synthesis and metabolism in the plastid envelope. *Physiol. Plant.* **100**: 65–77.
- Martinez, M.V. and Whitaker, J.R.** (1995). The biochemistry and control of enzymatic browning. *Trends Food Sci. Technol.* **6**: 195–200.
- Matsui, K., Shibata, Y., Tateba, H., Hatanaka, a, and Kajiwara, T.** (1997). Changes of lipoxygenase and fatty acid hydroperoxide lyase activities in bell pepper fruits during maturation. *Biosci. Biotechnol. Biochem.* **61**: 199–201.
- Mayne, S.T. and Parker, R.S.** (1989). Antioxidant activity of dietary canthaxanthin. *Nutr. Cancer* **12**: 225–36.
- Mazida, M.M., Salleh, M.M., and Osman, H.** (2005). Analysis of volatile aroma compounds of fresh chilli (*Capsicum annum*) during stages of maturity using solid phase microextraction (SPME). *J. Food Compos. Anal.* **18**: 427–437.
- van der Meer, I.M., Spelt, C.E., Mol, J.N.M., and Stuitje, A.R.** (1990). Promoter analysis of the chalcone synthase (*chsA*) gene of *Petunia hybrida*: a 67 bp promoter region directs flower-specific expression. *Plant Mol. Biol.* **15**: 95–109.
- Miallau, L., Alphey, M.S., Kemp, L.E., Leonard, G. a, McSweeney, S.M., Hecht, S., Bacher, A., Eisenreich, W., Rohdich, F., and Hunter, W.N.** (2003). Biosynthesis of isoprenoids: crystal structure of 4-diphosphocytidyl-2C-methyl-D-erythritol kinase. *Proc. Natl. Acad. Sci. U. S. A.* **100**: 9173–9178.
- Mikami, K., Sakamoto, A., and Iwabuchi, M.** (1994). The HBP-1 family of wheat basic/leucine zipper proteins interacts with overlapping cis-acting hexamer motifs of plant histone genes. *J. Biol. Chem.* **269**: 9974–9985.
- Minguez-Mosquera, M.I. and Hornero-Medez, D.** (1994). Formation and transformation of pigments during the fruit ripening of *Capsicum annum* cv. Bola and Agridulce. *J. Agric. ...*: 38–44.
- Minguez-Mosquera, M.I. and Hornero-Mendez, D.** (1993). Separation and quantification of the carotenoid pigments in red peppers (*Capsicum annum* L.), paprika, and oleoresin by reversed-

phase HPLC. *J. Agric. Food Chem.* **41**: 1616–1620.

- Minoia, S., Petrozza, A., D'Onofrio, O., Piron, F., Mosca, G., Sozio, G., Cellini, F., Bendahmane, A., and Carriero, F.** (2010). A new mutant genetic resource for tomato crop improvement by TILLING technology. *BMC Res. Notes* **3**: 69.
- Morais, H., Ramos, A.C., Tibor, C., and Forgács, E.** (2001). Effects of fluorescent light and vacuum packaging on the rate of decomposition of pigments in paprika (*Capsicum annuum*) powder determined by reversed-phase high-performance liquid chromatography. *J. Chromatogr. A* **936**: 139–44.
- Moran, N.A. and Jarvik, T.** (2010). Lateral Transfer of Genes from Fungi Underlies Carotenoid Production in Aphids. *Science* (80-.). **328**: 624–627.
- Morris, W.L., Ducreux, L.J.M., Hedden, P., Millam, S., and Taylor, M. a.** (2006). Overexpression of a bacterial 1-deoxy-D-xylulose 5-phosphate synthase gene in potato tubers perturbs the isoprenoid metabolic network: Implications for the control of the tuber life cycle. *J. Exp. Bot.* **57**: 3007–3018.
- Mortensen, a, Skibsted, L.H., and Truscott, T.G.** (2001). The interaction of dietary carotenoids with radical species. *Arch. Biochem. Biophys.* **385**: 13–19.
- Murata, N. and Los, D.A.** (1997). Membrane Fluidity and Temperature Perception. *Plant Physiol.* **115**: 875–879.
- Mustilli, A.C.** (1999). Phenotype of the Tomato high pigment-2 Mutant Is Caused by a Mutation in the Tomato Homolog of DEETIOLATED1. *PLANT CELL ONLINE* **11**: 145–158.
- Nogueira, M., Mora, L., Enfissi, E.M. a, Bramley, P.M., and Fraser, P.D.** (2013). Subchromoplast sequestration of carotenoids affects regulatory mechanisms in tomato lines expressing different carotenoid gene combinations. *Plant Cell* **25**: 4560–79.
- Ohlrogge, J. and Browse, J.** (1995). Lipid biosynthesis. *Plant Cell* **7**: 957–970.
- Ohmiya, A., Kishimoto, S., Aida, R., Yoshioka, S., and Sumitomo, K.** (2006). Carotenoid cleavage dioxygenase (CmCCD4a) contributes to white color formation in chrysanthemum petals. *Plant Physiol.* **142**: 1193–1201.
- Omenn, G.S., Goodman, G.E., Thornquist, M.D., Balmes, J., Cullen, M.R., Glass, A., Keogh, J.P., Meyskens, F.L., Valanis, B., Williams, J.H., Barnhart, S., and Hammar, S.** (1996). Effects of a Combination of Beta Carotene and Vitamin A on Lung Cancer and Cardiovascular Disease. *N. Engl. J. Med.* **334**: 1150–1155.
- Pan, Y. et al.** (2013). Network inference analysis identifies an APRR2-like gene linked to pigment accumulation in tomato and pepper fruits. *Plant Physiol.* **161**: 1476–85.
- Pandit, J., Danley, D.E., Schulte, G.K., Mazzalupo, S., Pauly, T. a, Hayward, C.M., Hamanaka, E.S., Thompson, J.F., and Harwood, H.J.** (2000). Crystal structure of human squalene synthase. A key enzyme in cholesterol biosynthesis. *J. Biol. Chem.* **275**: 30610–30617.
- Paran, I. and Van Der Knaap, E.** (2007). Genetic and molecular regulation of fruit and plant domestication traits in tomato and pepper. *J. Exp. Bot.* **58**: 3841–3852.
- Park, Y., Choi, Y., Lee, Y., Kang, J., and GU, S.** (2009). A Gene-based dCAPS Marker for Selecting old-gold-crimson (ogc) Fruit Color Mutation in Tomato. *J. Life Sci.* **19**: 152–155.
- Parsons, E.P., Popovvsky, S., Lohrey, G.T., Alkalai-Tuvia, S., Perzelan, Y., Bosland, P., Bebeli, P.J., Paran, I., Fallik, E., and Jenks, M. a.** (2013). Fruit cuticle lipid composition and water loss in a diverse collection of pepper (*Capsicum*). *Physiol. Plant.* **149**: 160–174.
- Perez-Fons, L., Steiger, S., Khaneja, R., Bramley, P.M., Cutting, S.M., Sandmann, G., and Fraser, P.D.** (2011). Identification and the developmental formation of carotenoid pigments in the

- yellow/orange *Bacillus* spore-formers. *Biochim. Biophys. Acta - Mol. Cell Biol. Lipids* **1811**: 177–185.
- Pérez-Gálvez, A., Garrido-Fernández, J., Mínguez-Mosquera, M.I., Lozano-Ruiz, M., and Montero-de-Espinosa, V.** (1999). Fatty acid composition of two new pepper varieties (*Capsicum annuum* L. cv. Jaranda and Jariza). Effect of drying process and nutritional aspects. *J. Am. Oil Chem. Soc.* **76**: 205–208.
- Perry, L. et al.** (2007). Strach fossils and the domestication and dispersal of chilli peppers (*Capsicum* spp. L.) in the Americas. *Science* **315**: 986–988.
- Pichersky, E., Noel, J.P., and Dudareva, N.** (2006). Biosynthesis of Plant Volatiles: Nature's Diversity and Ingenuity. **311**: 808–811.
- Pino, J., Fuentes, V., and Barrios, O.** (2011). Volatile constituents of Cachucha peppers (*Capsicum chinense* Jacq.) grown in Cuba. *Food Chem.* **125**: 860–864.
- Pino, J., Sauri-Duch, E., and Marbot, R.** (2006). Changes in volatile compounds of Habanero chile pepper (*Capsicum chinense* Jack. cv. Habanero) at two ripening stages. *Food Chem.* **94**: 394–398.
- Pogson, B.J., Woo, N.S., Förster, B., and Small, I.D.** (2008). Plastid signalling to the nucleus and beyond. *Trends Plant Sci.* **13**: 602–609.
- Popovsky, S. and Paran, I.** (2000). Molecular genetics of the γ locus in pepper: its relation to capsanthin-capsorubin synthase and to fruit color. *TAG Theor. Appl. Genet.* **101**: 86–89.
- Prebeg, T., Ljubescic, N., and Wrisher, M.** (2006a). Chromoplast biogenesis in *Chelidonium majus* petals. *ACTA Soc. Bot. Pol.* **75**: 107–112.
- Prebeg, T., Ljubešić, N., and Wrisher, M.** (2006b). Differentiation of Chromoplasts in *Cucumis sativus* Petals. *Int. J. Plant Sci.* **167**: 437–445.
- Qin, C. et al.** (2014). Whole-genome sequencing of cultivated and wild peppers provides insights into *Capsicum* domestication and specialization. *Proc. Natl. Acad. Sci. U. S. A.* **111**: 5135–40.
- Ramel, F., Birtic, S., Ginies, C., Soubigou-Taconnat, L., Triantaphylidès, C., and Havaux, M.** (2012). Carotenoid oxidation products are stress signals that mediate gene responses to singlet oxygen in plants. *Proc. Natl. Acad. Sci. U. S. A.* **109**: 5535–40.
- Rao, a. V. and Rao, L.G.** (2007). Carotenoids and human health. *Pharmacol. Res.* **55**: 207–216.
- Rey, P., Gillet, B., and Romer, S.** (2000). Over-expression of a pepper plastid lipid-associated protein in tobacco leads to changes in plastid ultrastructure and plant development upon stress. **21**: 483–494.
- Rodriguez-Uribe, L., Guzman, I., Rajapakse, W., Richins, R.D., and O'Connell, M. a.** (2012). Carotenoid accumulation in orange-pigmented *Capsicum annuum* fruit, regulated at multiple levels. *J. Exp. Bot.* **63**: 517–526.
- Rohmer, M., Knani, M., Simonin, P., Sutter, B., and Sahm, H.** (1993). Isoprenoid biosynthesis in bacteria: a novel pathway for the early steps leading to isopentenyl diphosphate. *Biochem. J.* **295 (Pt 2)**: 517–524.
- Romer et al** (1993). Expression of genes encoding early carotenoid biosynthetic enzymes in *Capsicum annuum*.: 1414–1421.
- Ronen, G., Carmel-Goren, L., Zamir, D., and Hirschberg, J.** (2000). An alternative pathway to beta-carotene formation in plant chromoplasts discovered by map-based cloning of beta and old-gold color mutations in tomato. *Proc. Natl. Acad. Sci. U. S. A.* **97**: 11102–11107.
- Ronen, G., Cohen, M., Zamir, D., and Hirschberg, J.** (1999). Regulation of carotenoid biosynthesis during tomato fruit development: expression of the gene for lycopene epsilon-cyclase is down-

- regulated during ripening and is elevated in the mutant *Delta*. *Plant J.* **17**: 341–351.
- Roudier, F. et al.** (2010). Very-long-chain fatty acids are involved in polar auxin transport and developmental patterning in *Arabidopsis*. *Plant Cell* **22**: 364–375.
- Rushing, J. and Huber, D.** (1985). INITIATION OF TOMATO FRUIT RIPENING WITH COPPER. *J. Am. Soc. Hortic. Sci.* **110**: 316–318.
- Van Ruth, S.M., Roozen, J.P., Cozijnsen, J.L., and Posthumus, M.A.** (1995). Volatile compounds of rehydrated French beans, bell peppers and leeks. Part II. Gas chromatography/sniffing port analysis and sensory evaluation. *Food Chem.* **54**: 1–7.
- Sadeghi-Bazargani, H., Banani, a., and Mohammadi, S.** (2010). Using SIMCA statistical software package to apply orthogonal projections to latent structures modeling. World Autom. Congr. (WAC), 2010.
- Sandmann, G.** (1994). Carotenoid biosynthesis in microorganisms and plants. *Eur. J. Biochem.* **223**: 7–24.
- Von Schantz, T., Bensch, S., Grahn, M., Hasselquist, D., and Wittzell, H.** (1999). Good genes, oxidative stress and condition-dependent sexual signals. *R. Soc.* **266**: 1–12.
- Schindler, U. and Cashmore, A.R.** (1990). DNA binding proteins involve ubiquitous. *EMBO J.* **9**.
- Schwartz, J.L., Singh, R.P., Teicher, B., Wright, J.E., Trites, D.H., and Shklar, G.** (1990). Induction of a 70kD protein associated with the selective cytotoxicity of beta-carotene in human epidermal carcinoma. *Biochem. Biophys. Res. Commun.* **169**: 941–946.
- Schweiggert, U., Kammerer, D.R., Carle, R., and Schieber, A.** (2005). Characterization of carotenoids and carotenoid esters in red pepper pods (*Capsicum annuum* L.) by high-performance liquid chromatography/atmospheric pressure chemical ionization mass spectrometry. *Rapid Commun. Mass Spectrom.* **19**: 2617–2628.
- Schwender, J., Seemann, M., Lichtenthaler, H.K., and Rohmer, M.** (1996). Biosynthesis of isoprenoids (carotenoids, sterols, prenyl side-chains of chlorophylls and plastoquinone) via a novel pyruvate/glyceraldehyde 3-phosphate non-mevalonate pathway in the green alga *Scenedesmus obliquus*. *Biochem. J.* **316** (Pt 1: 73–80.
- Shan, Q., Wang, Y., Li, J., Zhang, Y., Chen, K., Liang, Z., Zhang, K., Liu, J., Xi, J.J., Qiu, J.-L., and Gao, C.** (2013). Targeted genome modification of crop plants using a CRISPR-Cas system. *Nat. Biotechnol.* **31**: 686–8.
- Shewmaker, C.K., Sheehy, J. a., Daley, M., Colburn, S., and Ke, D.Y.** (1999). Seed-specific overexpression of phytoene synthase: Increase in carotenoids and other metabolic effects. *Plant J.* **20**: 401–412.
- Shumskaya, M., Bradbury, L.M.T., Monaco, R.R., and Wurtzel, E.T.** (2012). Plastid Localization of the Key Carotenoid Enzyme Phytoene Synthase Is Altered by Isozyme, Allelic Variation, and Activity. *Plant Cell* **24**: 3725–3741.
- Silletti, M.F., Petrozza, A., Stigliani, A.L., Giorio, G., Cellini, F., D’Ambrosio, C., and Carriero, F.** (2013). An increase of lycopene content in tomato fruit is associated with a novel *Cyc-B* allele isolated through TILLING technology. *Mol. Breed.* **31**: 665–674.
- Simkin, A.J., Gaffé, J., Alcaraz, J.P., Carde, J.P., Bramley, P.M., Fraser, P.D., and Kuntz, M.** (2007). Fibrillin influence on plastid ultrastructure and pigment content in tomato fruit. *Phytochemistry* **68**: 1545–1556.
- Simkin, A.J., Schwartz, S.H., Auldridge, M., Taylor, M.G., and Klee, H.J.** (2004). The tomato carotenoid cleavage dioxygenase 1 genes contribute to the formation of the flavor volatiles ??-ionone, pseudoionone, and geranylacetone. *Plant J.* **40**: 882–892.

- Simkin, A.J., Zhu, C., Kuntz, M., and Sandmann, G.** (2003). Light-dark regulation of carotenoid biosynthesis in pepper (*Capsicum annuum*) leaves. *J. Plant Physiol.* **160**: 439–43.
- Simpson, D.J., Baqar, M.R., and Lee, T.H.** (1977). Fine structure and carotenoid composition of the fibrillar chromoplasts of *Asparagus officinalis* L. *Ann. Bot.* **41**: 1101–1108.
- Simpson, D.J. and Lee, T.H.** (1976). The fine structure and formation of fibrils of *Capsicum annuum* L. chromoplasts. *Zeitschrift fur Pflanzenphysiologie*: 127–138.
- Stahl, W. and Sies, H.** (2003). Antioxidant activity of carotenoids. *Mol. Aspects Med.* **24**: 345–351.
- Stitt, M. and Sonnewald, U.** (1995). Regulation of metabolism in transgenic plants. *Annu. PhysiolMolBiol* **46**: 341–368.
- Takos, A.M., Jaffé, F.W., Jacob, S.R., Bogs, J., Robinson, S.P., and Walker, A.R.** (2006). Light-induced expression of a MYB gene regulates anthocyanin biosynthesis in red apples. *Plant Physiol.* **142**: 1216–1232.
- Tang, W. and Perry, S.E.** (2003). Binding site selection for the plant MADS domain protein AGL15. An in vitro and in vivo study. *J. Biol. Chem.* **278**: 28154–28159.
- Tepić, A.N. and Vujičić, B.L.** (2004). Colour change in pepper (*Capsicum annuum*) during storage. *Acta Period. Technol.* **280**: 59–64.
- Thorup, T.A., Tanyolac, B., Livingstone, K.D., Popovsky, S., Paran, I., and Jahn, M.** (2000). Candidate gene analysis of organ pigmentation loci in the Solanaceae. *Proc. Natl. Acad. Sci. U. S. A.* **97**: 11192–7.
- Toledo-Ortiz, G., Huq, E., and Rodríguez-Concepción, M.** (2010). Direct regulation of phytoene synthase gene expression and carotenoid biosynthesis by phytochrome-interacting factors. *Proc. Natl. Acad. Sci. U. S. A.* **107**: 11626–31.
- Uno, Y., Furihata, T., Abe, H., Yoshida, R., Shinozaki, K., and Yamaguchi-Shinozaki, K.** (2000). Arabidopsis basic leucine zipper transcription factors involved in an abscisic acid-dependent signal transduction pathway under drought and high-salinity conditions. *Proc. Natl. Acad. Sci. U. S. A.* **97**: 11632–11637.
- Vandesompele, J., De Preter, K., Pattyn, F., Poppe, B., Van Roy, N., De Paepe, A., and Speleman, F.** (2002). Accurate normalization of real-time quantitative RT-PCR data by geometric averaging of multiple internal control genes. *Genome Biol.* **3**: RESEARCH0034.
- van Verk, M.C., Bol, J.F., and Linthorst, H.J.M.** (2011). WRKY transcription factors involved in activation of SA biosynthesis genes. *BMC Plant Biol.* **11**: 89.
- Vidi, P.A., Kanwischer, M., Baginsky, S., Austin, J.R., Csucs, G., Dörmann, P., Kessler, F., and Bréhélin, C.** (2006). Tocopherol cyclase (VTE1) localization and vitamin E accumulation in chloroplast plastoglobule lipoprotein particles. *J. Biol. Chem.* **281**: 11225–11234.
- Vishnevetsky, M.** (1999). Carotenoid sequestration in plants: the role of carotenoid-associated proteins. *Trends Plant Sci.* **4**: 232–235.
- Vishnevetsky, M., Ovadis, M., Zuker, A., and Vainstein, A.** (1999). Molecular mechanisms underlying carotenogenesis in the chromoplast: Multilevel regulation of carotenoid-associated genes. *Plant J.* **20**: 423–431.
- Vogg, G., Fischer, S., Leide, J., Emmanuel, E., Jetter, R., Levy, A. a., and Riederer, M.** (2004). Tomato fruit cuticular waxes and their effects on transpiration barrier properties: Functional characterization of a mutant deficient in a very-long-chain fatty acid ω -ketoacyl-CoA synthase. *J. Exp. Bot.* **55**: 1401–1410.
- Vracar, L., Tepic, A., Vujicic, B., and Solaja, S.** (2007). Influence of the heat treatment on the color of ground pepper (*Capsicum annuum*). *Acta Period. Technol.* **190**: 53–58.

- Wade, H.K., Bibikova, T.N., Valentine, W.J., and Jenkins, G.I.** (2001). Interactions within a network of phytochrome, cryptochrome and UV B phototransduction pathways regulate chalcone synthase gene expression in arabidopsis leaf tissue. *Plant J.* **25**: 675–685.
- Wang, C.-J., Chou, M.-Y., and Lin, J.-K.** (1989). Inhibition of growth and development of the transplantable C-6 glioma cells inoculated in rats by retinoids and carotenoids. *Cancer Lett.* **48**: 135–142.
- Wang, C.Y. and Baker, J.E.** (1979). Effects of two free radical scavengers and intermittent warming on chilling injury and polar lipid composition of cucumber and sweet pepper fruits. *Plant Cell Physiol.* **20**: 243–251.
- Wang, Y.Q., Yang, Y., Fei, Z., Yuan, H., Fish, T., Thannhauser, T.W., Mazourek, M., Kochian, L. V., Wang, X., and Li, L.** (2013). Proteomic analysis of chromoplasts from six crop species reveals insights into chromoplast function and development. *J. Exp. Bot.* **64**: 949–961.
- Wang, Z., Zhu, Y., Wang, L., Liu, X., Liu, Y., Phillips, J., and Deng, X.** (2009). A WRKY transcription factor participates in dehydration tolerance in *Boea hygrometrica* by binding to the W-box elements of the galactinol synthase (*BhGolS1*) promoter. *Planta* **230**: 1155–1166.
- Wanke, M., Skorupinska-tudek, K., and Swiezewska, E.** (2001). Isoprenoid biosynthesis. **48**: 663–672.
- Weissenberg, M., Schaeffler, I., Menagem, E., Barzilai, M., and Levy, A.** (1997). Isocratic non-aqueous reversed-phase high-performance liquid chromatographic separation of capsanthin and capsorubin in red peppers (*Capsicum annum* L.), paprika and oleoresin. *J. Chromatogr. A*: 89–95.
- Welsch, R., Medina, J., Giuliano, G., Beyer, P., and Von Lintig, J.** (2003). Structural and functional characterization of the phytoene synthase promoter from *Arabidopsis thaliana*. *Planta* **216**: 523–534.
- Whitaker, B.D.** (1991). Growth conditions and ripening influence plastid and microsomal membrane lipid compositions in bell pepper fruit. *J. Am. Soc. Hort. Sci.* **116**: 528–533.
- Wolffe, A.P.** (1999). Epigenetics: Regulation Through Repression. *Science* (80-.). **286**: 481–486.
- Woodall, A. a., Britton, G., and Jackson, M.J.** (1997a). Carotenoids and protection of phospholipids in solution or in liposomes against oxidation by peroxy radicals: Relationship between carotenoid structure and protective ability. *Biochim. Biophys. Acta - Gen. Subj.* **1336**: 575–586.
- Woodall, A. a., Wai-Ming Lee, S., Weesie, R., Jackson, M., and Britton, G.** (1997b). Oxidation of carotenoids by free radicals: relationship between structure and reactivity. *Biochim. Biophys. Acta* **1336**: 33–42.
- Wrischer, M., Prebeg, T., Magnus, V., and Ljubešić, N.** (2007). Crystals and fibrils in chromoplast plastoglobules of *Solanum capsicastrum* fruit. *Acta Bot. Croat.* **66**: 81–87.
- Wuttke, H.** (1976). CHROMOPLASTS IN *ROSA-RUGOSA* - DEVELOPMENT AND CHEMICAL CHARACTERIZATION OF TUBULAR ELEMENTS. *ZEITSCHRIFT FÜR Naturforsch. C-A J. Biosci.* **31**: 456–&.
- Xiao, Y., Savchenko, T., Baidoo, E.E.K., Chehab, W.E., Hayden, D.M., Tolstikov, V., Corwin, J. a., Kliebenstein, D.J., Keasling, J.D., and Dehesh, K.** (2012). Retrograde signaling by the plastidial metabolite MEcPP regulates expression of nuclear stress-response genes. *Cell* **149**: 1525–1535.
- Xu, J., Duan, X., Yang, J., Beeching, J.R., and Zhang, P.** (2013). Enhanced Reactive Oxygen Species Scavenging by Overproduction of Superoxide Dismutase and Catalase Delays Postharvest Physiological Deterioration of Cassava Storage Roots. *Plant Physiol.* **161**: 1517–1528.
- Yanagisawa, S.** (2000). Dof1 and Dof2 transcription factors are associated with expression of multiple genes involved in carbon metabolism in maize. *Plant J.* **21**: 281–288.

- Ye, X., Al-Babili, S., Klöti, a, Zhang, J., Lucca, P., Beyer, P., and Potrykus, I.** (2000). Engineering the provitamin A (beta-carotene) biosynthetic pathway into (carotenoid-free) rice endosperm. *Science* **287**: 303–305.
- Yeats, T.H., Buda, G.J., Wang, Z., Chehanovsky, N., Moyle, L.C., Jetter, R., Schaffer, A. a., and Rose, J.K.C.** (2012). The fruit cuticles of wild tomato species exhibit architectural and chemical diversity, providing a new model for studying the evolution of cuticle function. *Plant J.* **69**: 655–666.
- Yeats, T.H. and Rose, J.K.C.** (2013). The formation and function of plant cuticles. *Plant Physiol.* **163**: 5–20.
- Ytterberg, a J., Peltier, J.-B., and van Wijk, K.J.** (2006). Protein profiling of plastoglobules in chloroplasts and chromoplasts. A surprising site for differential accumulation of metabolic enzymes. *Plant Physiol.* **140**: 984–997.
- Zheng, H., Rowland, O., and Kunst, L.** (2005). Disruptions of the Arabidopsis Enoyl-CoA reductase gene reveal an essential role for very-long-chain fatty acid synthesis in cell expansion during plant morphogenesis. *Plant Cell* **17**: 1467–1481.
- Zhou, X., Welsch, R., Yang, Y., Álvarez, D., Riediger, M., Yuan, H., Fish, T., Liu, J., Thannhauser, T.W., and Li, L.** (2015). Arabidopsis OR proteins are the major posttranscriptional regulators of phytoene synthase in controlling carotenoid biosynthesis. *Proc. Natl. Acad. Sci.* **112**: 201420831.